DISSERTATION

A MULTI-OBJECTIVE COMMUNITY-LEVEL SEISMIC RETROFIT OPTIMIZATION COMBINING SOCIAL VULNERABILITY WITH AN ENGINEERING FRAMEWORK FOR COMMUNITY RESILIENCY

Submitted by

Elaina N. Jennings

Department of Civil and Environmental Engineering

In partial fulfillment of the requirements

For the Degree of Doctor of Philosophy

Colorado State University

Fort Collins, Colorado

Spring 2015

Doctoral Committee:

Advisor: John W. van de Lindt

Rebecca Atadero
Hussam Mahmoud
Lori Peek

Copyright by Elaina N. Jennings 2015

All Rights Reserved

ABSTRACT

A MULTI-OBJECTIVE COMMUNITY-LEVEL SESIMIC RETROFIT OPTIMIZATION COMBINING SOCIAL VULNERABILITY WITH AN ENGINEERING FRAMEWORK FOR COMMUNITY RESILIENCY

This dissertation presents a multi-objective optimization framework for community resiliency by providing decision maker(s) at the local, state, or other government level(s) with an optimal seismic retrofit plan for their community's woodframe building stock. A genetic algorithm was selected to perform the optimization due to its robustness in multi-objective problem solving. In the present framework, the algorithm provides a set of optimal community-level retrofit plans for the woodframe building inventory based on the socio-demographic characteristics of the focal community, Los Angeles, California. The woodframe building inventory was modeled using 37 archetypes designed to several historical and state-of-the-art seismic design provisions and methodologies. The performance of the archetypes was quantified in an extensive numerical study using nonlinear time history analysis. Experimental testing was conducted at full scale on a three-story soft-story woodframe building. The experimental testing investigated the seismic performance of several retrofit strategies for use in the framework, and the results were used in development of a metric correlating inter-story drift limits with damage states used in the framework. A performance-based retrofit design is presented in detail, and the experimental testing results of four retrofits are provided as well.

The algorithm uses each archetype's seismic performance to identify the set of optimal community-level retrofit plans to enhance resiliency by minimizing four objectives: initial cost,

economic loss, number of morbidities, and recovery time. In the model, *initial cost* sums the cost of each new retrofit, e*conomic loss* incorporates direct and indirect costs; the *number of morbidities* includes injuries, fatalities, and persons diagnosed with post-traumatic stress disorder (PTSD); and a *recovery time* is estimated and may be used to represent the loss in quality of life for the affected population. The framework was calibrated to the estimated losses from the 1994 Northridge earthquake. An application of the framework is presented using Los Angeles County as the community. Two forecasted populations are also examined using the census data for Daly City, California and East Los Angeles to further exemplify the framework. Analyses were conducted at six seismic intensities. In all illustrative examples, the total financial loss (e.g., initial cost + economic loss) was higher for the initial population (i.e. un-retrofitted community). When combining this financial savings with the reduced number of morbidities, it is clear that the higher initial cost associated with retrofitting the woodframe building stock greatly outweighs the risks and losses associated with not retrofitting. The results also demonstrated how retrofitting the existing woodframe building stock greatly reduces estimated losses, especially for very large earthquakes. The resulting losses were further investigated to demonstrate the important role that the mental health of the population plays in a community's economy and recovery following disastrous events such as earthquakes. Overall, the results clearly demonstrate the necessity in including social vulnerability when assessing or designing for community-level resiliency for a seismic hazard.

ACKNOWLEDGMENTS

The author would like to express sincerest gratitude to her adviser, Dr. John van de Lindt, for his support, guidance, collaboration, and the many great opportunities he continued to present since the day we first met. The author would also like to thank and recognize her committee members, Dr. Rebecca Atadero, Dr. Hussam Mahmoud, and Dr. Lori Peek, for their support, inputs, and participation; each of which provided invaluable advice on topics of their own respect whether towards research and/or my professional development.

There were three major funding sources throughout the duration of this dissertation. The first year and most preliminary work was funded by the National Science Foundation through a graduate research diversity supplement awarded to the author.

The design studies presented in this dissertation were part of the NEES-Soft Project, which was partially supported by the National Science Foundation through EEC-1263155 and through CMMI-1314957. The author would like to recognize the entire NEES-Soft project team, contributors to the project, and the SEESL staff at the University at Buffalo.

The Department of Civil and Environmental Engineering at Colorado State University honored me with the opportunity to teach a course in my final semester. Their financial support and confidence in my abilities was greatly appreciated.

The author would also like to thank Franklin Sutley for consultation on many aspects of this dissertation, as well as, her research group, friends, and family for their support, and making this a very memorable and enjoyable experience.

TABLE OF CONTENTS

LIST OF TABLES

LIST OF FIGURES

Chapter 1: Introduction

Disasters affect communities without discrimination, and in the immediate moments following the event a social leveling may temporarily exist. This instance in time knows no social class, knows no race, knows no age, nor gender. However, the moments following this brief instance in time, during, after, and throughout the recovery stage, are extremely biased and affect individuals and communities in different ways and to different extents. The level to which an individual, a family, or a community is affected is based on their social vulnerability, and the time it takes them to recover is based on their resiliency. Hazards are not consistent everywhere, but rather vary in type and intensity by location. Loss happens to individuals and families, but recovery is a community effort. Therefore, addressing resiliency at the regional or community levels may be most beneficial.

Community disaster resiliency has become a mitigation focus worldwide. The World Bank and World Health Organization have hundreds of country-specific projects with this focus. Within the U.S. in the past several years, major research efforts have been established by the American Society of Civil Engineers (ASCE), the American Society of Mechanical Engineers (ASME), the Pacific Earthquake Engineering Research (PEER) Center, the National Earthquake Hazards Reduction Program (NEHRP) with the National Research Council (NRC), National Academies, the Department of Homeland Security (DHS), the Federal Emergency Management Agency (FEMA), the American Technology Council (ATC), the American National Standards Institute (ANSI), and the National Institute of Standards and Technology (NIST).

1.1 Resiliency

Vulnerability and resiliency are two well-developed concepts in the literature with many varying connotations across fields and focuses of study (i.e. engineering, sociology, psychology, geography, ecology, financial, biophysical, etc.). A comprehensive set of definitions found in the literature is provided in Cutter (1996) for vulnerability and in Norris et al. (2008) for resiliency. Social vulnerability is a pre-existing condition of an individual, or group, based on the social, economic, and political conditions of the place where the individual or group is located. Vulnerable subjects have a higher risk, and lack some category, or categories, of resources to recover efficiently, or recover fully, when exposed to a hazard. With this in mind, the relationship between risk and vulnerability may be expressed as

$$\text{Risk} = \text{Hazard} * \text{Vulnerability} \qquad \text{Eq. 1-1}$$

That is to say that social vulnerability is not measured so much by the hazard itself, but rather by those pre-existing conditions, and risk is the measurement of a vulnerable population to a hazard.

Throughout the past two decades, the United States government has made attempts at improving the resiliency of communities against disasters. In 1994, FEMA declared the National Mitigation Strategy which provided incentives for seismic mitigation. In 1997, Project Impact was initiated which declared a community to be disaster resistant if it met specific requirements and followed certain protocols, including the implementation of specific hazard risk reduction actions. In 2013, the city of San Francisco, California passed a local ordinance mandating the retrofit of at-risk soft-story woodframe buildings, and more recently, the city of Los Angeles is working toward a similar retrofit program for soft-story woodframe (and potentially older non-ductile concrete) buildings. Globally, there have been many efforts as well. A few of the

research efforts which have shaped how community disaster resilience is viewed today are presented below, but this review is not intended to be exhaustive.

In 2003, Bruneau et al. presented a quantitative framework to assess and enhance the seismic resilience of communities. The authors describe resiliency as consisting of four dimensions: technical, organizational, social, and economic. Each of the four dimensions, in its own way, must execute the four properties of resiliency: robustness, redundancy, resourcefulness, and rapidity, as they apply to physical and social systems. These four dimensions may be thought of as performance objectives for either the ends or the means to resiliency. Detailed examples of each dimension's performance measures are provided in terms of the four properties. Figure 1-1 provides a conceptual definition of measuring seismic resilience, with a community's functional capacity on the ordinate and time on the abscissa, where time could be in units of days, weeks, or even years. Referring to Figure 1-1, during the pre-event stage, a normal level of operation exists for a given community. The community's functional capacity may actually be improving due to pre-event planning. When an earthquake or other acute disturbance occurs, a sudden drop in the functional capacity is immediately realized potentially due to power outages, lifeline losses, infrastructure failures, etc. First responders follow the drop, and then the gradual process of recovery takes place until a new normal level of functional capacity is met. This new level could occur at the pre-event level of operation, or a new level of operation may be achieved with the potential to be better (or worse, but acceptable to the community) than the original level. Considering the conceptual notion in Figure 1-1, resiliency can be defined as minimized time to recovery.

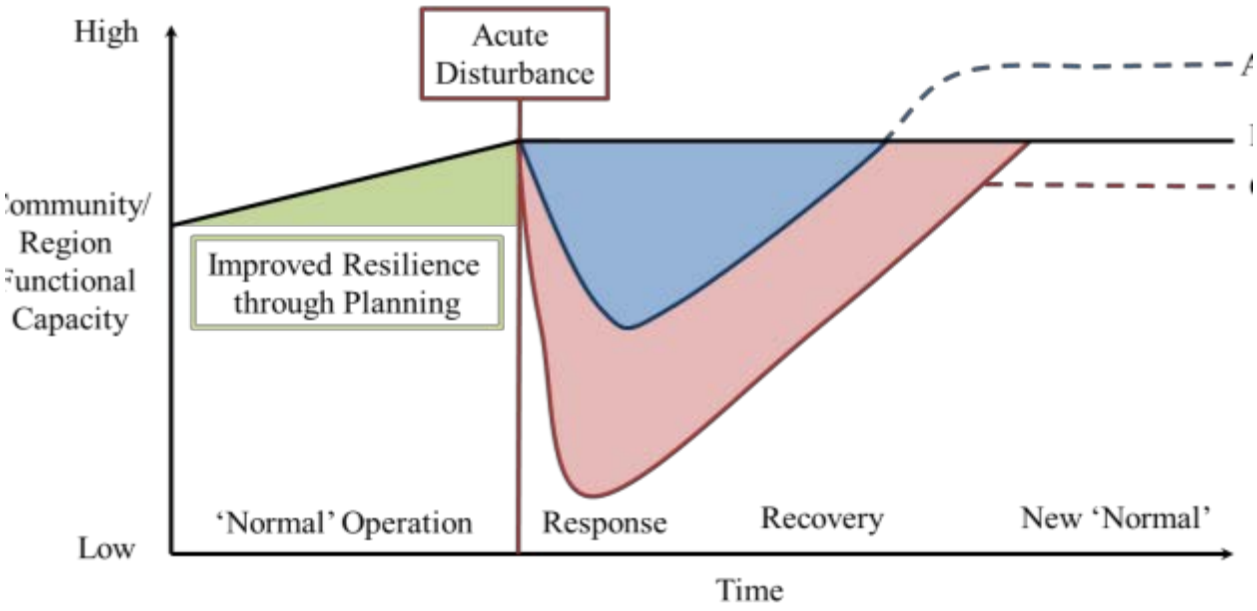

Figure 1-1: Concept of Resiliency

Some researchers have attempted to develop metrics for measuring and comparing community disaster resilience. For example, a disaster resilience of place (DROP) model was developed by Cutter et al. (2008) to provide a standard metric for measurement and comparison of a community's disaster resilience. The research was conducted following the U.S. federal agency's Subcommittee on Disaster Reduction (2005) grand challenges request for consistent factors and metrics to assess a community's resilience in order to provide assistance with vulnerability reduction. The DROP model provides a conceptual relationship between vulnerability and resiliency. The model suggests that there is an overlap between vulnerability and resiliency, providing an explanation of how pre-event characteristics of a place interact with an event. The community or region either possesses the appropriate amount of coping responses, or it does not, in which case a disaster occurs. Following recovery, there is a learning stage which provides preparation for the next disaster. The model is useful in a conceptual sense, but does not offer any type of measurement, solution or progression in resiliency.

Other groups of researchers, practitioners and planners have identified resiliency goals for implementation. For example, the San Francisco Planning and Urban Research Association (SPUR) [McAllister (2013)] identified goals for resilience defined in the context of disaster planning, and identified three phases of response: rescue, recovery, and rebuilding. The second phase focused on restoring neighborhoods and reestablishing the workforce (30-60 days), which identified 95% of residences with the ability to shelter-in-place as a resilience goal. The third phase consisted of the repair and reconstruction of the affected area (years). With respect to the present work, if in the pre-event stage, the community possesses a resilient built environment, i.e. robustness, then the time associated with phases two and three can be significantly reduced.

Additionally, NIST's Technical Note 1795 [McAllister (2013)] thoroughly addresses the role of the built environment in community resilience and presents major findings from two workshops for the Resilience Roundtable on Standards for Disaster Resilience for Buildings and Physical Infrastructure System which were sponsored by NIST, DHS, and ANSI-HSSP. Short term and long term activities in community resilience planning were identified. These included terminology for resilience objectives, developing risk-based performance goals, developing resilience metrics and tools, as well as, developing guidelines for standards to incorporate these metrics into codes. It was emphasized that in order for the desired community disaster resilience levels to be achieved, performance goals beyond the ones in current building codes would need to be established. Although acknowledged as driving the requirements for the performance of the built environment, other aspects of community disaster resiliency such as social issues related to human health, safety, and general welfare were not addressed.

1.2 Motivation

Severe earthquakes are low probability-high consequence events. In fact, in the past decade over 400,000 deaths were caused by just four out of hundreds of earthquakes occurring worldwide [Spence et al. (2011)]. The three most recent large earthquakes occurring in the United States were the 1971 San Fernando earthquake, the 1989 Loma Prieta earthquake, and the 1994 Northridge earthquake. These earthquakes were each devastating with respect to loss of life, casualties, building damage, economic loss, and loss in quality of life. In the latter two earthquakes, damage to woodframe structures was extensive resulting in more than $16.7 billion in losses in the Northridge earthquake alone [CUREE (2001)]. Considering that 90% of all residential buildings in the United States are of light-frame wood construction [Ellingwood et al. (2008)], improving the seismic resilience of the woodframe building stock would significantly improve resiliency at the community and/or regional level for regions in the United States.

Due to the devastating effects of earthquakes, loss estimation models have been a research topic of interest with the intention of predicting and therefore preventing loss while improving immediate recovery efforts. Many good earthquake loss estimation models are available in the literature at the single-building level and at the regional level. Models, such as Hazus [DHS (2003)], employ generic fragility functions based largely on expert opinion, which produces the end result of a generalized solution. What the literature lacks is an approach which employs a combination of analytical and empirical techniques with the efficiency associated with regional methods and the level of detail associated with building-specific methods.

May (2006) discussed the lack of adoption of performance-based seismic design (PBSD) procedures in engineering firms, and stated that it would be necessary for changes in building code provisions to fuel the widespread adoption. This is not an easy task however, because, as

May discusses, developing such guidelines is "fundamentally a value judgment that presumably requires some form of collective decision making" which may be aided by knowledge of the relevant seismic risk and cost-benefit relationships. May concluded that future guidelines should incorporate "what is desirable from the public point-of-view, and what is empirically achievable." Therefore, methodologies to be included in future PBSD guidelines should provide a range of solution options with tradeoffs for each of the performance objectives.

Additionally, thus far, the resiliency frameworks, hazard and vulnerability indices, and loss estimation models mention the importance of social vulnerability, however the explicit incorporation and/or quantification is generally neglected. The exception is in Hazus and MAEViz which consider social losses and use demographic information for determining shelter needs. Additionally, MAEViz computes a social vulnerability index to identify the specific area(s) of a region which are most vulnerable so that first-responder recovery efforts may be better directed. Neither Hazus or MAEViz, or other loss models, have directly incorporated the social vulnerability to determine the loss in quality of life for the affected population. Although a significant amount of uncertainty is associated with quantifying such subjective measures as post-traumatic stress disorder (PTSD) and loss in quality of life, there is a need to move beyond strictly qualitative measures. The available loss estimation models, community disaster resiliency and decision-making frameworks similarly lack this crucial characteristic of including social variables in their metrics.

The author has identified a major gap in the research which is to address community disaster resiliency by providing decision makers with a set of optimal retrofit plans for their community's built environment based on a regional loss estimation model that estimates loss by considering both social vulnerability and building performance. The optimal community retrofit

plans were based on performance objectives including the initial cost, associated economic loss, the impact on the mental health of society, the number of injuries and fatalities, and the time to recovery. This allows decision makers to develop comparisons between multiple resilience levels with the associated risk-based performance criteria.

1.3 Literature Review

A literature review is provided in this section. The initiation and transformation of performance-based seismic design (PBSD) is first discussed, then followed by a discussion on the state of the art in loss estimation models. Next, vulnerability, risk, and resiliency studies and their major findings and contributions to the field, such as the SoVI, are presented. Lastly, the role of mental health in recovery is discussed.

1.3.1 Performance-Based Seismic Design

Following the devastating earthquakes which occurred in the United States over the past several decades, important lessons were learned, and noteworthy changes were made to the existing building codes and seismic provisions of the time, as well as disaster preparedness planning, emergency protocols, and social vulnerability perceptions. Henceforth, a shift in the design paradigm emerged based on owner and stake-holder articulated performance expectations conditioned on pre-defined limit states. This new design methodology became known as performance-based design (PBD), or more pointedly with respect to this dissertation, performance-based seismic design (PBSD). Design procedures falling under the large umbrella of PBSD are often displacement-, or drift-based, rather than ultimate strength-based. A well-known procedure for PBSD of woodframe structures is the direct displacement design (DDD) procedure [Pang and Rosowsky (2010)], and the simplified direct displacement design (SDDD) procedure [Pang et al. (2010)].

Even more recently, PBSD has shifted away from the limit states "Immediate Occupancy", "Life Safety", "Collapse Prevention", etc., due to the realization that these can be difficult for owners and stakeholders to relate to and understand. A second generation of PBSD begins to emerge in which the limit states include "Number of Casualties", "Total Economic Loss", and "Recovery Time" [FEMA (2012b)].

FEMA 283 (1996), FEMA 349 (2000), and FEMA 445 (2006) were created as an initiation of the second generation of PBSD. The Pacific Earthquake Engineering Research (PEER) Center formulated the first framework which quantified the metrics mentioned above, and is being implemented in the ATC-58 project. The framework is probabilistic and addresses uncertainties in the performance objectives with probability distributions. Damage and economic loss are estimated using the results from seismic hazard analysis and response simulation. The framework is divided into four stages, where the results of each stage serves as input to the next stage. Stage 1 generates the probabilistic seismic hazard and intensity of the site, stage 2 determines the engineering demand parameters (EDP) (e.g., inter-story drift) and collapse capacity of the structure under consideration, stage 3 correlates the EDPs with damage measures (DM) using fragility functions, and stage 4 provides decision variables (e.g., economic losses) based on repair and replacement costs, which can be used by stakeholders to aid in decision making [Porter (2003)].

1.3.2 Loss Estimation Models

A significant amount of research has been conducted on loss estimation models in an effort to predict the direct and indirect losses caused at a static point in time due to a specific seismic intensity. There are many good earthquake loss estimation models available. Several informative and extensive reviews have been published on hazard loss estimation models.

Specifically, as part of the World Bank's disaster risk management (DRM), a study on 31 open source or open access hazard loss estimation softwares was published [GFDRR (2014)]. Eight models were covered for seismic hazards, including Hazus and MAEViz. The study provided details on the outputs of each software with the advantages and disadvantages.

Perhaps the most widely used loss estimation model in the United States is Hazus. In 1997, the Federal Emergency Management Agency (FEMA) released their natural hazard loss estimation software package Hazus. Hazus is applicable to earthquakes, floods, and hurricanes. The most recent version of Hazus uses Geographic Information Systems (GIS) technology to estimate physical, economic, and social impacts of disasters. This allows users to overlap maps and compare different scenarios. It applies Porter's [Porter (2001)] assembly based vulnerability (ABV) approach, which sums assembly level component losses to compute a structure's loss. The capacity spectrum method is employed for structural earthquake response. Hazus was intended to be used in macroscopic loss estimation, and was based on the estimated fragility of three types of building elements (structural drift-sensitive, nonstructural drift-sensitive, and nonstructural acceleration-sensitive). Hazus was largely based on expert opinion, which although may be the state-of-the-art, is subjective and full of uncertainty. However, this does allow the model to provide information, albeit subjective, for impacts on service outages for lifelines, estimates on fire ignitions and fire spread, potential for serious hazardous materials release, and indirect economic loss effects. Hazus estimations are based around GIS software which is integrated with detailed databases of the building stock and demography of the United States, and therefore the Hazus methodology is not easily extended outside of the U.S. The Hazus model uses the demographic information to provide estimates on social losses such as the number of casualties (injuries and fatalities) and the number of persons needing temporary

shelter. To compute the shelter needs, weights are assigned to five income categories, five ethnic categories, and three age categories, and applied to the shelter needs estimate based on building damage. Additionally, Hazus has been noted to consistently provide an overestimation of losses for small earthquakes (<M6) [CGS (2009)].

The Mid-America Earthquake (MAE) Center and the National Center for Supercomputing Applications (NCSA) developed a seismic risk assessment software, MAEViz, in 2008. MAEViz is based on Hazus with expansions in several categories including the damage states and social losses. Loss estimates are provided for business content loss, business interruption loss, business inventory loss, household and population dislocation, shelter requirements, and short term shelter needs. MAEViz uniquely computes the fiscal impact following an earthquake, and the social vulnerability of sub-areas within the affected region by scoring each from 1-10 based on the demographic information of the neighborhood areas. The software uses a modified approach from Hazus to compute shelter needs and population dislocation.

More recently and within the ATC-58 Project [FEMA (2012b)], the PEER methodology was developed into a loss estimation tool for its execution: the Performance Assessment and Calculation Tool (PACT) software. PACT provides a way to keep track of all of the building inventory details, and to perform the intensive calculations for probabilistic computations and accumulation of losses. Inputs include all of the building system and component information. The user may select which component fragilities to use out of the database of component fragilities. Monte Carlo simulation is performed to account for the variability of the building performance for a specific seismic intensity. Results from the simulation and structural analysis

are used to determine the three performance objectives (number of deaths, repair and replacement costs, and downtime). The results are presented in a user-friendly and logical format for easy realization of losses.

Ramirez and Miranda (2009) presented a building-specific loss estimation method for a simplified approach of performance-based earthquake engineering. The study considered the PEER methodology and noted that the building-specific loss estimation was extremely detailed by requiring a full inventory of the building being evaluated and computationally-intensive by requiring the integration of many random variables. The authors stated that improvement could be made in an effort toward simplification, and that simplification of the procedure may be the key to the successful adoption of performance-based design. Some of the major contributions of their work included the development of the simplified methodology which took a more realistic and practical approach at computing direct loss due to building damage. The approach summed the losses by repair needed per sub-contractor and by building story, rather than by existing methods of computing losses at the component level. To estimate the mean economic loss, the second step in the PEER methodology was skipped and the engineering demand parameters (EDP) were used to compute the mean economic loss by consolidating fragility functions and repair costs. Generic fragility functions were employed where existing ones were not available, and lastly the loss estimation considered, for the first time, buildings which did not collapse, but resulted in such excessive drift such that demolition was required. There were other outcomes of their research; however those are not mentioned here. The story-based loss estimation methodology developed distributions of total cost amongst the building stories. The distribution is based on the fact that the bottom story often has a different layout from above stories consisting of a main entrance and lobby, as well as different façades and finishes, and therefore

has a different associated cost than a typical story which is consumed by many office units. This again has a different associated cost than the top story which typically hosts the building's mechanical equipment. Using data from RS Means conjunctively with engineering judgment, story cost distributions were developed and applied in the framework. Economic loss was computed by including the expected value of the loss at DBE, expected annual losses, and the present value for life-cycle costs. The issue with using generic fragility functions, as in their study, is that the basis is largely dependent on expert opinion which can have substantial variation. However, these types of generic fragility functions provide good relative insight into this complex problem, and as more data becomes available the uncertainties can be reduced.

In 2007, Pei and van de Lindt developed a novel long-term loss estimation framework at the single building level for progression of and incorporation into performance based seismic design (PBSD). The framework considered a response-damage-loss relationship and employed damage fragility systems to quantitatively model the uncertainty associated with that relationship. This study was the first time that economic loss was considered in PBSD of woodframe structures. The framework incorporated the assembly-based vulnerability (ABV) procedure [Porter (2001)]. Bayesian techniques were used for modeling subjective uncertainty and objective randomness. The program SAPWood was used for modeling and analyzing the structure using nonlinear time history analysis using a suite of ground motion records. Response parameters (i.e. EDPs) output and were used to generate cost-based correlation of the response parameters with damage fragilities. Summing the costs for all damageable components, a single earthquake loss sample was obtained. The process was repeated for multiple seismic intensities and the results were combined into vulnerability functions to be used in the long-term loss model. For the damage fragilities, four damage levels were defined. The probability of a

structure exposed to an earthquake falling into one of the four damage levels was accounted for by conducting Monte-Carlo simulation using the response parameters to obtain damage level information. The variables that were explicitly modeled, along with their associated uncertainties, included construction quality, building materials, repair costs, future earthquake intensity, earthquake ground motion, and number of earthquake events in the estimation period. Shearwall, drywall, door, and window responses were explicitly modeled, whereas contents were aggregated into a single variable with an associated mean and standard deviation for damage level and repair costing, i.e. loss estimation. Case studies were presented for two residential woodframe houses, and logical results were achieved which corresponded well with empirical data from the 1994 Northridge earthquake. Although the authors conducted specific case studies on woodframe buildings, the methodology is extendable to other structure types.

The loss estimation model presented in Pei and van de Lindt (2007) was extended, applied, and used to define performance objectives for woodframe buildings in terms of economic loss in Black et al. (2010). The study presented in Black et al. (2010) offers the first detailed and comprehensive implementation of the PEER ABV approach to woodframe buildings. The first-generation PBSD performance objectives of Immediate Occupancy, Life Safety, and Collapse Prevention were redefined in terms of direct economic loss. The study considered woodframe building floor plans and incorporated a building variant factor to account for the many potential variations of woodframe buildings. The direct economic loss probability distribution presented did not include loss associated with downtime or casualties. The authors did explicitly model six variations of partition and shearwall assemblies using the ABV approach. The loss analysis module used an EDP output from the nonlinear time history analysis (NLTHA), correlated this output with pre-determined damage states based on fragility functions,

and then estimated economic loss based on the damage state and performance group. Output from the model included loss as a percentage of building cost varying with earthquake intensity. Uncertainty, such as ground shaking intensity and corresponding building loss, was addressed explicitly by four potential refined performance objectives.

The Pei and van de Lindt (2007) loss estimation model was again extended, this time to a regional sense, and employed in Han et al. (2013). The Han et al. (2013) study contributed a hazard module to more accurately represent the regional hazard while eliminating some uncertainty, and explicitly accounting for the remaining uncertainty. The study employed the Pei and van de Lindt (2007) loss model to woodframe buildings, and presented a new building variant selection method for identifying building designs specific to stated performance objectives. The authors defined a "performance policy", as a set of one or more performance objectives to all be satisfied in design, and concluded that performance policies at the regional scale must consider limits of what is reasonably achievable.

In 2004, Dodo et al. presented three optimization methods for the selection of regional earthquake mitigation strategies. The three optimization methods consisted of two linear programs and one stochastic program which were intended to be integrated into loss estimation models, such as Hazus, for a complete loss estimation analysis. The authors identified many challenges associated with community decision making for disaster mitigation, and demonstrated that pre-earthquake mitigation investment was less expensive than post-earthquake recovery spending, while making note on the preservation of life achieved by the former case. The optimization methods used simplified measures for design levels (i.e., built to low, moderate or high seismic code), and non-descriptive damage states (e.g., no damage, slight damage, moderate damage) as potential outcomes for buildings following a seismic event. Outcomes provided how

to distribute mitigation amongst buildings based on construction type (e.g., wood, steel moment frame, steel braced frame, concrete shear walls, etc.) and occupancy type (e.g., residential, commercial, etc.). The results were generalized to the simplified building stock and therefore did not capture the variability that exists in the actual building stock which would directly affect performance after an earthquake.

There are many other loss estimation models available in the literature today. The models presented above are similar in the fact that the loss estimations were point estimates in time and did not take into account structural aging or damage to structures caused by previous earthquakes. However, resiliency and vulnerability are time varying processes. To account for these time variant processes, researchers have proposed numerous approaches. Van de Lindt and Niedzwecki (2000) introduced a performance-based approach to estimate the time variant reliability of structures exposed to earthquakes. Davidson et al. (2003) developed a quantitative model to forecast changes in hurricane vulnerability for the woodframe building stock of a specific area using a Markov-based model. The model accounted for changes in building vulnerability due to changes in building code content, changes due to technological innovations, structural aging, and building upgrades. As time intervals progressed in the model, only the applicable vulnerability changes would be applied to previously existing buildings versus newly constructed buildings. Although developed for hurricane vulnerability, the model could be extended to seismic vulnerability. Rojas et al. (2008) developed a genetic algorithm for optimal design of steel frames by minimizing the weight of the steel frame and simultaneously minimizing economic annual loss using Hazus for damage assessment. To account for time, the probability of all potential earthquakes that may occur during a single year and the mean

probability of occurrence of each were combined with the probable economic loss due to each possible earthquake to determine the annual economic loss for the structure.

Additionally, there are many rapid earthquake loss assessment models (e.g., PAGER for the United States). Erdik et al. (2011) provided a review of the previous decade's worth of development of new approaches and applications for earthquake rapid response systems which oftentimes incorporate a quasi-real time earthquake loss assessment. These models provide data in the immediate aftermath of an earthquake at the location of the event to aid in the allocation of immediate recovery operations until more detailed information is known. Details of such models will not be discussed here; however it was felt that the literature review would be incomplete without the acknowledgment of their existence.

1.3.3 Social Vulnerability

There are three recognized categories of disasters: natural, technological, and mass violence. Natural disasters, including earthquakes, hurricanes, tornados, tsunamis, floods, etc., are forces caused by nature. Although it is thought by some that society is not merely a victim of natural disasters, but a contributor or modifier when considering global warming and its effects. Technological disasters include chemical or hazardous materials emergencies, dam failures, nuclear events, power outages, cyber security breaches, explosions, etc. These are events caused by the malfunction of technological entities oftentimes with human error at the source or industrial disasters which can be due to accident, negligence or incompetence. Lastly, mass violence disasters include terrorist attacks during a time of peace, mass shootings, bombings, etc. Many researchers have concluded that mass violence disasters are the most traumatic causing the most adverse mental health effects on the victimized population because they are human-induced and possess the characteristic of intention. Technological and/or industrial disasters are

considered to cause more adverse consequences than natural disasters, because they are also caused by humans out of callousness and/or negligence [Norris et al. (2002a)]. These three categories of disasters are very different by their nature, but share the ability to adversely affect large groups of people simultaneously. The literature review that follows covers studies that have identified predictors of poor mental health following natural disasters and studies that have attempted to quantify influential factors of, or develop metrics for quantifying, social vulnerability. This is followed by a discussion regarding the role of mental health in community disaster resiliency and the associated economic loss.

1.3.3.1 Quantitative Measures of Vulnerability

Disastrous events, such as earthquakes, can have very adverse effects on the mental health of the exposed population. Post-traumatic stress disorder (PTSD) has been shown to be, by far, the most common psychological problem for victimized people to develop, followed by depression [Norris et al. (2002b)]. It is also the most commonly assessed and observed psychological problem in post-disaster population studies [Norris et al. (2002b)]. Prevalence of PTSD following disasters ranges dramatically based on many external factors such as the category of the disaster (natural, technological, or mass violence), the size and location of the area affected by the disaster, the number of deaths and injuries, the number of building collapses, or mass property damage, etc. PTSD prevalence following earthquake disasters has been shown in the literature to range from 13% - 73% of the exposed population. This wide discrepancy in prevalence of PTSD is due to sample size and sample content, PTSD measurement scale, distance from the epicenter, as well as the factors just mentioned. There are also numerous factors that are more internal factors of vulnerability to PTSD for an individual, such as previous experience with an earthquake (or other applicable disaster), previous history of mental illness,

exposure to the dead and dying, fearing for one's life, major property damage, being female, being a single mother, being an ethnic or racial minority, having low socioeconomic status, among many others. It is important to identify groups of people that are more vulnerable to PTSD so that appropriate pre-event and post-event measures may be taken.

Norris et al. (2002a) and Norris et al. (2002b) presented a profound two-part review of empirical disaster studies published from 1981 to 2001, "60,000 Disaster Victims Speak". Analyzing surveys from 160 samples of disaster victims, the authors conducted regression analysis to identify common predictors for adverse mental health following a disaster. The intentions of the study were to "determine what is known about (1) the potential range, magnitude, and duration of a disaster's effects on the mental health of the stricken community, and (2) the experiential, demographic, and psychosocial factors that influence who within that community is most likely to be adversely affected." Although the study was conducted for disasters in all three categories, it is assumed to be relevant here, for the single category of natural disasters, for general understanding. The identified vulnerable persons started with women, which were shown to almost always be twice as susceptible to PTSD as men. This statistic held true for female children too. Mexican women were shown to be even more vulnerable, but African American women were shown to be less vulnerable, which indicated a cultural difference in the severity of gender as a predictor. Children were shown to be more susceptible than adults to falling into the range of severe impairment. Adult age was shown to be quite variable but also associated with culture. Minority populations such as Hispanics and African Americans were shown to be at a higher risk in almost all surveys considered. Socioeconomic status, which included income, education, literacy and occupational prestige, was shown to be a high predictor, with persons of low socioeconomic status being more vulnerable.

Lastly, marital status and having children was examined. Prevalence of PTSD with respect to marital status and being a parent differed by both gender and culture. A relationship was found indicating that as the number of stressors and vulnerable characteristics increased so did the number and severity of the participant's PTSD symptoms. Additionally, the authors found that earthquake disasters in the United States showed lower prevalence of PTSD as compared to earthquakes which occurred in other developed nations and developing nations. Interestingly, the developing countries showed lower prevalence of PTSD than the developed nations outside of the U.S. Lastly, the authors found that longitudinal data suggested that symptoms of PTSD peak during the first year, and levels of immediate symptoms were good predictors for the levels of symptoms several months down the road.

Another large body of work was conducted on the development and application of the Social Vulnerability Index (SoVI), developed by Cutter et al. (2003). Socioeconomic and demographic information collected at the county-level from 1990 data was input as 42 variables. The factor-analytic approach identified eleven composite factors that contributed 76% of the variance in social vulnerability status. These eleven factors were listed in order of "percent variation explained" (i.e. order of influence): personal wealth, age, density of the built environment, single-sector economic dependence, housing stock and tenancy, being of African American race, being of Hispanic ethnicity, being of Native American ethnicity, being of Asian race, occupation, and infrastructure dependence. The SoVI was developed using these 11 variables. To compute the SoVI, county-level information was uploaded, and the summation of variable scores represents the index value. The regression analysis, which identified the 11 most influential variables, identified personal wealth to be the most significant factor accounting for 12.4% of the variation, specifically per capita income. This result is logical and can be explained

by the fact that wealthier individuals and communities typically have a larger quantity of financial, educational, and social resources to aid in recovery. It also goes along well with the findings in Norris et al. (2002).

Cutter and Finch (2008) conducted a study on the temporal changes in social vulnerability to natural hazards using Cutter et al.'s Social Vulnerability Index (SoVI). Five periods in time were analyzed: 1960, 1970, 1980, 1990, and 2000. The authors provided which demographic factors played the most significant role in each of the analyses, and for each of the five decades, the SoVI consistently indicated that socioeconomic status, level of development of the built environment, age, gender, and race/ethnicity were the most influential factors for all of the decades. Socioeconomic status was also consistently shown to be the most influential factor. Albeit, the percent of the variance explained by socioeconomic status varied for each decade (from 13.3% to 18.4%), it was still consistently the controlling factor. Over five decades, the four of the top five contributing demographic factors to social vulnerability were consistent and only varied by a few percent in each case. A nation-wide case study was conducted using county data of the 48 conterminous United States via GeoData software for the spatial statistics calculations. High social vulnerability was defined as being two standard deviations above the mean, and low social vulnerability was determined as being two standard deviations below the mean. The study showed that New York County, NY was the most vulnerable county for all decades due to its urban development, race and ethnicity demographic, and low socioeconomic status of a large portion of the population. Using the SoVI in this manner, comparing decades for the same place, can help to understand if and how the social vulnerability of a place changes. The study indicated that counties with increasing social vulnerability occurred due to either extreme depopulation (Great Plains) or population growth (Orange County, CA). This

knowledge can lead to a better understanding of vulnerability, and help with the allocation of funds at the local and federal level by knowing which places need support the most.

Schmidtlein et al. (2008) conducted a study on the sensitivity of the SoVI to a larger subset of variables, to changes in the geographic scale of the analyzed region, and variations in its construction. An analysis was conducted comparing the index values and most influential factors when using 33 and 26 variables. The results were fairly consistent showing wealth, race and poverty, age, Hispanic immigrants, and gender all being in the list of 8 and 6, respectively, most influential factors. Analyses were also conducted using the original index at the county level, intermediate level, and census tract level. The results for all three geographic levels varied, but were similar. Of the top seven contributing factors for social vulnerability, as dictated by the SoVI, race and poverty, Hispanic immigrants, age, and a form of gender and wealth appeared for all three analyses, albeit in a slightly different order with slightly different percentages. The final analysis investigated the robustness of the index based on constructing it in different ways. Varying its construction showed large differences in the resulting values, consistent with the change in construction, a very logical outcome. Based on the study, it may be concluded that there is some discrepancy in the results when changing the number of variables and geographic scale; however there is significant consistency in the results and therefore still reliable.

Prior to the SoVI, in 1997 the Earthquake Disaster Risk Index (EDRI) was introduced [Davidson (1997)]. The EDRI compares the disaster risk of different cities worldwide. The index considered hazard, exposure, vulnerability, external context (i.e. the city's prominence on the world stage), and emergency response and recovery capability as the five main factors which contribute to earthquake disaster risk. The EDRI identifies seismically vulnerable cities, and

their sources of vulnerability, however similar to the SoVI, it does not offer a solution. The EDRI acknowledges geological, engineering, economic, social, political, and cultural factors as contributing to earthquake disaster risk; however it does not explicitly incorporate social or cultural factors.

Then in 2003, Rashed and Weeks conducted a study employing GIS to assess urban vulnerability to earthquake hazards through a spatial multicriteria analysis using fuzzy logic. The authors explain that the spatial variability of vulnerability is possibly due to a causal linkage between socioeconomic and demographic characteristics, as well as culture and how hazards are viewed by the culture. Vulnerability was assessed through a combination of factors associated with the physical conditions of the geography and the social conditions of the population. The evaluation criteria was organized into three categories: (1) criteria for social risks (percentage of households that might seek temporary shelter and total economic cost); (2) criteria for physical induced risk (area of land that could be exposed to fire and amount of debris); and (3) criteria for systemic vulnerability (percentage of loss of functionality for hospitals, fire and police services, power utilities, highways, and bridges). The criteria were mapped using fuzzy logic for the analysis. The analysis was run for various earthquake scenarios which defuzzified (i.e. un-mapped) the criteria to identify vulnerability "hot spots". The methodology was intended to be used in conjunction with a loss estimation model, such as Hazus, which was employed during the case study conducted on Los Angeles County, California.

1.3.3.2 The Role of Mental Health

Poor mental health, such as depression or post-traumatic stress disorder (PTSD), can be the direct effect of a disaster. Mental health plays a critical role in the functioning and progression of society. Following a disaster, the mental health of the affected community or

region is central to the recovery process. When a person has poor mental health, the direct effect on the economy is through the practice of absenteesim and presenteeism. Absenteesim is the habitual practice of missing work, or willful absence, without good reason. Presenteeism is attending work while sick, or attending work when only capable of sub-par performance. This effect on the economy is in addition to the effect on the individual's loss due to the financial costs of seeking medical help. The following studies are in an effort to quantify the economic cost to society in which a portion of its community is stricken with PTSD.

Kessler and Frank (1997) conducted a study to examine the relationships between DSM-III-R (Diagnostic and Statistical Manual of Mental Disorders, third edition, revised) psychiatric disorders and work impairment in major occupational groups in the U.S. The data was collected via face-to-face in-home interviews with 8098 respondents. The respondents ranged in age from 15-54 years old. The results indicated substantial variation across occupations with respect to the prevalence of DSM-III-R psychiatric disorders, but did not vary substantially across occupations with respect to work loss and work cut-back days. Considering those with DSM-III-R psychiatric disorders, an average of 6 work loss days per month per 100 workers and 31 cut-back days per month per 100 workers were identified. DSM-III-R psychiatric disorders include affective disorders such as depression and mania, anxiety disorders such as panic disorder and PTSD, and substance disorders such as dependence and abuse of alcohol or substances. The occupations considered in the study included four professional occupations, two managerial/administration occupations, three craftsmen occupations, three clerical and sales worker occupations, and four laborers and operative worker occupations. A bivariate linear regression analysis was conducted to show the relationships between 30-day DSM-III-R disorders and psychiatric work-impairment days. The results indicated that PTSD was one of the

most positively associated disorders with work loss and work cut-back days. The quantitative survey results explicitly showed the influence of education, salary, and occupational prestige on the susceptibility of various psychiatric disorders including depression and PTSD. The results also demonstrated that once a person has depression or PTSD, the response was similar and independent of education, salary, or occupational prestige, that is to say that the average number of work loss and work cut-back days does not change based on socioeconomic status.

A large study was conducted to determine how much illness costs in terms of impairment and disability by the World Health Organization (WHO) Global Burden of Disease (GBD). Kessler and Greenberg (2002) suggest that the results were severely underestimated and therefore the authors reviewed evidence on the economic burdens of anxiety and stress disorders by focusing the high societal costs as being influenced by eight specific factors. These factors included frequency of occurrence, prevalence, onset, adverse effects and comorbidity. The authors stated that patients with PTSD commonly "work at low-paying jobs because they are unable to cope with the stresses of higher paying jobs. This would be considered a cost of illness from the societal perspective, but not from the perspective of the employer." The authors identified that out of six anxiety disorders PTSD was associated with the highest number of work-cutback days (4.9 days per month). However, none of the six disorders were significantly associated with work-loss days indicating that quality of performance was most affected, rather than the amount of time spent at work.

Zahran et al. (2011) calculated the economic costs of poor mental health days added by exposure to Hurricanes Katrina and/or Rita. Particular focus was given to single mothers versus the general public. The analyses indicated that poor mental health days increased by approximately 19% and 72% for all persons and single mothers, respectively, when exposed to a

hurricane. Hurricane intensity was determined to be a predictor of more poor mental health days for both population groups. Considering a $228.17 per day economic contribution made by the average worker, single mothers were estimated to have "suffered over $130 million in productivity loss from added post-disaster stress and disability." The total loss due to poor mental health caused by hurricane exposure was estimated at $460.4 million. The authors conducted a negative binomial analysis to identify the predictors of poor mental health days, and identified single mothers, poor physical health, post-exposure period, exposed area, education, income, and social support to all be predictors, listed in the order of highest to lowest influence on all persons. This study showed how vulnerable groups, such as single mothers, are more susceptible to poor mental health, and how that directly affects the economy and the achievement of full recovery.

1.4 Objectives and Overview

Mitigation against disasters can be a difficult task when it comes to deciding where money is best allocated such that it protects the population and preserves the quality of life. This is especially true considering the pronounced diversity of some geographically adjacent communities, and therefore becomes an issue that is best addressed by local governments. The framework presented here applies retrofit techniques such as those explored in the NEES-Soft Project [Jennings et al. (2014a), Jennings et al. (2014b)], a project which explored various soft-story building retrofit techniques, by taking a multi-disciplinary approach to disaster mitigation caused by large earthquakes at the regional level. The work proposed here aims to answer three questions. (1) How can a local government best allocate funds to mitigate damage to woodframe structures caused by earthquakes? (2) How can the probability of fatality, probability of injury, and the probability of a person developing PTSD be decreased by retrofitting the existing

woodframe building stock of a community? (3) Can an earthquake resilient community be established without considering the socioeconomic characteristics of the region?

The problem decision makers have had in answering the first two questions lies with the conflicting objectives. Ideally, any mitigation plan seeks to minimize the initial cost and minimize the total economic loss, while maximizing the preservation of life and maximizing the quality of life for the population at hand. The problem researchers have had in answering the third question is due to the highly subjective nature of quantifying qualitative measures like how a person's age, ethnicity, gender, etc. influences their likeliness of developing PTSD.

This dissertation addresses community disaster resilience of the built environment considering community resilience planning and performance goals. Performance objectives include minimizing: initial cost, economic loss, the number of morbidities, and the time to recovery, where the time to recovery may be considered as a comparison for the loss in quality of life. This planning provides improvements to be made in the short term and long term. The performance goals were quantified for each building design option and summed for the building stock of the community considering the population demographics, and serve as the resilience metrics. The optimization is executed via genetic algorithm (GA). Iterations (i.e. generations) were run in an effort to obtain the full pareto-optimal set of solutions, however computation power was a limiting factor. Obtaining the pareto-optimal set allows for comparisons between planning methods, and allows the community decision maker(s) to examine multiple resilience levels with the associated risk-based performance criteria. The GA was re-run for multiple hazard intensities so that the results could be presented as fragilities. The pareto-optimal set of solutions and fragilities provided risk-based performance criteria for various resilience levels for use by the decision maker(s) of communities. Case studies are presented for Los Angeles

County, California using the 2010 U.S. census data, and two forecasted populations using the 2010 census data for Daly City California and East Los Angeles, California.

In the optimization of a community seismic mitigation plan, a single, known (i.e., convergent) solution cannot be identified due to the uncertainty in the decision maker. Preferences were not employed for the selection of a single optimal solution. Rather, 5 solutions were selected and analyzed more extensively. The final mitigation plan selection would be left to the decision maker. A single solution could be identified if the decision maker preferences were employed as weights on the four objectives.

The remainder of this dissertation presents the method, both analytically and numerically, providing several illustrative examples to demonstrate its application. Chapter 2 presents the performance objectives employed in the framework and their relevance to community disaster resilience. The four performance objectives are minimizing: the initial cost, the total economic loss, the number of morbidities, and the time to recovery. Chapter 3 provides the theoretical formulation for the combined engineering-social loss model, along with its limitations.

The numerical modeling of the engineering variables is presented in Chapter 4, starting with the designs, the numerical modeling, and the nonlinear analyses of the building archetypes. Chapter 5 continues the discussion on the engineering variables presenting the design and testing of a performance-based seismic retrofit of a soft-story woodframe building. The correlation between the damage states and visual damage obtained from full-scale experimental tests is presented in Chapter 5 as well. Chapter 6 presents a thorough literature review of the population studies used for the quantification of socioeconomic variables, followed by the modeling of the socioeconomic variables. In Chapter 7, a brief description of the genetic algorithm is presented in biological terms, and then it is presented in its application for this study.

Several illustrative examples of the framework are presented in Chapter 8. The illustrative examples were conducted on the three communities. The first community was Los Angeles County, California, the second and third communities were investigated as potential population forecasts for Los Angeles County, using the 2010 U.S. census data for Daly City, California and East Los Angeles. The analyses were conducted at six seismic hazard levels with and without the incorporation of the socioeconomic factors. Comparisons are discussed for the various applications. Finally in Chapter 9, the study conclusions and contributions are discussed, and followed by recommendations.

Chapter 2: Performance Objectives for Community Resiliency

Three research questions were posed in section 1.4 regarding government allocations of mitigation funds and the influence of social factors on community disaster resiliency. This work employs four performance objectives to answer those questions and to aid decision makers by providing comparisons between planning methods based on multiple resilience levels. The four performance objectives are set forth in the form of minimizations and include the initial cost, economic loss, number of morbidities, and the time to recovery. These four objectives are not mutually exclusive, but are interdependent. For example, the probability of PTSD (a category of morbidity to be discussed later in Chapter 5) is dependent on the time to recovery, which is dependent on the number of persons with PTSD. However, modeling interdependency was outside of the scope of this study, and therefore the objectives were treated for the dependence on one another, but not interdependence. For example, if the initial cost was spent on retrofitting existing structures and on building new structures to higher seismic resiliency, we expect to see a reduction in the number of morbidities and the economic loss (which includes the cost to repair building damage as well as the cost of each morbidity). Additionally, the time to recovery is dependent on the economic loss and the number of morbidities. The detailed conceptualization of each objective is discussed throughout this chapter.

2.1 Initial Cost

Ideally, every community would be designed to 100% resiliency for any event. What limits this in application is the required initial cost. Initial cost is an imperative objective as it usually governs any decision. The goals of decision makers are only realized to the extent of the budget which funds the community. Its presence here provides discrepancy between the other

three objectives requiring the algorithm to provide diverse solutions to then be presented to the decision makers. In this study, the initial cost was computed by summing the cost of retrofitting the required number of existing buildings in the community in order to minimize the other objectives. There were 37 archetypes used in this study; seven floor plans designed or retrofitted following five different seismic provisions or retrofit procedures, and then additionally two of the floor plans retrofitted by a sixth procedure. The detailed account of the 37 archetypes is provided in Chapter 4.

Following the 1994 Northridge earthquake, a study was conducted by CUREE which provided detailed sub-assembly cost estimations for four example archetypes including detailed new construction cost estimates [see CUREE Publication No. 29; Reitherman and Cobeen (2003), for details]. The archetypes used in that study serve as four of the thirty-seven archetypes in this study, with the floor plans representing four of seven total floor plans used in this study. In this study, the detailed CUREE new construction cost estimates were divided by the respective archetype square footage to provide a cost per square foot (cost/sf) value for the four archetypes. These four archetypes consist of a one-story single family dwelling (SFD), a two-story single family dwelling, a two-story multi-family townhome, and a three-story multi-family apartment building. Making the assumption that new construction costs are approximately the same for all one-story single-family dwellings of the same structural type (i.e. light woodframe construction), the computed value from the CUREE study was applied to all archetypes which were one-story single-family dwellings (7 in total), after adjusting for inflation. This same procedure was repeated for all similar archetypes, including the two-story single-family dwellings, the two-story multi-family townhomes, and the three-story multi-family apartment buildings. There is one additional archetype considered in this study, a four-story

office building. The new construction cost per square foot was obtained from Reed Construction (RSMeans) data [RSMeans Online (2014)]. The new construction costs obtained from the CUREE study were adjusted for inflation (from 2001 to 2014 dollars). Although the CUREE study was of excellent quality, and the RSMeans' values are assumed to be a reasonable representation of actual construction costs, there is still an associated uncertainty in cost values as these differ across contractors and across regions. Therefore cost values were represented by lognormal distributions with associated mean and standard deviation values. The mean values were the values provided in the CUREE study and on the RSMeans website. The standard deviation values were set as one-third of the mean values. The new construction cost values were used for estimating economic loss based on the cost of collapsed buildings being rebuilt. The new construction cost distributions were fit with a lognormal distribution. The lognormal distribution parameters are provided in Appendix A.

The retrofits employed in this study were not similar to the retrofits in the CUREE study with respect to performance goals, and therefore the CUREE retrofit cost estimations were not used in this study. Retrofit cost per square foot values were obtained and adjusted from two sources [Porter and Cobeen (2009), Samant et al. (2009)]. The study by Samant et al. (2009) provided retrofit costs per square foot for three retrofit schemes. The third retrofit scheme had the same performance objectives as the ASCE 7-05 procedure used in this study, and therefore the mean value ($9/sf) was used here for the archetypes retrofitted following the ASCE 7-05 methodology. The study by Porter and Cobeen (2009) provided the average building square footage for the buildings considered in their study, and the average retrofit cost per building for three retrofit schemes. The third retrofit scheme was designed to a similar level as the performance-based seismic retrofit to the Life Safety (PBSR-LS) limit state used in this study.

By dividing their third retrofit scheme's cost by the average building square footage, the mean value for the retrofit cost per square foot for the PBSR-LS archetypes was determined ($28/sf). The final retrofit cost per square foot is for the archetypes retrofitted by a PBSR to Immediate Occupancy (PBSR-IO) limit state. The mean value for these retrofits was adjusted from the PBSR-LS value using an amplification factor of 1.2 ($34/sf). The retrofit cost per square foot values were multiplied by each archetype's area (sf) which served as the mean retrofit cost. The standard deviation values were set as one-third of the mean value. The retrofit cost random variables were fit with lognormal distributions, where the lognormal distribution parameters are provided for each applicable archetype in Appendix A.

2.2 Economic Loss

Although the most important aspect of community disaster resilience is the preservation of life, the economic loss following earthquakes can be tremendous and have lasting effects on the exposed community which can in turn lessen the quality of life. The exact value of economic loss is subjective and would be virtually impossible to quantify in an exact manner, however monetary values for economic loss are published following all disaster events. These values range across publications depending on the extent of indirect costs considered in the calculation. The economic loss caused by the 1994 Northridge earthquake is most often reported as $49 billion. Similar to the way financial constraints were discussed in section 2.1 with the initial cost, decision makers put importance on the potential negative economic impact of a disaster on their community. Therefore, when considering community disaster resilience, the economic loss plays a very important role.

In this study, the economic loss includes direct and indirect costs. The direct costs considered in this study include the repair cost of buildings based on the amount of damage

caused to each building, any temporary relocation costs (i.e. shelter-out-of-place costs), contents damage, the medical bills and downtime associated with each injury severity level and for treating PTSD, and a monetary value for each lost life. The repair costs were based on a building's damage state. In this study, like the cost of new construction and retrofit, the repair costs were represented by random variables and fit with lognormal distributions. The CUREE study [Reitherman and Cobeen (2003)] which provided the new construction estimates used herein also provided detailed subassembly repair cost estimates based on the damage state of the building. The damage states used in that study were adopted in this study, and therefore the subassembly repair costs were directly incorporated into this study after adjusting for inflation. The number of subassembly units per archetype was determined for the computation of an archetype's total repair cost based on the damage states. This value served as the mean, and the standard deviation was computed as one-third of the mean. The repair cost distribution for each archetype for each damage state was fit with a lognormal distribution. The complete set of repair cost distribution parameters for the 37 archetypes and the five damage states are provided in Appendix A. Contents damage was computed as a percentage of the total repair cost value.

Once a building reaches the fourth damage state, shelter-out-of-place was modeled as a requirement. The daily costs for sheltering out-of-place were estimated using the same procedure as Hazus, which determined the relocation costs based on occupancy class, floor area, damage state, and whether the damaged structure was rented or owned. These values, although still uncertain, were employed as strict values and therefore were not fit with a probability distribution.

The costs due to injury increased with increasing injury severity. The costs were set as the values the U.S. government assigns to each injury severity level including fatality [FHWA

(1994)]. These values are comprehensive costs covering pain, lost quality or life, medical costs, legal costs, lost earnings, lost household production, etc. No uncertainty is included in the analysis of these values since they are the actual values that federal government agencies use in cost-benefit analysis and were assigned as deterministic for this study. The one-year treatment costs ($5,400) for a person with PTSD were determined from a study conducted by the Veteran's Health Administration (VHA) [CBO (2012)] and incorporated in the economic loss.

The indirect costs considered in this study included the downtime from work associated with each injury severity level and with PTSD. The downtime due to injury and fatality was accounted for in the direct cost value from the government. The downtime from work due to PTSD was modeled using work-loss days as well as work cut-back days caused by absenteeism and presenteeism, respectively. The shelter-out-of-place costs, injury costs, fatality costs, PTSD treatment costs, and losses due to downtime caused by PTSD were all set as strict values, and not represented by random variables with distributions.

This is clearly not the full story of what total economic loss involves, however it was felt to be an adequate representation for this study. The detailed analytical quantification of the economic loss considering direct and indirect loss is provided in Chapter 3.

2.3 Number of Morbidities

The most important objective in any structural design is the preservation of life. The tragically high number of morbidities which follow disasters has inspired research on safety for decades. Just in the past decade, nearly half a million lives have been lost worldwide due to earthquakes. This study puts great importance on the preservation of life by setting the reduction

in the total number of morbidities, where morbidities include the number of injured individuals, the number of fatalities, and the number of persons diagnosed with PTSD, as one of the four main objectives.

In order to incorporate the number of morbidities into this research, injury rates based on five different injury severity levels (e.g., minor, moderate, severe, critical, and fatal) had to be quantified. The combined injury severity rates and PTSD rate are discussed collectively as the morbidity rates throughout this work. The morbidity rates are influenced by engineering variables and socioeconomic variables. The morbidity rates are defined by the damage state, which is directly related to the building performance. The other variables are used as factors to modify the morbidity rates. Building performance and the age, quality, and density of the built environment are critical factors in morbidity rates. During an earthquake, most injuries and deaths occur to people inside buildings. In a dense built environment (i.e. urban setting), if buildings experience high responses to ground motions, then the morbidity rate of people outside of buildings will likely increase due to fallen building debris. Older buildings and buildings with lower construction quality will perform poorly relative to newer buildings and buildings with a high quality of construction in protecting building occupants. Newer buildings are also likely to have less debris fall.

To measure and quantify building performance, an engineering variable was employed, i.e. peak inter-story drift (ISD). Peak ISD has been shown to be well correlated to damage caused to woodframe structures [Filiatrault and Folz (2002)]. The full relationship employed here is as follows: building damage is the result of building response, which is measured by the peak inter-story drift, which is the result of building capacity, construction quality and earthquake intensity. If an earthquake occurred which caused severe damage to a building, one

can expect the number of casualties to be higher than the number of casualties resulting from a less damaged building. Morbidity rates, as a function of building performance, differ by building damage state (the categorized level of damage). That is, there is a single morbidity rate for each injury severity level and for each damage state, and there are five damage states considered in this study. For example, the percentage of building occupants which experienced an injury placing them in critical condition is greater when the building has collapsed compared to if the building had only experienced minimal drywall damage. In this study, inter-story drift was used to quantify the six morbidity rates for the five building damage states.

There is considerable uncertainty associated with morbidity rates caused by building response due to an inability to conduct experiments and difficulty in obtaining true counts from past earthquakes. Therefore, in this study, the morbidity rates were represented as random variables. The mean values of the morbidity rates for each damage state are the values used in Hazus [DHS (2003)], and the standard deviation was one-third of the mean value. The Hazus values were determined from the ATC-13 values and adjusted based on a study conducted after the 1994 Northridge earthquake which used hospital records and GIS mapping of the victims [DHS (2003)]. There were more injury severity levels considered in this study than in Hazus, however the damage states are the same. Therefore, linear interpolation was used on the Hazus injury severity rates to provide the complete set of injury severity rates for the damage states.

The rate of PTSD is newly considered by this study. The rate of PTSD similarly changes with respect to the damage state. PTSD rates based on damage states were modeled after the Hazus severe injury rates. The details of this quantification are discussed later in Chapter 6. The rate of PTSD is dependent on the number of building collapses, the number of injured persons, the number of fatalities, and the recovery time. In this study, the rate of PTSD was related to

these other factors through the damage state. The morbidity rates caused by building response were represented by lognormal distributions. The full set of lognormal distribution parameters for the morbidity rates based on damage states used in this study are provided in Appendix A.

In addition to engineering factors, socioeconomic factors also influence the morbidity rates. For example, it has been shown that individuals aged approximately 60 years and older are more susceptible to death or injury during an earthquake [Mahue-Giangreco et al. (2001)]. Surveying the literature, one will find that many socioeconomic factors have been linked with injury, fatality, and PTSD diagnosis. These linkages are found in population surveys conducted after disasters on the exposed population. A detailed account of the meta-data analysis conducted on the population surveys used in this study is provided later in Chapter 6. The socioeconomic variables used to quantify the morbidity rates in this study include: age, gender, ethnicity, family structure, and socioeconomic status. Many socioeconomic variables play a role in the probability of injury, fatality, and PTSD; however these variables were chosen here due to their higher accessibility in population surveys. In this study, the socioeconomic variables were only used as an influence on the overall morbidity rates. The socioeconomic variables were not used in any specific characterization of injury severity levels or damage states. The engineering variable, peak inter-story drift, was strictly used for differing between injury severity levels and damages states. The detailed analytical quantification of the resiliency objectives is provided in Chapter 3.

For quantifying the probability of injury and fatality, three socioeconomic variables were modeled, age, gender, and socioeconomic status. These three variables were selected due to their accessibility of their influence on injury and fatality in the population studies. It has been shown that age influences the injury and fatality rates due to the physical limitations of elderly

individuals and their general inability to respond quickly. In this study, the number of persons aged 65 years and older within the community was modeled such that it resulted in an increase in the overall injury and fatality rates. The number of persons aged 64 years and younger were grouped together and determined to have no age-related effect on the overall injury and fatality rates. This age grouping was a simplification, but felt to be reasonable and well-representative of the actual influence of age on the injury and fatality rates.

The literature has demonstrated that during a typical moderate to large intensity earthquake, more females than males are injured and killed [Peek-Asa et al. (1998)]. Therefore, in this study, females of all ethnicities were grouped together to have a gender-specific impact on the injury and fatality rates in the marginalized community. Socioeconomic status was the third and final socioeconomic variable used to quantify the injury and fatality rates. Here, socioeconomic status included annual income and educational attainment. This makes the assumption, based on the literature, that the more educated an individual is, the more likely they will take necessary precautions in order to insure their safety during an earthquake, and be able to respond appropriately. Additionally, the wealthier an individual is, the more likely they will have the means to actually take these necessary precautions, such as install seismic restraints on non-structural components and contents in the building, and have earthquake insurance. Wealthy individuals are also, in general, more likely to live and work in buildings of higher construction quality and designed using seismic provisions. There are three levels of socioeconomic status considered in this study, low, moderate and high, which were quantified relative to the community being analyzed, and not relative to the country as a whole.

In addition to the preservation of life and injury prevention, maintaining the quality of life and the mental health of the community is also very important. To quantify the mental health

of the community the rate of PTSD, or the probability of PTSD, was computed. Chapter 1 discussed the many variables which have been shown to increase a person's risk for developing PTSD. Five socioeconomic variables were used in this study to quantify the number of individuals developing PTSD: age, gender, ethnicity and race, family structure and socioeconomic status. Older individuals have been shown to be more resilient to PTSD, mostly due to previous life experiences. Females have been shown to have nearly twice the risk of developing PTSD than males. Ethnic and racial minorities, regardless of what race or ethnicity the minority is, have been shown to be more susceptible to PTSD following earthquakes mostly due to lack of resources (social support and political support). Single parents and people living in single-person households have been shown to be more susceptible to developing PTSD mostly due to a lack of social support. Finally, households of lower income and lower education (i.e. lower socioeconomic status) have been shown to be much more susceptible to PTSD also mostly due to a lack of resources.

Detailed accounts of how each of the five socioeconomic variables influences the morbidity rates is provided in Chapter 6 of this dissertation. Specific analytical quantification of the morbidity rates considering all variables discussed in this section is provided in Chapter 3. The population demographic data including the number of persons in each age group, in each race/ethnicity group, in each gender group, in each family structure group, and in each socioeconomic status group, were used as inputs to the optimization, and were obtained from U.S. census data [U.S. Census (2012)] for the specified community.

2.4 Time to Recovery

The fourth objective is the time to recovery. Referring back to Figure 1-1, resiliency was shown to be directly related to time to recovery. A resilient community has a short recovery

time. As demonstrated in Figure 1-1, recovery time can vary depending on what is considered as recovery. Recovery could be when the pre-event state or better is achieved, but it also can mean a lower state which is still within the manageable and acceptable operating state for the community. This complicates the quantification for time to recovery, so much that these specific differences were not explicitly modeled here. In this study, time to recovery was estimated based on the repair time, and the physical and emotional health recovery times. Repair time was measured as the total amount of time for all damaged structures to be fully repaired; a factor dependent on the number of crews available for conducting the repairs. The CUREE study [Reitherman and Cobeen (2003)] provided subassembly repair times. Archetype repair times for each damage state were computed the same way archetype repair costs were computed using the CUREE subassembly repair time values. The mean value was obtained from the CUREE study, the standard deviation was set as one-third of the mean, and the repair time random variable was fit with a lognormal distribution. Appendix A provides the distribution parameters for the repair time for each archetype for each damage state.

Physical health-recovery time varies with the injury severity level. PTSD recovery time was set as one year (365 days) based on the Norris et al. (2002a and 2002b) study which demonstrated that the most severe PTSD symptoms occur during the first year. The community recovery time does not vary with the number of persons diagnosed with PTSD. That is, the recovery time due to PTSD is not cumulative over the number of persons diagnosed with PTSD because all persons can recover simultaneously. Strict values were assigned to the physical health and mental health recovery times.

Time to recovery may also be considered as the time to improve the loss in quality of life for the community. That is, the more people suffering from PTSD, the more people injured or

who had family members or loved ones injured, or had family members or loved ones killed during the earthquake, as well as the amount of physical building damage and damage to personal belongings present within the community all takes a toll on the mental health of the community and the population's quality of life. The drop in mental health may be considered as a drop in the quality of life, and the quicker the mental health of the community can be restored to a pre-disaster state or better, the more resilient that community is considered to be.

At the end of the multi-objective optimization, the Pareto-optimal set of solutions is provided with tradeoffs between resiliency objectives such as initial cost versus time to recovery. Decision makers may have resiliency goals such as "*90% shelter in place for all single family dwellings*" or "*no collapse of soft-story woodframe buildings*" during and following a seismic event of specified intensity. The results from this study provide the mitigation plan for the decision makers to accomplish these goals along with an estimate of initial cost, economic loss, the number of morbidities, and the time for recovery for the exposed population. Examples are provided in Chapter 8 with the outputted pareto-optimal set of solutions for the Los Angeles County community.

Chapter 3: Theoretical Formulation for Combined Engineering and Socioeconomic Loss Model

The framework presented here applies retrofit techniques, such as those explored in the NEES-Soft Project [van de Lindt et al. (2011)], by taking a multi-disciplinary approach to disaster mitigation caused by large earthquakes at the community level. The community-level mitigation plans are identified by solving a multi-objective optimization problem via genetic algorithm which minimizes the four performance objectives discussed in Chapter 2. The diagram provided in Figure 3-1 demonstrates the dissertation framework and how each aspect connects, where ngen refers to the generation count in the genetic algorithm, and nROW refers to the number of weights to be applied to the objectives . To use the framework, first, community leaders, building owners, or decision makers in general, must collectively formulate the resiliency-based optimization problem by defining the seismic hazard to which their community should be resilient. The population socioeconomic data is then uploaded from U.S. census data, and all other inputs are provided. The framework computes socioeconomic variable factors based on the required input values and information from the meta-data analysis conducted on population studies. The meta-data analysis computed odds ratios for each variable subcategory relative to the other subcategories (e.g., odds ratios between female and male gender, odds ratio between young age group and older age group, etc.). The odds ratios were determined for each performance objective. For example, gender subcategory odds ratios differ for the probability of injury, the probability of fatality, and the probability of developing PTSD. Table 3-1 provides

which variables were considered in each damage measure and performance objective. Detailed accounts of the population studies used in the meta-data analysis are provided in Chapter 6. A detailed categorized account of all input data is provided as follows:

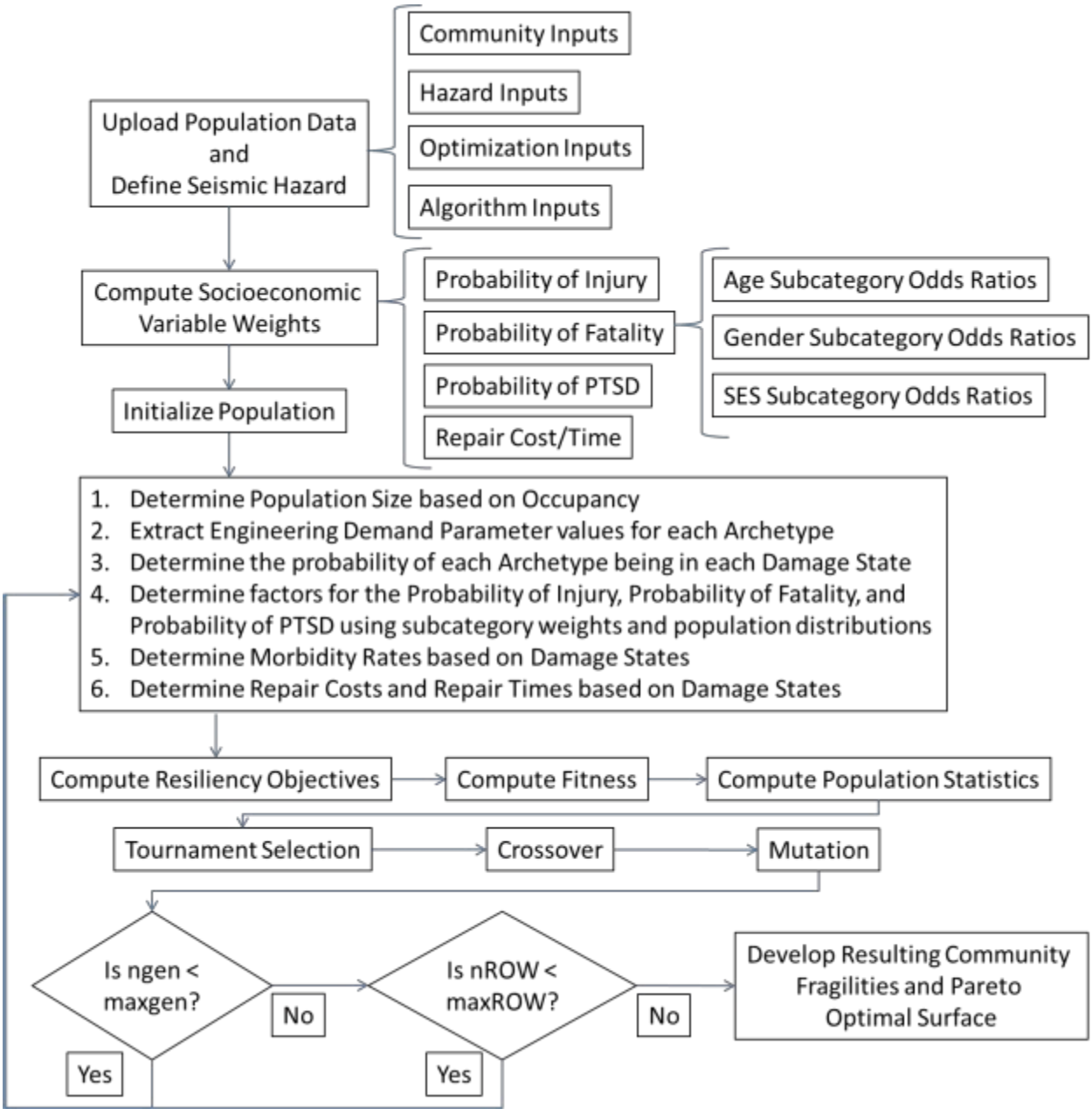

Figure 3-1: Dissertation Framework

Archetype-specific inputs: detailed floor plan and subassembly count (e.g., number of interior wall, exterior wall, and ceiling 64sf units, number of windows, and number of water

heaters), total floor area (sf), occupancy (number of persons occupying each archetype), unit cost of new construction, unit cost of retrofit ($/sf), contents value (% of total construction cost).

Community-specific inputs: density of the built environment (e.g., urban or rural), the percentage of families with children living in the household, the average annual salary of the population, the number of construction crews available for repair work following a large earthquake, the percentages of each age, ethnicity, family structure, gender, and socioeconomic status group present within the community (see Table 3-2), and the average number of persons per household.

Hazard-specific inputs: the spectral acceleration of the scenario earthquake (*Sa* = 0.1g – 0.4g in 0.1g increments), the inter-story drift collapse limit (taken as 10% for woodframe buildings in this study), and the time of day in which the scenario earthquake occurs (occupancy is dependent on time of day).

Optimization-specific inputs: the nonexceedance probability of the engineering demand parameter(s), the quality level of population data to be used in formulation of the socioeconomic variable factors, the economic category for the country that the socioeconomic variable information was collected from (e.g., developed nations only, or both developed and developing nations), the average number of hours per day in which an individual does not work due to PTSD (studies show 2 hours), and the full set of performance objective weights to be used in the development of the pareto-optimal surface of solutions.

Algorithm-specific inputs: the number of individuals in the population (i.e. the number of communities), the maximum number of generations, the probability of crossover, and the probability of mutation.

Referring back to Figure 3-1, once all inputs are provided, the genetic algorithm (GA) begins by initializing the population. Here, an individual in the genetic algorithm is a modeled community (i.e. a collection of building archetypes). The detailed account of the genetic algorithm is provided in Chapter 7. Preliminary computations are conducted prior to employment of the GA operators. These preliminary computations include: determining the population size based on the number of each building in the community and its respective occupancy, extracting the engineering demand parameter(s) for each archetype based on the seismic hazard and optimization inputs, using the socioeconomic data to determine damage measure factors, and determining the damage measures (e.g., morbidity rates, repair costs, repair times) based on the damage state. These preliminary calculations are used to quantify the performance objectives. For computing the fitness, the performance objectives are normalized by the minimum value of each respective performance objective in the current population so that each performance objective has the same order of magnitude. The normalized performance objectives were summed together representing the fitness for each community in the population. Population statistics were recorded and then plotted, such as the maximum, minimum, and mean population values for each damage measure, each performance objective, and fitness for each generation. These plots demonstrate the convergence of the fitness and show the resulting trend in the performance objectives and damage measures. Following the computation of the fitness values, the three GA-operators selection, crossover and mutation are employed. The fitness is re-calculated and the GA operators are employed again. This process repeats until the maximum number of generations is reached. Once this occurs, the GA reruns, starting with re-initialization of the population, for each set of weights applied to the performance objectives in an effort to achieve diverse solutions for forming the pareto-optimal surface. The pareto-optimal surface

represents the optimal tradeoffs between the resiliency objectives. The optimal tradeoff solutions would be provided to the decision maker(s) so that decisions can be made based on the preference over the performance objectives.

The following sections provide the quantification of the damage measures and performance objectives, and discussion on the limitations. Random (uncertain) variables are denoted by capital letters, particular values are denoted by lower case, probability is denoted by P[ ], and conditional probability is denoted by P[A|B]. The probability plots are theoretical distributions for exemplary purposes. Within the framework, these distributions are adjusted based on the seismic hazard inputs and community demographics.

Table 3-1: Variables Considered in Performance Objectives

Performance Objectives		*Density/Age of Built Environment*	*Inter-Story Drift*	*Age*	*Eth-nicity*	*Gender*	*Family Structure*	*Socio-economic Status*
Initial Cost								
Economic Loss	Building Damage	×	×					
	Morbidity	×	×	×	×	×	×	×
Number of Morbidities	Injuries	×	×	×		×		×
	Fatalities	×	×	×		×		×
	PTSD		×	×	×	×	×	×
Time to Recovery		×	×	×	×	×	×	×

Table 3-2: Variable Subcategories

Variable	*Subcategory*
Age	Young
	Old
Built Environment	New Rural
	Old Rural
	New Urban
	Old Urban
Ethnicity	Majority
	Minority
Family Structure	Single
	Single Parent
	Partnered
	Partnered Parents
Gender	Female
	Male
Socioeconomic Status	Low
	Moderate
	Upper

3.1 Damage States

Five damage states were considered in this study based on major damage categories identified for woodframe structures. These were determined based on experience of the author's from experimental tests to be discussed in Chapter 5, but also matched the Hazus [DHS (2003)] and CUREE (Reitherman and Cobeen (2003)] damage states. Table 3-3 provides a description for each damage state with respect to the physical damage observed for woodframe structures. In this study, the damage states were centered on inter-story drift values observed from full-scale experimental tests. Inter-story drift has been shown to be well-correlated with physical damage to woodframe structures [Filatrault and Folz (2002)]. The detailed determination of the overlapping inter-story drift ranges for each damage state is discussed in detail in Chapter 5.

Table 3-3: Damage State Descriptions

Damage State	*Level*	*Description*
1	No Damage	Structure can be immediately occupied, no repairs required.
2	Slight	Structure can be immediately occupied, minor drywall repairs required.
3	Moderate	Shelter-in-place allowed, drywall replacement required.
4	Severe	Shelter-in-place prohibited, structural damage incurred.
5	Collapse	Structure is not safe for entry, must be reconstructed.

Within the framework, once the spectral acceleration, probability of nonexceedance and collapse limit values are set by the user, the engineering demand parameter (EDP), i.e. peak inter-story drift, is extracted from fragility functions developed for each archetype. Using the extracted peak inter-story drift values, the probability of each archetype being in each damage state is then determined. Lognormal cumulative distribution functions (CDFs) were developed for each damage state using the respective inter-story drift ranges determined in Chapter 5, and shown in Figure 3-2. The damage states were modeled sequentially. The probability of each damage state given a specific inter-story drift value was determined using the following relationship for sequential damage states and their respective CDFs:

$$P[DS = ds|ISD = x]$$

$$= \begin{cases} 1 - P[DS \geq ds|ISD = x] & ds = 1 \\ P[DS \geq ds|ISD = x] - P[DS \geq ds + 1|ISD = x] & 2 \leq ds \leq n_{ds} - 1 \\ P[DS \geq ds|ISD = x] & ds = n_{ds} \end{cases}$$

Eq. 3-2

where = 5 in this study, and

$$\sum_{ds=1}^{n_{ds}} P[DS = ds|ISD = x] = 1.0 \qquad \text{Eq. 3-3}$$

Eq. 3-1 uses the extraction of the EDPs based on the input seismic hazard. The probability of the sequential damage states given a peak inter-story drift value is provided in Figure 3-3. In this study, the damage states provide the connection between the damage measures (e.g., building

performance, morbidity rates, repair costs, relocation costs, and repair times). The quantification of building performance is provided in Chapter 4. The following sections demonstrate the quantification of the remaining damage measures.

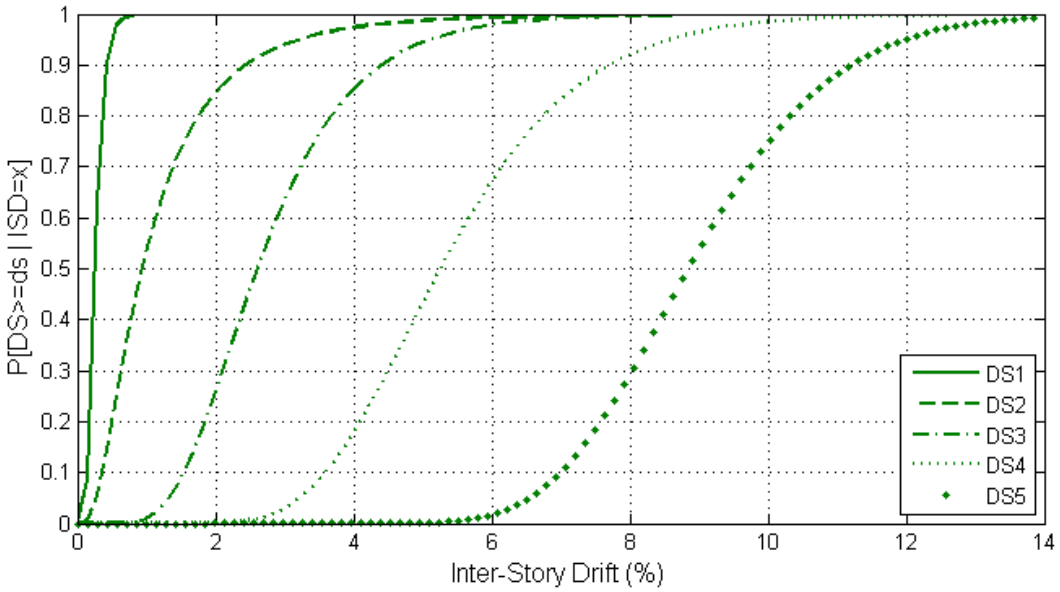

Figure 3-2: Damage State Lognormal CDFs given Inter-Story Drift

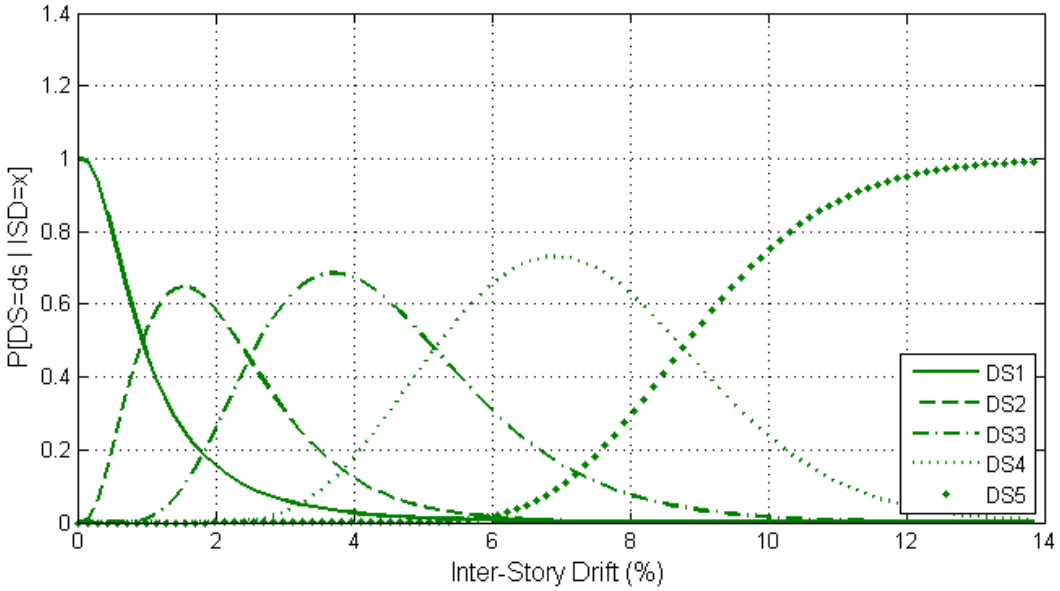

Figure 3-3: Probability of Sequential Damage States given Inter-Story Drift

3.2 Number of Morbidities

The preservation of life is the central goal in any structural design. In this dissertation it is proposed that preserving quality of life should also be considered as a design goal using the population's mental health as a metric. The number of morbidities was determined through the morbidity rates for injury, fatality, and PTSD diagnoses. PTSD diagnoses were incorporated into the loss model to represent the mental health of the population by means of a count of the number of persons expected to be diagnosed with PTSD. The morbidity rates were determined as a function of the damage states and adjusted based on the demographics of the population. The population demographics were incorporated through the socioeconomic factors, the applicable variables for each morbidity rate was shown in Table 3.1. The morbidity rates for the injury severity levels were computed as

$$MR_{is,ds} = (F_{age,MR} \cdot F_{env,MR} \cdot F_{gen,MR} \cdot F_{ses,MR}) \cdot IS_{is,ds} \quad \text{Eq. 3-4}$$

and the morbidity rate for PTSD was computed as

$$MR_{pr,ds} = (F_{age,MR} \cdot F_{env,MR} \cdot F_{eth,MR} \cdot F_{fam,MR} \cdot F_{gen,MR} \cdot F_{ses,MR}) \cdot PR_{ds} \quad \text{Eq. 3-5}$$

where , , , , , and are the socioeconomic factors for age, environment, ethnicity, family, gender, and socioeconomic status, respectively, and where the *MR* subscript refers to the factor value for either injury severity rate or PTSD rate. ,*ds* and are the probability of injury severity level *is* and PTSD diagnosis rate for damage state *ds*, respectively. The morbidity rates were incorporated into the computation of three performance objectives: economic loss, number of morbidities, and time to recovery. The number of morbidities, , was computed by multiplying the morbidity rates by the population size of the community:

$$RO_3 = \sum_{ds=1}^{n_{ds}} \left[\left(\sum_{is=1}^{n_{is}} MR_{is,ds} + MR_{pr,ds} \right) \cdot \sum_{i=1}^{n_{arch}} \left(n_{i,ds} \cdot occ_i \right) \right] \quad \text{Eq. 3-6}$$

where $_{,ds}$ is the number of each archetype *i* for the damage state *ds*; is the occupancy for each archetype *i*. The number of morbidities included the number of people in all injury severity levels, including fatalities, and the total number of PTSD diagnoses.

3.2.1 Injury Severity Rates

There are five injury severity levels considered in this study: minor injury, moderate injury, severe injury, critical injury, and fatal injury. The fatal injuries cover both assumed instantaneous deaths caused by the earthquake and deaths occurring in the immediate days following the earthquake in hospitals due to critical injuries or other unresolved health conditions attributed to the earthquake. Table 3-4 provides the description for each injury severity level. The latter four injury severity levels are analogous to those in Hazus. The minor injury severity level can be difficult to quantify due to the lack of record available caused by the nature of it being self-treated. It was not included in Hazus, but was included in this study.

Table 3-4: Description of Injury Severity Levels

Injury Severity Level	*Description*
Minor	Self-treated injuries
Moderate	Injuries requiring basic medical aid
Severe	Hospitalized injuries
Critical	Life threatening injuries
Fatal	Deaths and non-survivable injuries

The injury severity rates for each respective damage state, $_{,ds}$, were modeled as random variables using the lognormal distribution parameters provided in Appendix A, where the mean value was obtained from Hazus [DHS (2003)] for the latter four severity levels. The mean value for the minor injury severity level was determined by dividing the moderate injury severity rates by a factor of 10. The factor of 10 was chosen due to its use by Hazus in several instances for increasing/decreasing from one injury severity rate to the next. The lognormal CDFs for each

injury severity level for each damage state conditioned on casualty rate are provided in Figure 3-4 through Figure 3-8, where some of the curves appear to overlap (DS2, DS3, and/or DS4) due to the scale of the plot, but in fact differ slightly. The percentage, $_{,i}$, of each archetype *i* being in each damage state *ds* was computed as

$$P_{ds,i} = P_{ds,isd} \cdot n_i \qquad \text{Eq. 3-7}$$

where $_{,isd} = P[DS = ds|ISD = x]$, i.e. the probability of archetype *i* being in damage state *ds* as determined in Eq. 3-1, and is the total number of archetype *i* present in a single community. The percentage of buildings in the community whose occupants would be in injury severity level *is* was computed as

$$P_{is} = IS_{is,ds} \cdot \sum_{i=1}^{n_{arch}} P_{ds,i} \qquad \text{Eq. 3-8}$$

where $_{,ds}$ may also be described as a strict probability conditioned on the damage state, shown in Figure 3-9, and expressed as

$$IS_{is,ds} = P[IS = is|DS = ds] \qquad \text{Eq. 3-9}$$

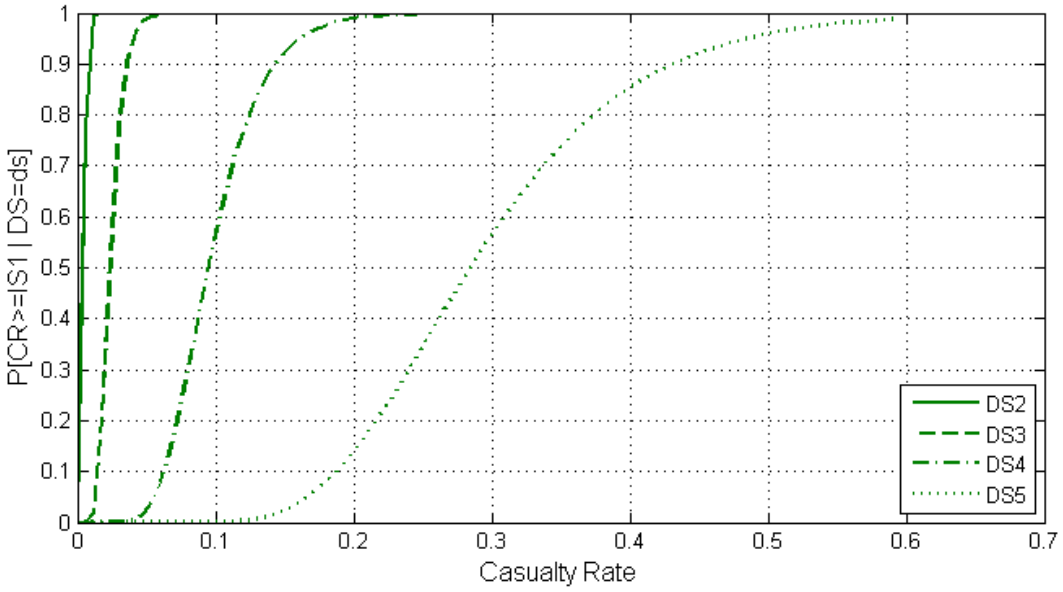

Figure 3-4: Nonexceedance Probability for Injury Severity Level 1 for each Damage State

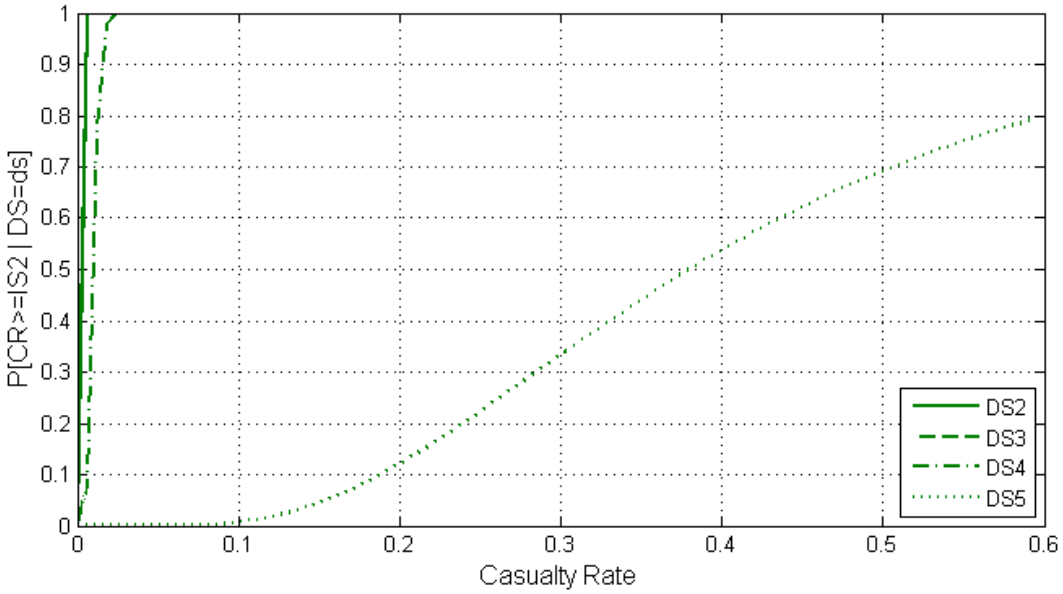

Figure 3-5: Nonexceedance Probability for Injury Severity Level 2 for each Damage State

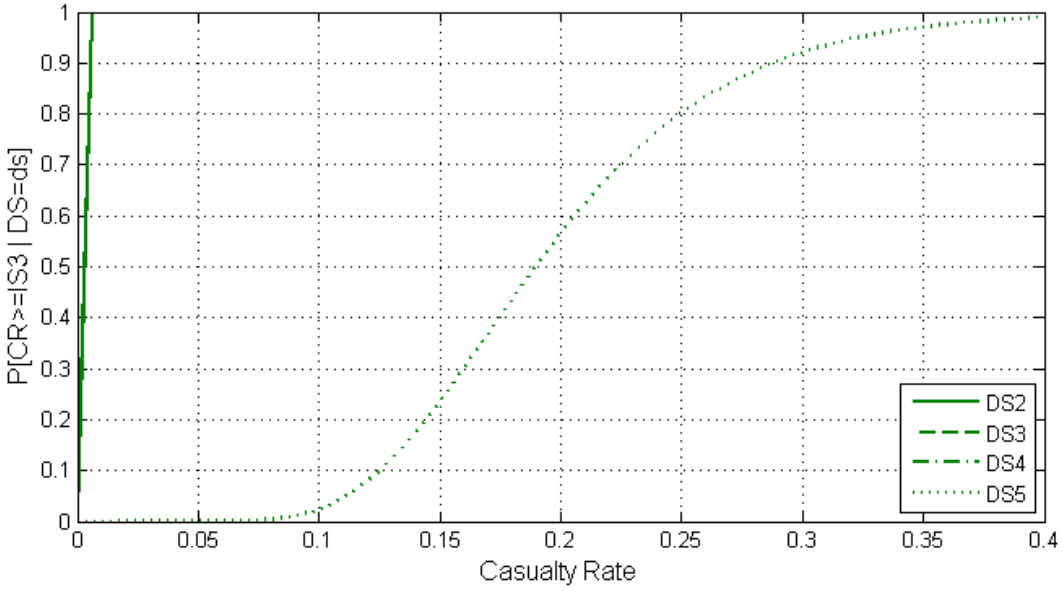

Figure 3-6: Nonexceedance Probability for Injury Severity Level 3 for each Damage State

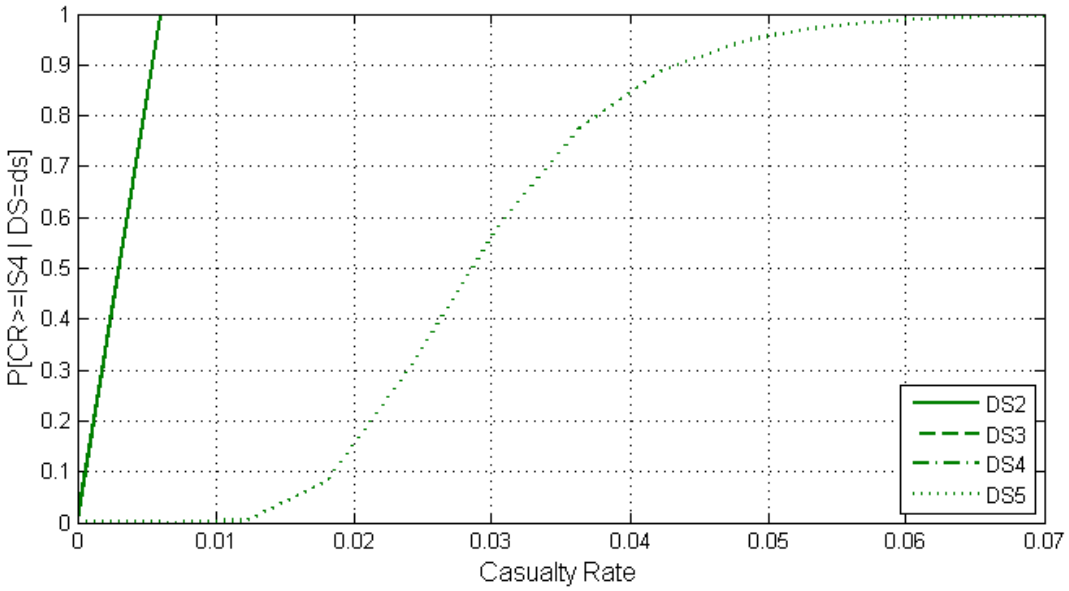

Figure 3-7: Nonexceedance Probability for Injury Severity Level 4 for each Damage State

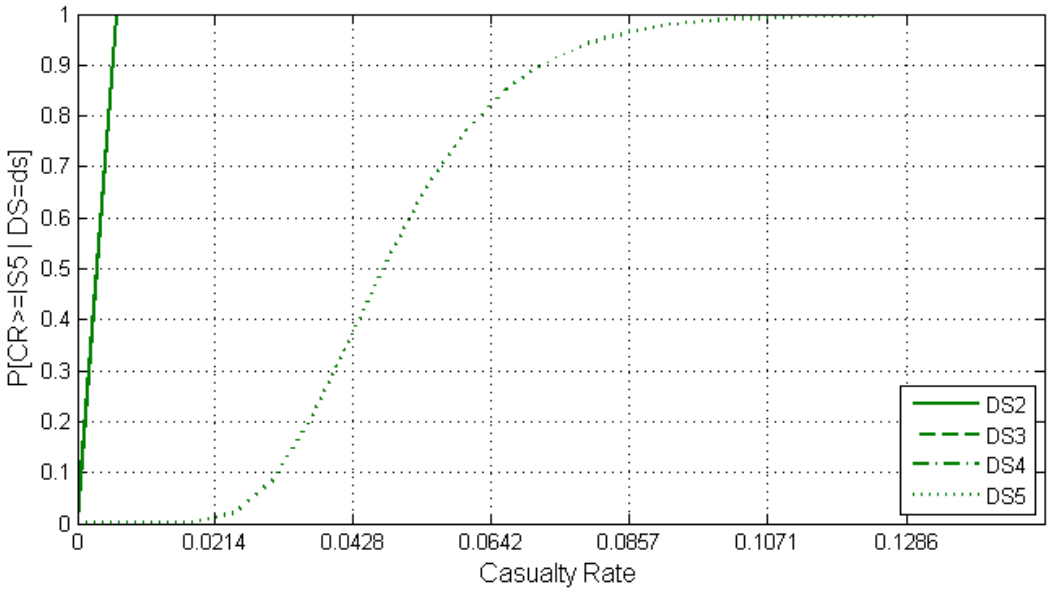

Figure 3-8: Nonexceedance Probability for Injury Severity Level 5 for each Damage State

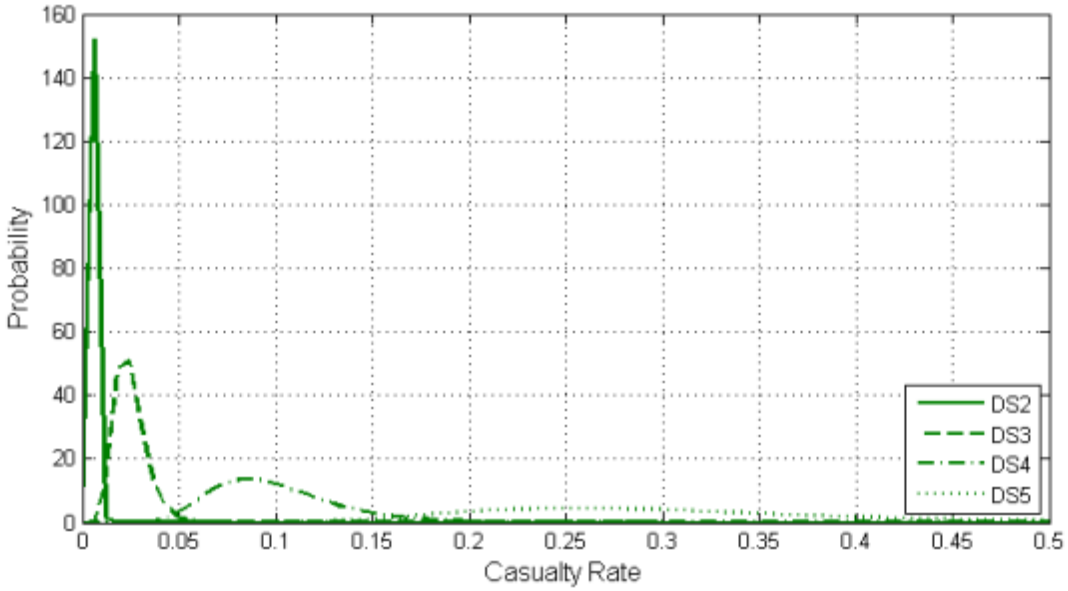

Figure 3-9: Probability of Injury given each Damage State

3.2.2 Rate of PTSD Diagnosis

The rate of PTSD diagnosis was conditioned on the damage state, and is expressed as a random variable. The mean value for each damage state was set to be the same as the severe injury rates. The distribution parameters were provided in Appendix A. The lognormal CDF for the rate of PTSD for all damage states is provided in Figure 3-10. The percentage of the population that would be diagnosed with PTSD following a scenario earthquake, , was determined similarly as the percentage of the population that would sustain a specific injury severity level, it was expressed as

$$R_{PTSD} = \sum_{ds=1}^{n_{ds}} \left[PR_{ds} \cdot \sum_{i=1}^{n_{arch}} \left(P_{ds,i} \cdot n_i \right) \right] \qquad \text{Eq. 3-10}$$

where is the lognormal probability density function for PTSD diagnosis rate for damage state *ds*, $_{,i}$ was determined in Eq. 3-6, and is the number of archetypes *i* in the community. may also be described as a strict probability conditioned on the damage state and expressed

as

$$PR_{ds} = P[PR = pr|DS = ds] \quad \text{Eq. 3-11}$$

The probability of PTSD diagnosis given a specific damage state is expressed graphically in Figure 3-11. Eq. 3-7 and Eq. 3-9 provide the injury severity rates and PTSD diagnosis rate for the community based on the damage state used in Eq. 3-3 and Eq. 3-4. To get the actual count, or number of people diagnosed with PTSD, Eq. 3-9 should be multiplied by the occupancy of each archetype.

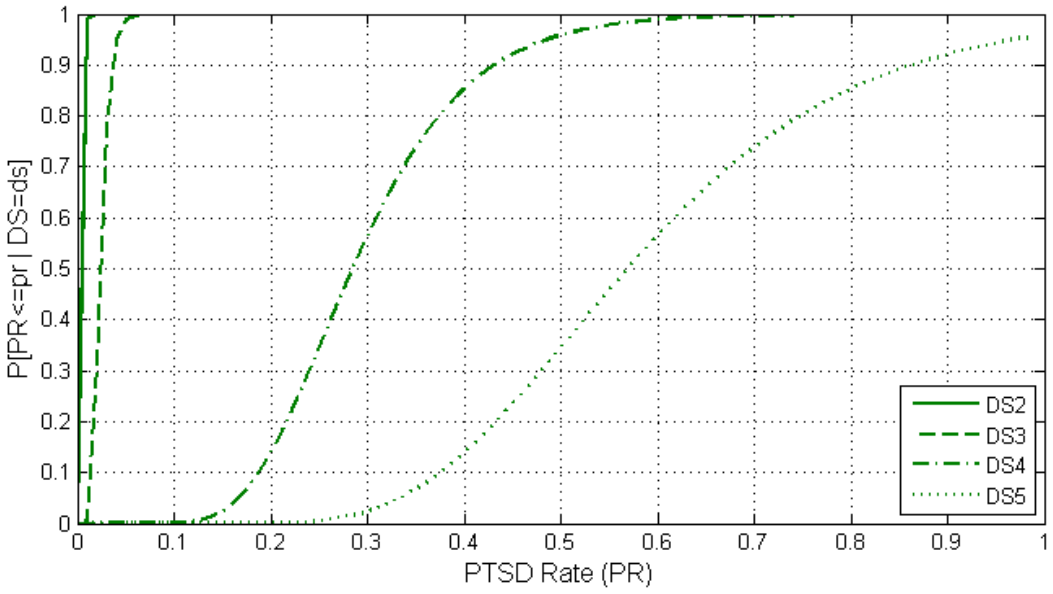

Figure 3-10: Nonexceedance Probability for the Rate of PTSD for each Damage State

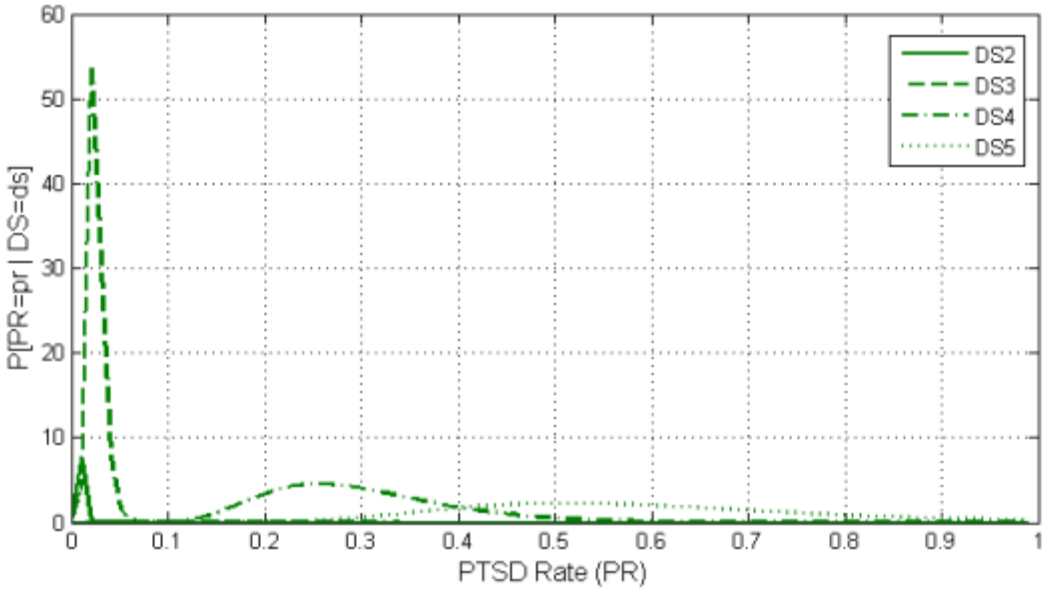

Figure 3-11: Probability for the Rate of PTSD for each Damage State

3.3 Initial Cost

The initial cost was computed as the cost for all new retrofits, , it may be expressed as

$$RO_1 = ic_{ret} \quad \text{Eq. 3-12}$$

The new retrofit costs were strict values computed using a unit cost per square foot for the respective archetype and respective retrofit, multiplied by the total floor area of the archetype. The quantity of new retrofits was determined by subtracting the total number of buildings retrofitted by modern provisions (i.e. ASCE7-05, SDDD-LS, SDDD-IO, and FEMA P-807 designs) for the current generation from the initial population in . This may be expressed as

$$ic_{ret} = \sum_{i=i}^{n_{arch,ret}} cost_{ret,i} \cdot fa_i \cdot (n_{gen,i} - n_{gen_0,i}) \quad \text{Eq. 3-13}$$

3.4 Economic Loss

The economic loss was computed as the sum of direct and indirect costs. These costs included: repair costs (including rebuild costs), , loss due to contents damage, , relocation

costs, , and morbidity costs, , (e.g., injury costs, PTSD treatment costs, PTSD downtime costs, and the value of a lost life). The second objective, , (i.e. economic loss) may be expressed as

$$RO_2 = EL_{RC} + EL_{RL} + EL_M \quad \text{Eq. 3-14}$$

3.4.1 Repair Costs

The economic losses due to repair costs, rebuild costs, and contents damage were grouped together. The mean values for the repair costs were obtained from Reitherman and Cobeen (2003), as discussed in Chapter 2. These repair costs were provided at the subassembly level for exterior walls (64sf unit size), interior walls (64sf unit size), ceilings (64sf unit size), windows (individual unit size) and water heaters (individual unit size). Therefore, to determine the repair costs for archetype *i*, the number of units for each of the five subassemblies was determined. To compute the total archetype repair cost for each damage state, $_{,i}$, the lognormal inverse CDF for the subassembly repair costs, $\phi^{-1}(_{,k})$, was multiplied by thirty percent of the number of subassembly units, $_{,k}$, and summed together for all subassemblies *k*, expressed as

$$RC_{ds,i} = \sum_{k=1}^{5} 0.3 \cdot n_{unit,k} \cdot \Phi^{-1}(RC_{ds,k}) \quad \text{Eq. 3-15}$$

Only 30% of the subassembly units were used in determining the repair costs, because in reality, not every single 8 ft by 8 ft wall interior wall, exterior wall, and ceiling segments will be damaged on the building. Based on the author's experience discussed in Chapter 5, assuming 30% of the subassembly units is still conservative. The lognormal CDF for the repair cost for each damage state is provided in Figure 3-12.

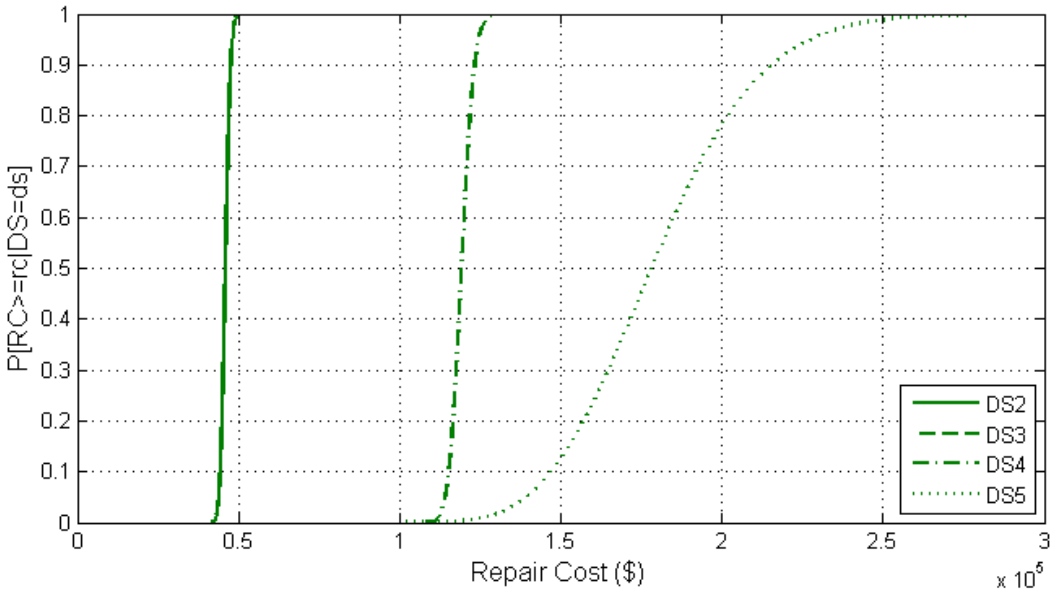

Figure 3-12: Nonexceedance Probability of Repair Cost for each Damage State

Economic loss due to rebuild costs were computed using the cost per square foot values determined in Chapter 2 from Reitherman and Cobeen (2003). These values were multiplied by the archetype floor area and summed for all archetypes reaching damage state 5. The economic loss due to rebuild costs may be expressed as

$$RB_{DS5,i} = cost_i \cdot n_{ds5,i} \qquad \text{Eq. 3-16}$$

Economic loss due to contents damage was set as 50% of the repair cost value for residential structures and 100% of the mean repair cost value for commercial structures. The contents values, , were used in DHS (2003) as percentages of the structure value. The mean contents damage, $_{,i,}$ may be expressed as

$$CD_{ds,i} = RC_{ds,i} \cdot CV_i \qquad \text{Eq. 3-17}$$

To compute the economic loss due to all archetypes in the community over all damage states, , the sum of the archetype *i* repair cost for damage state *ds*, $_{,i}$, the archetype rebuild costs for archetypes reaching damage state 5, $_{,i}$, and the archetype *i* contents damage for damage state

ds, $_{,i}$, was multiplied by the total number of archetypes i in the community and summed together. The economic loss due to all archetypes in the community over all damage states may be expressed as

$$EL_{RC} = \sum_{ds=1}^{n_{ds}} \sum_{i=1}^{n_{arch}} (RC_{ds,i} + RB_{DS5,i} + CD_{ds,i}) \cdot n_i \quad \text{Eq. 3-18}$$

The strict probability of repair cost given each damage state, $P[RC = rc|DS = ds]$, is provided in Figure 3-13.

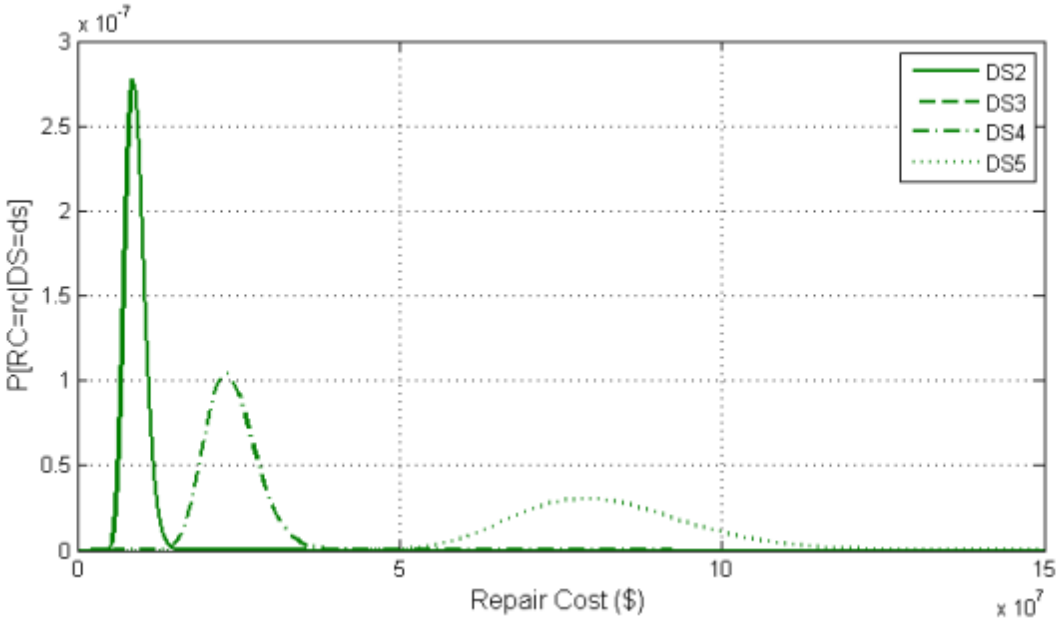

Figure 3-13: Probability of Repair Cost for each Damage State

3.4.2 Relocation Count and Cost

Following the scenario earthquake, if a building reached DS4 or DS5, then temporary relocation of the building occupants would be required. The ability for building occupants to shelter in place is important to decision makers and community leaders. If persons are displaced for too long, they may decide to permanently relocate to another community which will have significant impact on the community both financially and culturally. The number of relocated

persons was computed as the number of buildings reaching damage states 4 and 5 multiplied by the specific building's occupancy, expressed as

$$n_{rel} = n_{i,DS4} * occ_i + n_{i,DS5} * occ_i \quad \text{Eq. 3-19}$$

where, = number of relocated persons; $_{,DS4}$ = number of archetypes *i* in damage state 4; $_{,DS5}$ = number of archetypes *i* in damage state 5; = number of persons occupying archetype *i*. The number of relocated persons is provided as a fragility function conditioned on the initial cost, expressed as

$$P[nRel \leq n | ic = ic_i] \quad \text{Eq. 3-20}$$

where *n* = the number of relocated persons caused by ; *ic* = initial cost; = the initial cost of the specific community mitigation plan *i*. The computation of the cost for relocation was adopted from the Hazus methodology, and incorporated into the performance objective economic loss. The relocation cost may be expressed as

$$rel_i = fa_i \cdot \left[(1 - per_i) \cdot \sum_{ds=4}^{5} \left(p_{ds,i} \cdot dc_i \right) + per_i \cdot \sum_{ds=4}^{5} \left(p_{ds,i} \cdot (dc_i + rent_i + rt_{ds,i}) \right) \right]$$

Eq. 3-21

where, = the relocation costs for archetype *i* based on occupancy class; = the floor area of archetype *i*; $_{,i}$ = the probability of archetype *i* being in damage state *ds*; = the disruption costs for archetype *i* based on occupancy class in units of dollars per square foot ($/sf); $_{,i}$ = recovery time for archetype *i* in damage state *ds*; is the percent owner occupied for archetype *i*; = the rental cost for archetype *i* based on occupancy class in units of $/sf/day. The values for , , and were obtained from Hazus and are provided in Table 3-5, where SFD is a single family dwelling, and MFD is a multi-family dwelling. The values for $_{,i}$ were the mean values for $_{,i}$ provided in Appendix A. To determine the economic loss due to relocation, , the relocation cost for

archetype *i* is multiplied by the total number of archetypes *i* in the community, and summed for all archetypes, expressed as

$$EL_{RL} = \sum_{i=1}^{n_{arch}} rel_i \cdot n_i \qquad \text{Eq. 3-22}$$

Table 3-5: Relocation Cost Parameter Values

Parameter	*Archetype Category*	*Hazus Value*
dc ($/sf)	Residential SFD	0.82
	Residential MFD	0.82
	Commercial	0.95
per (%)	Residential SFD	75
	Residential MFD	35
	Commercial	55
rent ($/sf/month)	Residential SFD	0.68
	Residential MFD	0.61
	Commercial	1.36

3.4.3 Economic Loss due to Morbidity

The economic loss due to morbidity, , was determined as the sum of the economic loss caused by the number of persons in each morbidity category (five injury severity levels, including fatality, and PTSD diagnoses), expressed as

$$EL_M = \sum_{i=1}^{5} EL_{Inj,is} + EL_{PTSD} \qquad \text{Eq. 3-23}$$

where $_{,is}$ is the economic loss due to injury for injury severity level *is*, and is the economic loss due to PTSD. The community economic losses due to each injury severity level were modeled as random variables. The mean value, $_{,is}$, was determined by multiplying the particular cost value associated with each injury severity level, $_{,is}$, by the respective mean value of the injury severity rate distribution, , respectively. The standard deviation, $_{,is}$, was determined similarly, but by taking one-third of the particular cost value. Throughout the framework, if the standard deviation was unknown, it was assumed as one-third of the mean. The mean and standard deviation for the economic loss due to injury based on injury severity rate may be expressed as

$$mEL_{Inj,is} = cost_{Inj,is} \cdot mIS_{is}$$ Eq. 3-24

$$sEL_{Inj,is} = \left(\frac{1}{3}\right) \cdot cost_{Inj,is} \cdot mIS_{is}$$ Eq. 3-25

The parameters in Eq. 3-24 and Eq. 3-25 were used to determine the lognormal distribution parameters. The particular cost values for each injury severity level were set as the values the U.S. government assigns to each injury severity level, including fatality [FHWA (1994)], and adjusted for inflation to 2014 dollars. These values are comprehensive costs covering pain, lost quality of life, medical costs, legal costs, lost earnings, lost household production, etc. Table 3-6 provides the cost values for each injury severity level.

Table 3-6: Injury Severity Costs

Injury Severity Level	*Minor*	*Moderate*	*Severe*	*Critical*	*Fatality*
Cost ($)	8,000	64,000	785,000	3,170,000	4,165,000

The economic loss due to PTSD is the sum of economic losses due to treatment of PTSD, $_{,trmt}$, and the downtime due to PTSD considering absenteeism from work, $_{,Abs}$, and presenteeism at work, $_{,Pres}$, expressed as

$$EL_{PTSD} = EL_{PTSD,trmt} + EL_{PTSD,Abs} + EL_{PTSD,Pres}$$ Eq. 3-26

To model the economic loss due to PTSD as a random variable, the process above was similarly repeated by first combining the particular costs (or mean values) for treatment, downtime due to absenteeism, and downtime due to presenteeism, expressed as

$$cost_{PTSD} = cost_{PTSD,trmt} + cost_{PTSD,abs} + cost_{PTSD,pres}$$ Eq. 3-27

$$mEL_{PTSD} = cost_{PTSD} \cdot mPTSD$$ Eq. 3-28

$$sEL_{PTSD} = \left(\frac{1}{3}\right) \cdot cost_{PTSD} \cdot sPTSD$$ Eq. 3-29

Recall from Chapter 2, that the treatment cost of PTSD was determined from a study conducted by the Congressional Budget Office on veterans [CBO (2012)] as $5400 per year.

3.4.4 Absenteeism and Presenteeism

The equations used for determining the number of work loss days and work cut back days due to PTSD were obtained from Goetzel et al. (2004). The annual rate of absenteeism due to PTSD was computed as

$$R_{Abs} = n_{WLD} \cdot (P_{PTSD} \cdot n_{pop})/240 \qquad \text{Eq. 3-30}$$

where is the average annual number of work loss days per person obtained from Kessler and Frank (1997), is the population size based on building occupancy, and *240* is the total number of work days per year. The total loss due to absenteeism was estimated by multiplying the annual rate of absenteeism, , by the average salary of the population, expressed as

$$cost_{PTSD,Abs} = R_{abs} \cdot salary \qquad \text{Eq. 3-31}$$

The annual rate of presenteeism due to PTSD is

$$R_{Pres} = n_{WCBD} \cdot (P_{PTSD} \cdot n_{pop}) \cdot hr_{WCB} \cdot 0.125/240 \qquad \text{Eq. 3-32}$$

where is the average annual number of work cut back days per person due to PTSD [Kessler and Frank (1997)], is the average number of hour per day in which work is cut back due to PTSD [Kessler and Frank (1997)], and *0.125* represents 8 hours per work day. The total loss due to presenteeism was estimated using the average salary of the population, expressed as

$$cost_{PTSD.Pres} = R_{Pres} \cdot salary \quad \text{Eq. 3-33}$$

Eq. 3-31 and Eq. 3-33 are incorporated into Eq. 3-27, along with the value for treating PTSD, for computing the mean value for the total economic loss due to PTSD.

3.5 Time to Recovery

As mentioned in Sec. 3.2, the quality of life and mental health of the population are important in order for a community to have a successful economy. One way to measure the impact on the quality of life of the population is through the estimated recovery time. To compute the community time to recovery, the maximum was taken over the recovery time for each morbidity category and the total repair time, expressed as

$$RO_4 = max\begin{Bmatrix} RecT_M \\ RecT_{Rep} \end{Bmatrix} \quad \text{Eq. 3-34}$$

3.5.1 Recovery Time due to Morbidity Rates

The recovery time due to morbidity, , was determined by taking the maximum recovery time over the individual morbidity rates, , expressed as

$$RecT_M = max\begin{Bmatrix} mrt_{IS1} \\ mrt_{IS2} \\ mrt_{IS3} \\ mrt_{IS4} \\ mrt_{IS5} \\ mrt_{PTSD} \end{Bmatrix} \quad \text{Eq. 3-35}$$

Eq. 3-35 assumes that there are members of the population in all morbidity rate categories. In the model, the maximum value is only taken over the morbidity rates which have members of the population suffering from the specific morbidity. That is to say that, if the defined seismic hazard was for a very small earthquake, there may not be any members of the population which experience the latter two morbidity categories (e.g., fatality and PTSD). In which case, only the first four morbidity categories would be considered in Eq. 3-35.

The values for were set as the values list in Table 3-7 for the various morbidities. If a distribution for the recovery time due to each morbidity rate was desired, the values in Table 3-7 could be set as the mean values and the standard deviation set to one-third of the mean. Rather than doing this for each morbidity rate, the maximum value of all components of the recovery time, RO4, was taken as the mean value for the distribution and the standard deviation set as one-third of the mean. It is evident from the Eq. 3-34 and the values in Table 3-7 that the recovery time due to PTSD would normally control for larger earthquakes.

Table 3-7: Recovery Time due to Morbidity

Morbidity Rate	Injury Severity Level 1	Injury Severity Level 2	Injury Severity Level 3	Injury Severity Level 4	Injury Severity Level 5	PTSD
Time (weeks)	1	6	16	26	26	52

3.5.2 Time due to Repair

The recovery time due to repair time, , was determined the same way that the economic loss due to repair costs, , was determined. The mean values for the repair times were obtained from Reitherman and Cobeen (2003), as discussed in Chapter 2. These repair times were provided at the subassembly level for exterior walls (64sf unit size), interior walls (64sf unit size), ceilings (64sf unit size), windows (individual unit size) and water heaters (individual unit size). Therefore, to determine the repair times for archetype *i*, first the number of units for each of the five subassemblies was determined. To compute the total archetype repair time, $_{,i}$, for each damage state, the lognormal inverse CDF for the subassembly repair time, $\varphi^{-1}(_{,k})$ was multiplied by the number of subassembly units, $_{,k}$, and summed together for all subassemblies. The total archetype repair time may be expressed as

$$RT_{ds,i} = \sum_{k=1}^{5} n_{unit,k} \cdot \Phi^{-1}(RT_{ds,k}) \qquad \text{Eq. 3-36}$$

The lognormal CDF for the repair cost for each damage state is provided in Figure 3-14. To compute the repair time due to all archetypes in the community, , for all damage states, the archetype *i* repair time for damage state *ds*, $_{,i}$, is multiplied by the total number of archetypes *i* in the community, summed over the community, and then divided by the number of repair persons, . The number of repair crews was determined by the percentage of the Los Angeles County population that is in the construction industry (i.e. 5.7% on the 2010 U.S. census) divided by three to represent a three-person crew. The actual number of repair crews is full of uncertainty. What is known is that if a major disaster were to occur, repair crews from all surrounding areas would come for work. Therefore, conservatively assuming it this way accounts for non-professionals and out-of-towners offering repair, as well as the local repair companies. The community recovery time due to building repairs may be expressed as

$$RecT_{Rep} = (\sum_{ds=1}^{n_{ds}} \sum_{i=1}^{n_{arch}} RT_{ds,i} \cdot n_i)/n_{rep} \qquad \text{Eq. 3-37}$$

The strict probability of repair time given each damage state is provided in Figure 3-15.

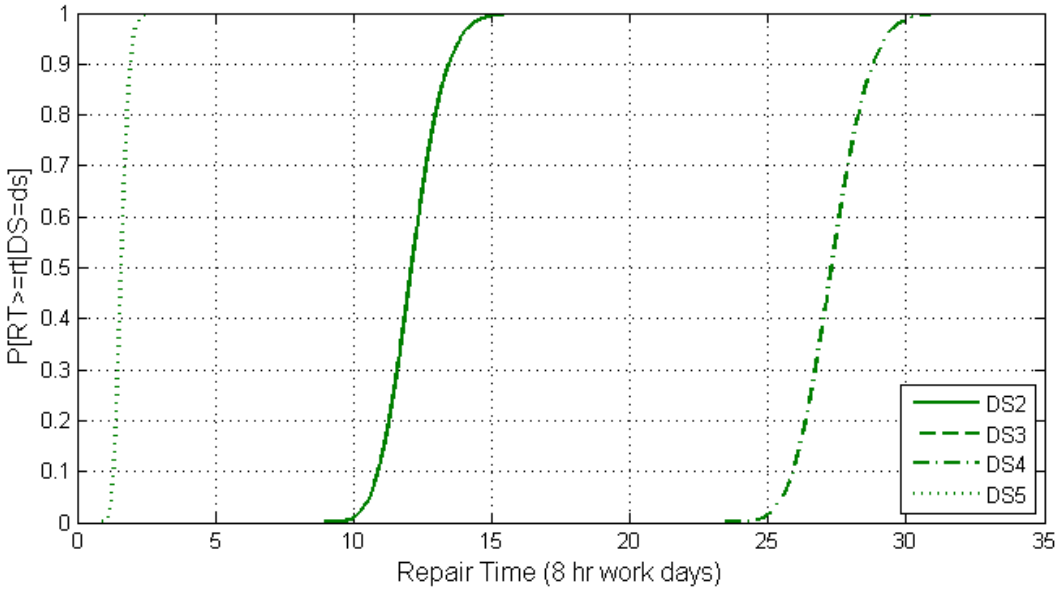

Figure 3-14: Nonexceedance Probability of Repair Time for each Damage State

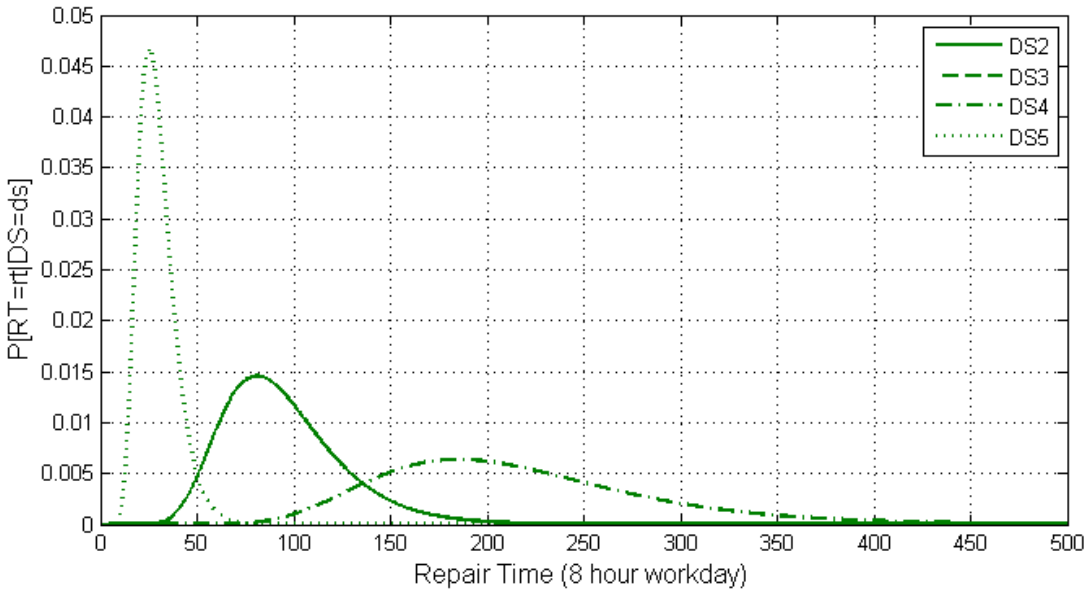

Figure 3-15: Probability of Repair Time for each Damage State

3.6 Limitations

Many factors influence an individual's social vulnerability and a community's resiliency to earthquakes, and not all of these factors were included in this dissertation. It is well known that the severity of the experience, proximity to the epicenter, magnitude of the earthquake, role

in the aftermath, severe damage caused to a person's home or personal belongings, the amount of physical damage caused to the built environment in the community, experiencing previous trauma, being widowed, being alone during the earthquake, lack of social support, previous psychiatric illness, injury to self or a loved one, loss of a loved one, having a disability, gender, ethnicity, education, socioeconomic status, family structure, amount of time in the country, and many other factors, all play a significant role in vulnerability and resiliency. Due to the limitations in this study, and the lack of data required for incorporating each influential factor, only the variables listed in Table 3-1 were considered here, although the importance of all factors is duly recognized. Additionally, in order for a community to be resilient, many other aspects of mitigation are important aside from structurally strengthening the woodframe building stock, such as preparedness, planning, and execution of recovery operations. Emergency facilities such as hospitals, police stations, fire stations, etc. must have access to power and water at all times. Food, shelter, and psychiatric services must be made available immediately after the event, as well as an effort to resume children's education.

The present study aims for quantification of disaster resiliency at the community level by retrofitting the existing woodframe building stock. This quantification proves a difficult task, even with its limitations, due to its subjective nature and the non-homogeneity of the existing research data. For example, the most recent devastating earthquake occurring in the United States was two decades ago. It may be assumed that in the past 20 years, a portion of the at-risk infrastructure has been rebuilt or retrofitted such that fewer buildings would collapse when subjected to a large earthquake, and thus causing fewer casualties. Therefore, statistics from the 1994 Northridge earthquake may be considered outdated. Earthquakes are one of the most frequently occurring natural disasters in the world and an abundance of somewhat current

statistical data on building damage and the affected populations is available. The problem then arises in comparing different societies and cultures in developing nations with more-developed nations, and applying the results globally. For example at the engineering-level, light-frame wood construction is by far the dominant construction type for residential buildings in the United States; however masonry-type structures dominate the residential buildings stock in many other countries. Therefore, statistics on such quantities as the number of buildings which collapsed, the number of injuries, and the number of fatalities may not be comparable. Borden and Cutter (2008), as well as Gall et al. (2008), discuss in depth the issues that arise when simultaneously using data from different databases, using data from one area and applying its statistics to another area in the world, the issue of changing the geographic scale of the measured data for an analysis, and comparing losses over time. Borden and Cutter (2008) demonstrate when considering public-access databases, the issue of "what constitutes a disaster" dictates which events are reported and the effect of this difference. Loss numbers are calculated differently, either by direct losses, or both direct and indirect losses. Data is collected at different levels: for a city, county, census tract, etc., with various and inconsistent surveys. In their study, Borden and Cutter (2008) demonstrated that a smaller county can sometimes show a very high fatality rate that can skew the conclusions. Thus, using that data which offers a high fatality rate for a certain group of people may not be accurately applied to a different location and different group of people. There are also many inconsistencies within the surveys used for collecting social demographic data; however these limitations will be discussed in Chapter 6.

In spite of the vast number of discrepancies with the available data, even still, this study attempts to quantify a selection of desired relationships to be inputted into the proposed framework. It is believed that the value of the framework itself does not decrease due to the

discrepancies with the data, although the accuracy of the output may be enriched with improvement in the consistency of the data collected. It is anticipated that the quality and consistency of data will improve over the years and may then be used to update the framework.

Aside from limitations with the socioeconomic data collection, there are other shortcomings with respect to defining the seismic hazard, modeling a set of archetypes, and determining the performance of the archetypes to the defined seismic hazard. These shortcomings start with the uncertainty associated with the magnitude and location of future earthquakes. This framework sets all buildings in the community an equal distance from the epicenter. This assumption will require case studies to be on smaller population subgroups selected as 100,000 buildings. The framework also assumes that all buildings are at full strength and stiffness, no degradation due to aging or past earthquakes is present. The framework allows seven floor plans to represent all woodframe building floor plans in a potential community. Although this is a shortcoming, it was felt to represent the larger quantity of woodframe building types present in the United States.

Chapter 4: Numerical Modeling of Building Archetypes

Structural design evolves as new information is gained from research and experiences. Major changes are often adopted in any type of design code or provision, and new guidelines are often published, following disastrous events that highlight existing or perceived deficiencies in calibration and sometimes philosophy. The work presented in this chapter chronicles the evolution of seismic design for woodframe structures from 1959 through current state-of-the-art methodologies available in 2014, providing a brief background on the historical significance and major changes adopted in each code or guideline. A set of seven base-archetypes were designed to five design or retrofit provisions selected based on their historical significance. An extensive nonlinear numerical analysis was conducted to quantify the difference in performance obtained by each newer methodology. The purpose of examining each of these is that a typical metropolitan statistical area (MSA) will have woodframe buildings designed to many different codes within its building inventory.

4.1 Previous Reviews on Historical Seismic Design

A number of other reviews are available in the literature providing historical timelines on various aspects of seismic design. McIntosh and Pezeshk (1997) compared the purpose, type of document and target audience, lateral forces, and analysis provisions provided in the early 1990's editions of the National Earthquake Hazard Reduction Program (NEHRP), Structural Engineers Association of California (SEAOC), American Society of Civil Engineers (ASCE) Standard 7, and the Uniform Building Code (UBC) seismic design provisions. Major differences in the design noted for these documents were that NEHRP and ASCE Standard 7 were based on strength design while SEAOC and UBC were based on allowable stress design, with many other

differences discussed in the review. The authors discussed the importance of maintaining consistency in selected provisions for the material design, detail requirements, and load provisions when exceeding the elastic limit state. A general review was provided with specific examples for steel and concrete framing systems. No specific examples were provided for woodframe structures.

In 2002, Beavers published a review on the history of seismic hazard maps, their development and use, and the use and adoption of seismic building codes in the United States from its first initiation to its state at that time (2002). Beavers (2002) provided a complete review on these topics, some of which were touched upon in this work, however details were not repeated.

Line (2006) provided a short review on benchmarking seismic design load and resistance values for woodframe shearwall structures over a span of approximately 50 years. The review started with the 1955 Uniform Building Code (UBC) and concluded with the 2006 International Building Code (IBC). Discussion on the changes in framing, wood structural panel, shearwall aspect ratios, nailing schedules, base shear, and shearwall resistance were provided. An analytical comparison was provided on the seismic base shear computations for a regular one-story woodframe structure with wood panel shearwalls for two aspect ratios and three locations in the United States.

Then, in 2008, Diebold et al. chronicled the SEAOC Blue Book from 1959-2008. The authors provided a historical lead up to the first Blue Book, its development, and the changes in the seismic design recommendations for each major time period.

Thus far in these reviews, limited equations were presented, no analytical comparisons were presented based on building performance, and the most current to date is still several years

old and did not include any performance-based seismic design methodologies or newer retrofit procedures. The present study focuses on the evolution of the seismic risk and performance of woodframe buildings based on historical changes in seismic design provisions from 1959 to 2014.

4.2 Design Codes

Six different historical design and/or retrofit provisions were selected for this study. Three of the six were selected due to fundamental changes in the building codes which occurred following major earthquakes in the United States. Others selected were two state-of-the-art performance-based seismic retrofit designs, and a new and economic soft-story-only retrofit guideline. The following subsections provide the motivation behind each provision, code, or guideline selection, and some of the detailed calculations within the respective document.

4.2.1 Pre-1971 San Fernando Earthquake Design

On February 9, 1971 at 6:01am PST a Richter scale M6.6 earthquake occurred in San Fernando Valley, California. Although only of moderate size on the Richter scale, in terms of motion, this was the strongest earthquake ever recorded in California at the time [Ritchie (2003)]. Governor Reagan, as well as, President Nixon declared Los Angeles County a disaster area. The death toll totaled 58, and property damage estimates exceeded $2 billion. The biggest impact of this earthquake for the region was the damage caused to several medical facilities. In fact, 49 of the 58 fatalities occurred due to the collapse of the Veterans Administration Hospital building, and four more persons died due to the collapse of the newly built Olive View Hospital. There were several significant outcomes directly resulting from the 1971 San Fernando earthquake. Perhaps the greatest conclusion drawn with respect to the building stock was the need for certain structures to be designed stronger than the minimum code requirements to

maintain functionality immediately after an earthquake, or other hazard, event. These structure types were to include hospitals, schools used as emergency shelters, emergency communication buildings, fire departments, and other disaster relief agencies. Furthermore, a new concept known as the "occupancy factor" was recommended after this event that would require greater resistance for buildings with large occupancy and special occupancy, such as schools, hospitals, theaters, etc. [Jennings (1971)]. Both the occupancy factor and building category were adopted into the building code as a direct result of the 1971 San Fernando earthquake.

To provide the design space with a pre-1971 San Fernando earthquake design, the 1959 SEAOC seismic recommendations [Seismology (1959)] and the 1970 Uniform Building Code [UBC (1970)] were selected. The 1959 SEAOC seismic recommendations, often referred to as the Blue Book, were the first seismic provisions published in the United States by the Structural Engineering Association of California. These provisions introduced the framing factor, *K*, which was to include the effect of the building's ductility in the design base shear, *V*. The design base shear, or minimum total lateral seismic force that a building was required to withstand in each of the building's main axes was computed as

$$\mathrm{V} = \mathrm{K} \cdot \mathrm{C} \cdot \mathrm{W} \qquad \text{Eq. 4 - 1}$$

where *K* was the horizontal force factor tabulated for buildings and other structures based on the building's structural system, *W* was the total dead load, and *C* was the numerical coefficient for base shear determined by

$$\mathrm{C} = \frac{0.05}{\mathrm{T}^{1/3}} \qquad \text{Eq. 4 - 2}$$

T was the fundamental period of vibration of the structure in seconds in the direction being considered. If this information was not known, the structural engineering could estimate *T* by

$$T = \frac{0.05 \cdot H}{\sqrt{D}} \qquad \text{Eq. 4 - 3}$$

where *H* was the height of the main portion of the building in feet above the base, and *D* was the dimension of the building in feet in a direction parallel to the applied forces. The distribution of the total lateral force, *V*, over the building height was provided as

$$F_x = \frac{V \cdot w_x \cdot h_x}{\sum w \cdot h} \qquad \text{Eq. 4 - 4}$$

where was the portion of *W* for level *x*, and was the height in feet above the base to level *x*. Further provisions were provided for the lateral force on parts or portions of buildings or other structures, but the presented provisions above was the extent to what was used in this study.

The 1970 UBC permitted the use of gypsum lath and plaster, gypsum sheathing board, and gypsum wallboard to provide lateral resistance for vertical diaphragms in wood framed wall assemblies. Table No. 47.1 (see Appendix B) from the 1970 UBC provided the allowable shear for seismic forces in pounds per square foot (psf) for these materials.

4.2.2 Pre-1994 Northridge Earthquake Design

Nearly exactly 23 years later, on January 17, 1994 at 4:31am, a magnitude 6.7 earthquake shook the nearly the same location as before in the San Fernando Valley area creating a near perfect "nature experiment" thus presenting the opportunity for evaluating the effectiveness of earthquake policy legislation, building code policies, updated disaster recovery efforts, and the like. Fortunately, this earthquake occurred on a holiday weekend, early in the morning, so the death toll was much lower than what could be expected on a typical Monday during typical working hours. Even still, 71 people died. Mayor Riordan of Los Angeles declared a state of emergency by 5:45am, and by 2:08pm, President Clinton announced a federal declaration of disaster for the area [Comfort (1994)]. Post 1971 San Fernando Valley earthquake, significant changes occurred in seismic hazard mapping, and the legislation and building code standards regarding earthquakes. Most structures built between these two earthquakes incorporated some

form of seismic design. Therefore, the count of 20,000 structures vacated and around 12,500 structures damaged, came as quite a surprise to some. Retrofitted structures were reported to have performed well, and post event, much more technical and complex seismic design provisions began being considered. With the realization that even moderate events can cause billions of dollars of damage, the resulting losses from the 1994 Northridge earthquake sparked a shift in the design paradigm for structural engineers. With damage estimates reaching $49 billion, making this the most costly natural disaster in U.S. history in terms of dollar loss, the birth of the Performance-Based Design (PBD) philosophy was generated.

To provide the design space with a pre-1994 Northridge earthquake and post-1971 San Fernando earthquake seismic design, the 1978 NEHRP provisions [ATC 3-06 (1978)] and the 1988 Uniform Building Code [UBC (1988)] were selected. In 1978, Congress mandated that the Federal Emergency Management Agency (FEMA) implement P.L. 95-124 and initiate the National Earthquake Hazard Reduction Program (NEHRP) in an effort to reduce risk from earthquakes [FEMA (2004)]. In collaboration with the Applied Technology Council (ATC), NEHRP published its first set of seismic provisions in 1978, titled: "Tentative Provisions for the Development of Seismic Regulations for Buildings." The lateral seismic base shear, *V*, which was now expressed as

$$\mathrm{V} = \mathrm{C_s} \cdot \mathrm{W} \qquad \text{Eq. 4 - 5}$$

where *W* is the total gravity load of the building , and is the seismic design coefficient expressed as

$$C_S = \frac{1.2 \cdot A_v \cdot S}{R \cdot T^{2/3}} \qquad \text{Eq. 4 - 6}$$

where is the coefficient for effective peak velocity-related acceleration, *S* is the coefficient for the soil profile characteristics, *R* is the response modification factor (equal to 6.5 for woodframe

structures (Table 3-B in the 1978 NEHRP Provisions)), and *T* is the fundamental period of the building computed using the expression provided in Eq. 4-3. The lateral seismic shear force, , induced at any level was expressed by

$$F_x = C_{vx} \cdot V \qquad \text{Eq. 4 - 7}$$

where

$$C_{vx} = \frac{w_x \cdot h_x^k}{\sum_{i=1}^{n} w_i \cdot w_i^k} \qquad \text{Eq. 4 - 8}$$

where *k* is an exponent related to the building period (*k* = 1 for buildings with a period of 0.5 seconds or less, and k = 2 for buildings with a period of 2.5 seconds or higher, and linear interpolation was used for periods between 0.5 and 2.5 seconds). By this time period (post-1971 to pre-1994), several major changes were made to the seismic provisions: (1) in the computation of the seismic base shear, which now included peak acceleration, soil profile characteristics, and the structural framing system, and (2) the building period was considered through an exponent in the vertical distribution of lateral forces, where buildings with lower periods would have a linear force distribution, and buildings with higher periods would have an exponential force distribution.

Per section 4714(a) of the 1988 UBC, the use of gypsum lath and plaster, gypsum sheathing board, and gypsum wallboard were permitted to provide lateral resistance for vertical diaphragms in wood framed wall assemblies. Table No. 47.1 (see Appendix B) from the 1988 UBC provided the allowable shear for seismic forces in pounds-per-square foot (psf) for these materials.

4.2.3 Modern Seismic Design

Following the two major earthquakes previously discussed, a wealth of research was conducted in an effort to make systematic and powerful changes to the building codes and

seismic provisions so that the disastrous aftermaths of these two earthquakes would not be seen again following future earthquakes. First introduced in the 1991 NEHRP Provisions, but not incorporated until much later, modern seismic design uses maps representing the exceedance probability of seismic intensity in terms of spectral values in a set number of years (10% PE in 250 years, i.e. 1500-year event) based on spectral accelerations for two periods (0.3 sec and 1.0 sec). The seismic hazard equations were set on the B-C boundary (site class), and eventually conversions from the B-C boundary were provided for other site conditions. Modern seismic design codes provide two probabilistic seismic hazard levels: (1) the design basis earthquake (DBE) (10% PE in 50 years, i.e. 500-year event), and (2) the maximum considered earthquake (MCE) (2% PE in 50 years, i.e. 2500-year event).

The ASCE Standard 7-05 [ASCE (2005)] and 2006 International Building Code [IBC (2006)] were selected for the modern seismic design provisions. In the ASCE Standard 7-05, the lateral seismic base shear, *V*, was expressed as it was in Eq. 4 - 5. However, now, the seismic design coefficient, , incorporates the occupancy importance factor, *I*, and the new representation of the seismic hazard using the spectral response acceleration parameters, along with the response modification factor, *R*, and fundamental period, *T*. The computation of becomes significantly more complicated in the modern design codes with the new seismic hazard maps. Five equations are used to determine the final value of , and will not be presented here due to the complexity and also the associated incompleteness without providing a full description of defining the seismic hazard. The approximate fundamental period was expressed as

$$T_a = C_t \cdot h_n^x \qquad \text{Eq. 4 - 9}$$

where is the height in feet above the base to the highest level of the structure, and the coefficients and x are determined based on the structure system ($= 0.02$ and $x = 0.75$ for

woodframe structures). The vertical force distribution is determined the same as was expressed in Eq. 4-7 and Eq. 4-8. It is important to note the significance in the change from previous seismic design being conducted for a single seismic hazard for all of the United States versus now seismic design being based on the actual seismic hazard at the specific building site.

4.2.4 Performance-Based Seismic Retrofit Design

Performance-based seismic design (PBSD) was centered on well-articulated performance objectives based on building owner/stakeholder performance goals. PBSD is used for designing for extreme events, taking the design further than what traditional seismic design provisions provide guidance for. Two performance-based seismic retrofit (PBSR) designs were used in this study, both of which employed the Simplified Direct Displacement Design (SDDD) procedure [Pang et al. (2010)].

Traditional seismic design was based around strength criteria. The height of woodframe construction was limited to four stories, and engineered wood construction was not based on a global seismic design philosophy. Wood elements were not designed at the system-level with collective performance considered, but rather as individual elements which fit together [Pang et al. (2010)]. These facts and shortcomings were the impetus for the SDDD procedure. Pang and Rosowsky (2010) developed the Direct Displacement Design (DDD) procedure which required modal analysis and a set 50% probability of non-exceedance (PNE) for drift limits. The SDDD procedure is a simplified version of DDD which does not require modal analysis, and may be performed at any PNE through an adjustment factor. Once the PNE is selected, and the adjustment is made through an adjustment factor , a design inter-story drift must be selected. Because inter-story drift has been shown to be well-correlated with damage to woodframe structures [Filiatrault and Folz (2004)], the design inter-story drift provides the basis of the limit

states and performance objectives. The vertical distribution of the base shear is computed using the same expression as in Eq. 4-8. A substitute structure is analyzed by applying the centroid of the lateral force distribution at an effective height, which may be expressed as

$$h_{eff} = \sum_i C_{v_i} \cdot h_{oi} \qquad \text{Eq. 4 - 10}$$

where is the vertical distribution factor for the floor provided in Eq. 4-8 , and is the floor height with respect to the ground for the floor. Interpolation was used to determine the effective displacement, , at the effective height. An effective seismic weight, , of the substitute structure was determined by

$$W_{eff} = \frac{(\sum_i W_i \cdot \Delta_{oi})^2}{\sum_i W_i \cdot \Delta_{oi}^2} \qquad \text{Eq. 4 - 11}$$

where is the seismic weight of the floor, and is the displacement of the floor with respect to the ground. The damping reduction factor was computed as

$$\beta_\zeta = \frac{4}{5.6 - \ln(100 \cdot \zeta_{eff})} \qquad \text{Eq. 4 - 12}$$

where

$$\zeta_{eff} = \zeta_{int} + \zeta_{hyst} \qquad \text{Eq. 4 - 13}$$

where is the intrinsic damping and assumed to be 1% in this study, and is the hysteretic damping, which based on experimental studies was determined to be expressed as

$$\zeta_{hyst} = 0.32 e^{-1.38 \frac{K_S}{K_o}} \qquad \text{Eq. 4 - 14}$$

where / was set as 0.3 for this study. The design base shear coefficient was determined using the capacity spectrum approach, and was expressed by

$$C_c = min \begin{cases} \frac{C_{NE} S_{XS}}{B_\zeta} \\ \frac{g}{4\pi^2 \Delta_{eff}} \left(\frac{C_{NE} S_{X1}}{B_\zeta} \right)^2 \end{cases} \qquad \text{Eq. 4 - 15}$$

where g is the acceleration due to gravity, and and are the short period and one second spectral parameters, which are based on the seismic hazard and site conditions, and are also used in the ASCE Standard 7-05 design procedure. Lastly, the design forces are computed, which include the base shear, lateral forces, story shears, overturning moments, and required story secant stiffness. These expressions are not provided here but can be found in Pang et al (2010). Shearwalls are then selected and distributed throughout the building floorplan using the shearwall backbone forces at the target ISD to meet the required story shear.

4.2.5 Soft-Story-Only Retrofit Design

Soft-story woodframe buildings have long been recognized as a disaster preparedness issue. FEMA began the Applied Technology Council (ATC) Project 71.1 which would eventually result in the FEMA P-807 Guidelines [FEMA (2012a)] for retrofitting soft-story woodframe buildings. The FEMA P-807 Guidelines were developed to aid practicing engineers in retrofitting soft-story woodframe buildings in a cost-effective and practical manner for quick and consistent implementation. Within the FEMA P-807 Guidelines, the retrofit is to be constrained to the soft-story with the intent of limiting disruption to the building's occupants. The soft-story-only retrofit must be adequate to prevent the building from collapsing at the first story while not being too stiff or strong to potentially collapse the upper stories by driving the earthquake forces upward. The building owner and other stakeholders can set specific performance objectives for retrofitting the building. The FEMA P-807 Guidelines emphasize that the retrofit is not meant to prevent the soft-story building from being damaged during a seismic event, but rather to prevent the building from collapse and to achieve shelter-in-place following the earthquake. It is critical to note here that the FEMA P-807 Guidelines do not

necessarily provide a soft-story structure with a full design code-compliant retrofit. This decision is left to the stakeholders including local and regional governments and building officials.

The FEMA P-807 Guidelines were selected as one of the retrofit options in this study due to their uniqueness in methodology relative to the other selected provisions, and assumed future widespread use. In order for a retrofit to meet the FEMA P-807 Guidelines it must meet the criteria in three categories: (1) eligibility constraints, (2) strength requirements, and (3) an eccentricity limit. The eligibility constraints are based on geometry and construction, the details of which can be found in the FEMA P-807 (2012a). The general eligibility requirements restrict the building to no more than four woodframe above-grade stories without an above-grade concrete podium supporting the structure, and require that appropriate soil type and site class adjustment factors be used. The strength requirements specify that the retrofitted building's spectral capacity in each principal direction exceeds the spectral demand. Drift limits are provided for two cases in association with the strength requirements: (1) 4% maximum drift is acceptable for high-displacement capacity stories; and (2) 1.25% maximum drift is acceptable for the low-displacement capacity stories. The FEMA P-807 Guidelines specify the various materials that can qualify a building story as either high-displacement (i.e. wood structural panels, horizontal wood siding, gypsum wall board, etc.) or low-displacement (i.e., stucco, plaster on wood or gypsum lath, diagonal wood sheathing, etc.). The premise of the methodology focuses on eliminating torsion since it exacerbates the soft-story condition and gives rise to structural collapse. In support of this, the eccentricity limits recommend that zero eccentricity between the first-story center of strength and second-story center of strength remains following the retrofit. If this is not possible, the maximum acceptable eccentricity must be less

than 10% of the corresponding building dimension. A free downloadable software, the weak-story tool, is available from FEMA's website for executing the FEMA P-807 procedure.

4.3 Shearwall Parameters

For the pre-1971 San Fernando Earthquake design used in this dissertation, horizontal wood siding (HWS) was used as the exterior wall sheathing material and plaster on wood lath was used as the interior wall sheathing material. These walls were modeled by the CUREE 10-parameter hysteretic model [Folz and Filatrault (2001)] graphically represented in Figure 4-1. The 10 parameter hysteretic model for the HWS walls was obtained from Bahmani and van de Lindt (2013). In that study, cyclic tests were conducted on a number of 8 ft × 8 ft (2.44 m × 2.44 m) shearwalls sheathed with various materials. The specimens with HWS were composed of a single layer of 1×8 (25 mm × 203 mm) Spruce-Pine-Fir (SPF) wood siding attached to the framing studs by 8d common nails with a shank diameter of 0.134 in. (3.4 mm), shank length of 2.5 in. (63.5 mm), and head diameter of 9/32 in (7.1 mm). The framing consisted of 2×4 dimension lumber spaced at 16 in. (406.4 mm) on center, with a single bottom plate and double top plate. The 10 parameter hysteretic parameters for the plaster on wood lath (PWL) were provided in Pang et al. (2012), which were obtained from experimental testing conducted in the 1950s at the Forest Products Laboratory [Trayer (1956)]. The PWL walls were composed of the same framing method and spacings as previous walls, but with No. 1 common well-seasoned southern yellow pine lumber. The experimentally tested PWL walls were 9 ft × 14 ft, (2.74 m × 4.27 m) which required 12 in. (304.8 mm) spacing between the outer studs on each side of the wall. The wood lath were 4 ft (1.22 m) long, spaced at 0.25 in. (6.35 mm) and nailed with 3d nails, and grounds were 0.75 in. (19.05 mm). The plaster proportions were 100 lbs to 175 lbs of plaster to sand, respectively. Two coats were applied to the wall, and allowed one week to cure

prior to testing. In the pre-1971 San Fernando Earthquake designs, only the allowable shear for the PWL walls was used to meet the required design shear, and not the HWS. Although the use of gypsum wallboard was allowed by the 1970 UBC, it was not typical of this era to use such a sheathing material. Therefore, it was not used in the pre-1971 San Fernando Earthquake designs.

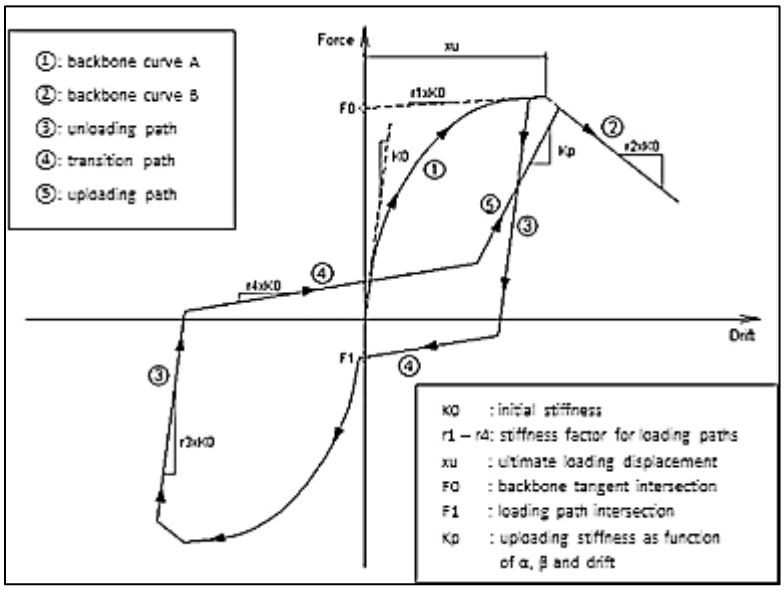

Figure 4-1: CUREE 10-Parameter Hysteretic Model
(figure excerpted from Pei and van de Lindt (2010))

For the pre-1994 Northridge Earthquake design, stucco was used as the exterior wall sheathing material and gypsum wallboard was used as the interior wall sheathing material. Only the allowable shear of the GWB was used in the archetype design to meet the required design shear. In this case, the full wall assembly was modeled using either GWB sheathing on both sides of the framing, or GWB on one side and stucco on the other side. The double-sided GWB shearwall was modeled using the CUREE 10-parameter hysteretic model. The stucco/GWB wall was modeled using the 16-parameter Evolutionary Parameter Hysteretic Model (EPHM) hysteretic model [Pang et al. (2007)], graphically represented in Figure 4-2. The GWB, GWB/GWB, Stucco, and Stucco/GWB parameter sets were obtained from Bahmani and van de Lindt (2013). The GWB assembly was composed of 0.5 in. (12.7 mm) thick regular GWB

fastened to framing studs with #6 coarse thread bugle head drywall screws at 16 in spacing. The GWB panels were installed vertically and the edge at the middle was sealed with mud and mesh tape. The stucco assembly was composed of 7/8 in. (22.2 mm) thick stucco consisting of five sub layers: a weather barrier layer, wire lath, a scratch coat, a brown coat, and a finish coat. For the experimental testing conducted by Bahmani and van de Lindt (2013), the stucco walls were intended to resemble 1920's to 1950's construction styles as closely as possible, and the stucco specimens were stated to have fully cured prior to the cyclic testing.

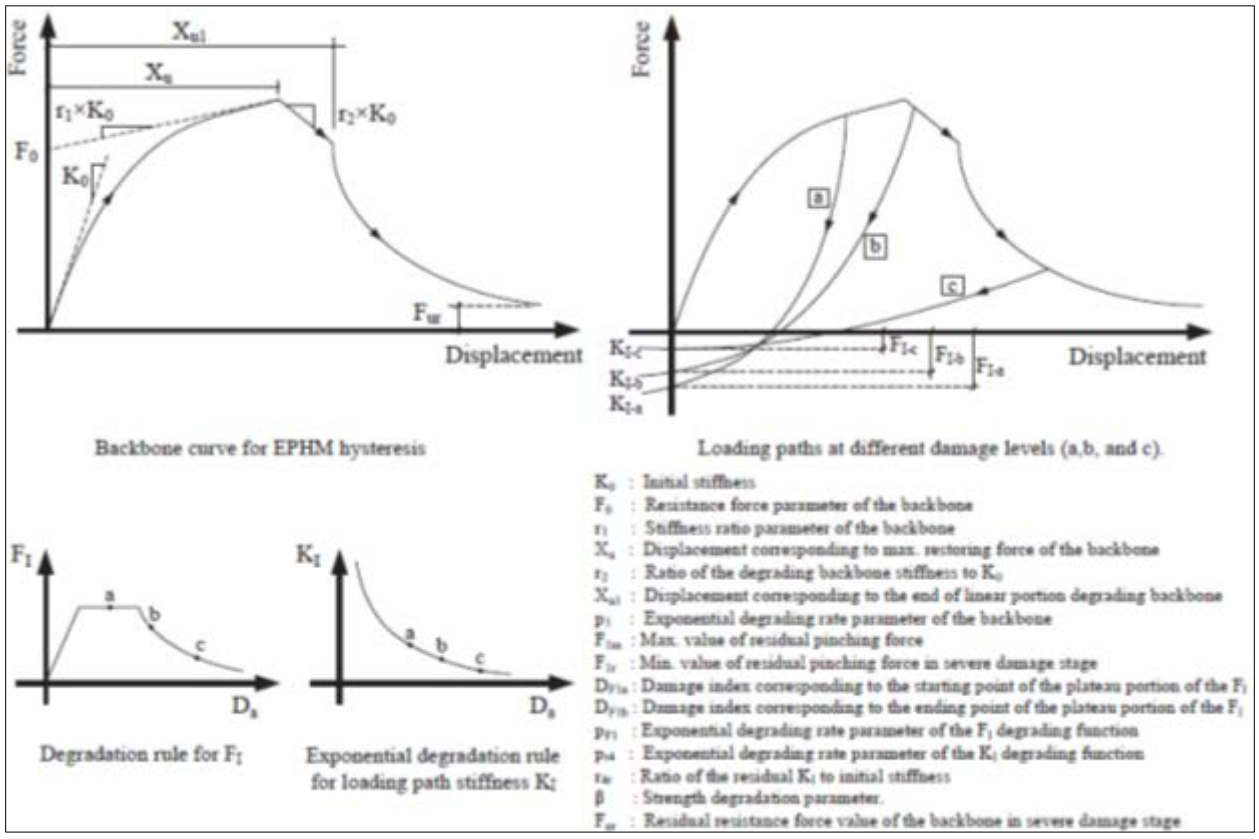

Figure 4-2: EPHM sixteen-parameter hysteretic model
(figure excerpted from Bahmani and van de Lindt (2013))

For all of the modern seismic design codes and retrofits (post-1994 Northridge Earthquake designs), stucco was used as the exterior wall sheathing material, GWB was used as the interior wall sheathing material, and 15/32 in. oriented strand board (OSB) sheathing was

used as the shearwall sheathing material. Only the allowable shear of the OSB-sheathed shearwalls was used for providing the lateral resistance for the archetypes. The non-structural walls were modeled as complete wall assemblies, either GWB/GWB or Stucco/GWB. For the portions of these walls which needed to be modified to shearwalls, the OSB sheathed wall was modeled separately and the multiple wall assemblies were superimposed in the numerical model. The shearwalls were distributed throughout the floor plan to provide lateral symmetry to the furthest extent possible avoiding the addition of shearwall length above the design requirement. The 10-parameter hysteretic models for all OSB sheathed shearwalls were obtained from Pang et al. (2010).

Table 4-1 provides the 10 parameter hysteretic models in per-foot values for all wall types used in this study. Table 4-2 provides the 16 parameter hysteretic models in per-foot values for all wall types used in the study. The seismic coefficient, C or , for the archetypes designed by the 1959 SEAOC provisions, 1978 NEHRP provisions, and the 2005 ASCE-7 Standard were 0.10, 0.15, and 0.154, respectively. Table 4-3 provides the weight, W, and the design base shear, V, used in the design for each of the archetypes.

Table 4-8: CUREE 10-hysteretic parameters for walls

Sheathing	*K0 (k/in/ft)*	*F0 (k/ft)*	*F1 (k/ft)*	*r1*	*r2*	*r3*	*r4*	*Xu (in)*	*α*	*β*
	0.110	0.050	0.020	0.128	-0.050	1.03	0.070	8.19	0.395	1.075
	2.146	0.395	0.047	0.020	-0.330	1.02	0.007	0.669	0.800	1.050
Stucco	2.695	0.295	0.040	0.045	-0.038	1.00	0.005	0.745	0.775	1.050
	0.520	0.090	0.010	0.045	-0.059	1.04	0.007	1.135	0.750	1.050
GWB/GWB	1.0625	0.187	0.02	0.045	-0.059	1.03	0.006	1.14	0.75	1.05
SPly (6/12)[4]	2.359	0.675	0.091	0.025	-0.049	1.01	0.019	1.841	0.714	1.286
SPly (4/12)	3.028	1.006	0.146	0.026	-0.056	1.01	0.022	1.850	0.759	1.286
SPly (3/12)	3.787	1.277	0.170	0.032	-0.060	1.01	0.023	1.898	0.714	1.286
SPly (2/12)	4.232	1.989	0.248	0.030	-0.073	1.01	0.033	1.972	0.759	1.241
DPly (6/12)[5]	3.459	1.499	0.087	0.009	-0.054	1.01	0.028	1.652	0.759	1.286
DPly (4/12)	4.171	2.202	0.121	0.013	-0.068	1.01	0.035	1.735	0.759	1.241
DPly (3/12)	4.582	2.916	0.155	0.024	-0.084	1.01	0.040	1.791	0.814	1.241
DPly (2/12)	5.171	4.315	0.255	0.046	-0.114	1.01	0.053	1.990	0.723	1.150

Horizontal wood siding [Bahmani and van de Lindt (2013)]
on wood lath [Pang et al. (2012)]
wallboard [Bahmani and van de Lindt (2013)]
-ply OSB sheathing [Pang et al. (2010)]
[5] Double-ply OSB sheathing [Pang et al. (2010)]

Table 4-9: EPHM 16-hysteretic parameters for wall

Wall	*K0 (k/in/ft)*	*F0 (k/ft)*	*r1*	*Xu (in)*	*r2*	*Xu1 (in)*	*P1*	*F1m (k/ft)*
Stucco/GWB	2.75	0.525	0.05	1.25	-0.15	1.5	-0.48	0.3125
Wall	*F1r (k/ft)*	*Df1a (in)*	*Dflb (in)*	*PF1*	*Pr4*	*r4r*	*β*	*Fur (k/ft)*
Stucco/GWB	0.00625	0.625	1.5	-0.2	-0.5	0.0001	1.07	0.1063

Table 4-10: Archetype parametric values used in seismic design codes

Design Code	*1959 SEAOC*		*1978 NEHRP*		*ASCE7-05*	
Floor Plan	*W (kip)*	*V (kip)*	*W (kip)*	*V (kip)*	*W (kip)*	*V (kip)*
1	29	2.9	25.7	3.9	24.2	3.7
2	67.1	6.7	68	10.4	57.8	8.9
3	201	20.1	181	27.8	147.5	22.7
4	371	40	351.7	54.1	288.7	44.4
5	34.1	3.4	31.7	4.9	28.6	4.4
6	43.7	4.4	41.2	6.3	40	6.2
7	489.5	57	443	68.1	392.2	60.3

4.4 Archetypes

Seven floor plans were selected as the base archetypes for this study, these include: (1) a one-story house without a garage, (2) a two-story house with a garage, (3) a two-story three-unit townhouse, (4) a three-story ten-unit soft-story apartment building with tuck-under parking, (5) a one-story house with a garage, (6) a two-story house with a garage, (7) a four-story soft-story commercial mid-rise office building with large open space on the bottom story creating a torsional irregularity. The base floor plans for these seven buildings are provided in Figure 4-3 through Figure 4-9, respectively. The first four floor plans came from Reitherman and Cobeen (2003), the remaining fifth and sixth floor plans came from Pei (2007), and the seventh floor plan was taken from FEMA (2012a) with new dimensions assigned. Together, the seven were felt to be representative of the woodframe building stock present in California. Each of the seven archetypes were designed to the four design codes previously discussed: 1959 SEAOC Blue Book (1959 Blue Book), 1978 NEHRP, ASCE Standard 7-05 (ASCE7-05), and the Simplified Direct Displacement Design (SDDD). The archetypes were designed twice by the SDDD procedure. The first SDDD was a superior level design to the limit state of life safety (SDDD-

LS) which was set to have a 50% PNE of 3.00% ISD when subjected to a MCE seismic hazard. The second SDDD was an excellent level design to the limit state of immediate occupancy (SDDD-IO) which was set to have a 50% PNE of 1.00% ISD when subjected to a MCE seismic hazard. Additionally, the two soft-story woodframe buildings (see Figure 4-6 and Figure 4-9) were retrofitted following the FEMA P-807 procedure using the weak-story tool. This provided a total of 37 archetypes for the design space. The floor plans presented in Figure 4-3 through Figure 4-9 provide limited dimensions with wall identification numbers labeled. The wall identification numbers were assigned to those walls which were available to be structural shearwalls in any of the 37 archetype designs. The sheathing and length for each shearwall in each of the archetypes are provided in Table 4-4 through Table 4-12 for each floor plan, respectively, with the seismic design provision listed. The sheathing was listed by short hand using the same notation as in Table 4-1.

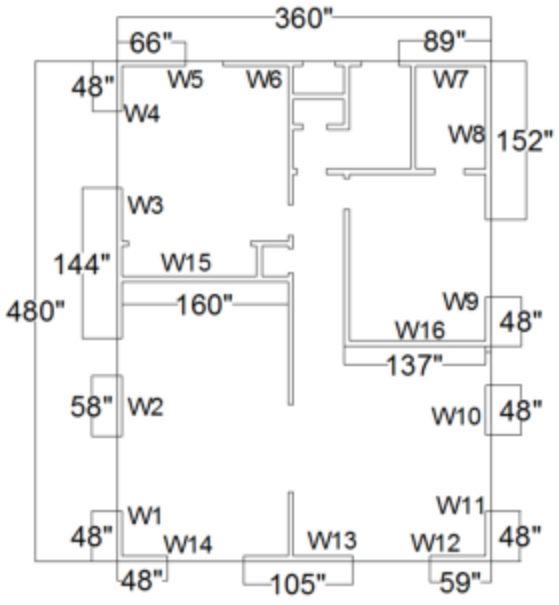

Figure 4-1: Floor Plan 1 - One-Story House without a Garage

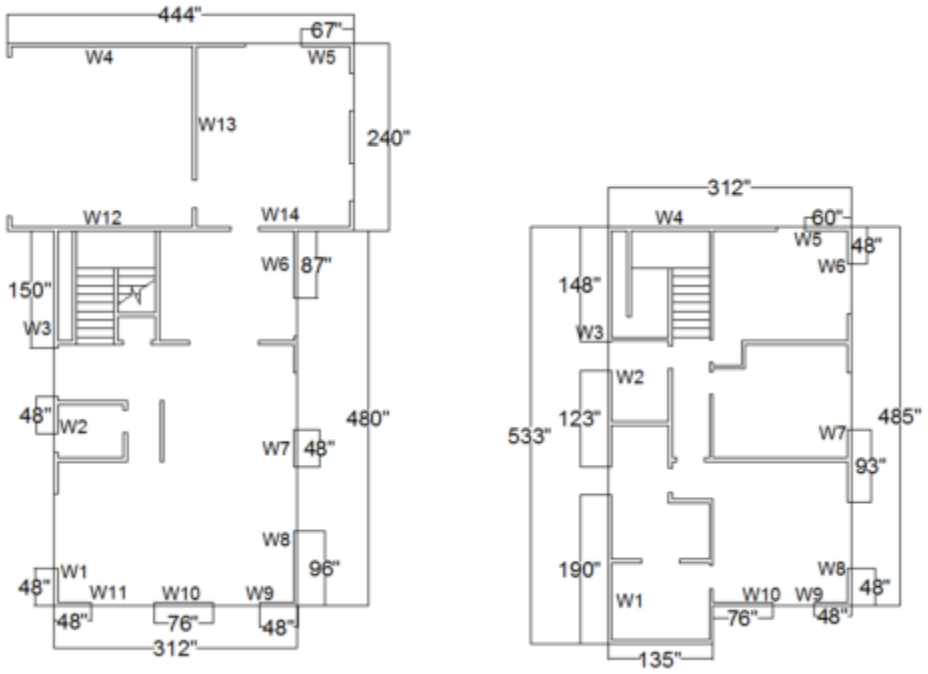

(a) (b)

Figure 4-2: Floor Plan 2 - Two-Story House with a Garage: (a) First Story; (b) Second Story

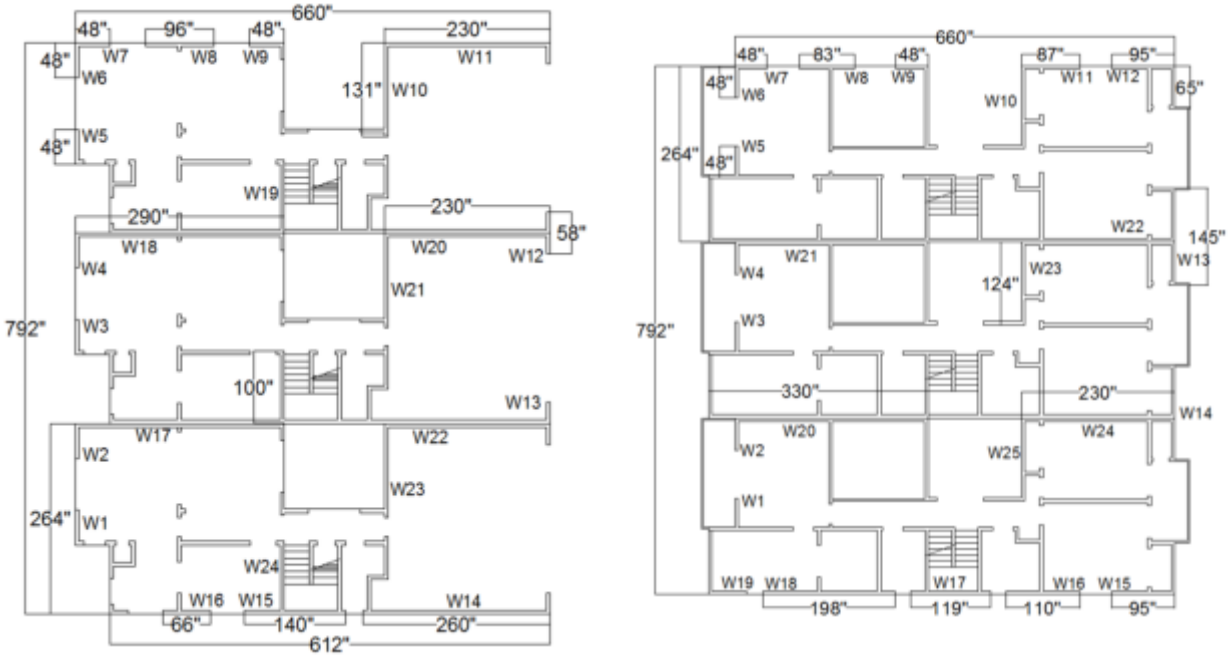

(a) (b)

Figure 4-3: Floor Plan 3 - Two-Story Three-Unit Townhouse: (a) Unit 1; (b) Unit 2; (c) Unit 3

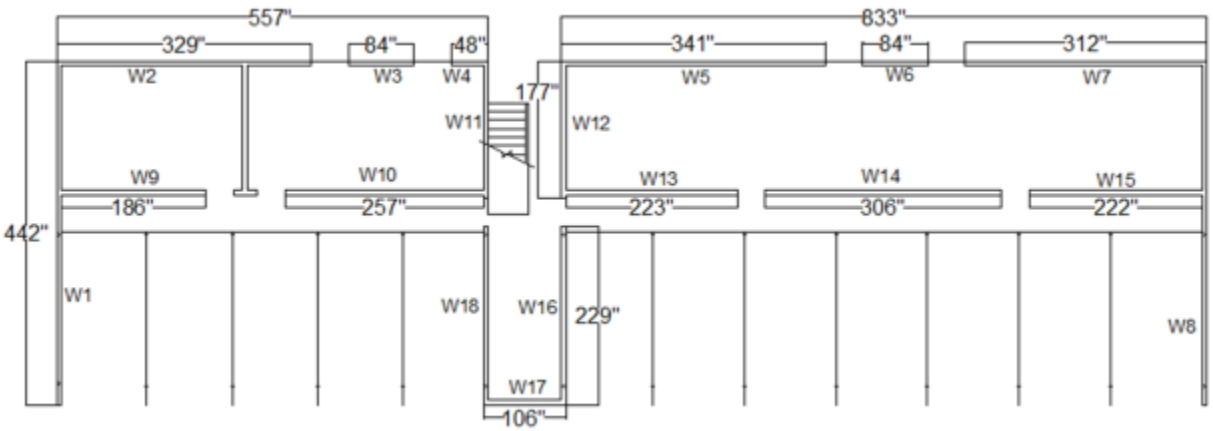

(a)

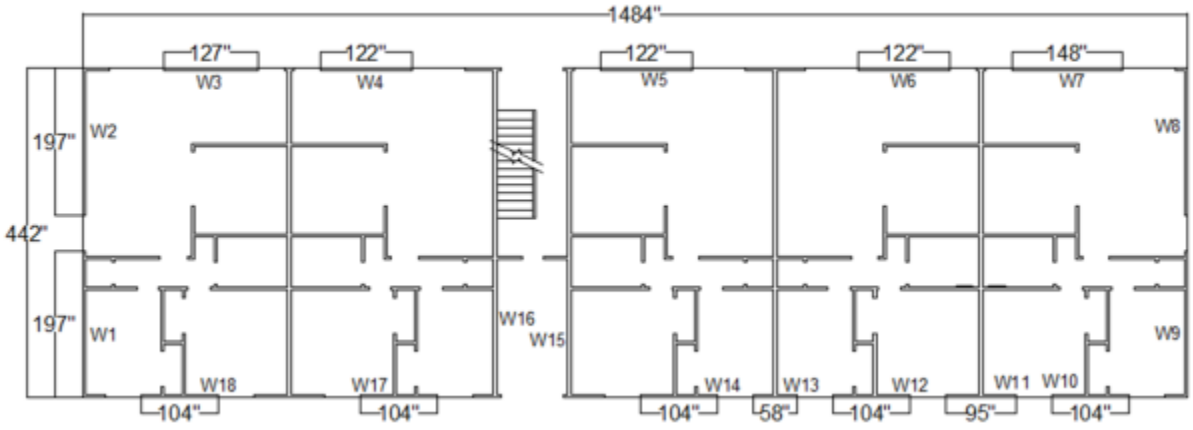

(b)

Figure 4-4: Floor Plan 4 - Three-Story Ten-Unit Soft-Story Apartment Building: (a) First Story; (b) Upper Stories

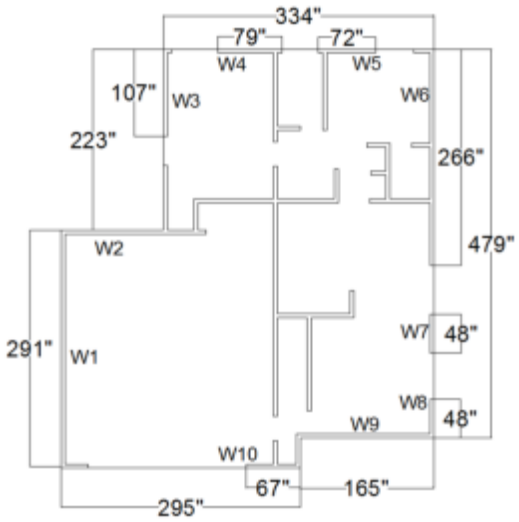

Figure 4-5: Floor Plan 5 – One-Story House with a Garage

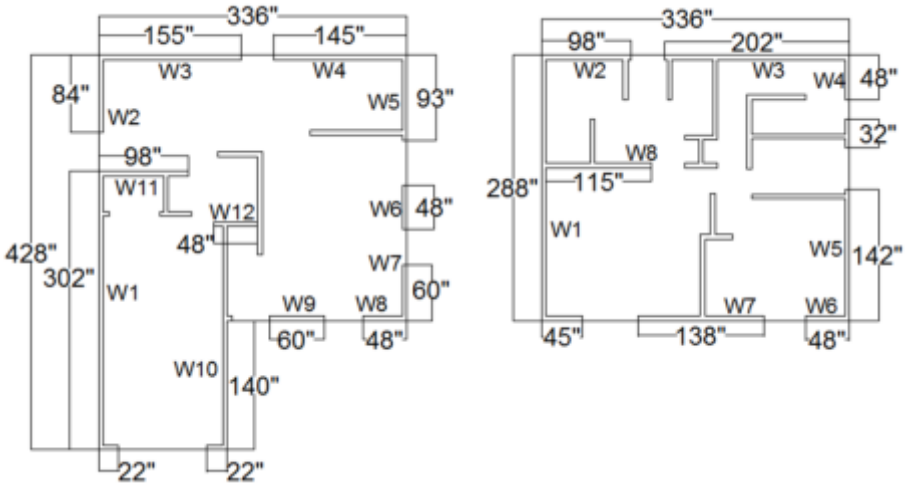

Figure 4-6: Floor Plan 6 - Two-Story House with a Garage

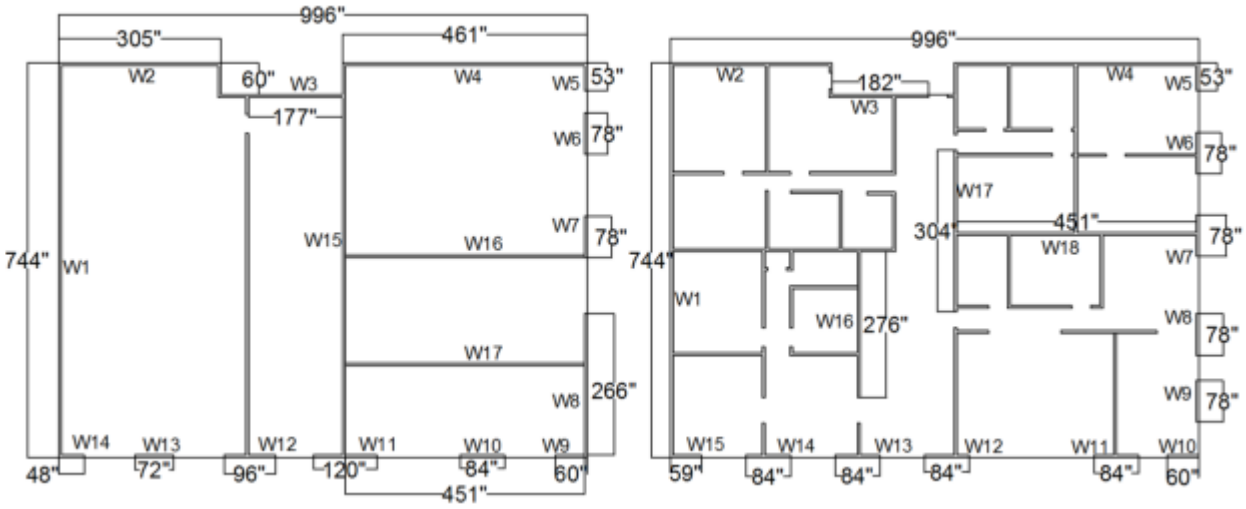

(a) (b)

Figure 4-7: Floor Plan 7 – Four-Story Soft-Story Office Building with Garage Doors Lining Large Portions of Bottom Story: (a) First Story; (b) Upper Stories

Table 4-11: Floor Plan 1 – Shearwall Locations

Design Code	*ASCE7-05*		*SDDD-LS*		*SDDD-IO*	
Wall ID	*Retrofit Length (in)*	*Retrofit ID*	*Retrofit Length (in)*	*Retrofit ID*	*Retrofit Length (in)*	*Retrofit ID*
W1	-	-	48	SPly (6/12)	48	SPly (6/12)
W2	-	-	48	SPly (6/12)	48	SPly (6/12)
W3	48	SPly (6/12)	48	SPly (6/12)	48	SPly (6/12)
W4	-	-	48	SPly (6/12)	48	SPly (6/12)
W5	-	-	48	SPly (6/12)	48	SPly (6/12)
W6	48	SPly (6/12)	48	SPly (6/12)	48	SPly (6/12)
W7	-	-	48	SPly (6/12)	48	SPly (6/12)
W8	-	-	96	SPly (6/12)	96	SPly (6/12)
W9	48	SPly (6/12)	-	-	-	-
W10	-	-	48	SPly (6/12)	48	SPly (6/12)
W11	-	-	48	SPly (6/12)	48	SPly (6/12)
W12	-	-	48	SPly (6/12)	48	SPly (6/12)
W13	48	SPly (6/12)	48	SPly (6/12)	48	SPly (6/12)
W14	-	-	48	SPly (6/12)	48	SPly (6/12)
W15	-	-	48	SPly (6/12)	48	SPly (6/12)
W16	-	-	48	SPly (6/12)	48	SPly (6/12)

Table 4-12: Floor Plan 2 - Shearwall Locations

Design Code		*ASCE7-05*		*SDDD-LS*		*SDDD-IO*	
Story	*Wall ID*	*Retrofit Length (in)*	*Retrofit ID*	*Retrofit Length (in)*	*Retrofit ID*	*Retrofit Length (in)*	*Retrofit ID*
Story 1	W1	48	SPly (6/12)	48	SPly (6/12)	48	SPly (3/12)
	W2	-	-	48	SPly (6/12)	48	SPly (3/12)
	W3	-	-	87	SPly (6/12)	150	SPly (3/12)
	W4	-	-	84	SPly (4/12)	48	SPly (3/12)
	W5	-	-	67	SPly (4/12)	67	SPly (3/12)
	W6	-	-	87	SPly (6/12)	87	SPly (3/12)
	W7	-	-	48	SPly (6/12)	48	SPly (3/12)
	W8	-	-	48	SPly (6/12)	48	SPly (3/12)
	W9	48	SPly (6/12)	48	SPly (6/12)	48	SPly (3/12)
	W10	48	SPly (6/12)	76	SPly (6/12)	76	SPly (3/12)
	W11	-	-	48	SPly (6/12)	48	SPly (3/12)
	W12	48	SPly (6/12)	80	SPly (6/12)	60	SPly (3/12)
	W13	48	SPly (6/12)	144	SPly (6/12)	120	SPly (3/12)
	W14	48	SPly (6/12)	60	SPly (6/12)	60	SPly (3/12)
Story 2	W1	-	-	48	SPly (6/12)	48	SPly (3/12)
	W2	48	SPly (6/12)	48	SPly (6/12)	48	SPly (3/12)
	W3	-	-	48	SPly (6/12)	48	SPly (3/12)
	W4	48	SPly (6/12)	48	SPly (6/12)	80	SPly (3/12)
	W5	-	-	48	SPly (6/12)	60	SPly (3/12)
	W6	-	-	48	SPly (6/12)	48	SPly (3/12)

	W7	48	SPly (6/12)	48	SPly (6/12)	48	SPly (3/12)
	W8	-	-	48	SPly (6/12)	48	SPly (3/12)
	W9	-	-	48	SPly (6/12)	48	SPly (3/12)
	W10	48	SPly (6/12)	48	SPly (6/12)	76	SPly (3/12)

Table 4-13: Floor Plan 3 - Multi-Story Shearwall Locations

Design		*ASCE7-05*		*SDDD-LS*		*SDDD-IO*	
Story	*Wall ID*	*Retrofit Length (in)*	*Sheathing Material*	*Retrofit Length (in)*	*Retrofit ID*	*Retrofit Length (in)*	*Retrofit ID*
Story 1	W1	-	-	48	SPly (6/12)	48	SPly (6/12)
	W2	48	SPly (6/12)	48	SPly (6/12)	48	SPly (6/12)
	W3	-	-	48	SPly (6/12)	48	SPly (6/12)
	W4	48	SPly (6/12)	48	SPly (6/12)	48	SPly (6/12)
	W5	-	-	48	SPly (6/12)	48	SPly (6/12)
	W6	48	SPly (6/12)	48	SPly (6/12)	48	SPly (6/12)
	W7	48	SPly (6/12)	48	SPly (6/12)	48	SPly (6/12)
	W8	-	-	96	SPly (6/12)	96	SPly (6/12)
	W9	-	-	48	SPly (6/12)	48	SPly (6/12)
	W10	48	SPly (6/12)	131	SPly (6/12)	131	SPly (6/12)
	W11	48	SPly (6/12)	230	SPly (6/12)	230	SPly (6/12)
	W12	48	SPly (6/12)	58	SPly (6/12)	58	SPly (6/12)
	W13	48	SPly (6/12)	58	SPly (6/12)	58	SPly (6/12)
	W14	48	SPly (6/12)	144	SPly (6/12)	66	SPly (6/12)
	W15	-	-	140	SPly (6/12)	140	SPly (6/12)
	W16	48	SPly (6/12)	66	SPly (6/12)	66	SPly (6/12)
	W17	48	SPly (6/12)	-	-	290	SPly (6/12)
	W18	48	SPly (6/12)	-	-	290	SPly (6/12)
	W19	-	-	-	-	100	SPly (6/12)
	W20	48	SPly (6/12)	-	-	230	SPly (6/12)
	W21	48	SPly (6/12)	131	SPly (6/12)	131	SPly (6/12)
	W22	48	SPly (6/12)	-	-	230	SPly (6/12)
	W23	48	SPly (6/12)	131	SPly (6/12)	131	SPly (6/12)
	W24	-	-	-	-	100	SPly (6/12)
Story 2	W1	-	-	48	SPly (6/12)	48	SPly (6/12)
	W2	48	SPly (6/12)	48	SPly (6/12)	48	SPly (6/12)
	W3	-	-	48	SPly (6/12)	48	SPly (6/12)
	W4	48	SPly (6/12)	48	SPly (6/12)	48	SPly (6/12)
	W5	-	-	48	SPly (6/12)	48	SPly (6/12)
	W6	48	SPly (6/12)	48	SPly (6/12)	48	SPly (6/12)
	W7	48	SPly (6/12)	48	SPly (6/12)	48	SPly (6/12)
	W8	-	-	83	SPly (6/12)	83	SPly (6/12)
	W9	-	-	48	SPly (6/12)	48	SPly (6/12)
	W10	48	SPly (6/12)	124	SPly (6/12)	124	SPly (6/12)
	W11	-	-	87	SPly (6/12)	87	SPly (6/12)
	W12	48	SPly (6/12)	95	SPly (6/12)	95	SPly (6/12)
	W13	58	SPly (6/12)	58	SPly (6/12)	58	SPly (6/12)
	W14	58	SPly (6/12)	58	SPly (6/12)	58	SPly (6/12)
	W15	48	SPly (6/12)	95	SPly (6/12)	66	SPly (6/12)

	W16	-	-	-	-	-	-
	W17	-	-	119	SPly (6/12)	119	SPly (6/12)
	W18	-	-	66	SPly (6/12)	66	SPly (6/12)
	W19	48	SPly (6/12)	-	-	-	-
	W20	48	SPly (6/12)	-	-	290	SPly (6/12)
	W21	48	SPly (6/12)	-	-	290	SPly (6/12)
	W22	48	SPly (6/12)	-	-	-	-
	W23	48	SPly (6/12)	-	-	-	-
	W24	48	SPly (6/12)	-	-	230	SPly (6/12)
	W25	48	SPly (6/12)	124	SPly (6/12)	124	SPly (6/12)

addition to the designs shown in the table, the 1978 NEHRP design required three SPly (6/12) on walls W3, W4, and W21, with lengths 48”, 48”, and 131”, respectively.

Table 4-14: Floor Plan 4 - Multi-Story Shearwall Locations

Design Code		*ASCE7-05*		*SDDD-LS*		*SDDD-IO*	
Story	*Wall ID*	*Retrofit Length (in)*	*Sheathing Material*	*Retrofit Length (in)*	*Retrofit ID*	*Retrofit Length (in)*	*Retrofit ID*
Story 1	W1	288	SPly (6/12)	442	SPly (6/12)	442	SPly (2/12)
	W2	192	SPly (6/12)	329	SPly (6/12)	329	SPly (3/12)
	W3	-	-	-	-	84	SPly (3/12)
	W4	-	-	-	-	48	SPly (3/12)
	W5	-	-	-	-	341	SPly (3/12)
	W6	-	-	-	-	84	SPly (3/12)
	W7	192	SPly (6/12)	312	SPly (6/12)	312	SPly (3/12)
	W8	288	SPly (6/12)	442	SPly (6/12)	442	SPly (2/12)
	W9	96	SPly (6/12)	186	SPly (6/12)	186	SPly (4/12)
	W10	-	-	-	-	257	SPly (4/12)
	W11	-	-	-	-	177	SPly (4/12)
	W12	-	-	177	SPly (6/12)	177	SPly (2/12)
	W13	-	-	-	-	223	SPly (4/12)
	W14	-	-	-	-	306	SPly (4/12)
	W15	96	SPly (6/12)	222	SPly (6/12)	222	SPly (4/12)
	W16	72	SPly (6/12)	229	SPly (6/12)	229	SPly (2/12)
	W17	96	SPly (6/12)	106	SPly (2/12)	106	SPly (2/12)
	W18	72	SPly (6/12)	-	-	229	SPly (4/12)
Story 2	W1	96	SPly (6/12)	197	SPly (6/12)	197	SPly (2/12)
	W2	96	SPly (6/12)	197	SPly (6/12)	197	SPly (2/12)
	W3	96	SPly (6/12)	127	SPly (6/12)	127	SPly (2/12)
	W4	-	-	122	SPly (6/12)	122	SPly (2/12)
	W5	-	-	122	SPly (6/12)	122	SPly (2/12)
	W6	-	-	-	-	122	SPly (2/12)
	W7	96	SPly (6/12)	148	SPly (6/12)	148	SPly (2/12)
	W8	96	SPly (6/12)	197	SPly (6/12)	197	SPly (2/12)
	W9	96	SPly (6/12)	197	SPly (6/12)	197	SPly (2/12)
	W10	96	SPly (6/12)	104	SPly (6/12)	104	SPly (2/12)
	W11	-	-	-		95	SPly (2/12)
	W12	-	-	104	SPly (6/12)	104	SPly (2/12)
	W13	-	-	-	-	58	SPly (2/12)
	W14	-	-	104	SPly (6/12)	104	SPly (2/12)
	W15	-	-			442	SPly (6/12)
	W16	-	-	-	-	442	SPly (3/12)
	W17	-	-	104	SPly (6/12)	104	SPly (2/12)
	W18	96	SPly (6/12)	104	SPly (6/12)	104	SPly (2/12)
Story 3	W1	60	SPly (6/12)	148	SPly (6/12)	197	SPly (3/12)
	W2	60	SPly (6/12)	148	SPly (6/12)	197	SPly (3/12)
	W3	60	SPly (6/12)	127	SPly (6/12)	127	SPly (3/12)

	W4	-	-	-	-	122	SPly (3/12)
	W5	-	-	-	-	122	SPly (3/12)
	W6	-	-	-	-	-	-
	W7	60	SPly (6/12)	148	SPly (6/12)	148	SPly (3/12)
	W8	60	SPly (6/12)	148	SPly (6/12)	197	SPly (3/12)
	W9	60	SPly (6/12)	148	SPly (6/12)	197	SPly (3/12)
	W10	60	SPly (6/12)	104	SPly (6/12)	104	SPly (3/12)
	W11	-	-	-	-	-	-
	W12	-	-	-	-	104	SPly (3/12)
	W13	-	-	-	-	-	-
	W14	-	-	104	SPly (6/12)	104	SPly (3/12)
	W15	-	-			442	SPly (6/12)
	W16	-	-	-	-	-	-
	W17	-	-	-	-	104	SPly (3/12)
	W18	60	SPly (6/12)	104	SPly (6/12)	104	SPly (3/12)

Table 4-15: Floor Plan 4 - Soft-Story-Only Shearwall Locations

Design Code	*1959 Blue Book*		*1978 NEHRP*		*FEMA P-807*	
Wall ID	*Retrofit Length (in)*	*Shearwall ID*	*Retrofit Length (in)*	*Shearwall ID*	*Retrofit Length (in)*	*Retrofit ID*
W1	442	SPly (6/12)	442	SPly (6/12)	-	-
W2	-	-	-	-	-	-
W3	-	-	-	-	-	-
W4	-	-	-	-	-	-
W5	-	-	-	-	-	-
W6	-	-	-	-	-	-
W7	-	-	-	-	-	-
W8	442	SPly (6/12)	442	SPly (6/12)	264	SPly (4/12)
W9	186	SPly (6/12)	186	SPly (6/12)	-	-
W10	-	-	-	-	257	SPly (2/12)
W11	-	-	-	-	-	-
W12	-	-	-	-	-	-
W13	-	-	-	-	223	SPly (2/12)
W14	-	-	-	-	-	-
W15	222	SPly (6/12)	222	SPly (6/12)	-	-
W16	-	-	-	-	229	SPly (4/12)
W17	106	SPly (3/12)	106	SPly (3/12)	107	DPly (2/12)
W18	-	-	-	-	229	DPly (2/12)

Table 4-16: Floor Plan 5 - Shearwall Locations

Design Code	*ASCE7-05*		*SDDD-LS*		*SDDD-IO*	
Wall ID	*Retrofit Length (in)*	*Retrofit ID*	*Retrofit Length (in)*	*Retrofit ID*	*Retrofit Length (in)*	*Retrofit ID*
W1	48	SPly (6/12)	144	SPly (6/12)	144	SPly (6/12)
W2	-	-	126	SPly (6/12)	126	SPly (6/12)
W3	-	-	107	SPly (6/12)	107	SPly (6/12)
W4	48	SPly (6/12)	79	SPly (6/12)	79	SPly (6/12)
W5	-	-	72	SPly (6/12)	72	SPly (6/12)
W6	48	SPly (6/12)	155	SPly (6/12)	155	SPly (6/12)
W7	-	-	48	SPly (6/12)	48	SPly (6/12)
W8	-	-	48	SPly (6/12)	48	SPly (6/12)
W9	-	-	165	SPly (6/12)	165	SPly (6/12)
W10	48	SPly (6/12)	67	SPly (6/12)	67	SPly (6/12)

Table 4-17: Floor Plan 6 - Shearwall Locations

Design Code		*ASCE7-05*		*SDDD-LS*		*SDDD-IO*	
Story	*Wall ID*	*Retrofit Length (in)*	*Retrofit ID*	*Retrofit Length (in)*	*Retrofit ID*	*Retrofit Length (in)*	*Retrofit ID*
Story 1	W1	48	SPly (6/12)	132	SPly (6/12)	188	SPly (6/12)
	W2	-	-	48	SPly (6/12)	84	SPly (6/12)
	W3	-	-	48	SPly (4/12)	155	SPly (6/12)
	W4	48	SPly (6/12)	48	SPly (4/12)	145	SPly (6/12)
	W5	-	-	48	SPly (6/12)	93	SPly (6/12)
	W6	48	SPly (6/12)	48	SPly (6/12)	48	SPly (6/12)
	W7	-	-	-	-	-	-
	W8	-	-	48	SPly (4/12)	48	SPly (3/12)
	W9	48	SPly (6/12)	48	SPly (4/12)	60	SPly (3/12)
	W10	-	-	84	SPly (6/12)	140	SPly (6/12)
	W11	-	-	48	SPly (6/12)	48	SPly (6/12)
	W12	-	-	-	-	48	SPly (4/12)

Story 2	W1	48	SPly (6/12)	96	SPly (6/12)	132	SPly (4/12)
	W2	-	-	48	SPly (6/12)	96	SPly (6/12)
	W3	48	SPly (6/12)	48	SPly (6/12)	96	SPly (6/12)
	W4	-	-	48	SPly (6/12)	48	SPly (4/12)
	W5	48	SPly (6/12)	48	SPly (6/12)	48	SPly (4/12)
	W6	-	-	48	SPly (6/12)	48	SPly (4/12)
	W7	48	SPly (6/12)	48	SPly (6/12)	60	SPly (4/12)
	W8	-	-	-	-	48	SPly (6/12)

Table 4-18: Floor Plan 7 – Multi-Story Shearwall Locations

Design Code		*ASCE7-05*		*SDDD-LS*		*SDDD-IO*	
Story	*Wall ID*	*Retrofit Length (in)*	*Sheathing Material*	*Retrofit Length (in)*	*Retrofit ID*	*Retrofit Length (in)*	*Retrofit ID*
Story 1	W1	288	SPly (4/12)	744	SPly (6/12)	744	DPly (4/12)
	W2	96	SPly (4/12)	305	SPly (6/12)	305	DPly (4/12)
	W3	96	SPly (3/12)	-	-	230	DPly (4/12)
	W4	96	SPly (4/12)	461	SPly (6/12)	461	DPly (4/12)
	W5	48	SPly (3/12)	53	SPly (3/12)	53	DPly (2/12)
	W6	-	-	78	SPly (3/12)	78	DPly (2/12)
	W7	-	-	78	SPly (3/12)	78	DPly (2/12)
	W8	48	SPly (3/12)	266	SPly (3/12)	266	DPly (2/12)
	W9	48	SPly (3/12)	60	SPly (3/12)	60	DPly (2/12)
	W10	-	-	84	SPly (3/12)	84	DPly (2/12)
	W11	96	SPly (4/12)	120	SPly (3/12)	120	DPly (2/12)
	W12	96	SPly (4/12)	96	SPly (3/12)	96	DPly (2/12)
	W13	-	-	72	SPly (3/12)	72	DPly (2/12)
	W14	48	SPly (3/12)	48	SPly (3/12)	48	DPly (2/12)
	W15	192	SPly (6/12)	-	-	744	SPly (3/12)
	W16	-	-	-	-	461	SPly (6/12)
	W17	-	-	-	-	-	-
Story 2	W1	288	SPly (6/12)	744	SPly (6/12)	744	SPly (2/12)
	W2	48	SPly (6/12)	305	SPly (6/12)	305	SPly (2/12)
	W3	96	SPly (6/12)	-	-	-	-
	W4	96	SPly (6/12)	461	SPly (6/12)	461	SPly (2/12)
	W5	48	SPly (3/12)	53	SPly (3/12)	53	DPly (2/12)
	W6	-	-	78	SPly (3/12)	78	DPly (2/12)

	W7	48	SPly (3/12)	78	SPly (3/12)	78	DPly (2/12)
	W8	-	-	78	SPly (3/12)	78	DPly (2/12)
	W9	48	SPly (3/12)	78	SPly (3/12)	78	DPly (2/12)
	W10	60	SPly (6/12)	60	SPly (4/12)	60	DPly (2/12)
	W11	-	-	84	SPly (4/12)	84	DPly (2/12)
	W12	72	SPly (4/12)	84	SPly (4/12)	84	DPly (2/12)
	W13	72	SPly (4/12)	84	SPly (4/12)	84	DPly (2/12)
	W14	-	-	84	SPly (4/12)	84	DPly (2/12)
	W15	48	SPly (6/12)	59	SPly (4/12)	59	DPly (2/12)
	W16	-	-	-	-	276	SPly (3/12)
	W17	-	-	-	-	304	SPly (3/12)
	W18	-	-	-	-	451	SPly (3/12)
Story 3	W1	196	SPly (6/12)	540	SPly (6/12)	744	SPly (2/12)
	W2	48	SPly (6/12)	240	SPly (6/12)	305	SPly (2/12)
	W3	-	-	-	-	-	-
	W4	72	SPly (4/12)	240	SPly (6/12)	461	SPly (2/12)
	W5	48	SPly (4/12)	53	SPly (4/12)	53	DPly (2/12)
	W6	-	-	78	SPly (4/12)	78	DPly (2/12)
	W7	48	SPly (4/12)	78	SPly (4/12)	78	DPly (2/12)
	W8	-	-	78	SPly (4/12)	78	DPly (2/12)
	W9	48	SPly (4/12)	78	SPly (4/12)	78	DPly (2/12)
	W10	60	SPly (6/12)	60	SPly (4/12)	60	DPly (2/12)
	W11	-	-	84	SPly (4/12)	84	DPly (2/12)
	W12	-	-	84	SPly (4/12)	84	DPly (2/12)
	W13	-	-	84	SPly (4/12)	84	DPly (2/12)
	W14	-	-	84	SPly (4/12)	84	DPly (2/12)

	W15	48	SPly (6/12)	59	SPly (4/12)	59	DPly (2/12)
	W16	-	-	-	-	-	-
	W17	-	-	-	-	304	SPly (6/12)
	W18	-	-	-	-	-	-
Story 4	W1	120	SPly (6/12)	312	SPly (6/12)	744	SPly (4/12)
	W2	48	SPly (6/12)	144	SPly (6/12)	305	SPly (4/12)
	W3	-	-	-	-	-	-
	W4	60	SPly (6/12)	144	SPly (6/12)	461	SPly (4/12)
	W5	48	SPly (6/12)	-	-	53	SPly (2/12)
	W6	-	-	78	SPly (6/12)	78	SPly (2/12)
	W7	-	-	78	SPly (6/12)	78	SPly (2/12)
	W8	-	-	78	SPly (6/12)	78	SPly (2/12)
	W9	48	SPly (6/12)	78	SPly (6/12)	78	SPly (2/12)
	W10	60	SPly (6/12)	60	SPly (6/12)	60	SPly (2/12)
	W11	-	-	84	SPly (6/12)	84	SPly (2/12)
	W12	-	-	-	-	84	SPly (2/12)
	W13	-	-	-	-	84	SPly (2/12)
	W14	-	-	84	SPly (6/12)	84	SPly (2/12)
	W15	48	SPly (6/12)	59	SPly (6/12)	59	SPly (2/12)
	W16	-	-	-	-	-	-
	W17	-	-	-	-	-	-
	W18	-	-	-	-	-	-

Table 4-19: Floor Plan 7 - Soft-Story Only Shearwall Locations

Design Code		*1959 Blue Book*		*1978 NEHRP*		*FEMA P-807*	
Story	*Wall ID*	*Retrofit Length (in)*	*Shearwall ID*	*Retrofit Length (in)*	*Shearwall ID*	*Retrofit Length (in)*	*Retrofit ID*
Story 1	W1	240	SPly (6/12)	240	SPly (6/12)	360	SPly (2/12)
	W2	-	-	-	-	-	-
	W3	230	SPly (6/12)	230	SPly (6/12)	230	SPly (2/12)
	W4	-	-	-	-	216	SPly (2/12)
	W5	53	SPly (3/12)	53	SPly (6/12)	-	-
	W6	-	-	78	SPly (6/12)	-	-
	W7	-	-	78	SPly (6/12)	-	-
	W8	266	SPly (6/12)	266	SPly (6/12)	228	SPly (2/12)
	W9	60	SPly (6/12)	60	SPly (6/12)	-	-
	W10	-	-	-	-	-	-
	W11	120	SPly (6/12)	120	SPly (6/12)	48	SPly (2/12)
	W12	96	SPly (6/12)	96	SPly (6/12)	98	SPly (2/12)
	W13	-	-	-	-	72	SPly (2/12)
	W14	48	SPly (6/12)	48	SPly (6/12)	-	-
	W15	-	-	-	-	-	-
	W16	-	-	-	-	-	-
	W17	-	-	-	-	-	-

4.5 Quantifying Archetype Performance

All archetypes were modeled in SAPWood (Seismic Analysis Package for Woodframe Structures) [Pei and van de Lindt (2010)] using the 10 or 16 parameter hysteretic models provided above. All structural and nonstructural walls were modeled. To quantify the seismic performance of the 37 buildings presented in the previous section, nonlinear time history analysis (NLTHA) was conducted in SAPWood [Pei and van de Lindt (2010)]. The specific NLTHA method used was a multi-record incremental dynamic analysis (IDA) using the FEMA P695 [FEMA (2009)] suite of 22 bi-axial ground motion records scaled to 40 spectral accelerations

totaling 1,760 NLTHA for each archetype. The IDA results for the first story of each of the 37 archetypes are provided in Appendix C. These results were used to develop fragility curves conditioned on peak inter-story drift (ISD). The peak inter-story drift fragility curves for each story of each of the archetypes are presented in Figure 4-10 through Figure 4-16 for a spectral acceleration equal to 1.5g (MCE seismic hazard for Los Angeles, California). These fragility curves may be expressed as

$$P[peak\ ISD \leq ISD | Sa = 1.5g] \qquad \text{Eq. 4 - 16}$$

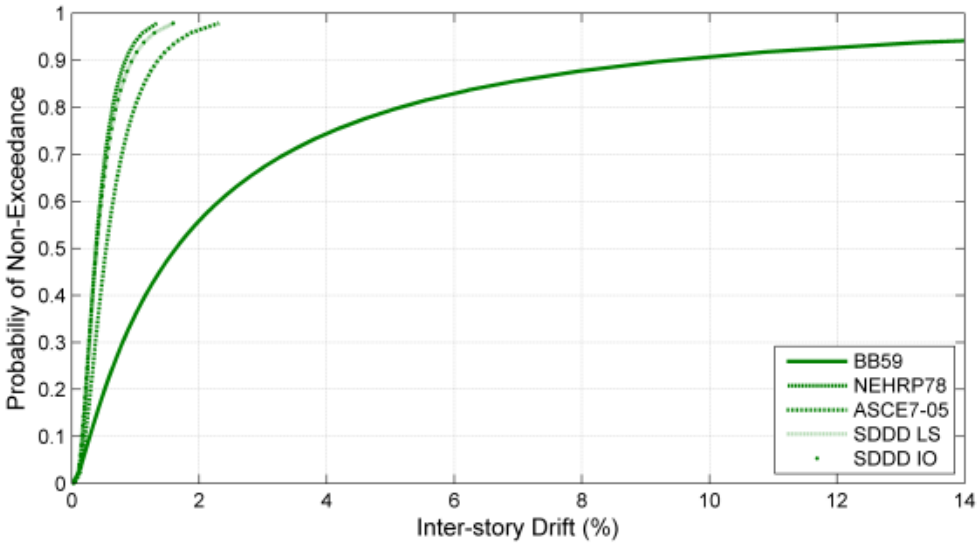

Figure 4-8: Floor Plan 1 - Peak Inter-Story Drift Probability of Non-Exceedance

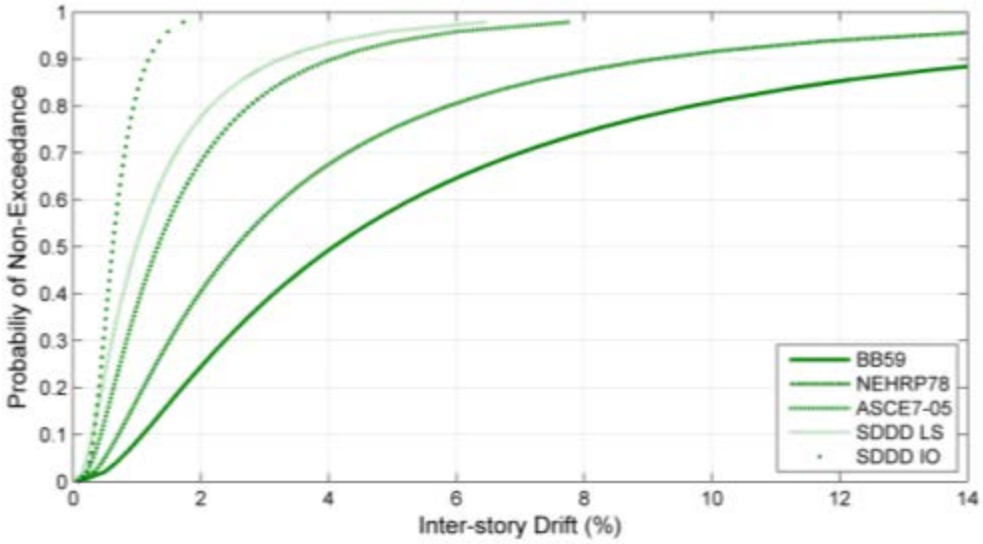

(a)

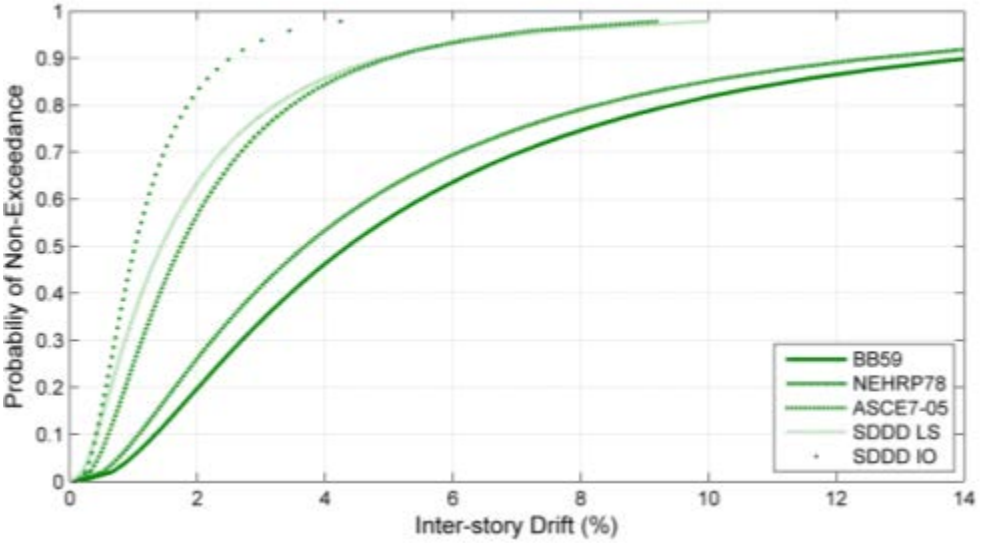

(b)

Figure 4-9: Floor Plan 2 - Peak Inter-Story Drift Probability of Non-Exceedance: (a) First Story; (b) Second Story

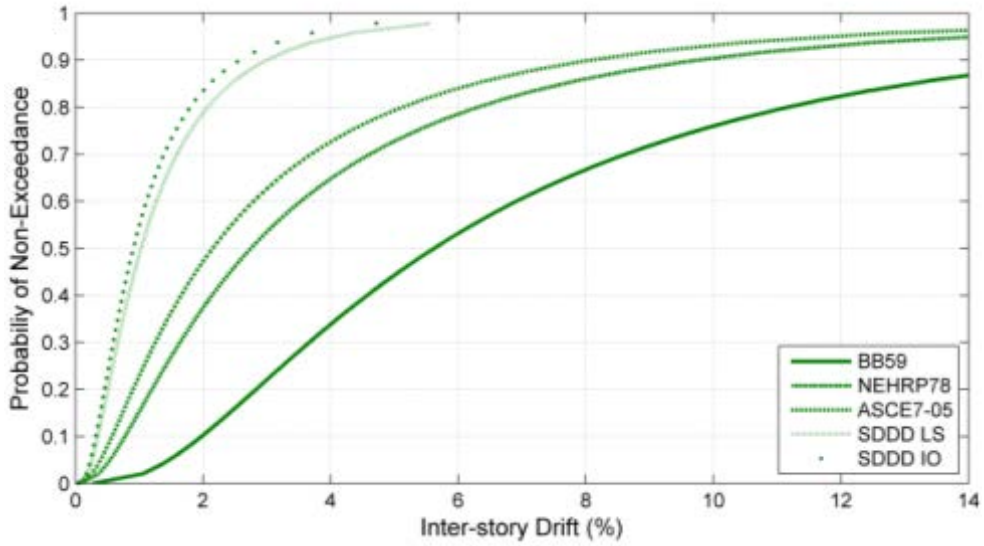

(a)

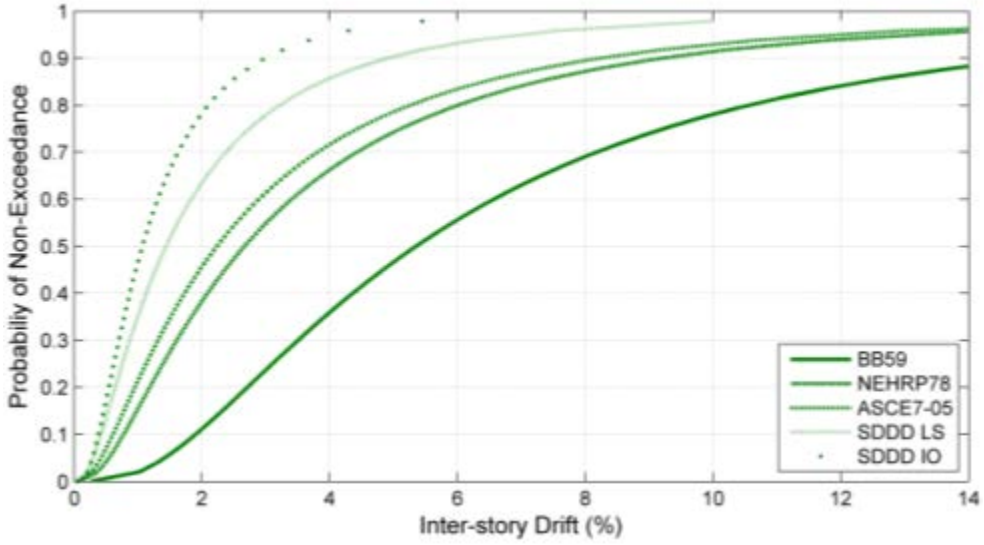

(b)

Figure 4-10: Floor Plan 3 - Peak Inter-Story Drift Probability of Non-Exceedance: (a) First Story; (b) Second Story

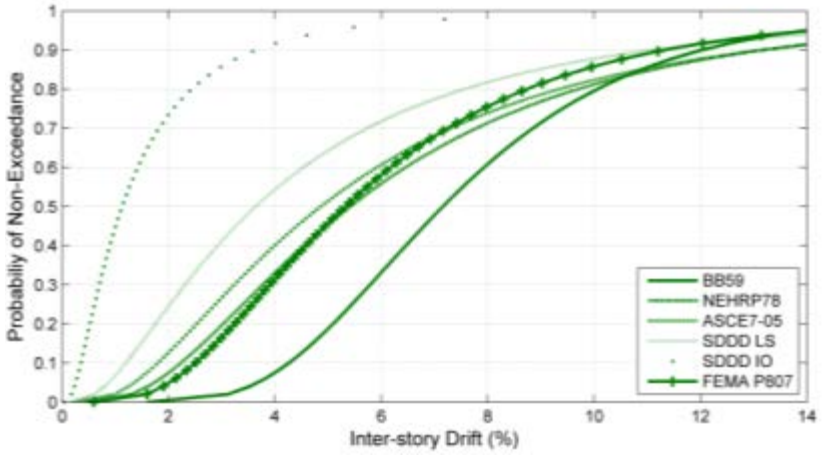

(a)

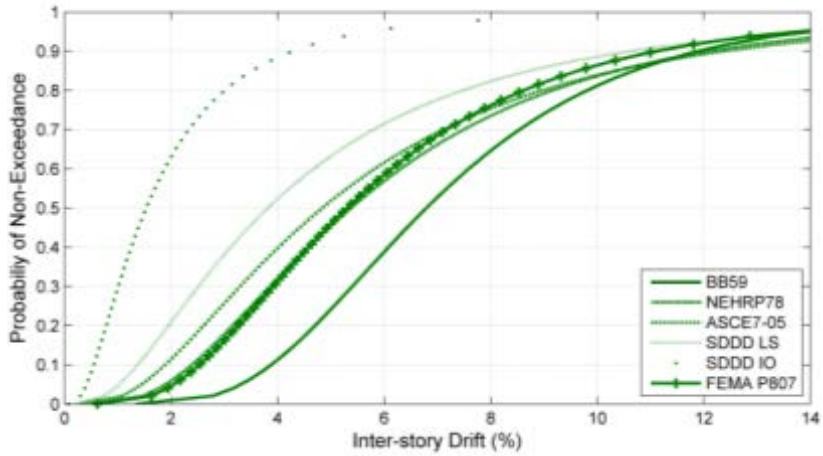

(b)

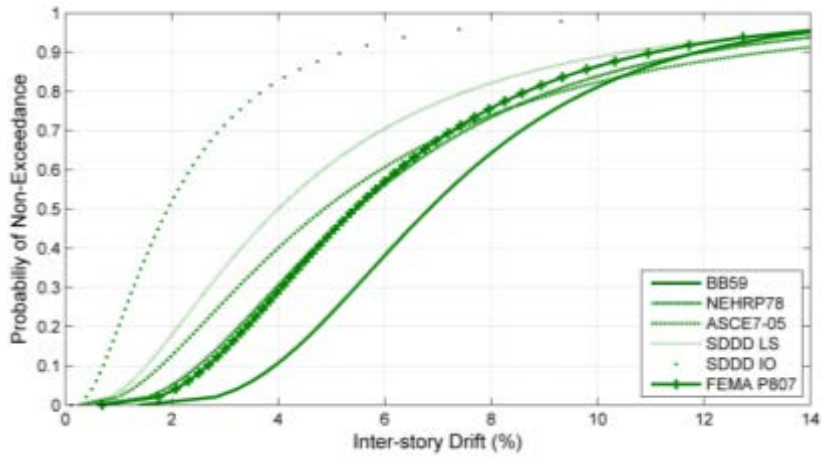

(c)

Figure 4-11: Floor Plan 4 - Peak Inter-Story Drift Probability of Non-Exceedance: (a) First Story; (b) Second Story; (c) Third Story

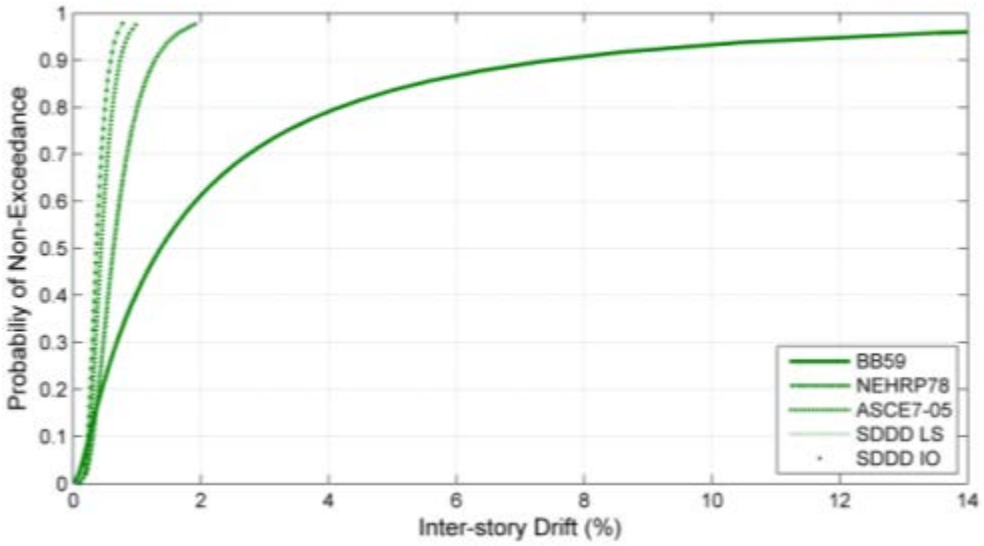

Figure 4-12: Floor Plan 5 - Peak Inter-Story Drift Probability of Non-Exceedance

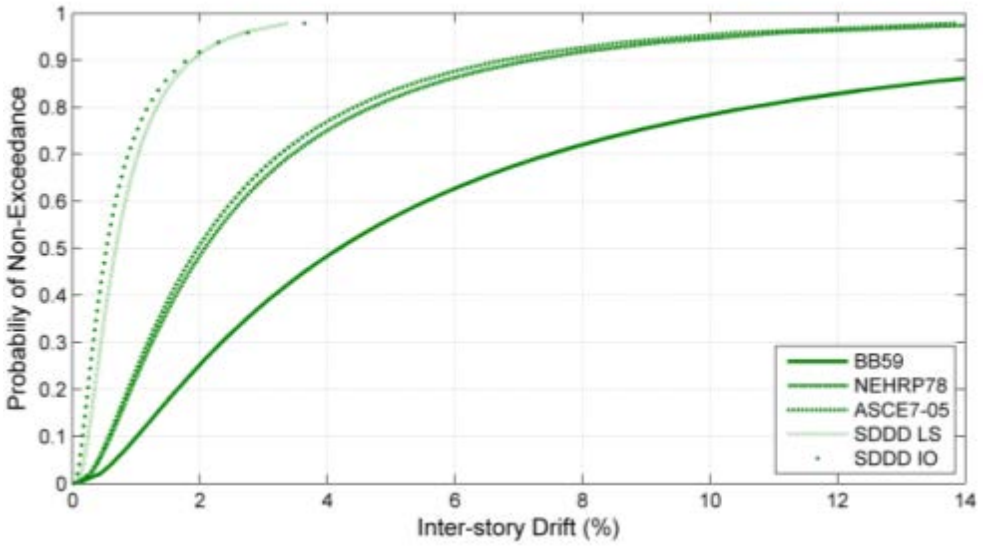

(a)

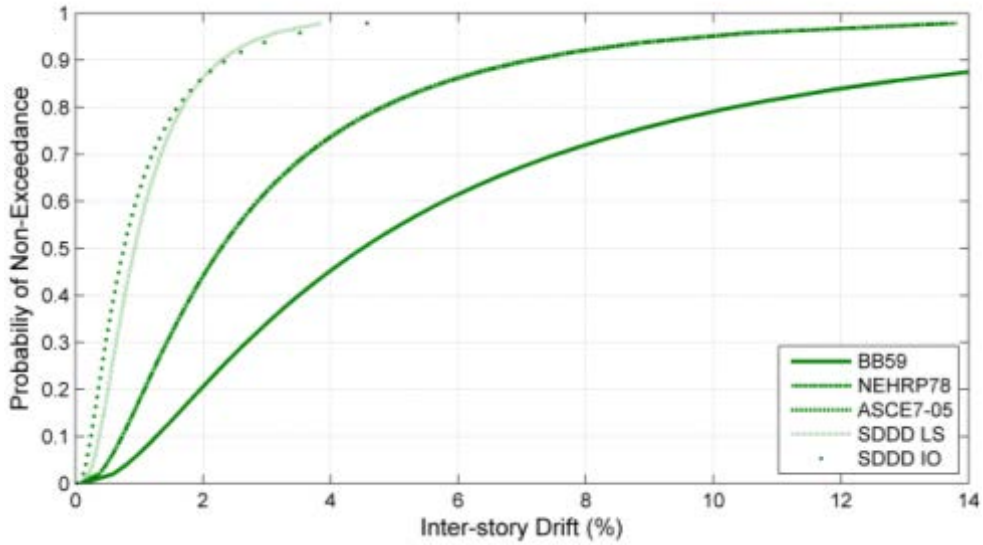

(b)

Figure 4-13: Floor Plan 6 - Peak Inter-Story Drift Probability of Non-Exceedance: (a) First Story; (b) Second Story

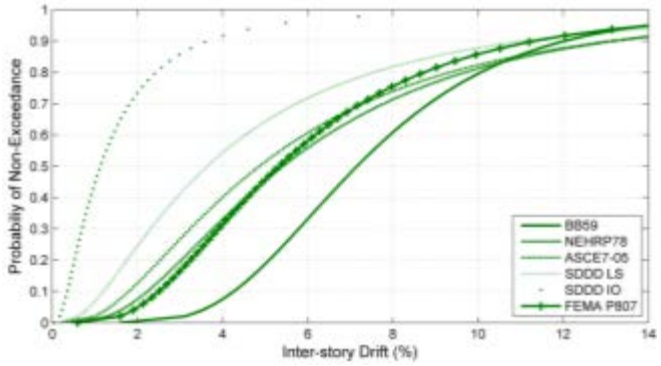

(a)

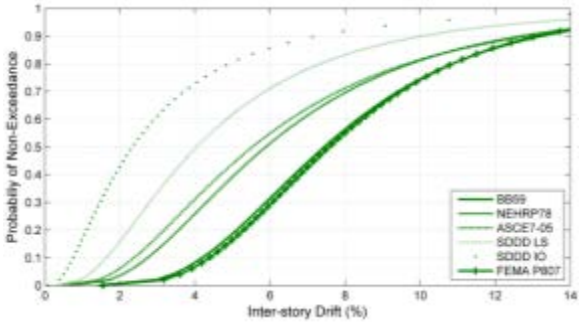

(b)

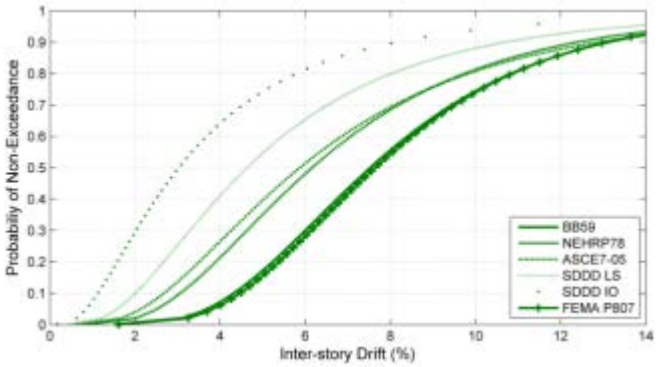

(c)

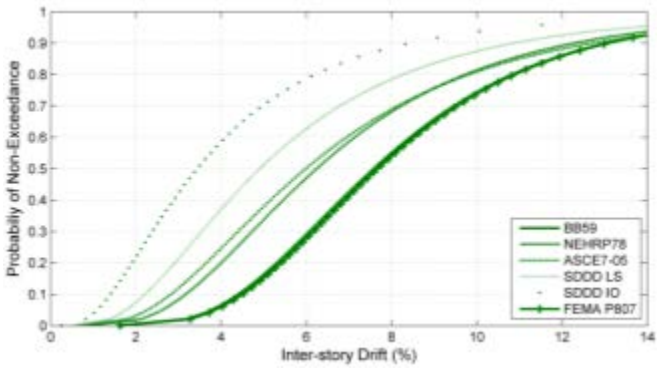

(d)

Figure 4-14: Floor Plan 7 - Peak Inter-Story Drift Probability of Non-Exceedance: (a) First Story; (b) Second Story; (c) Third Story; (d) Fourth Story

Referring to Figure 4-10 through Figure 4-12, and Figure 4-14 and Figure 4-15, it can be seen that the fragility curves line up, relative to each design, exactly as one might expect, i.e. that each newer design was an improvement upon the previous. The 1959 Blue Book design is shown to be the worst performing design, followed by the 1978 NEHRP, the ASCE7-05, the SDDD-LS, and then with the SDDD-IO as the best performing design. This trend was generally consistent, but with several overlapping fragility curves on the two one-story buildings (see Figure 4-10 and Figure 4-14).

There was uncertainty associated with where the FEMA P-807 retrofit fragility curve would fall within the other designs due to the fact that is not necessarily code compliant. Looking at the fragility curves for the two-story floor plans in Figure 4-13 and Figure 4-16, the same general trend was seen with the SDDD-IO design as the best performing, followed by the SDDD-LS design, for all stories in both of the original soft-story buildings. The 1959 Blue Book design was the worst performing for all three stories of the three-story building, and the worst performing design for the first story of the four-story building. The 1959 Blue Book design and the FEMA P-807 retrofit design overlap and essentially provided the same fragility for the upper three stories of the four-story building, shown in Figure 4-16(b-d). In both Figure 4-13(a) and Figure 4-16(a), the FEMA P-807 retrofit design fragility curve fell approximately between the fragility curves for the 1959 Blue Book and 1978 NEHRP designs until approximately 35% PNE, then between the fragility curves of the 1978 NEHRP and ASCE7-05 design from 50% PNE until approximately 70% PNE, and ended by overlapping the fragility curves of the ASCE7-05 and 1959 Blue Book designs. In these two figures, at the first stories, the SDDD-IO design was significantly stronger than any other design. At 50% PNE, the SDDD-IO design showed a peak ISD value of approximately 1.2% for both buildings, the SDDD-LS

design showed a peak ISD value of approximately 3.7% for both buildings, and all other designs showed nearly or greater than 5% peak ISD for both buildings. Similar trends were seen for the upper stories.

The fragility curves presented in this section were incorporated into the decision framework presented herein, and became the basis of the damage states based on experimental studies, as discussed in Chapter 3. The experimental studies and damage state definitions are provided in Chapter 5. Community fragility curves were developed using the fragility curves presented in this section to provide decision makers with a graphical display of the community's overall building performance. The concept of community fragilities was first developed by Park et al. (2013). The community fragility is the combination of each building's fragility curve for every building in the community which may be expressed as a weighted summation of the single building fragilities. The expression for the community fragility is

$$F_c = \sum_{i=1}^{n} \lambda_i^b F_i^b \qquad \text{Eq. 4 - 17}$$

where is the community fragility, is the fragility for the building, *n* is the total number of buildings in the community, and is a weighting factor for the building, which may be expressed as

$$\lambda_i^b = \frac{I_i^b}{\sum_{i=1}^{n} I_i^b} \qquad \text{Eq. 4 - 18}$$

where is an importance parameter for the building and can be used to account for the number of people living in the buildings, the overall area of the buildings, and the importance of the building in the community. In this study, was set equal to 1.0, such that each building was assigned equal importance.

Chapter 5: Experimental Testing and Damage State Development

In this chapter, the damage states discussed in Chapter 3 are developed. To do this, first several soft-story retrofit schemes were designed and modeled, to evaluate the retrofitted building's performance through hybrid testing at full scale. In order to provide enough variety in the design space of the algorithm, multiple design methodologies had to be identified. The motivation behind the retrofit design and experimental testing presented in this chapter was to evaluate the efficacy of more modern and state-of-the-art retrofit design methodologies which do not currently have historical record of building performance. The two retrofit procedures experimentally investigated were a performance-based seismic retrofit procedure and the FEMA P-7807 soft-story retrofit procedure. The FEMA P-807 procedure needed to be experimentally tested due to the associated uncertainty considering that it is not necessarily code compliant, and since it has not been tested in an in-situ condition thus far and therefore real data was not available. Similarly for the performance-based seismic retrofits, real-world data does not currently exist for such new methodologies and therefore needed to be investigated experimentally.

A secondary motivation for the testing was the development of the damage state fragilities in an effort to fully utilize all of the data obtained from the testing. Recall in Chapter 3, the probability of a building being in each sequential damage states, *ds*, was expressed as

$$P[DS = ds|ISD = x]$$

$$= \begin{cases} 1 - P[DS \geq ds|ISD = x] & ds = 1 \\ P[DS \geq ds|ISD = x] - P[DS \geq ds + 1|ISD = x] & 2 \leq ds \leq n_{ds} - 1 \\ P[DS \geq ds|ISD = x] & ds = n_{ds} \end{cases}$$

Eq. 5-38

where = 5 in this study, and

$$\sum_{ds=1}^{n_{ds}} P[DS = ds|ISD = x] = 1.0 \qquad \text{Eq. 5-39}$$

The inter-story drift, *ISD*, and conditional probability expressions used in Eq. 5-1 were obtained from the nonlinear time history analysis and resulting fragility curves presented in Chapter 4 for the 37 archetypes. This chapter focuses on the development of the damage states which were based on correlating physical damage with inter-story drift measurements from the full-scale experimental testing at the University at Buffalo. Those soft-story woodframe building tests were part of the NEES-Soft Project [van de Lindt et al. (2012)]. In this study, damage states are defined based on the non-structural and structural damage to woodframe structures, primarily walls. Five damage states are utilized herein. A description for each damage state was initially provided in Table 3-3, but is repeated in Table 5-1 for convenience.

Table 5-20: Damage State Descriptions

Damage State	*Level*	*Description*
1	No Damage	Structure can be immediately occupied, no repairs required.
2	Slight	Structure can be immediately occupied, minor drywall repairs required.
3	Moderate	Shelter-in-place allowed, drywall replacement required.
4	Severe	Shelter-in-place prohibited, structural damage incurred.
5	Collapse	Structure is not safe for entry, must be reconstructed.

Categorizing damage to woodframe buildings using engineering demand parameters (i.e. inter-story drift or peak floor acceleration) is a popular method. In 2002, Filiatrault and Folz ported the Direct Displacement Design procedure to woodframe buildings; a displacement-based approach within performance-based seismic design rather than the traditional codified strength-based design procedure. The method, originally developed for concrete buildings [Priestly (1998)], was ported to woodframe following the 1994 Northridge earthquake where it was observed that excessive drifts caused cracking of interior and exterior wall finishes and

accelerations caused extensive damage to contents. Continuing on the drift-damage path, in 2005, van de Lindt articulated a damage-based seismic reliability concept by expressing damage as a linear combination of peak displacement and hysteretic energy dissipated by shearwalls within a structure during an earthquake. The predictive capability of this model was investigated in van de Lindt and Gupta (2006) for several woodframe shearwalls with performance comparisons provided by experimental tests. The model was used again in Park and van de Lindt (2009) for developing damage fragilities for a six-story light-frame wood building.

These studies set the stage for drift correlation with damage to woodframe buildings, providing concepts used throughout this dissertation. Prior to defining the inter-story drift ranges associated with each damage state used in this study, a brief introduction on the experimental testing is presented.

5.1 Full-Scale Experimental Testing

Hybrid testing is an emerging earthquake engineering experimental method which evaluates system-level response by testing only a portion of the system. To carry out the testing, a hybrid model was created consisting of two complementary parts: (1) an experimental substructure which is a physical test structure representing a portion of the full structure, and (2) a numerical substructure which is a numerical model representing the remainder of the full structure. The physical model provides force and/or displacement feedback to the numerical substructure model to yield global responses. The two substructures were fully coupled for system evaluation. The advantage of hybrid testing is that the portion of a structural system that is well-understood can be represented numerically, thus saving cost to the experiment, and allowing more testing on the less understood portion of the system. In this study, the hysteretic behavior of the retrofits and their effects on the soft-story were reasonably known, thus the

retrofitted soft-story served as the numerical substructure. The behavior of the un-retrofitted upper stories, and more specifically with the effect of the first story retrofit on their behavior, was less understood; hence the physical substructure consisted of the upper two stories which were constructed at full-scale in the laboratory. Figure 5-1 presents a schematic showing the hybrid testing process employed here. The hybrid test controller coordinated the two substructures by sending the displacement commands from the numerical substructure to the physical substructure (solid arrow) through the actuator controller and xPC target, and feeding the measured forces from the physical substructure back to the numerical substructure through the same path (dashed arrow) which would be used to update the full model for the next time step. For more details on the hybrid testing algorithm and the numerical substructure model, the interested reader is referred to Shao et al. (2014) and Pang et al. (2012), respectively.

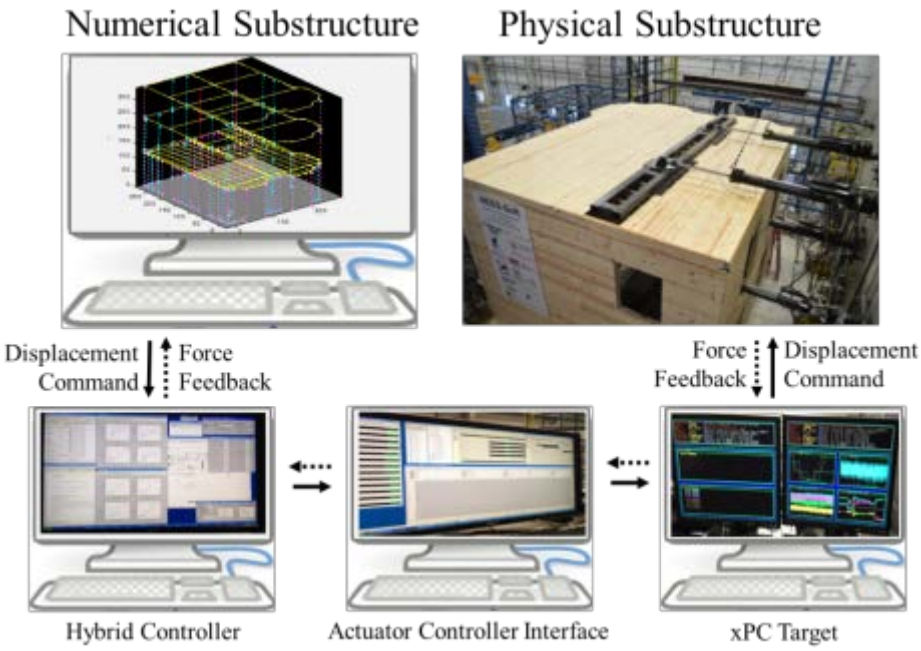

Figure 5-1: Hybrid Test Process

5.1.1 Test Building

The un-retrofitted building was a three-story soft-story woodframe building (6.18 m x 7.40 m plan dimension) modeled after typical 1920's to 1940's style construction to be representative of current structurally deficient soft-story woodframe buildings in Northern California. The first story served as a parking garage with only two interior walls surrounding a stairwell, and the rest of the first story remained open for vehicle parking. The two upper stories were identical in plan and consisted of single unit apartments. The first story floor plan with dimensions is shown in Figure 5-2(a), and the dimensioned floor plan of the two upper stories is shown in Figure 5-2(b). It is worth noting that these types of soft-story woodframe buildings are typically larger in plan, but building dimension limitations for this test program were constrained by the site of the NEES facility at the University at Buffalo.

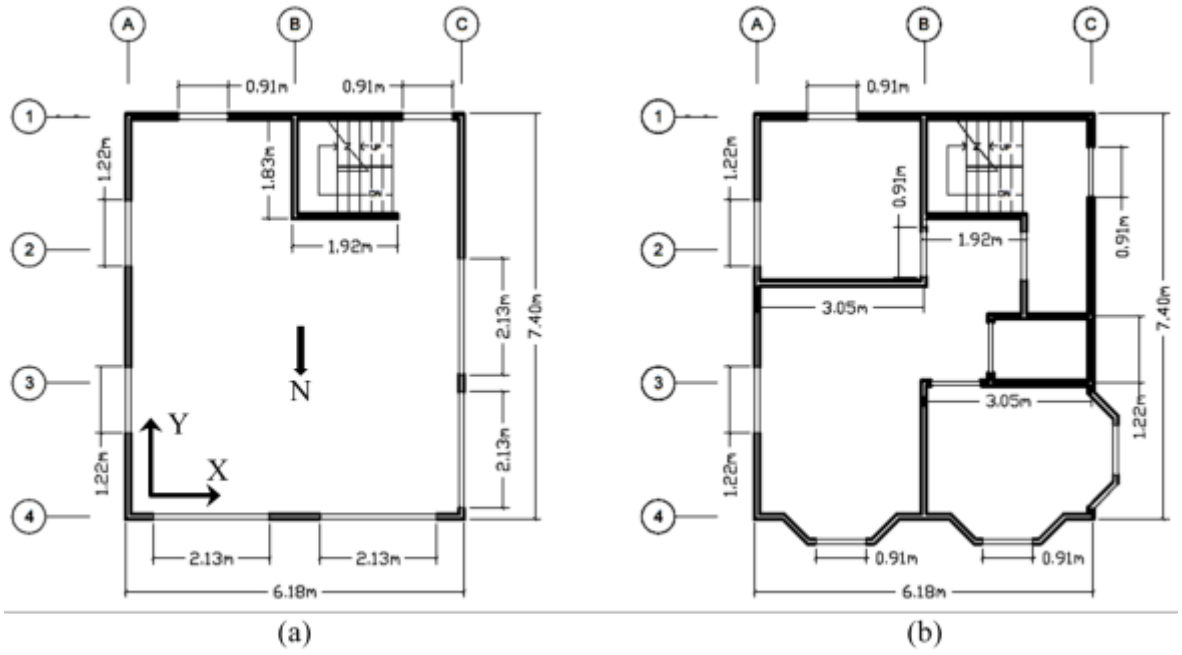

Figure 5-2: Floor Plan of Un-retrofitted Test Building:
(a) First Story; (b) Second and Third Stories

For the design of the physical substructure, typical construction for this era was reproduced to the extent possible based on several site visits to soft-story woodframe buildings in Northern California including two that were in the process of undergoing retrofit and renovation. The physical substructure consisted of the upper two stories of the building previously described, constructed at full-scale with finishing materials (Figure 5-2(b)). The physical substructure was anchored to the strong floor through the second story sill plates which rested on top of a MC6×15.3 steel channel. A 4×4 (88.9 mm × 88.9 mm) (3.5 in × 3.5 in) dimension lumber wood nailer provided the interface between the sill plates and steel channel. Douglas Fir-Larch (DFL) dimension lumber was used for constructing the wall framing, the floor diaphragm, and the roof diaphragm. Horizontal wood siding (HWS) made from 1x10 (19.0 mm × 235 mm) (0.75 in × 9.25 in) DFL dimension lumber planks was used as the exterior sheathing, as seen in Figure 5-3(a). For fastening, two 8d common nails were hand-driven per board spaced vertically at each stud location at 406.4 mm (16 in) on center which formed a couple-moment when racking. One aspect that differed from the typical 1920's to 1960's construction was that gypsum wallboard (GWB) was used as the interior wall sheathing as opposed to stucco or plaster on wood lath due to project financial and repair time constraints. Often soft-story woodframe buildings have been renovated with GWB as the interior sheathing, and the retrofits were designed based on GWB, thus no significant effect on test or project outcomes is envisioned as a result of this substitution.

(a) (b)

Figure 5-3: Physical Substructure: (a) Exterior with Top Actuators Connected to roof Diaphragm; (b) Actuator Connection to Floor Joists

Four actuators were attached to the floor joists of the third floor and roof diaphragms through a load transfer system, shown in Figure 5-3(b). Two actuators with a stroke capacity of +/- 1.0 m (40 in) and +/- 13 degrees of rotational freedom in the horizontal direction were mounted at the third floor diaphragm and at the roof diaphragm. Two actuators at each level allowed for control of both translation and in-plane rotation. The two top actuators connected at the roof diaphragm can be seen in Figure 5-3(a), and the bottom two can be seen going through openings at the second (physical) level.

5.1.2 Retrofit Designs

Seven different retrofits were designed and tested on the three-story building. Three retrofits were designed following the procedure provided in FEMA P-807 [FEMA (2012a)] using cross-laminated timber (CLT) rocking walls, steel cantilevered columns (CC), and viscous fluid dampers (VFD) as the retrofit elements. A fourth retrofit was designed as an alternative using a woodframe distributed knee brace (DKB) as the retrofit elements. These four retrofits were soft-story-only retrofits and did not retrofit or otherwise alter the upper stories. Two other retrofits were design using performance-based seismic design (PBSD) limit states which required upper

story retrofits. The two PBSD retrofit elements were shape memory alloy (SMA) devices and steel moment frames (SMF). Ordinary plywood-sheathed shearwalls with an anchor tiedown system for overturning restraint were used as the upper story retrofits. A final retrofit using a soft-story-only layout of the SMA devices with the intention of over-strengthening the first-story forcing the seismic demand into the second story was tested during the final collapse test phase. The SMA PBSR and collapse test layouts were designed as part of this dissertation work and thus only the SMA PBSR will be presented here in detail. The interested reader is referred to Jennings et al. (2014a) for more detail on the CLT and CC retrofits, Tian and Symans (2012) for more detail on the VFD retrofit, Gershfeld et al. (2014) for more detail on the DKB retrofit, Jennings et al. (2014b) for more detail on the SMA retrofit, and Jennings et al. (2014c) for more detail on the collapse tests.

5.1.2.1 SMA PBSR Design for Building Performance

A seismic retrofit using a SMA-steel device in the scissor-jack brace [Jennings et al. (2014c)] was designed for a soft-story woodframe building using performance-based seismic design (PBSD) criteria to meet a superior building performance based on the needs of a potential building owner (or other stakeholder). To achieve the superior performance, the performance objectives for the seismic retrofit design considered two limit states: immediate occupancy (IO) and life safety (LS). The IO limit state was defined by 1.5% inter-story drift with a 50% probability of nonexceedance (PNE) of the design basis earthquake (DBE) for San Francisco, CA. The LS limit state was defined by 2.5% inter-story drift with a 50% PNE of a maximum considered earthquake (MCE) for San Francisco, CA.

5.1.2.2 Procedure used in SMA PBSR Design

The retrofit design focused on eliminating the soft-story condition and eliminating the torsional response from the building while meeting the inter-story drift criteria set for both limit states. The retrofit design was centered on maintaining all original functionality of the parking garage without compromising any of the building's architectural features. The Simplified Direct Displacement Design (DDD) procedure [Pang et al. (2010)] was followed to determine the additional capacity required for retrofitting the un-retrofitted building and fine-tuned using nonlinear time history analysis (NLTHA) in SAPWood. The SMA-steel device was selected to provide the additional strength and stiffness required for removing the soft-story condition from the bottom story. An appropriate number of SMA devices were selected based on the computed design story shear for the first story. An attempt was made at only retrofitting the soft-story; however, reviewing the results from the multi-record NLTHA revealed the seismic demand had been shifted into the second story causing damage and indicated the need for upper story retrofits. This is not surprising since the upper stories of these older buildings are typically structurally deficient like the soft-story, although not as deficient as the soft-story. Ideally the upper story retrofits would perform adequately and be cost effective, but it would be necessary to minimize the interruption time for the building occupants. Due to the available wall length on the upper stories and the less expensive material assembly and installation procedure associated with traditional shearwalls, plywood-sheathed wood shearwalls with an anchor tiedown system (ATS) for overturning restraint were selected as the upper story retrofits. This approach of using the traditional shearwalls as the retrofit elements was not employed on the soft-story due to the lack of available wall length and the need to position retrofit elements to eliminate the eccentricity of the soft-story. Of course, key was the objective of maintaining full functionality

of the parking garage. Using the design story shears from the simplified DDD calculations on the upper stories, an appropriate number of shearwalls with corresponding nail patterns were selected. The general step-by-step procedure used in the design process is presented in Figure 5-4. The detailed procedure for determining the location of the individual retrofits is more building-specific and will be discussed later.

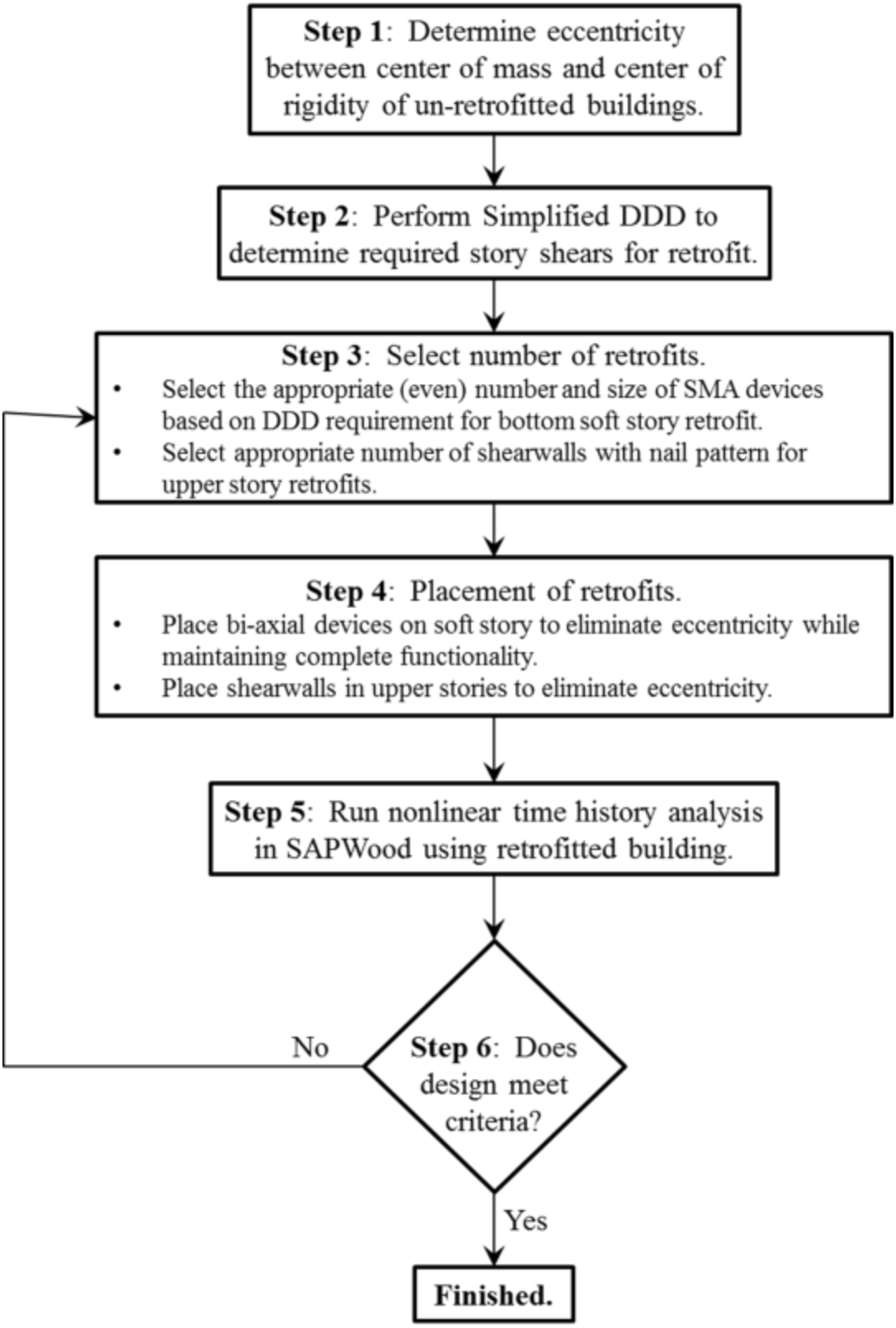

Figure 5-4: SMA Soft-Story Seismic Retrofit Design Procedure

5.1.2.3 Layout of Retrofit Elements in Building

Four SMA-steel devices in scissor-jack braces were numerically placed on the first story of the three-story building. Figure 5-5 provides a schematic of a bi-axial pair of scissor jack braces with a close-up on the SMA-steel device. Braces were placed in sets of two, oriented at 90° from each other in an 'X' like position at 45° and 135° from the principle building axes so that each device responded to motion in both directions. The retrofit layout on all three stories is provided in Figure 5-6. The braces in such a retrofit would not be incorporated into the walls, but set out from the wall with a 0.44 (4.7 sq. ft) footprint to be enclosed by partition walls with a service door for maintenance. The footprint of the retrofit element did not block any parking or decrease any of the functionality of the parking garage, as indicated in Figure 5-6(a). The scissor-jack braces were connected to the above floor system by a welded steel plate on top of the brace. Thin steel plates were welded perpendicular to the top plate and bolted onto the floor joists ensuring the load transfers through the floor diaphragm. The same type of connection was used at the base of the brace to transfer load into the foundation, connecting to the floor joists below the scissor-jack braces (see Figure 5-5).

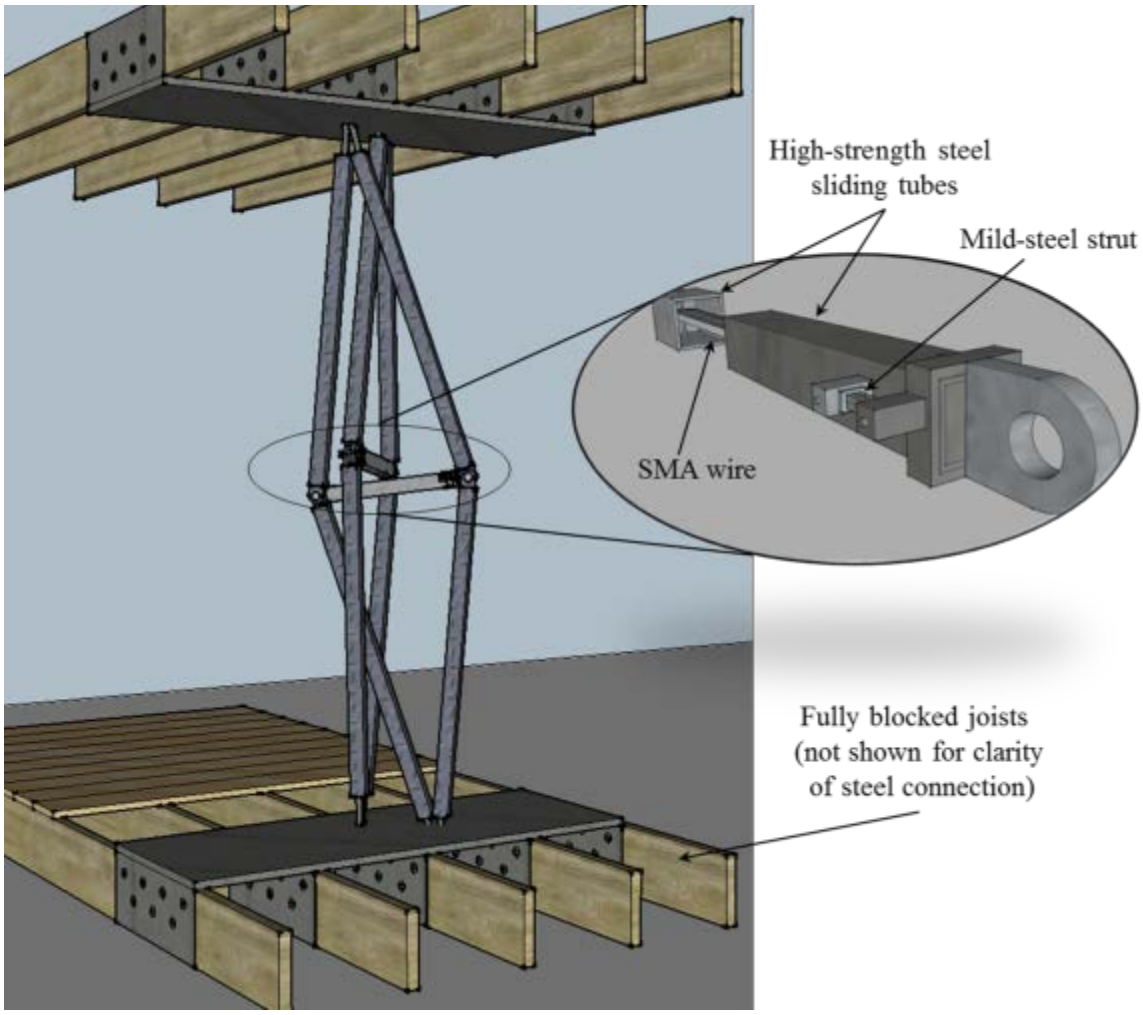

Figure 5-5: Bi-axial Pair of Scissor Jack Braces with SMA-Steel Device

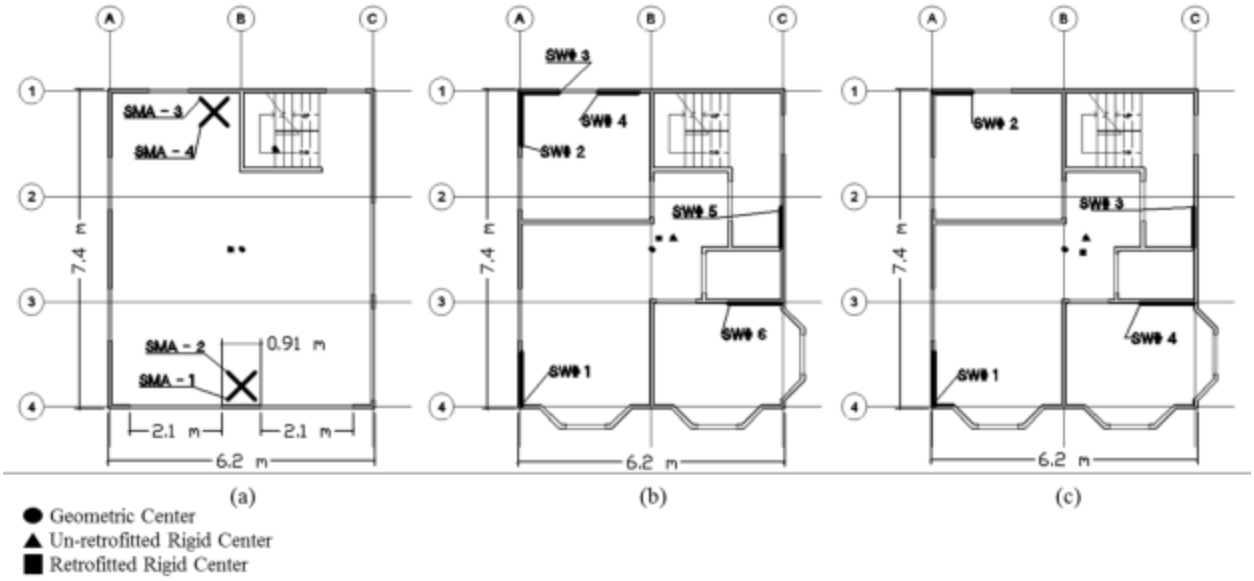

Figure 5-6: SMA-Retrofitted Test Building Floor Plan with Centers:
(a) First Story; (b) Second Story; (c) Third Story

The placement of the braces was determined using a weighted average of the stiffness of each existing wall, its center coordinates, and the additional stiffness from the four devices, back calculating for the best locations. Due to the constraints imposed by maintaining the complete functionality of the parking garage, the potential device locations were limited and a small eccentricity remained in both principle building directions. The layout of the devices on the first story with three 'centers-of-interest' labeled is provided in Figure 5-6(a). In Figure 5-6, the circle marker represents the approximate center of mass, the triangle marker represents the center of rigidity of the un-retrofitted story, and the square marker was placed at the center of rigidity of the retrofitted story. Prior to retrofitting, the resultant eccentricity existing between the approximate center of mass and center of rigidity equaled 2.4 m on the first story. Following the seismic retrofit, the center of rigidity of the first story was relocated to very near the approximate center of mass with a resultant eccentricity of 0.3 m.

The upper story retrofit components were modeled by the same 10-parameter hysteretic model with the more common wood shearwall shape (e.g., see van de Lindt (2004)). In total, ten walls with 12.7 mm (½ in) thick plywood sheathing fastened with 10d common nails were modeled in the upper stories. Six shearwalls were required for meeting the design story shear on the second story with 50.8 mm (2 in) perimeter nail spacing, and four shearwalls were required on the third story with 152.4 mm (6 in) perimeter nail spacing. All shearwalls were modeled with 304.8 mm (12 in) field nailing. The method used for placement of the shearwalls followed the same logic as was used on the first story. A weighted average of the stiffness from the shearwalls and the existing walls was used with a desire to keep the shearwalls on the building perimeter, although this was not entirely possible. The layouts of the shearwalls for the second and third story retrofits were provided in Figure 5-6(b) and (c) where the shearwalls were shown by the bold lines and labeled SW #1 – 6. Following the design of the seismic retrofit, the decrease in calculated eccentricity was not as profound for the upper stories as the first story due to their symmetry. Table 5-2 lists the coordinate locations of all three centers for each story with the coordinate axis set at the bottom left corner of each floor plan.

Table 5-21: Coordinate Location of Building Centers

Center	*Approximate Center of Mass*		*Un-retrofitted Rigid Center*		*Retrofitted Rigid Center*	
	x	*y*	*x*	*y*	*x*	*y*
Story 1	3.09 m	3.71 m	3.86 m	6.01 m	2.82 m	3.71 m
Story 2	3.09 m	3.71 m	3.59 m	3.96 m	3.25 m	3.94 m
Story 3	3.09 m	3.71 m	3.59 m	3.96 m	3.54 m	3.65 m

5.1.2.4 Numerical Validation using Nonlinear Time History Analysis

Multi-record NLTHA was conducted in SAPWood on the three-story building using the FEMA P695 [FEMA (2009)] suite of 22 far-field bi-axial earthquake ground motions. Two analyses were conducted, each at different seismic intensities, i.e. the earthquake records scaled

to the DBE and MCE for San Francisco, California. The results from the NLTHA were rank ordered creating a PNE of the selected damage measure, i.e. maximum inter-story drift, shown in Figure 5-7 for each story. Vertical lines were plotted at the design limit states. As can be seen from Figure 5-7, at 50% PNE, the design meets both limit states for all three stories.

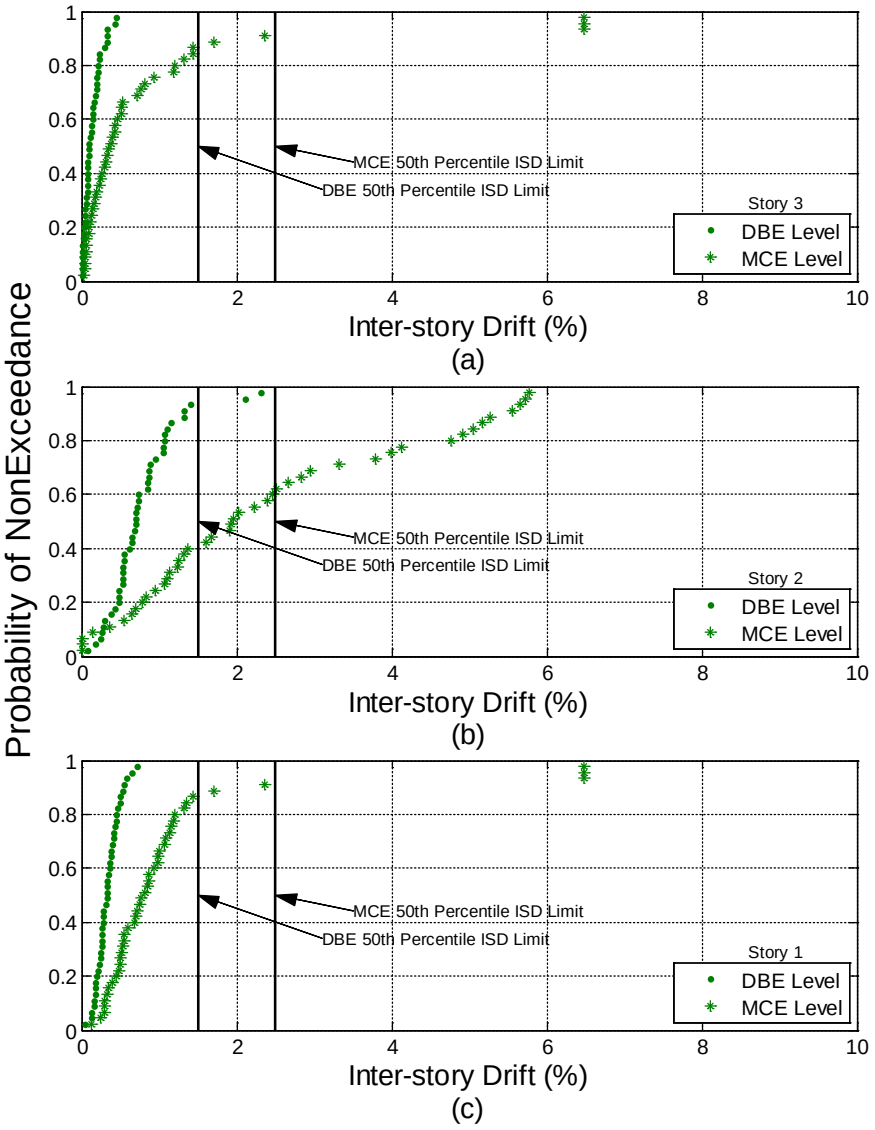

Figure 5-7: Inter-Story Drift Probability of Non-Exceedance Curve for Retrofitted SAPWood Model: (a) Third Story; (b) Second Story; (c) First Story

5.1.3 Hybrid Testing, Results and Discussion

During the fall of 2013, slow pseudo-dynamic hybrid testing was carried out at the NEES facility at the University at Buffalo on the retrofitted three-story soft-story woodframe building described earlier. Testing was conducted slowly at full-scale. Table 5-3 summarizes the testing program including the earthquake ground motion with component, seismic hazard level, scaled peak ground acceleration (PGA), and the peak inter-story drift (ISD) response with the story it occurred in.

Table 5-22: Description of Hybrid Tests

Retrofit	*Test No.*	*Ground Motion with Component*	*Seismic Hazard Level*	*Scaled PGA (g)*	*Peak ISD Response (Story)*
Cross-Laminated Timber Rocking Walls (CLT)	CLT01	Loma Prieta @ Capitola – 2	Low Percentile SRE	0.199	2.28% ()
	CLT02	Loma Prieta @ Capitola - 2	Low Percentile DBE	0.453	1.60% ()
	CLT03	Loma Prieta @ Gilroy - 1	High Percentile DBE	0.645	1.51% ()
	CLT04	Loma Prieta @ Capitola - 2	Low Percentile MCE	0.680	2.62% ()
Cantilevered Column (CC)	CC02	San Fernando @ LA – 2	High Percentile DBE	0.474	1.72% ()
	CC03	Cape Mendocino @ Rio – 2	Low Percentile MCE	0.893	3.10% ()
	CC04	Loma Prieta @ Gilroy - 1	High Percentile MCE	0.976	2.29% ()
Distributed Knee Brace (DKB)	DKB01	Loma Prieta@ Gilroy – 2	Low Percentile DBE	0.427	1.30% ()
	DKB02	Loma Prieta@ Gilroy – 1	High Percentile DBE	0.645	3.00% ()
	DKB03	Loma Prieta@ Gilroy - 2	Low Percentile MCE	0.645	4.10% ()
Fluid Viscous Damper (FVD)	FVD01	Loma Prieta@ Gilroy – 2	Low Percentile DBE	0.427	1.6% ()
	FVD02	Loma Prieta@ Gilroy – 1	High Percentile DBE	0.645	1.0% ()
	FVD03	Loma Prieta@ Gilroy – 2	Low Percentile MCE	0.645	3.8% ()

	FVD04	Loma Prieta@ Gilroy - 1	High Percentile MCE	0.976	N/A
Shape Memory Alloy Devices	SMA01	Loma Prieta @ Gilroy – 2	Low Percentile MCE	0.645	1.4% ()
	SMA02	San Fernando @ LA – 2	High Percentile MCE	0.687	1.9% ()
	SMA03	Loma Prieta @ Gilroy – 1	High Percentile MCE	0.976	2.2% ()
	SMA04	Loma Prieta @ Gilroy – 1	Low Percentile DBE	0.623	1.7% ()
	SMA05	Loma Prieta @ Gilroy - 2	High Percentile DBE	0.427	1.7% ()
Steel Moment Frame (SMF)	SMF01	Sinusoidal Load	PGA=0.25*g	0.250	3.60% ()
	SMF02	Sinusoidal Load	PGA=0.50*g	0.500	5.37% ()
	SMF03	Sinusoidal Load	PGA=0.50*g	0.500	6.11% ()
	SMF04	Sinusoidal Load	PGA=0.25*g	0.250	3.32% ()
Collapse (COL)	COL01	Loma Prieta @ Capitola – 2	MCE	0.680	-
	COL02	Loma Prieta @ Capitola – 2	MCE	0.680	3.13% ()
	COL03	Loma Prieta @ Capitola – 2	2.5*DBE	1.13	9.84% ()
	COL04	Loma Prieta @ Capitola – 2	3*DBE	1.36	10.8% ()
	COL05	San Fernando @ LA - 2	2.5*DBE	1.19	11.4% ()

5.1.3.1 FEMA P-807 Retrofit Results and Discussion

The test program results presented herein sought to validate the FEMA P-807 soft-story retrofit procedure such that it could be used as an option in the decision-making framework. The validation was articulated by meeting the design, namely two inter-story drift limits: (1) a 4% inter-story drift limit identified as the on-set of collapse in FEMA P807 for the predetermined seismic intensity and DBE, and (2) a 7% inter-story drift limit for MCE intensity, the latter of which is believed to be closer to when collapse actually begins to occurs. In all cases, the retrofitted soft-story woodframe building performed well meeting the 4% drift limit set in FEMA P-807 at an even higher intensity than designed (= 1.14g). The test results demonstrated the effectiveness of the soft-story-only retrofit in strengthening the soft-story while not transferring

enough force into the upper stories as to exceed the drift limit or on-set collapse, and in eliminating torsional response. Overall the results indicated that the FEMA P-807 procedure results in building performance as was intended during the development of the guideline document and is a viable retrofit option for the decision-making framework presented in this dissertation.

5.1.3.2 Performance-Based Seismic Retrofit Results and Discussion

Similarly, the experimental testing conducted on the PBSR sought to include it in the decision-making framework as the highest level of design. The results validated that the performance-based seismic retrofit would provide superior performance. Detailed, but limited, results are presented on the SMA-steel device seismic retrofit. The SMA-steel device seismic retrofit was based on the drift criteria discussed above, and only the detailed results to the higher intensity MCE hybrid tests are presented for brevity, since they governed the design. The first test, SMA01, was conducted using the Loma Prieta ground motion, recorded at Gilroy, and scaled to MCE intensity for San Francisco, CA; the ISD time history for all three stories is provided in Figure 5-8. Minimal ISD was seen in the first story where the SMA-steel devices were modeled. The most significant drift occurred in the second story with the peak ISD reaching 1.4%, meeting the Life Safety limit state set at 2.5%. The third story follows a similar trend to the second story, but with only about half the ISD amplitude. Figure 5-9 provides the ISD time history for SMA02. Similar to the SMA01, the ground motion was scaled to MCE intensity, minimal ISD was seen on the first story, and the most significant ISD occurred on the second story with the peak ISD reaching 1.9%, still within the Life Safety limit state. The ISD time history for SMA03 is provided in Figure 5-10. This test, compared to the previous two hybrid tests, produced the largest ISD response from the building on all three stories. This was

expected due to the accumulated damage from the previous tests. The peak ISD occurred on the second story reaching 2.2%, just less than the Life Safety limit state.

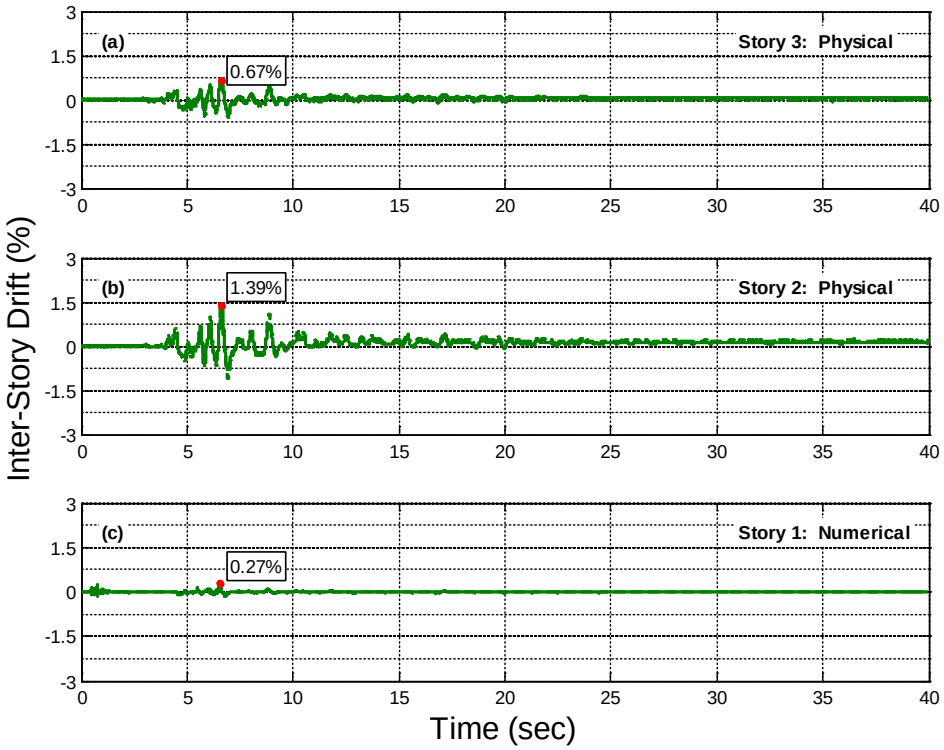

Figure 5-8: Inter-story Drift Time History for SMA01:
(a) Third Story; (b) Second Story; (c) First Story

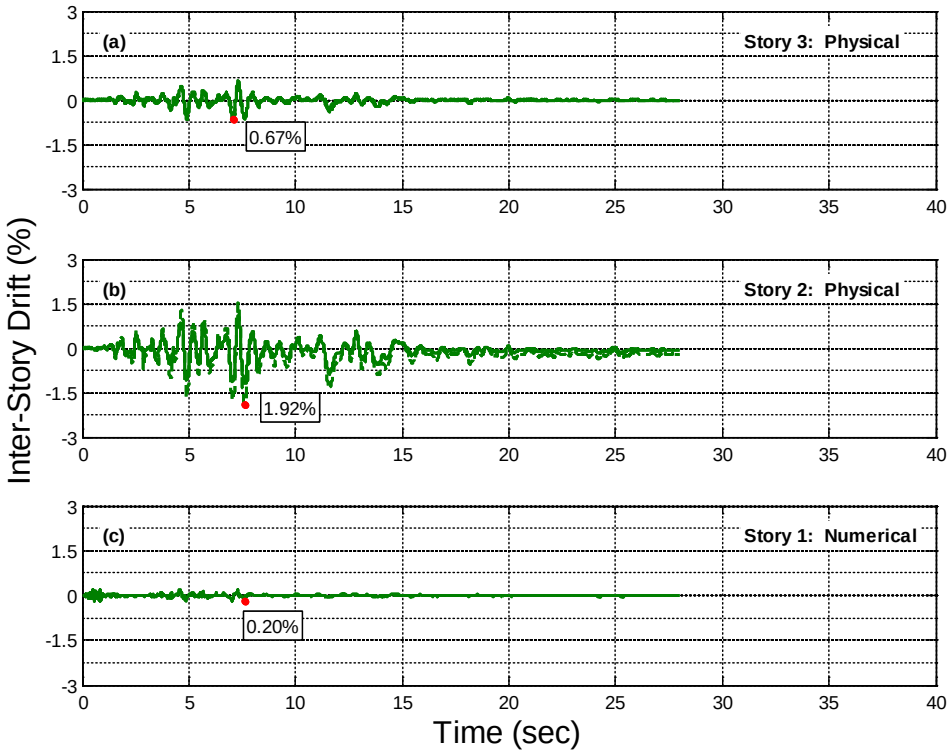

Figure 5-9: Inter-story Drift Time History for SMA02:
(a) Third Story; (b) Second Story; (c) First Story

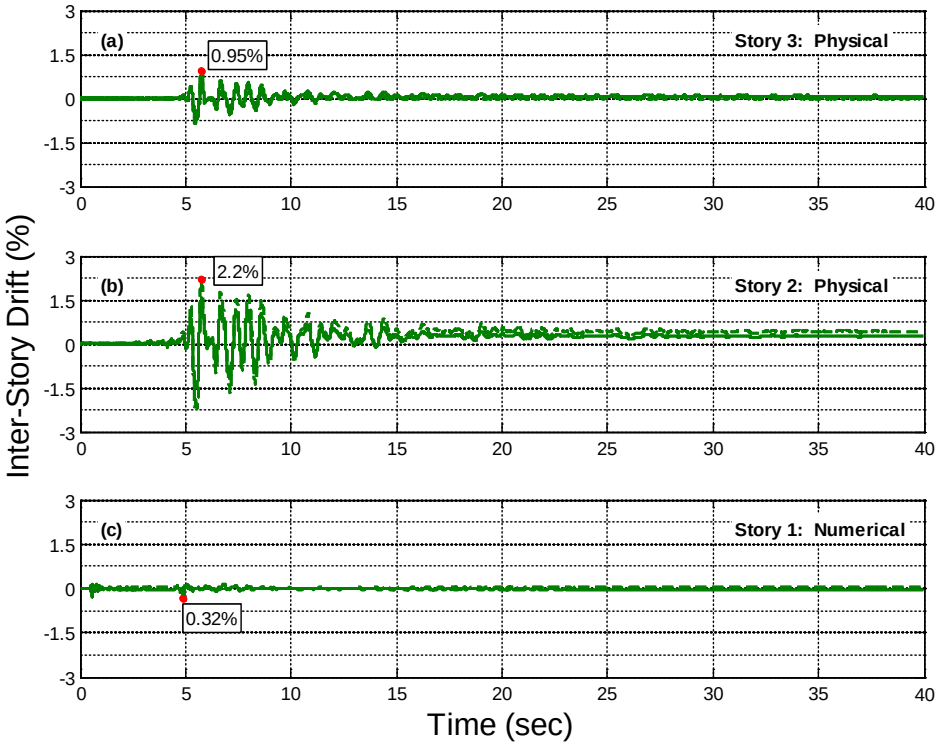

Figure 5-10: Inter-story Drift Time History for SMA03:
(a) Third Story; (b) Second Story; (c) First Story

Hybrid test results verified that the building performed slightly better than its design target and met the performance criteria which were based on peak inter-story drift. It is believed that an adequately performing retrofit could have been achieved by using traditional plywood-sheathed wood shearwalls as the retrofit elements on all building stories. For this particulate soft-story building, this would have required a large portion of the soft-story's walls to be retrofitted thereby impacting the functionality of the parking areas at ground level and therefore the SMA-steel devices were selected as the retrofit elements. Repeated testing of the retrofit scheme in the soft-story woodframe building demonstrated the resilience of the retrofit to withstand a mainshock earthquake of high intensity and large aftershocks that might follow.

As an aside, it should be noted that the numerical and hybrid test results confirmed the adequacy of the proposed retrofit scheme using the SMA-steel device in the scissor-jack brace.

Prior to implementation into practice, the device should be optimized to use a shorter SMA wire length to provide for more options in providing shear capacity so that a linear distribution of the seismic demand per story for all building stories may be possible. Furthermore, if the soft-story building being retrofitted has longer external wall segments, the scissor-jack brace configuration should be elongated to improve the magnification factor. The work presented here showed that the bi-axial scissor-jack brace pair is a new promising configuration that may be able to host any type of damper and should be further explored experimentally.

5.1.3.3 Collapse Test Results and Discussion

The collapse tests aimed to develop fragilities conditioned on the collapse limit of woodframe buildings. There was uncertainty in using traditional collapse limits for structurally deficient woodframe buildings constructed with archaic building materials. To investigate the collapse limit for a structurally deficient woodframe building constructed with archaic building materials, the numerical model of the bottom soft-story was over-strengthened such that the seismic demand would be shifted into the un-retrofitted structurally-deficient upper stories. Following five high intensity real-time open-loop hybrid tests, collapse of the second story was identified following a very intense earthquake. The Loma Prieta – Capitola record, a MCE level test (COL02) did not result in collapse at the second story. It was shown that when 250% of the design basis earthquake was applied, which is equivalent to 167% of the MCE for Loma Prieta – Capitola, the structure immediately collapsed at the second story. Thus, it can be concluded that for this record a second story collapse due to over-strengthening of the first story would likely occur at approximately 125% to 150% MCE for this earthquake record. It was also of interest to identify drift limits where the various damage states occurred and what mechanisms caused the onset of each damage state. Softening of the upper two stories was observed throughout the

collapse test program. COL04 softened the upper two stories such that it was deemed collapsed. The mechanisms indicating the collapsed state were the 6.7% residual drift and multiple nail push-outs which resulted in a dramatic increase in the fundamental period. The seismic demand shifted into the upper stories at the low seismic intensity level of COL02. The collapse capacity of the archaic and un-retrofitted upper two stories may be quantified at approximately a 20 kN lateral strength capacity and 8% lateral drift capacity. Structural damage was observed following test COL03 which was the first test to collapse the second story.

5.1.3.4 System Identification and Damage Inspections

Prior to each hybrid test, a system identification (system ID) test was conducted on the physical substructure to identify building properties, specifically the stiffness matrix of the physical substructure and its fundamental period. The displacement protocol used in the System ID test is provided in Figure 5-10. The first actuator moved forward to 2.54 mm (0.1 in), then backward through zero, continuing to -2.54 mm (-0.1 in), and then back to zero, while the other three actuators were held to zero displacement. This was repeated for each of the four actuators and followed by the top two actuators moving together, the bottom two actuators moving together, and then all four actuators moving together. The identified properties served three purposes: (1) used in the preliminary numerical analysis to estimate the structural response and check for numerical instabilities prior to hybrid testing; (2) in conjunction with a visual inspection of the building to determine whether the damage caused by previous tests was too severe to continue; and (3) as the physical substructure properties in the initial integration step of the hybrid simulation. The system ID tests helped determine the physical damage by comparing the stiffness matrix and period for the first three modes. Figure 5-12 provides the physical substructure stiffness matrix comparison for all tests conducted as part of the NEES-

Soft@Buffalo testing program. Referring to the top left plot in Figure 5-12, a steady drop in stiffness is seen as tests progress, where rises in the curve were typically due to repairs. Figure 5-13 provides the physical substructure period comparison for the first three modes for all tests conducted as part of the NEES-Soft Project at the University at Buffalo. Here again, drops in the fundamental period imply softening of the structure, and most rises were due to repairs. Comparing the change in stiffness, change in period and visual damage observations provided an effective method for quantifying damage to the physical substructure.

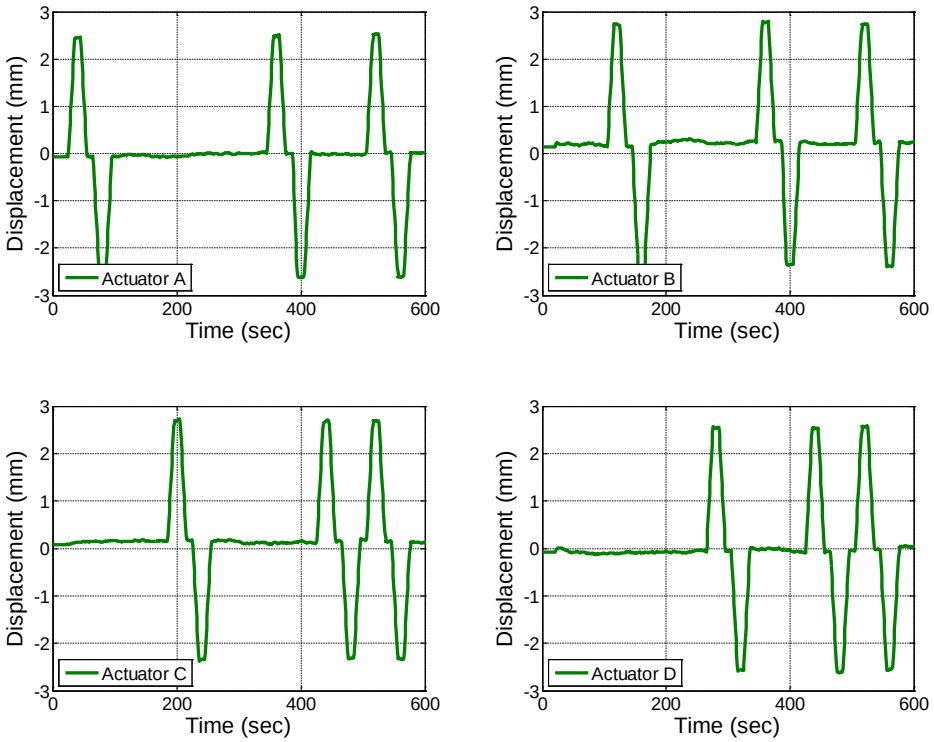

Figure 5-11: System ID Displacement Protocol

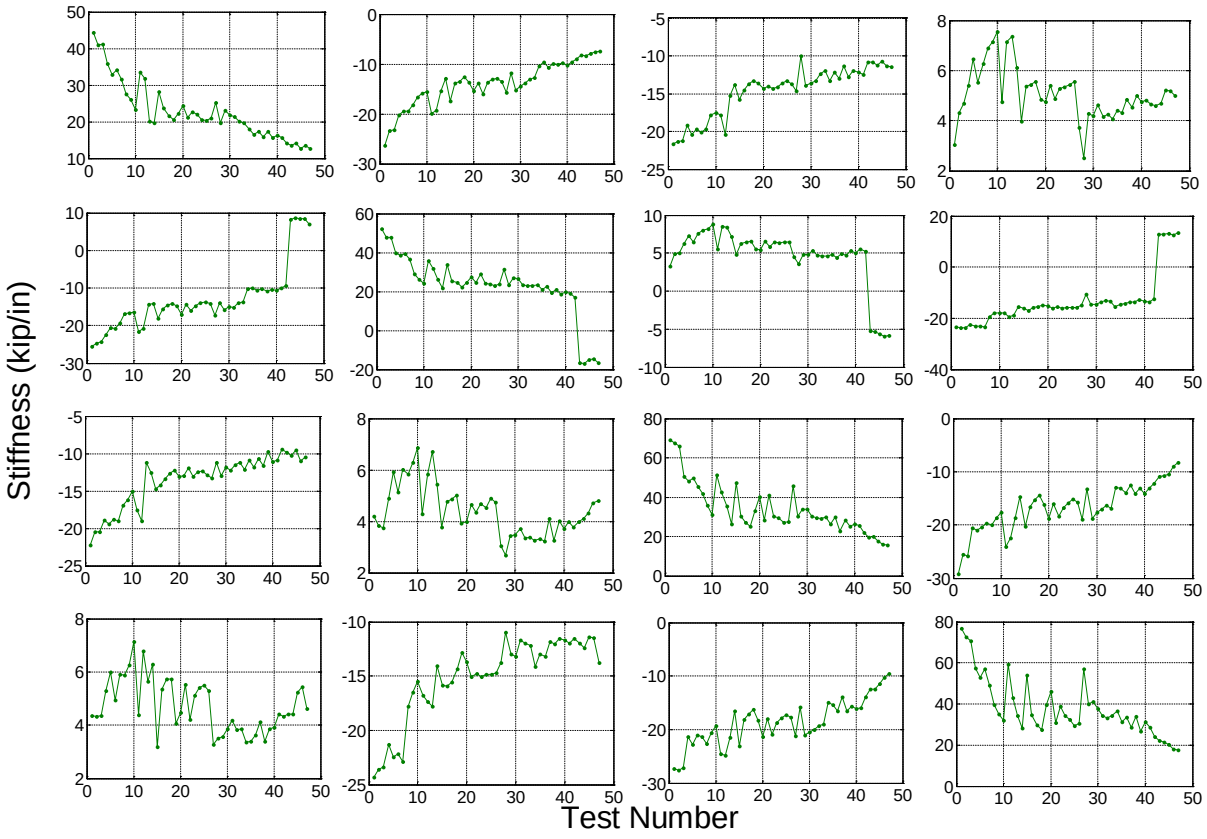

Figure 5-12: Stiffness Comparison

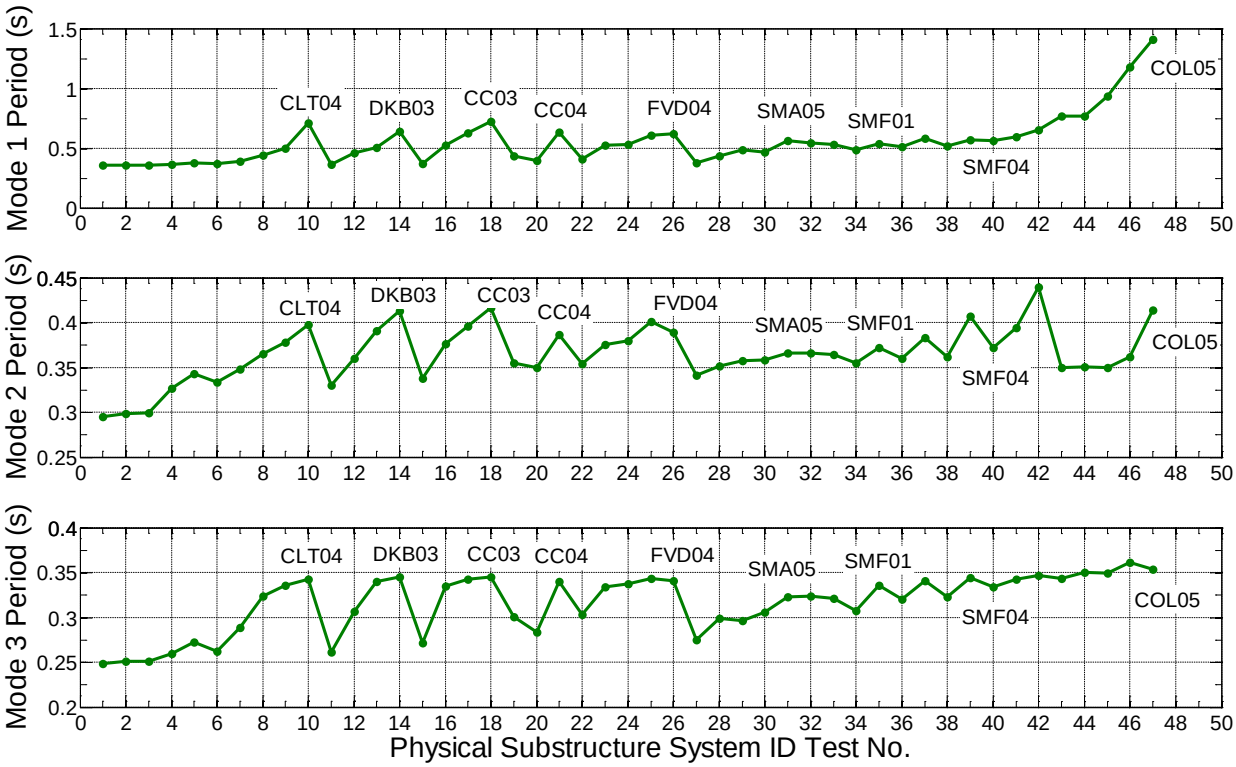

Figure 5-13: Period Comparison for First Three Modes

Damage observations were recorded following each hybrid test as part of the routine inspections of the physical substructure, and quantitatively by an increase in fundamental period and decrease in stiffness based on the System ID tests. Figure 5-14 provides six images chronicling the physical damage observed through the test program. Figure 5-14(a) was taken after SMA01 of the southeast wall (see Figure 5-2) where a peak inter-story drift of 1.06% was recorded. Here, cracking along the drywall panel seems may be seen. Figure 5-14(b) was taken following SMA02 where a peak inter-story drift of 1.30% was measured on the same wall. Figure 5-14(c) – (f) were taken following SMA03, COL02, COL03, and COL05, respectively with peak inter-story drift measurements reaching approximately 2.00%, 3.10%, 9.80%, and 11.4%, respectively. In each progressing image, the cracking along panel lines becomes more severe from minor cracking, minor spalling, to major spalling with tape separation, until finally

the panels detached. Although not evident in the photographs, panel crushing was observed in Figure 5-14(c) – (f) at the bottom corners, along with multiple drywall screw push-outs.

(a)

(b)

(c)

(d)

(e)

(f)

Figure 5-14: Photos Chronicling Damage Observed to South Wall in Stairwell: (a) SMA01; (b) SMA02; (c) SMA03; (d) COL02; (e) COL03; (f) COL05

5.2 Correlating Damage with Inter-story Drift

Figure 5-15 provides an image taken following experimental test CLT01 where the damage would be categorized as damage state 2. The peak inter-story drift of this wall was measured as 1.64%. In the photo one can see cracking along the panel edges, with minor spalling and tape separation in the adjoining wall corner. There is no crushing, cracking, or separation of the panels evident, nor drywall screw pull-outs, and therefore immediate occupancy would be safely allowed. However, the home owner or resident would want these minor repairs conducted.

Figure 5-15: Damage State 2 Example

Figure 5-16 provides a photo taken following CLT04. The wall instrumentation measured a peak inter-story drift of 2.57%. From the photo one can see cracking along the panel edges, spalling and tape separation along the adjoining wall corners, and large shear cracks extending off of the window corners through the panels. This damage would be categorized as damage state 3, and would require replacement of at least four drywall panels on this wall. With no drywall screw push-outs and no panel separation evident, and with this being one of the more severely damage walls in the building, shelter-in place would be permitted to the residents following an initial safety check.

Figure 5-16: Damage State 3 Example

Structural damage was identified only during the collapse test phase, and following COL03 where the peak inter-story drift 9.8% and a 1.9% residual drift was observed. Figure 5-17 provides a photo taken following COL03. The panel separation shown in Figure 5-17 would be representative of damage state 4, while the residual drift in the wall framing is representative of damage state 5. In this case, extensive drywall replacement would be required, minor structural damage would have occurred, and the building occupants would be required to shelter-out-of place until repairs were complete. Figure 5-18 provides two photos taken following COL05. Figure 5-18(a) shows an approximately 2 in. separation between the second story ceiling and third story floor diaphragm. Figure 5-18(b) provides an image of the building exterior with a 7.0% residual inter-story drift. The damage shown in Figure 5-18 would be categorized as damage state 5. This building would not be safe for entry, would be red-tagged, and would likely require demolition. For safety during the experimental tests, a crane was

positioned directly over the physical substructure and a slackened strap positioned through the actuator openings on the roof. The strap, along with the actuators, ensured the building would not physically fall over risking injury and damage to equipment. If these two restraints were not provided, the building would have physically collapsed.

Figure 5-17: Damage State 4 and Damage State 5 Example

(a) (b)

Figure 5-18: Damage State 5 Example: (a) Separation between Upper Stories; (b) 7.0% Residual Drift on Physical Substructure

Based on these damage inspections, the inter-story drift ranges identified to correspond to each damage state are provided in Table 5-4, where the upper bound limit for damage state 5 is shown as 14.0% for practical purposes. This limit was imposed on the nonlinear time history

analysis data to overcome numerical anomalies. It is assumed that a woodframe building would be overcome by the gravity load if reaching 14.0% inter-story drift. There were not enough measurements from the experimental tests to clearly define damage state 4. The ranges in Table 5-4 for damage state 4 were based on a combination of damage observations from the experimental testing and researcher opinion. The values shown in Table 5-4 were used in the lognormal distribution model for developing the sequential damage state expressions in Eq. 5-1 and in Chapter 3.

Table 5-23: Damage State Inter-story Drift Ranges

Damage State	*Inter-story Drift Range (%)*		
	Lower Bound	*Upper Bound*	*Mean*
1	0.00	0.52	0.26
2	0.14	4.00	1.2
3	1.00	4.50	2.75
4	3.50	9.00	5.50
5	7.00	14.0	9.00

Chapter 6: Modeling of Socioeconomic Variables

This chapter focuses on quantifying the effect of socioeconomic variables on social vulnerability and recovery time. Complexities include high variability associated with the socioeconomics of different places, social vulnerability of different places, and the different hazards associated with those places. Socioeconomics and social vulnerability are dynamic measures constantly evolving and changing. Currently, social vulnerability is not well understood and neither is its dynamic nature. What is understood is that the change in social vulnerability differs for different communities. When grouping the current understanding and data availability with the randomness of earthquake occurrence and earthquake intensity, it becomes increasingly complex to quantify a community's social vulnerability at any point in time. There is enough information to statically model a generalized quantification of social vulnerability for a selected community using their socio-demographic data for scenario earthquakes. This chapter presents the methodology used in this dissertation for such quantification.

Five socioeconomic variables were incorporated into this study to help quantify three morbidity rates: the rate of injury, the rate of fatality, and the rate of post-traumatic stress disorder (PTSD) diagnoses. The five variables are: age, ethnicity/race, family structure, gender, and socioeconomic status. The age and density of the built environment together were modeled as a sixth variable used in quantifying the three morbidity rates. This variable was not considered a socioeconomic variable; however it was modeled identically to the socioeconomic variables, and therefore is discussed conjunctively in this chapter. Not all six variables were used to quantify all three morbidity rates. Table 6-1 provides which variables were included in

modeling each of the three morbidity rates. These variables were selected due to their highly demonstrated influence on the morbidity rates and their availability in the literature. A similar, but more inclusive table (Table 3-1) was presented in Chapter 3.

Table 6-24: Variables Considered in Morbidity Rates

Morbidity Rate	*Variable*					
	Age	*Built Environment*	*Ethnicity*	*Family Structure*	*Gender*	*Socioeconomic Status*
Injury Rate	×	×			×	×
Fatality Rate	×	×			×	×
PTSD Diagnosis Rate	×	×	×	×	×	×

6.1 Literature Review/Meta-Data Analysis

An extensive meta-data analysis was conducted prior to quantifying the six variables listed in Table 6-1. The data collection process was essentially a case study of case studies, or an empirical evaluation of the empirical literature. Many references were used in the conceptual development of the socioeconomic variables, however only 33 references were used in the analytical modeling of the socioeconomic variables. Table 6-2 summarizes the list of references that were used to quantify the six variables, providing which morbidity rate(s) and which variable(s) were gained from each study, the reported PTSD prevalence rate, if applicable, along with a brief description on the method of data collection, which earthquake the study followed, and the geographic scale in which data was gathered. The meta-data analysis was only conducted on studies which looked at populations affected by earthquakes, and not any other kind of disaster. References covering marginalized populations caused by other disasters are referenced in other places throughout this work. The references which make up Table 6-2 are population studies conducted by sociologists, anthropologists, psychologists, psychiatrists, or other medical doctors after earthquakes. The purpose of these studies is to survey the exposed

population and identify the marginalized population so that recovery efforts are efficient and to further our understanding of earthquake disasters on people and how the impact changes with demographic factors. There were 16 earthquake events covered in the meta-data analysis which are listed in Table 6-3. These earthquakes began with an earthquake occurring in 1993 in India, and concluded with the 2011 Tohoku, Japan earthquake. There is a large variation in earthquake magnitude (and intensity presumably) and location. These earthquakes were selected due to the availability of data provided in the literature on the affected population. PTSD prevalence rates ranged from 2.5% to 60% among the sample populations. The large range was expected due to the wide variety in sample size, PTSD diagnostic tool, post-event measurement time, severity of the event, and the socioeconomic variability associated with the marginalized populations. Major conclusions from this analysis regarding the variables' relationship to the morbidity rates are provided in the following subsections, headed by each variable.

Table 6-25: Summary of Meta-Data Analysis References

Earthquake	*Morbidity Rate*	*Variables gained from study*	*Description of data collection method*	*Geographic scale*	*PTSD Prevalence*	*Source*
1993 India	PTSD	Age, Gender	Semi-structured interview using questions based on DSM-III- criteria conducted 1 mo. post event	Three villages: Mangrul, Nandurga, and Hasalgan	23%	Sharan et al. (1996)
1994 Northridge	PTSD	Gender	Interview questions based on Diagnostic Interview Schedule/Disaster Supplement 32 weeks post event.	City blocks with the greatest concentration of property damage, most of which were in the Northridge area.	13%	McMillen et al. (2000)
1994 Northridge	PTSD	Age, Ethnicity, Gender, SES	Computer-assisted telephone survey using Civilian Mississippi Scale conducted 8-12 mo. post event.	Los Angeles County and Ventura County	Not Provided	Siegel (2000)
1994 Northridge	Injury, Fatality	Age, Ethnicity, Gender	Records from 78 hospitals within two weeks post event.	Los Angeles County	NA	Peek-Asa et al. (1998)
1994 Northridge	Injury, Fatality	Age, Ethnicity, Gender	Records from 4 hospitals within three weeks post event.	Los Angeles County	NA	Mahue-Giangreco et al. (2001)
1994 Northridge	Injury, Fatality	Gender	Computer-assisted telephone survey conducted 6-24 mo. post event	Los Angeles County	NA	Shoaf et al. (1998)
1995 Hanshin-Awaji, Japan	Injury, Fatality	Age, Gender	Records from 48 affected and 47 unaffected hospitals up to 15 days post event.	48 affected and 47 unaffected hospitals	NA	Tanaka et al. (1997)

1998 Ceyhan, Turkey	PTSD	Age, Gender, Family Structure, SES	for DSM-administered 1 mo. and 13 mo. post event.	Patients of the medical school of Dicle Univ. in Ceyhan.	42% and 23%	Altindag et al. (2005)
1999 Chi-chi, Taiwan	PTSD	Gender	Self-report administered by research psychiatrists using the 6 weeks post event.	Chungliao (worst affected region)	21.70%	Hsu et al. (2002)
1999 Chi-chi, Taiwan	PTSD	Gender, SES	distributed 10 mo. post event.	Two of the most severely damaged villages.	10%	Chang et al. (2005)
1999 Chi-chi, Taiwan	PTSD, Injury	Age, Gender, SES	Interviewed using the -Chinese one year post event.	Victims in temporary housing units from severely affected regions	16.50%	Kuo et al. (2007)
1999 Chi-chi, Taiwan	Injury, Fatality	Age, Gender, SES	Records through the Family Registration Database.	22 municipalities officially affected by the earthquake	NA	Chou et al. (2004)
1999 Kocaeli, Turkey	PTSD	Gender	Psychiatric interview using the for DSM-administered 6-20 weeks post event.	Schools in two townships of Adapazari located in the epicentre of the earthquake.	60%	Eksi et al. (2006)
1999 Kocaeli, Turkey	Injury, Fatality	Age, Gender, SES	Home interview conducted 19-21 mo. post event.	One of the hardest hit cities, Gölcük.	NA	Ramirez et al. (2005)
2000 Iceland	PTSD	Gender, SES	Post-distributed three mo. post event.	Five exposed local government areas	24%	Bodvarsdottir and Elklit (2004)
2002 Molise, Italy	PTSD	Age, Gender, SES	Mental Health Team administered the for PTSD six mo. post event.	Five most affected villages	14.50%	Priebe et al. (2009)
2003 Bam, Iran	PTSD	Age, Family Structure, Gender, SES	Interviews by trained personnel using the GHQ- conducted 5 mo. post event.	Bam, Iran	NA	Montazeri et al. (2005)

2005 Pakistan	PTSD	Age, Family Structure, Gender, SES	Trained personnel administered the 30 mo. post event.	Three districts close to the epicenter.	41.30%	Ali et al. (2011)
2007 Pisco, Peru	PTSD	Age, Family Structure, Gender, SES	Interviews by trained personnel using the and conducted 5 mo. post event.	City of Pisco	25.20%	Cairo et al. (2010)
2007 Pisco, Peru	PTSD	Age, Family Structure, Gender, SES	PCL- questionnaire administered by professionals 4 years post event.	Urban or peri-urban areas of 5 districts in the province of Pisco.	15.90%	Flores et al. (2014)
2008 Wenchuan, China	PTSD	Age, Ethnicity, Gender	PCL- questionnaire administered by professionals 4, 6, 9, and 12 mo. post event.	Three secondary schools in Wenchuan	11.2%, 8.8%, 6.8%, 5.7%	Liu et al. (2010)
2008 Wenchuan, China	PTSD	Age, Gender	Interview with psychiatrist based on scale score, conducted 6.5 mo. post event.	Three middle schools in Mianzhu city	2.50%	Ma et al. (2011)
2008 Wenchuan, China	PTSD	Age, Ethnicity, Family Structure, Gender, SES	PCL- administered by professionals 15 months post event.	Two of the most severely affected sub-districts - 39 villages	15.20%	Jia et al. (2010a)
2008 Wenchuan, China	PTSD, Injury	Age, Ethnicity, Family Structure, Gender, SES	In-person interviews by trained personnel using the CPTSD-conducted 15 months post event.	Two of the most severely affected sub-districts - 39 villages	12.40%	Jia et al. (2010b)

2008 Wenchuan, China	PTSD	Age, Family Structure	Professional-administered self-report PCL-questionnaires conducted 6 mo. post event.	9 different counties within the earthquake region	4.50%	Liu et al. (2012)
2008 Wenchuan, China	PTSD	Age, Ethnicity, Gender, SES	Self-report using PCL- one year post event.	19 severely affected counties	40.10%	Jin et al. (2014)
2008 Wenchuan, China	PTSD, Fatality	Age, Ethnicity, Family Structure, Gender, SES	Interviews by trained personnel using the 3 mo. post event.	Four areas in Sichuan Province.	47.30%	Kun et al. (2013)
2009 L'Aquila, Italy	PTSD	Age, Gender	TALS- distributed 10 mo. post event.	Town of L'Aquila	37.50%	Dell'Osso et al. (2011)
2009 L'Aquila, Italy	PTSD	Age, Gender	TALS- distributed 10 mo. post event.	Town of L'Aquila	41.30%	Dell'Osso et al. (2012)
2009 Padong, Indonesia	Injury, Fatality	Age, Family Structure, Gender	Health records from the Health Office, Handicap International (NGO), five general hospitals, and a specific list of injured victims obtained from five villages.	Padang, Indonesia	NA	Sudaryo et al. (2012)
2010 Haiti	PTSD	Age, Family Structure, Gender, SES	In person interview by trained personnel using the modified to include DSM-IV-, conducted 2-3.5 mo. post event.	Nazon area of Port-au-Prince	24.60%	Cerda et al. (2010)

2010 Haiti	PTSD	Age, Gender, SES	In-person interviews by trained personnel using the life events checklist, , IES-questionnaires conducted 30 months post event.	Port-au-Prince and surrounding municipalities	36.75%	Cenat and Derivois (2014)
2011 Tohoku, Japan	PTSD	Age, Gender	Self-report PTSSC-eight mo. post event.	Schools in Ishinomaki City	42.60%	Usami et al. (2012)

: Clinician-Administered PTSD Scale.
: Children's Interview for Psychiatric Syndromes.
: Davidson Trauma Scale.
: Harvard Trauma Questionnaire.
for PTSD: Breslau Short Screening Scale for PTSD.
-12: 12-Item General Health Questionnaire.
-C: PTSD Check List – Civilian.
: Children's Revised Impact of Event Scale.
-RI: Child PTSD Reaction Index.
-SR: Trauma and Loss Spectrum – Self Report.
: Peritraumatic Distress Inventory.
-R: Impact of Event Scale-Revised.
-15: Post traumatic stress symptoms for children 15 items.
: Diagnostic and Statistical Manual of Mental Disorders

Table 6-26: Earthquake Events Surveyed in Meta-Data Analysis

1993 India	2000 Icelandic	2009 Padong, Indonesia
1994 Northridge, USA	2002 Italy	2009 L'Aquilla, Italy
1995 Hanshin-Awaji, Japan	2003 Bam, Iran	2010 Haiti
1998 Ceyhan, Turkey	2005 Pakistan	2011 Tohoku, Japan
1999 Chi-chi, Taiwan	2007 Pisco, Peru	
1999 Kocaeli, Turkey	2008 Wenchuan, China	

6.1.1 Age

Infants and the elderly represent the most vulnerable age groups to injury and fatality during and following an earthquake. There is essentially no information regarding the morbidity rates on infants and only a little information regarding the morbidity rates on children after earthquakes. Of this information, children are sometimes considered to be the most vulnerable age group [Jia et al. (2010b), Hsu et al. (2002), Liu et al. (2010), Zahran et al. (2008)]. This is

due to their physical size, muscular development, and psychological development with less of a conscious to react to a disastrous situation correctly [Zahran et al. (2008)]. Specifically, infants and young children are completely dependent on their care-givers. Amongst the larger quantity of available data, elderly people are often deemed the most vulnerable to injury and fatality [Chou et al. (2004), Peek-Asa et al. (1998), Mahue-Giangreco et al. (2001)]. This may be due to the assumption that the elderly are generally more likely to be resistant to taking precautionary actions, and due to aging.

The literature is quite mixed on which age group is most vulnerable to PTSD. Elderly people are often deemed the most vulnerable to PTSD [Jia et al. (2010a), Cenat and Derivois (2014), Altindag et al. (2005), Priebe et al. (2009), Flores et al. (2014)]. This basis comes from the understanding that elderly people are less likely to have the financial savings to recover following a natural disaster and more likely to rely on Social Security or other sources for their income. However, elderly people have a lifetime of experiences to help them emotionally recover from the traumatic events. Prior exposure to disastrous events has been shown to make individuals both more emotionally resilient and less emotionally resilient to future disastrous events. Some studies have shown that younger persons are more vulnerable to PTSD [Sharan et al. (1996), Kuo et al. (2007), Cerda et al. (2013), Sudaryo et al. (2012)]. Children are often overlooked, especially older children and their abilities to help during a disastrous situation. Peek (2008) discussed how parents and teachers often become distracted and distraught following a natural disaster and therefore may not properly attend to the emotional needs of children and reestablish their sense of security post-event, making the children vulnerable to PTSD and depression. Middle-aged adults have been shown to have the highest rate of PTSD

[Kuo et al. (2007)] attributed to responsibilities and pressures to provide income and the family's needs.

6.1.2 Built Environment

Widespread building damage to a community and damage to personal property have been linked to a higher rate of PTSD [Sharan et al. (1996), Shoaf et al. (1998), Siegel (2000), Ramirez et al. (2005), Altindag et al. (2005), Priebe et al. (2009), Liu et al. (2010), Usami et al. (2012)]. The majority of deaths and injuries resulting from earthquakes are due to building damage or collapse. A highly dense built-up environment creates a vulnerable population due to the larger potential for more buildings to collapse, collapse into each other creating debris missiles, and create a more congested area for egress. Cutter et al. (2003) identified the density of the built environment as one of the eleven major contributors to vulnerability based on the significant potential for structural losses. This vulnerability is exacerbated if the infrastructure is older and/or of poor quality. Being in an urban environment does not always equate to a higher vulnerability. If the major damage from an earthquake were to occur in a rural environment, it could be assumed that a lower number of buildings would be damaged, and likely a lower number of people injured or killed. However, access to aid and resources for the immediate and prolonged recovery efforts could be much lower for a rural community potentially making the rural community more vulnerable.

6.1.3 Ethnicity/Race

There is a dearth of knowledge on the impact of earthquakes on ethnicity and race. Ethnicity and race have been shown to be linked with social vulnerability, specifically in the United States, those cultures which are also non-English speaking [Siegel (2000)]. Noticing this, significant progress has been made in the United States during the past 20 years to release

information regarding disasters in multiple languages. People in ethnic and racial minority groups have been identified as more vulnerable than those in non-minority ethnic and non-minority racial groups [Kun et al. (2013), Jia et al. (2010), Liu et al. (2010)]. This is due to the fact that minorities generally have a lower political power, lower access to resources, and lower social support. Some ethnic groups are associated with fatalism, a term describing a person that thinks he/she is above natural hazard events; this is discussed in Fothergill and Peek (2004). This belief prevents the person from taking cover during an event and can lead to an increased probability of injury or fatality, as well as PTSD. Perilla et al. (2002) reported that Latinos (38%) were the most likely to develop PTSD, followed by African-Americans (23%), and the least likely being Caucasians (15%) amongst victims of Hurricane Andrew in a study of 404 residents in southern Florida. These percentages were not used in the socioeconomic model, but do provide some information regarding the prevalence sequence based on the United States population percentages of each ethnic and racial group.

6.1.4 Family Structure

Cutter et al. (2003) identifies female-headed households to be highly vulnerable, and African-American female-headed households to be among the most vulnerable. In a study by Zahran et al. (2011), hurricane-exposed single mothers were shown to never fully return to pre-disaster levels of mental health. Whether a female- or male-headed household, if a child resides in the household it has been shown that parents are more likely to respond to disaster warnings [Peek and Stough (2010)], which down the road should lead to a lower chance of developing PTSD. Peek and Stough (2010) reported that if a parent develops PTSD, one or more of their children are more likely to develop PTSD as well. On the other hand, single persons without children have been shown to be the least likely to develop PTSD when compared to their

partnered counterparts [Atlindag et al. (2005), Jia et al. (2010a), Flores et al. (2014)], which may be due to their independence. This does not necessarily hold true if the single-household consists of a widowed elderly person.

6.1.5 Gender

Females are consistently shown to be at a greater risk to post-traumatic stress disorder following a natural disaster [Kuo et al. (2007), Kilic and Ulusol (2003), Bodvarsdottir and Elklit (2004), Priebe et al. (2009), Ali et al. (2011), Delll'Osso et al. (2011), Jin et al. (2014), Kim et al. (2013), Jia et al. (2010a), Jia et al. (2010b), Cenat and Derivois (2014), Sharan et al. (1996), Sharan et al. (2013), Flores et al. (2014)] with a few exceptions that observed the opposite [Galea et al. (2004), Dell'Osso et al. (2013), Xu and He (2012), Atlindag et al. (2005), Chang et al. (2005)]. This finding has been observed as especially true for females with children living in the household, i.e. mothers, and for female-headed households with or without children living in the household [Zahran et al. (2011)]. Females may also be more susceptible to physical injury, or death [Mahur-Giangreco et al. (2001), Ramirez et al. (2005), Peek-Asa et al. (1998), Shaof et al. (1998), Chou et al. (2004)] during a large earthquake. The statistics may be coincidental, but it is more likely that they are due to the general difference in biological makeup between genders such as physical strength and emotional coping mechanisms.

6.1.6 Socioeconomic Status

Throughout the literature, social vulnerability is linked to socioeconomic status. Although being poor is not the only factor that makes a person or community vulnerable, it has been identified by many to be the most influential factor [Fothergill and Peek (2004), Cutter et al. (2003)]. In a study by Fothergill and Peek (2004), the poor were shown to be the most cautious and fearful of disasters, however they were also shown to take the least pre-cautionary

actions. This may be rationalized by considering that the poor generally do not have great job security, live in lower quality housing, and cannot afford, nor have the authority if renting, to take pre-cautionary actions such as buying earthquake insurance and properly strengthening their homes. The poor are generally associated with having lower political power, and less access to resources. In 2003, Cutter et al. developed the Social Vulnerability Index (SoVI), during the process of which eleven composite factors that contributed the most to social vulnerability were identified. Personal wealth was identified to be the most significant factor. Wealthier individuals and communities likely have a larger quantity of, and generally more expensive, material items to lose, however they also have the means to replace and recover. There are several case studies that have shown that the less-educated members of a society are more vulnerable to PTSD, injury, and death [Kuo et al. (2007), Galea et al. (2004), Bodvarsdottir and Elklit (2004), Priebe et al. (2009), Jin et al. (2014), Zahran et al. (2008), Schmidtlein et al. (2008), Cutter and Finch (2008), Altindag et al. (2005), Jia et al. (2010a), Cenat and Derivois (2014), Chang et al. (2005), Flores et al. (2014)]. Education generally goes hand-in-hand with annual income, i.e. the more educated are also wealthier, but not always. Regardless of annual income, intuitively, a higher education lends itself to people being more educated on the threat of a disaster, and the need to take more precautionary actions which allows one to react more effectively in disastrous situations.

6.2 Socioeconomic Variable Subcategories

Each variable consists of smaller subcategories. The subcategories were originally presented in Table 3-2, and now repeated for convenience in Table 6-4. The subcategories were selected based on the information available in the literature which demonstrated their influence on the morbidity rates. Originally, subcategories matched the subcategories available in census

data however there was not enough detailed information for most variables forcing simplifications and groupings of census subcategories. For example, here, age has six subcategories: child, adolescent, young adult, middle-aged adult, older adult, and elder. Census data breaks age down into 30 different age groups. Following the meta-data analysis discussed in the previous section, it was concluded that there was not enough information at this time to quantify the difference in any morbidity rate for children aged 2-3 versus 4-5 versus 6-7, etc., years old, although there is evidence to support that differences do in fact exist for younger and older children [Peek (2008)]. The meta-data analysis was conducted over many studies, nearly all of which split the age groups differently: some by decade, some by different physical and emotional developmental periods, some by convenient splits based on the congregated data, and some in other ways. Due to these differences, the conclusion which was revealed from these studies was the very evident difference in morbidity rates for children versus older adolescents versus young adults versus older adults versus the elderly. The lines drawn between these subcategories were a little grey, but determined to be at the ages shown in Table 5-3 for this study. There was no available data on the prevalence of PTSD for children aged 0-9, and therefore this subcategory was left out of the modeling of that morbidity rate.

Table 6-27: Variable Subcategories

Variable	*Subcategory*
Age	Child (0 - 9 y.o.)
	Adolescent (10 - 18 y.o.)
	Young Adult (19 - 29 y.o.)
	Middle-Aged Adult (30 - 45 y.o.)
	Older Adult (46 - 64 y.o.)
	Elder (65+ y.o.)
Built Environment	New Rural
	Old Rural
	New Urban
	Old Urban

Ethnicity/Race	Majority
	Minority
Family Structure	Single
	Partnered
	Parent
Gender	Female
	Male
Socioeconomic Status	Low
	Moderate
	Upper

This same process was followed for the variable ethnicity/race. There are numerous ethnicities and races present in the United States, and available in more modern U.S. census data. The studies surveyed in the meta-data analysis covered earthquakes that occurred worldwide. The various ethnicities and races present in different parts of the world can be very different from the United States as a whole, and especially when looking at specific communities in the United States. Detailed PTSD prevalence following earthquakes amongst the more common ethnic and racial minorities in the United States is not readily available. The last major earthquake which occurred in the United States was 20 years ago, and major progress has been accomplished with respect to disaster recovery for ethnic and racial minorities. What was concluded from the meta-data analysis was that there was a clear difference in the morbidity rates for persons in under-represented groups, or minorities, versus non-minority groups (here termed as majority), where these minority/majority groups were based on the larger region, e.g., the country where the earthquake occurred [Kun et al. (2013), Jia et al. (2010), Liu et al. (2010)]. When looking at the state of California in the United States, and zooming into specific communities, the demographics can be quite different. In one community, white/Caucasian, non-Hispanic, may be the majority, and in another community Latino/Hispanic may be the majority. Looking back to the 1971 San Fernando Earthquake, the majority of the affected area occurred in a Latino/Hispanic community. Following that earthquake, post-disaster recovery aid

was distributed at the state and federal levels, at which levels the Latino/Hispanic ethnic group was a minority. It was seen that the general response and time to recovery for members of the Latino/Hispanic ethnic group were mirrored to those of a minority group. Many people were not familiar with the disaster-recovery process and were steered away due to their inability to speak English and their immigration status. In the present framework, the white/Caucasian group was considered the majority, and all other ethnicities and races were grouped together as the minority in quantifying the morbidity rates. This is not a perfect representation of the difference in morbidity rates based on ethnicity and race mostly due to the large number of groups which were lumped together as the minority. Also, due to the fact that the literature reveals that people whom are non-English speaking or have English as a second language and currently live in the United States are generally more vulnerable than those minority members who have English as their native language [Siegel (2000)]. Although a legitimate fact, there was not enough information to quantify this difference into a new subcategory for the ethnicity/race variable. Especially when considering the lack of reliability in the U.S. census data to fully represent the number of persons in a community which would fall into that category.

Family structure required a similar process. There are at least six subcategories for family structure which differ from the three listed in Table 6-4 by distinguishing between being a single parent or partnered parent, and between being a single never married person, single-divorced person, or single-widowed person. However, in reality there are even more than six, and in this study all single-person households were grouped together without differentiating by previous marital status. Zahran et al. (2011) demonstrated how single mothers were more vulnerable, and how single mothers required a longer recovery time following Hurricane Katrina. There was not enough information following the meta-data analysis to quantify the difference in

morbidity rates for single parents, or specifically single mothers. There was also not enough information to distinguish between why a person was single and the resulting impacts. What was revealed in the meta-data analysis was that parents respond differently and generally take more precautions than non-parents [Peek and Stough (2010)], which influences morbidity rates. The meta-data analysis also revealed that single person households were generally less likely to take any precautions thereby influencing the morbidity rates negatively [Sudaryo et al. (2012)].

The subcategories for socioeconomic status were modified from U.S. census data based on what was learned from the meta-data analysis. Similar to the age and ethnicity/race variables, U.S. census data provides numerous subcategory breakdowns for annual income and education level. There was not enough information to quantify the difference in the morbidity rates for households with annual income of $46,000 versus $50,000 versus $54,000, etc. The referenced population surveys differed by identifying the group of people with the least monetary and social resources as a variety of terms such as the poor, working class, people of low income, or low socioeconomic status. Educational brackets varied significantly worldwide relative to the educational brackets more traditionally used in the United States. There was not enough information to quantify the difference in morbidity rates for persons with a high school diploma versus some college. More common educational brackets found in the meta-data analysis included “no education” versus “literacy”. What became very evident was that in each survey within the affected community there were fewer people in each of the morbidity categories that were in the highest income subcategory and/or in the highest education subcategory. There was a significant amount of information regarding annual income and education level, but many studies did not provide information on both. These two are generally linked, that is a person with a lack of education generally has a low income and a person with a more education

generally has a higher income. Therefore annual income and education level were modeled collectively as socioeconomic status in this study. Three subcategories were chosen: low, moderate, and high, each set relative to national averages. When developing the three subcategories, annual income extremes were used as cut-offs regardless of education level. That is to say, that annual income was decided to play a greater role in vulnerability than education. For example, as mentioned earlier, when looking at the state of California, and zooming into specific communities, the demographics can be quite different. In one community in Southern California the mean income may be over $200,000, and in another community in Southern California the mean income may be less than $42,000. Regardless of education, no one in the $200,000 mean annual income community would be expected to experience similar morbidity rates to someone of low socioeconomic status. Furthermore, the national mean income has been between $51,000 and $57,000 for the past ten years. Therefore, no one, regardless of education, in the $42,000 mean annual income community would be expected to experience similar morbidity rates to someone of high socioeconomic status. Table 6-5 provides the breakdown on the requirements to be in each socioeconomic status subcategory. This shows that regardless of education, a household is placed in the low socioeconomic status subcategory if the annual income is less than $25,000, and a household is placed in the high socioeconomic status subcategory if the annual income is $150,000 or greater. No modifications or groupings were used for the gender subcategories: male and female.

Table 6-28: Description of Socioeconomic Status Subcategories

Subcategory	*Annual Income*	*Education Level*
Low	Less than $25,000	Any
	$25,000-$75,000	High school diploma
Moderate	$25,000 - $100,000	College degree
	$75,000 - $150,000	Some college
High	Greater than $75,000	College degree
	$150,000+	Any

6.3 Socioeconomic Variable Weighting Functions

The variables discussed throughout this chapter were used to develop adjustment factors for the three morbidity rates. As discussed in Chapter 3, within the framework the morbidity rates were originally developed as a function of the damage states, and then adjusted based on the demographics of the population using the developed adjustment factors. The expressions for the morbidity rates were originally provided in Eq. 3-3 and Eq. 3-4, but are repeated here for convenience. The morbidity rates for injury and fatality are identical, and were expressed as

$$MR_{is,ds} = (F_{age,MR} \cdot F_{env,MR} \cdot F_{gen,MR} \cdot F_{ses,MR}) \cdot IS_{is,ds} \qquad \text{Eq. 6 - 1}$$

The morbidity rate for PTSD diagnosis was expressed as

$$MR_{pr,ds} = (F_{age,MR} \cdot F_{env,MR} \cdot F_{eth,MR} \cdot F_{fam,MR} \cdot F_{gen,MR} \cdot F_{ses,MR}) \cdot PR_{ds} \quad \text{Eq. 6 - 2}$$

where , , , , , and are the socioeconomic category factors for age, environment, ethnicity, family, gender, and socioeconomic status, respectively, and where the *MR* subscript refers to the factor value for either injury severity or PTSD rate. $_{,ds}$ and are the probability of injury severity level *is* and PTSD diagnosis rate for damage state *ds*, respectively, which were developed in Chapter 3. This section develops the socioeconomic factors in Eq. 6-1 and Eq. 6-2. Each factor was modeled by the same procedure. In each of the studies listed in Table 6-2, the authors surveyed members of the population in a specified area following an earthquake event. The intention of those studies was to identify the vulnerable population members so that aid may be

provided, and to extend the existing knowledge on social vulnerability and the predictors for injury, fatality, or PTSD. In most cases, tabulated outputs, and sometimes statistical analysis, were provided in the referenced publications providing the number or the percentage of a certain demographic which were victim to one of the morbidity rates. Generally, the studies recorded the demographic information of the surveyed population distinguishing between whichever morbidity rate was relevant to their study. These tabulated values were used to develop odds ratios between the subcategories used in this study. The odds ratio provides the quantity of how much more likely was one demographic to be victim of one of the morbidities than another demographic. A detailed example of how the odds ratios were computed is provided using the injury and fatality data given in Peek-Asa et al. (1998).

Odds Ratio Example

Following the 1994 Northridge earthquake, a survey was conducted over the 78 hospitals in Los Angeles County, California for earthquake admissions. Overall, 171 earthquake-related injuries were identified in 16 hospitals. In order to be considered an earthquake admission the patient had to have been admitted within two weeks after the mainshock, and the patient had to have been admitted due to a physical injury. "Injuries were defined as earthquake-related if the injury was due to consequences of earthquake activity." Deaths were identified by the Los Angeles County Office of the Coroner, and had to have resulted from a physical injury to be considered in the study. Table 6-6 is a regenerated version of the demographic data presented in Peek-Asa et al. (1998) for the 171 individuals. The population numbers presented in Table 6-6 were 1990 U.S. census estimates for Los Angeles County. The 95% confidence intervals for the odds ratios were provided in Peek-Asa et al. (1998), but were not included here.

Table 6-29: Earthquake-Related Injuries and Population Rates of Injury (Data from Peek-Asa et al. (1998))

Characteristic		*No. Earthquake-Related Injuries*	*Population*	*Odds Ratio*
Total		171	8,863,164	N/A
Severity	Fatal	33	8,863,164	1.00
	Hospitalized	138	8,863,164	4.10
Gender	Male	78	4,421,398	1.00
	Female	93	4,441,766	1.20
Age	0 – 9 y.o.	5	1,384,014	1.00
	10 – 19 y.o.	5	1,223,397	1.00
	20 – 39 y.o.	55	3,797,209	3.78
	40 – 59 y.o.	44	1,910,925	5.87
	60 – 79 y.o.	36	859,369	10.92
	80+ y.o.	25	188,498	34.58
Ethnicity/Race	White, non-Hispanic	102	3,618,850	1.00
	Hispanic	38	3,351,242	0.40
	African American	6	934,776	0.23
	Asian/Pacific Islander	12	907,810	0.47

The odds ratios in the last column of Table 6-6 were computed using the population values for Los Angeles County to show the relative risk of injury for each demographic group over the entire population. The odds ratio is expressed as

$$OR = \frac{a/b}{c/d} = \frac{a \times d}{b \times c} \qquad \text{Eq. 6 - 3}$$

where *a* is the number in the exposed group from demographic *a*, *b* is the number in the exposed group from demographic *b*, *c* is the number in the control group of demographic *a*, and *d* is the number in the control group of demographic *b*. For example, using the values in Table 6-6, the odds ratio for male gender was computed by

$$OR_{male} = \frac{78 \times 4{,}421{,}398}{78 \times 4{,}421{,}398} = 1.00 \qquad \text{Eq. 6 - 4}$$

and the odds ratio for female gender was computed by

$$OR_{female} = \frac{93 \times 4{,}441{,}766}{78 \times 4{,}421{,}398} = 1.20 \qquad \text{Eq. 6 - 5}$$

These odds ratios imply that females have a relative risk of 1.2:1.0 compared to males for an earthquake-related injury. Or better stated as, females are 1.2 times more likely than males to suffer from an earthquake-related injury.

Similar odds ratios were computed for all of the studies listed in Table 6-2, providing a range of relative risk values for each subcategory. The mean value of all odds ratios for each subcategory was taken as the subcategory factor, , which may be expressed as

$$f_{MR(sub)} = mean\left(f_{MR(sub,i)}\right); \qquad i = 1{:}\, n_{f_{sub}} \qquad \text{Eq. 6 - 6}$$

where MR is for the respective morbidity rate. This computation was executed for all subcategories listed in Table 6-4. The socioeconomic category factors, , used in Eq. 6-1 and Eq. 6-2 were computed by multiplying the subcategory factors by the percentage of the population in each subcategory, , and summing for all subcategories. The socioeconomic category factor may be expressed as

$$F_{MR(cat)} = \sum_{i=1}^{n_{sub}} f_{MR(sub,i)} \cdot p_{sub,i} \qquad \text{Eq. 6 - 7}$$

This effectively applies a factor (or weight) to the population data. For example, if = 2 and = 1, and if there were 50% of each gender in the population, then would be computed as

$$F_{gender} = 1(0.5) + 2(0.5) = 1.5 \qquad \text{Eq. 6 - 8}$$

This would imply that the rate of PTSD diagnosis is expected to be 150% of the baseline rate for the specified community following the scenario earthquake, where the baseline rate is determined based on building damage. The final expected rate of PTSD diagnoses will increase further, or decrease, based on the other category factors.

6.4 Limitations

Some limitations to the work proposed in this dissertation were mentioned in Chapter 3. Those limitations were not felt to overcome the quality or intention of this work. Limitations

directly related to the modeling of the socioeconomic variable subcategories were discussed in Sec. 6.2. Other limitations associated with the socioeconomic model are as follows.

There was not enough information to model the subcategory factors for the built environment, , in the same way as the socioeconomic variables. Rather than averaging over several identified odds ratios, a set odds ratio was assigned to each subcategory of the built environment for each morbidity rate based on engineering judgment. The values selected as the subcategory factors for the built environment for the three morbidity rates are provided in Table 6-7. Very little scatter was assumed for the injury and fatality rates, and only a bit more difference was assigned to the PTSD diagnosis rate.

Table 6-30: Subcategory factors for the Built Environment

Subcategory	*Morbidity Rate*		
	Injury	*Fatality*	*PTSD Diagnosis*
New Rural	0.95	0.90	1.10
Old Rural	1.00	1.00	1.30
New Urban	1.05	1.00	1.00
Old Urban	1.15	1.10	1.20

Odds ratios were computed from the referenced population data for modeling the subcategory factors. Not all odds ratios were created equally. That is, the quality of data collection was not consistent for all studies. To account for this, quality ranks from 1 to 3, with 3 being the highest quality, were assigned to each study. The user of the framework may select to use only studies with a quality rank of 3, quality rank of 2 and 3, or all data regardless of quality rank. For the studies providing data for PTSD diagnoses, there were three potential factors which could reduce the quality rank.

Factor 1: The data collection process for predictors of PTSD followed one of three methods: (1) computer-assisted phone interview, (2) self-report symptom checklist, or (3) in-person interview with trained personnel. Considering these three methods, the bias in the sample

was assumed to decrease one quality rank level from method one to method two to method three, respectively. That is, the assigned quality rank decreased a level for each decreasing method.

Factor 2: A major controversy in the field is on the different measurement scales that may be used to diagnose Post-Traumatic Stress Disorder (PTSD). For example, in a brief survey of the literature four different scales used are the (1) Davidson Trauma Scale (DTS) [Kuo et al. (2007)], (2) the Breslau Short Screening Scale for PTSD [Priebe et al. (2009)], (3) the Harvard Trauma Questionnaire [Cairo et al. (2010)], and (4) the PTSD Check List [Flores et al. (2014)], to name a few. The instrument used for diagnosing PTSD was often modified from the Diagnostic and Statistical Manual of Mental Disorders (DSM) diagnosis or used an incomplete tool. The quality rank of studies which used modified or incomplete PTSD assessment tools was decreased by one point.

Factor 3: PTSD may not be properly diagnosed until it has been present for at least one month. Some of the studies referenced in this work reported population estimates for PTSD prior to the one month requirement. In this case, the quality rank of the study was decreased by one point.

For studies which provided data for injury or fatality, only one detail was identified which reduced the quality rank which regarded the data collection method. Data collected from medical records was considered of high quality. Data collected from computer-assisted phone interviews were considered to have a quality rank of one level less.

In addition to the difference in quality of the published data, studies were collected from earthquakes occurring worldwide. This worldwide data collection method was under the assumption that relative risk of people in other countries subjected to an earthquake disaster could be applied to a United States earthquake disaster better than applying the relative risk from

different disaster types only occurring within the United States. The latter would require using relative risk data from the terrorist attack on 9/11, Hurricane Katrina, Hurricane Sandy, the tornados in Joplin, MS, Tuscaloosa, AL, or Moore, OK, etc. to be applied to a potential earthquake disaster. This route was rejected due to the fact that people respond differently to different disaster types, especially a natural disaster versus a terrorist attack. Even still, the assumption that was employed is imperfect, especially when comparing information from developing nations and applying it to a developed nation. The World Factbook [CIA (2011)] lists 34 developed countries (DC). The user of the framework may select to only use studies conducted in DC, or they may select to use data from all countries to account for this assumption.

As mentioned briefly in Sec. 3.6, there is a noted discrepancy in the literature on the accuracy of comparing losses over time and the accuracy of using statistical demographic data collected at one geographic scale and applying it to another geographic scale. Both of these controversial methods are proposed to be used in the present framework and present a limitation to the study. To combat these limitations, two studies are presented. In 2008, Cutter and Finch conducted a study on the temporal changes in social vulnerability to natural hazards using Cutter's Social Vulnerability Index (SoVI). Five time periods were analyzed: 1960, 1970, 1980, 1990, and 2000. The authors provided which demographic factors played the most significant role in each of the analyses, and for each of the five decades, the SoVI indicated that socioeconomic status was the most influential factor. Albeit, the percent of the variance explained by socioeconomic status varied for each decade, it was still the controlling factor. Three other factors, development, gender, and age, showed up in the five most significant contributors for all five analyses, and race showed up in all but one. Over five decades, the four

of the top five contributing demographic factors to social vulnerability were consistent and only varied by a few percent in each case. Also in 2008, Schmidtlein et al. conducted a similar study on the sensitivity of the SoVi to change in the geographic scales. Analyses were conducted at the county level, intermediate level, and census tract level. The results for all three geographic levels varied, but were similar. Of the top seven contributing factors for social vulnerability, as dictated by the SoVI, race and poverty, Hispanic immigrants, age, gender, and wealth appeared for all three analyses, albeit in a slightly different order with slightly different percentages. Based on these two studies, although not perfect arguments for the present framework, it may be concluded that there is some discrepancy in the results when changing the time scale or geographic scale, however there is reasonable consistency in the results as well. Therefore, these methods are proposed to be used here, but as noted limitations of the study.

Chapter 7: Genetic Algorithm

To perform the optimization within the socioeconomic framework for identifying the optimal retrofit plans, a multi-objective genetic algorithm (GA) was employed. A genetic algorithm is a search algorithm which generates multiple solutions at each iteration and continues until an optimal solution is found. The optimal solutions are identified by the fitness function based on the objective function and constraints. The objectives discussed in Chapter 2 (i.e. initial cost, economic loss, number of morbidities, and recovery time) are minimized as the multi-objective function in this study.

7.1 Genetic Algorithms

Genetic algorithms (GA) are a subcategory of Evolutionary Algorithms, and are based on the mechanism of natural genetics and natural selection. The theory behind GAs is a direct analogy to Charles Darwin's Theory of Evolution. GAs imitate biology by optimizing a population of chromosomes consisting of a set of genes. Consider human beings where the genetic makeup of a human is described by a chromosome. The chromosome consists of various genes such as eye color, hair color, gender, etc. Each gene has various alleles, i.e. the value of the gene. For example, the alleles of eye color are brown, hazel, blue, green, etc. The world consists of an entire population of human beings. Two humans will mate and produce offspring. The alleles of the offspring are a combination of the dominant genes from the two parents. Throughout time, dominant genes may change, but the dominant genes are the ones that survive and continue on to the next generation. Fitness is the term used to measure each chromosome's dominance, i.e. survival of the fittest.

Within a genetic algorithm, chromosomes are series of real numbers or binary strings which represent certain characteristics, features, or mechanisms (i.e. genes). Each gene has a characteristic value denoted as its allele. The chromosomes, genes, and alleles are problem-specific. For example, in the present study, the chromosomes represent a community's woodframe building stock rather than humans. The genes are the different types of buildings present in the community (i.e. the 37 archetypes). The alleles are the quantity of each archetype present within the community.

The first generation in a genetic algorithm is typically randomly generated. In this study, the initial population is based on the input building statistics of the community (the quantity of woodframe buildings of each age and size that are actually present in the community). Mating is represented by the crossover operator. Two parent chromosomes "mate" and produce two offspring for the next generation. This consists of swapping a single or group of genes between the two chromosomes. A mutation operator is employed to maintain diversity within the population. This operator was introduced into the numerical algorithm, rather than being representative of actual biology. Mutation helps prevent premature convergence of the solution. Constraints are imposed to prevent the number of structurally deficient and structurally obsolete archetypes from increasing in future generations. Following crossover and mutation, the offspring chromosomes go through a selection operator where they compete against each other. The dominant chromosomes, those which most satisfy the objective(s), survive. Consecutive generations are determined based on the problem-specific objective function and fitness. This process of crossover-mutation-selection repeats for a set number of generations or until a specified outcome is obtained.

7.2 Advantages of GAs over Other Optimization Methods

Genetic algorithms are simple in nature, but have the ability to solve most optimization problems making them quite robust. Due to the complex nature of the multi-objective community-level mitigation planning optimization addressed here, genetic algorithms have several advantages over other optimization methods. Goldberg (1989) discussed how genetic algorithms have four fundamental differences that allow them to be more robust than other optimization methods:

1. GAs work with a coding of the parameter set, not the parameters themselves. This is advantageous because often times the parameters are in different units or measurement scales and can be very difficult to model. It is also beneficial when the number of parameters in the multi-objective optimization problem is very large.
2. GAs search parallel from a population of points, not a single point. This is beneficial when there are multiple local optima because the GA will avoid premature convergence to local optimal solutions or false-peaks.
3. GAs use payoff (objective function) information, not derivatives or other auxiliary information. This is beneficial if the objective function is not smooth, or is nonlinear, or if there are a large number of parameters to which the gradient information is not known.
4. GAs use probabilistic transition rules, not deterministic ones making them quite robust and able to solve most optimization problems.

Genetic algorithms are especially beneficial in solving multi-objective optimization problems due to the population of solutions generated every iteration. In this study, the GA will produce the pareto-optimal set of solutions for the decision maker(s) by extracting diverse solutions generated at each iteration. The decision maker(s) could input preferences by

weighting the performance objectives and allowing the genetic algorithm to identify the optimal solution. In this study, multiple weights were used to generate diverse solutions so that the pareto-optimal set may be developed. Once the pareto-optimal set was obtained, then decision maker preference was employed.

7.3 Description of the Genetic Model

The general procedure for the GA to be employed here is shown in Figure 7-1. There are three major sub steps in any genetic algorithm: crossover, mutation, and selection. The population is initialized through building statistic inputs for each archetype based on census data for the region, and the population initial fitness is computed. If the population fitness does not meet a pre-defined value, the population goes through the selection, crossover, and mutation operators and the population fitness is re-calculated. If there is still diversity in the population fitness or if the number of generations is less than the maximum set number of generations, the next generation is spawned repeating the crossover, mutation and selection operators until the solution converges or meets the specified maximum number of generations.

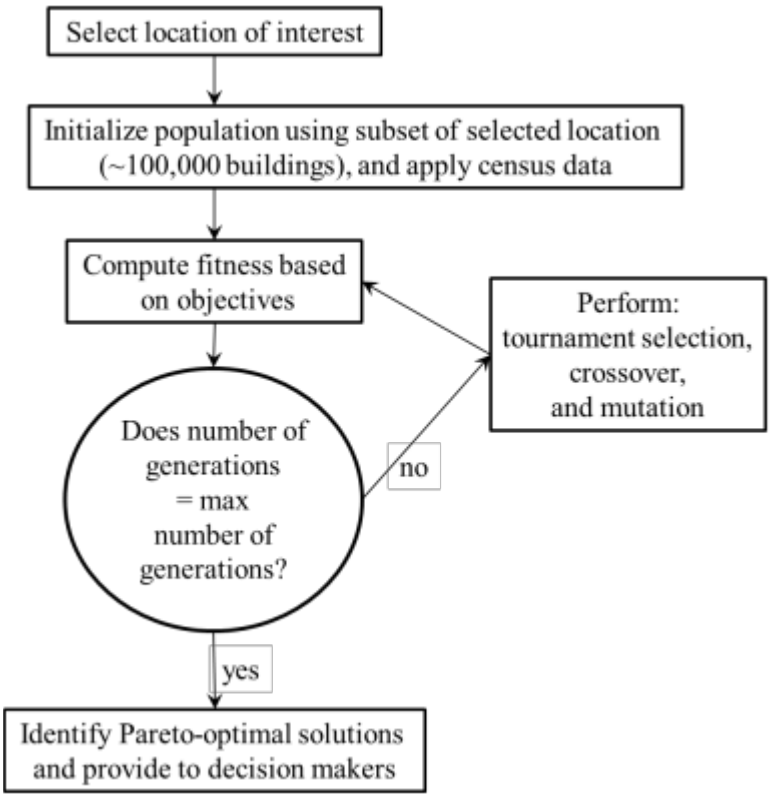

Figure 7-1: Generalized Genetic Algorithm Procedure

7.3.1 Fitness Formulation

The fitness function is a key part of the genetic algorithm. Genetic algorithms are based on the theory of evolution and survival of the fittest. The fitness function measures the "fitness" of each population member so that the most-fit member (i.e. optimal solution) may be identified. In this study, the fitness was computed by using only the mean values for each of the performance objectives to provide a strict number for comparison purposes. The mean performance objectives, , were normalized by the minimum population value of each respective performance objective in order to keep each on the same order of magnitude. Once normalized, the performance objectives were weighted, , and summed together. The fitness function may be expressed as

$$fitness = w_1 \cdot ro_1 + w_2 \cdot ro_2 + w_3 \cdot ro_3 + w_4 \cdot ro_4 \qquad \text{Eq. 7-40}$$

where the expressions for were provided in Eqs. 3-11, 3-13, 3-5, and 3-34 for initial cost, economic loss, number of morbidities, and time to recovery, respectively. The weights allow input of the decision maker preferences and can be changed to provide more diverse solutions. The lower the fitness value, the more fit the individual, and the more likely for it to be duplicated in future generations, this is the premise of a genetic algorithm.

7.3.2 Tournament Selection

The selection process uses the objective functions and fitness to determine which individuals will move on to the next generation. The tournament selection procedure is commonly used in optimization problems and was employed here. In tournament selection, each individual has two copies inserted into a mating pool, and therefore each individual competes in the tournament twice. Two individuals are randomly selected from the mating pool; the individual with the higher fitness value wins the tournament and moves on to the next generation. Another pair of individuals is drawn and the process continues until the new population has filled. Using this procedure, the most-fit individual in the population receives two copies in the new population, and the least-fit individual is removed from the new population. In this way, it is easy to see how the fitness of the population improves with future generations.

7.3.3 Double-Point Crossover

A crossover routine randomly exchanges characteristics (genes) between randomly selected individuals (chromosomes). The number of individuals selected to take on the crossover operator depends on the crossover rate, or probability of crossover, which is dictated by the user. The value of the crossover rate used in this study was 0.85. A single, or multiple, crossover

site(s) may be randomly generated or set. Many complicated crossover routines have been developed, however for this study; a double point crossover was employed due to the characteristic makeup of the chromosomes. The two crossover sites were set at the same locations for each chromosome entering into the crossover operator. Figure 7-2 provides a schematic demonstrating the crossover routine used in this study. Recall, within a chromosome the first seven genes are the number of each archetype designed by the 1959 Blue Book provisions, followed by the 1978 NEHRP designs, ASCE7-05 designs, SDDD-IO and SDDD-LS designs for all seven floor plans. The final two chromosomes are the two soft-story buildings retrofitted following the FEMA P-807 guideline. Referring to Figure 7-2, during crossover, the alleles of the modern designs (ASCE7-05 designs, SDDD-IO and SDDD-LS) of one parent are switched with the alleles of the other parent forming the two new offspring. The example genes in Figure 7-2 are all two-digit values for demonstrative purposes only.

Figure 7-2: Example of Double-Point Crossover Operator

7.3.4 Mutation

The mutation operator changes one or more alleles within a selected chromosome. The number of chromosomes which enter the mutation operator is based on the mutation rate, or probability of mutation which is similarly input by the user. The value of the mutation rate used in this study was 0.10; it is typically much lower than the crossover rate. The mutation operator helps maintain diversity in the population and keep the solution from premature and less than optimal convergence by randomly switching genes throughout the optimization process. To execute the mutation operator, a randomly selected single gene on a randomly selected individual mutates to a random (feasible) value. In this study, a single-point mutation site was used, and randomly selected as any of the first 14 gene within the chromosome (i.e. the 1959 Blue Book and 1978 NEHRP designs). The selected gene's allele mutates to a randomly generated number constrained by real number values to be between 0 and 1000. Figure 7-3 demonstrates the mutation operator on an example chromosome. The example genes in Figure 7-3 are all two-digit values for demonstrative purposes only.

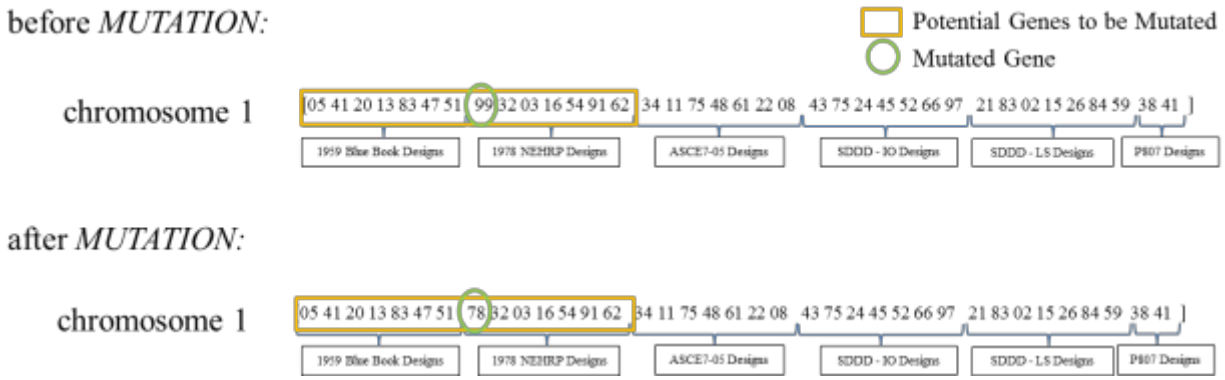

Figure 7-3: Example of Mutation Operator

7.4 Penalty Functions and Constraints

Penalty functions may be incorporated into a genetic algorithm as a way to impose constraints on the solutions, or to encourage the solution in a more optimal direction. There were

multiple penalty functions and constraints imposed in the GA used here. A constraint requires a solution to follow it. A solution may not meet the constraint imposed in a penalty function, and if it does not, then its fitness is altered in a negative way.

7.4.1 Constraints

The constraints imposed in this genetic algorithm were all based on controlling the number of each archetype, the total number of each floor plan over all designs, and the total number of all archetypes in a single solution. The constraints used in this study are provided as follows

- At all times, the total number of archetypes in the population is to remain at 100,000.
- At all times, the total number of floor plan, , over all designs, cannot be less than the original number of floor plan, , for the two outdated designs (1959 Blue Book and 1978 NEHRP) combined. This constraint ensures that the solution does not converge to having only a single floor plan present in the community. This constraint does allow more buildings of each building to be constructed, as long as the total number of archetypes does not exceed 100,000 as per the previous constraint.
- At all times, the total number of floor plan, , designed following the 1959 Blue Book provisions may not be greater than the original number of floor plan, , designed following the 1959 Blue Book provisions in the initial population. This same constraint is duplicated for all archetypes designed by the 1978 NEHRP provisions. These constraints ensure that the solution does not imply that more structurally obsolete or deficient buildings should be constructed.

7.4.2 Penalty Functions

There were three penalty functions imposed in the genetic algorithm. Two of the three penalty functions were imposed based on the budget input by the user, and the third penalty function was for further controlling the total number archetypes in the community. In each case, if the constraint was not met by the individual (solution), the corresponding fitness was multiplied by a factor of two. The first penalty function was for directing the initial cost of the optimal solution to be less than the budget set by the user. If the initial cost of the solution was greater than the budget, then its corresponding fitness value was multiplied by a factor of two. The first penalty function for limiting the initial cost may be expressed as

$$\begin{aligned} IF \quad & RO_{1,j} > budget \\ THEN \quad & fitness_j = 2 * fitness_j \end{aligned}$$

where is the initial cost of the individual in the current generation, as was defined in Eq. 3-11. The second penalty function was for directing the total economic loss of the optimal solution to be less than 10 times the budget set by the user. If the economic loss of the solution was greater than 10 times the budget, then its corresponding value was multiplied by a factor of two. The second penalty function for limiting the total economic loss may be expressed as

$$\begin{aligned} IF \quad & RO_{2,j} > 10 * budget \\ THEN \quad & fitness_j = 2 * fitness_j \end{aligned}$$

where is the economic loss of the individual in the current generation, as was defined in Eq. 3-13. The last penalty function was imposed for controlling the total number of archetypes in the community. If the total number of archetypes in the community was not equal to 100,000, then the corresponding fitness value was multiplied by a factor of two. The third penalty function may be expressed as

$$IF \quad \sum_{arch=1}^{37} n_{arch,j} \neq 100{,}000$$
$$THEN \quad fitness_j = 2 * fitness_j$$

The constraints were imposed following the Crossover and Mutation operators, and the penalty functions were imposed prior to the Selection operator. The factor of two was somewhat arbitrarily chosen, however through several trial runs it was identified to be an effective value. It should be noted that all coding for the genetic algorithm and socioeconomic framework was written in MATLab by the author.

Chapter 8: Application of Framework

In this chapter the community resiliency framework is applied to several illustrative examples over a subset of Los Angeles County, California. Prior to the illustrative examples, the framework was calibrated to the reported morbidity rates from the USGS Shakeout Scenario [USGS (2008)]. The USGS Shakeout Scenario looked at a much larger area, around 10,000,000 people. In this study, the framework is applied to a subset of 100,000 buildings, corresponding to approximately 1,000,000 people. The morbidity rates predicted in the Shakeout Scenario for a very large earthquake were approximately matched at a spectral acceleration of 2.5g, corresponding to a MCE seismic intensity which would be caused by a ground shaking intensity approximately equal to the worst section of what was examined in the Shakeout Scenario. At 2.5g spectral acceleration, the framework was applied using the Los Angeles County population without including the socioeconomic parameters, since these were not modeled in the Shakeout Scenario. Once a satisfactory level of calibration was achieved for the morbidity rates, the framework was reapplied using the socioeconomic parameters to compare the loss estimates with the reported losses from the 1994 Northridge earthquakes.

The 1994 Northridge earthquake was the last major earthquake which occurred in the United States. Most woodframe residential structures have fundamental periods of, or very near to, 0.2 seconds. A range of peak ground acceleration (PGA) values (less than 0.3g and up to greater than 0.6g) were recorded from the 1994 Northridge ground motion. The PGA for this study was taken as 0.5g resulting in an average spectral acceleration of 1.1g for the buildings with a fundamental period of 0.2 seconds. In 2003, a large federally-funded project known as the CUREE-Caltech Woodframe Project [Shierle (2003)] conducted an extensive investigation

on the damage to woodframe structures caused by the 1994 Northridge earthquake. The project reported various loss estimations, including the subassembly repair costs and repair times used in this study [Reitherman and Cobeen (2003)]. CUREE Publication No. W-09 reports that "About half of the $40 billion in property loss was in woodframe buildings." Therefore, the economic loss from the framework should be approximately, but less than, $20 billion. Applying the framework to the Los Angeles County population at 1.1g spectral acceleration at the same occupancy rates that might have been experienced during the Northridge earthquake (peak occupancy for residential structures), the percentile value for the economic loss was approximately $16 billion, which was felt to be close enough to the Northridge earthquake. Additionally, the CUREE publication reports "48,000 housing units were uninhabitable", therefore the total number of archetypes being classified in either damage state 4 or damage state 5 were summed and calibrated to equal approximately 48,000.

The calibrations discussed above were achieved by multiplying the resulting distributions for the estimated losses by factors to achieve the reported values. Eq. 3-5 presented the expression used for computing the number of morbidities. Rearranging this expression and incorporating the calibration factors, the expression for computing the number of morbidities becomes

$$RO_3 = F_{inj} \cdot \sum_{ds=1}^{n_{ds}} \left[\left(\sum_{is=1}^{4} MR_{is,ds} \right) \cdot \sum_{i=1}^{n_{arch}} \left(n_{i,ds} \cdot occ_i \right) \right] + F_{fat} \cdot \sum_{ds=1}^{n_{ds}} \left[MR_{is5,ds} \cdot \sum_{i=1}^{n_{arch}} \left(n_{i,ds} \cdot occ_i \right) \right] + F_{PTSD} \cdot \sum_{ds=1}^{n_{ds}} \left[MR_{pr,ds} \cdot \sum_{i=1}^{n_{arch}} \left(n_{i,ds} \cdot occ_i \right) \right] \quad \text{Eq. 8 - 1}$$

where , , and are the calibration factors for the injury, fatality, and PTSD diagnoses counts, respectively. These factors were determined to be 0.5 in all three cases. The remaining variables were defined in Chapter 3.

Once the framework was calibrated, illustrative examples were executed by analyzing three populations. The first population was the current demographic found in the 2010 U.S. census data for Los Angeles County, California. The second and third populations provide example demographics to further demonstrate the framework based on potential population growths, or population forecasts, for Los Angeles County. In each case, the framework was applied at six different seismic intensity levels, with and without incorporation of the socioeconomic variables. In total, 36 applications of the framework are presented demonstrating the significance of the socioeconomic variables, followed by three examples demonstrating the importance of the time of day.

Due to the framework's assumption that all buildings within the community are at an equal distance from the epicenter of the earthquake, a subset of the population size had to be used, rather than the entire population size for Los Angeles County as mentioned earlier. The subset population size was set as 100,000 buildings. There were several constants for the case studies presented below. These included the initial building inventory (see Table 8-1) which was selected as the building inventory of Los Angeles County based on 2010 U.S. census data. For the modernly design buildings, it was not evident from the census data which seismic provision was used in the design. Therefore, the quantity of modern buildings was evenly distributed over the last 23 genes for each respective floor plan. Subsequently the initial percentages for the subcategories of the built environment were constant for all case studies. In addition to the demographic and housing data, the genetic algorithm and optimization inputs were held constants for all examples. The probability of crossover was set to 0.85, the probability of mutation was set to 0.10, and the number of individuals in the population per generation was set to 50. The maximum number of generations was set to 100. A collapse limit of 10% inter-story

drift was employed. The peak inter-story drift values for each archetype from the nonlinear time history analyses were extracted at 50 percent probability on nonexceedance. The objective weights were set to unity in all cases so that the decision maker(s) could employ preferences at the end.

Table 8-31: Building Stock of Initial Population

Seismic Provision	*Floor Plan*	*Percentage of 100,000 in Initial Population*
1959 Blue Book	1	9.59%
	2	9.59%
	3	6.90%
	4	10.43%
	5	9.59%
	6	9.59%
	7	20.22%
1978 NEHRP	1	2.26%
	2	2.26%
	3	1.63%
	4	2.46%
	5	2.26%
	6	2.26%
	7	4.77%
ASCE7-05	1	0.26%
	2	0.26%
	3	0.19%
	4	0.21%
	5	0.26%
	6	0.26%
	7	0.41%
SDDD-IO	1	0.26%
	2	0.26%
	3	0.19%
	4	0.21%
	5	0.26%
	6	0.26%
	7	0.41%
SDDD-LS	1	0.26%
	2	0.26%
	3	0.19%
	4	0.21%
	5	0.26%
	6	0.26%
	7	0.41%
FEMA P-807	1	0.21%
	2	0.41%

8.1 Case Study 1: Los Angeles County, California

The first case study was conducted using the 2010 U.S. census data for Los Angeles County, California. The input values for each subcategory are provided in Table 8-2.

Table 8-32: Los Angeles County Community Inputs

Variable	*Subcategory*	*Input Value*
Total Population Size		9,818,605
Mean Annual Income		$81,729
Mean Household Size		2.98
Percentage of Households with Children		37.2%
Age	Child (0 - 9 y.o.)	13.1%
	Adolescent (10 - 19 y.o.)	14.6%
	Young Adult (20 - 29 y.o.)	15.4%
	Middle-Aged Adult (30 - 45 y.o.)	21.9%
	Older Adult (46 - 64 y.o.)	24.2%
	Elder (65+ y.o.)	10.9%
Ethnicity/Race	Majority	1.5%
	Minority	98.5%
Family Structure	Single	19.5%
	Partnered	80.5%
	Parent	37.2%
Gender	Female	50.3%
	Male	49.7%
Socioeconomic Status	Low	50.3%
	Moderate	34.9%
	Upper	14.5%

8.1.1 Illustrative Examples of the Optimization Framework

The examples presented in this subsection were conducted using the optimization framework for community-level resiliency. The analyses were conducted over the 2010 Los Angeles County population (see Table 8-2) at a MCE seismic hazard (Sa = 2.5g). The time of day was set to night (2:00am) such that peak occupancy of the residential structures would be achieved. Specifically, the occupancy percentage employed for the residential structures was 98%, and 25% for the commercial structures. The analysis was conducted once using the social vulnerability computations, and once without including the social vulnerability computations. In

each case, six plots are presented. The plots provide relationships between the percentile values for the objectives. Each point on a plot represents a different solution identified by the genetic algorithm. The same solutions are plotted on all six plots, but with the different objective values compared. Recall, the framework solution is a chromosome representing the number of each of the 37 archetypes present within the community. There are 5000 solutions on each plot, many of which are identical. The percentile values were extracted from the full lognormal distributions of each objective. The full distribution plots are provided in Appendix D for each of the objectives, as well as, several complimentary damage measures.

8.1.1.1 Community-Level Optimization of Los Angeles County at a MCE Seismic Hazard using Social Vulnerability

A community-level optimization was conducted using the resiliency framework on the 2010 Los Angeles County population at a MCE seismic hazard considering the social vulnerability of the community. The resulting percentile values for the four objectives are plotted in Figure 8-1 through Figure 8-6. The green circles highlight the pareto-optimal solutions in each figure. The pareto-optimal surface represents the optimal tradeoff with respect to the two objectives being compared. The pareto-optimal surface is not identical in the figures, because the identified solutions are optimal for only a subset of the objectives, and not all four objectives. Figure 8-1 provides the relationship between the estimated economic loss and the associated initial cost of the solutions. Three solutions formed the pareto-optimal surface for these two objectives. Figure 8-2 provides the relationship between the estimated number of morbidities and the associated initial cost of the solutions. Recall that the number of morbidities includes the total number of injuries, fatalities, and PTSD diagnoses. In this case, only two solutions were identified on the pareto-optimal surface. Figure 8-3 provides the relationship

between the estimated recovery time and the associated initial cost of the solutions, where only a single optimal solution was identified. Figure 8-4 provides the relationship between the estimated economic loss and the recovery time of the solutions, with only a single optimal solution identified. Figure 8-5 provides the relationship between the estimated number of morbidities and the recovery time of the solutions, again, with only a single optimal solution identified. Figure 8-6 provides the relationship between the estimated number of morbidities and the associated economic loss of the solutions. In this case, two solutions were identified to form the pareto-optimal surface. From these six plots, only three solutions were identified to form the pareto-optimal set of solutions for all four resiliency objectives. However, only two were extracted for further investigation. One of the two selected solutions provided the optimal tradeoff for the objectives number of morbidities and recovery time. The second selected solution provided the optimal tradeoff for the objectives initial cost and economic loss.

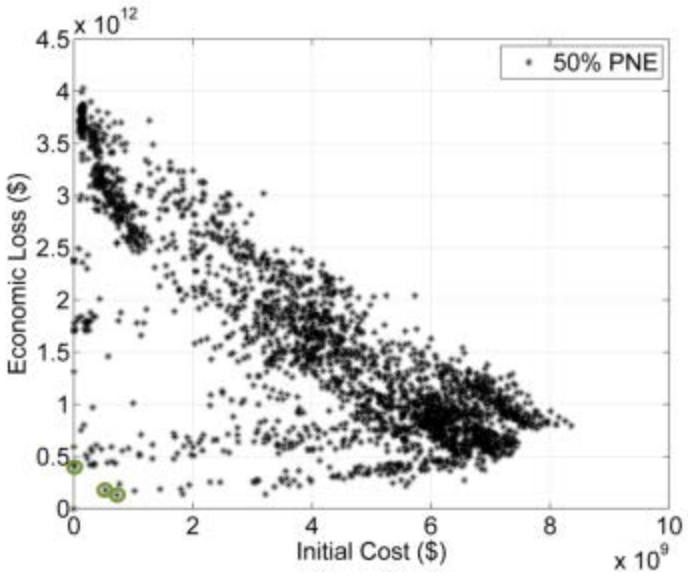

Figure 8-1: Percentile Values for Economic Loss vs. Initial Cost for Los Angeles County at MCE using Social Vulnerability with Pareto Optimal Surface Labeled

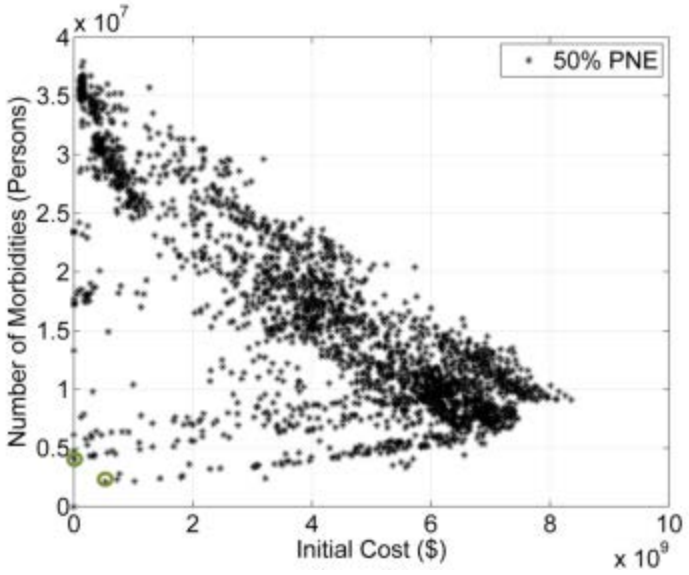

Figure 8-2: Percentile Values for Number of Morbidities vs. Initial Cost for Los Angeles County at MCE using Social Vulnerability with Pareto Optimal Surface Labeled

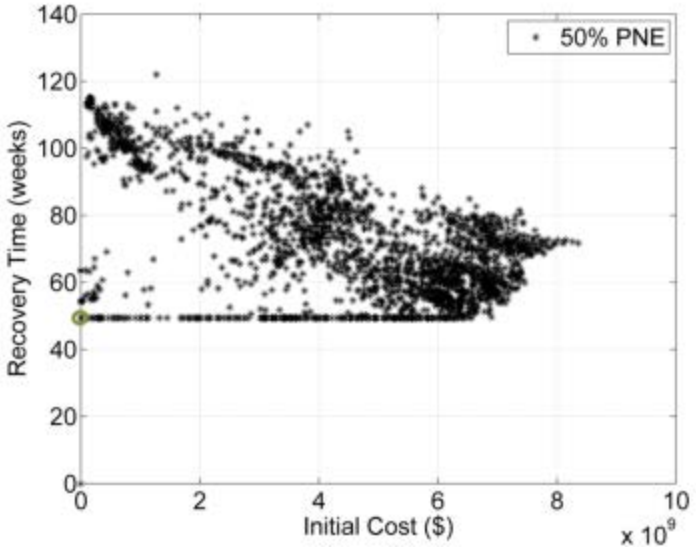

Figure 8-3: Percentile Values for Recovery Time vs. Initial Cost for Los Angeles County at MCE using Social Vulnerability with Pareto Optimal Surface Labeled

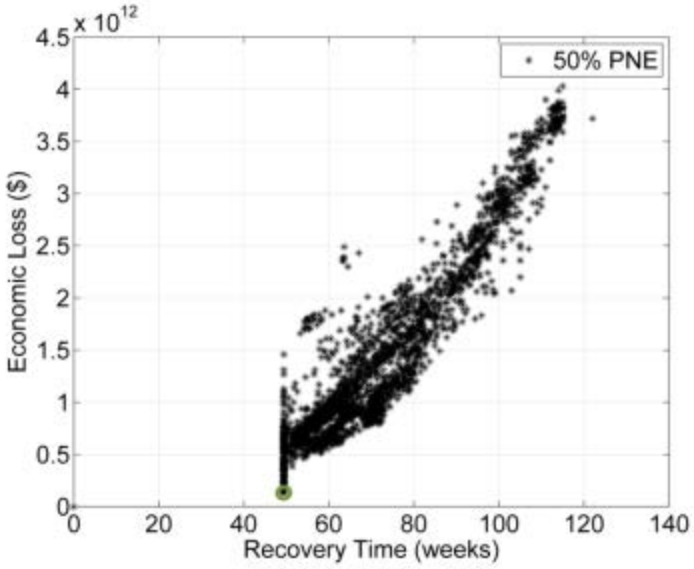

Figure 8-4: Percentile Values for Economic Loss vs. Recovery Time for Los Angeles County at MCE using Social Vulnerability with Pareto Optimal Surface Labeled

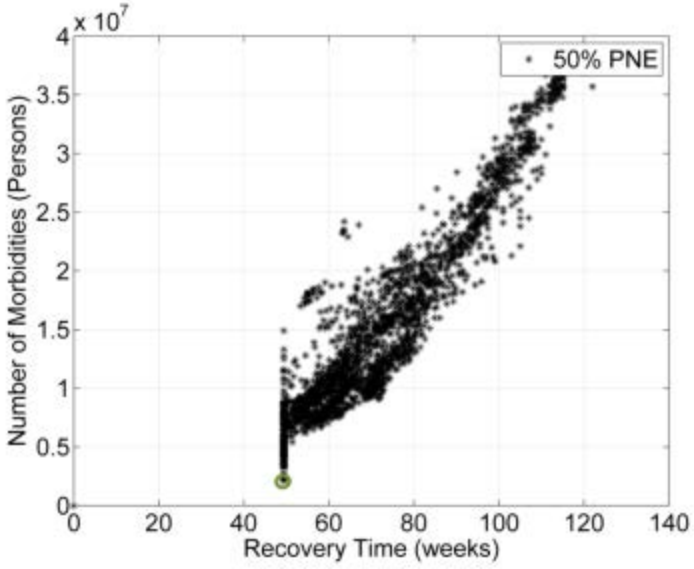

Figure 8-5: Percentile Values for Number of Morbidities vs. Recovery Time for Los Angeles County at MCE using Social Vulnerability with Pareto Optimal Surface Labeled

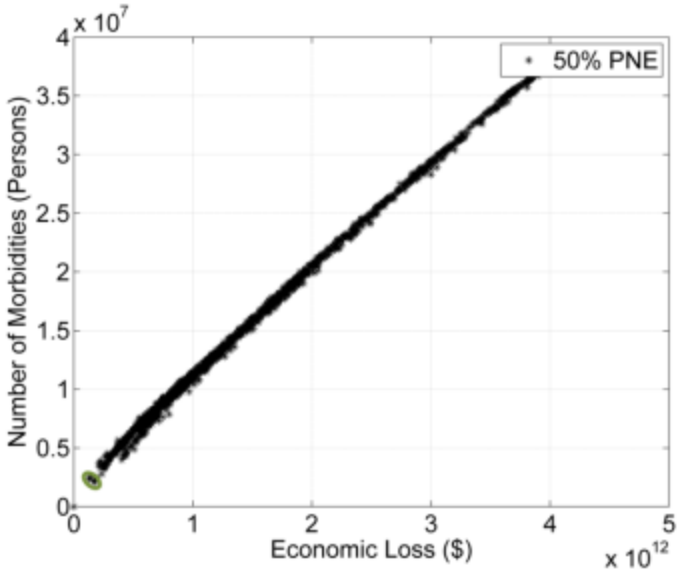

Figure 8-6: Percentile Values for Number of Morbidities vs. Economic Loss for Los Angeles County at MCE using Social Vulnerability with Pareto Optimal Surface Labeled

8.1.1.2 Community-Level Optimization of Los Angeles County at a MCE Seismic Hazard without using Social Vulnerability

A community-level optimization was conducted using the resiliency framework on the 2010 Los Angeles County population at a MCE seismic hazard without considering the social vulnerability of the community. The resulting percentile values for the four objectives were plotted in Figure 8-7 through Figure 8-12. Similar to the above discussion, the green circles highlight the pareto-optimal surface of solutions. Figure 8-7 provides the relationship between the estimated economic loss and the associated initial cost of the solutions. Five solutions were identified to form the pareto-optimal surface for these two objectives. Figure 8-8 provides the relationship between the estimated number of morbidities and the associated initial cost of the solutions. Four solutions were identified to form the pareto-optimal surface for these two objectives. Figure 8-9 provides the relationship between the estimated recovery time and the associated initial cost of the solutions. Figure 8-10 provides the relationship between the estimated economic loss and the recovery time of the solutions. Figure 8-11 provides the

relationship between the estimated number of morbidities and the recovery time of the solutions. The three figures (Figure 8-9 - Figure 8-11) which compare recovery time to another objective, all revealed only a single solution on the pareto-optimal surface. Figure 8-12 provides the relationship between the estimated number of morbidities and the associated economic loss of the solutions. Two solutions were identified to form the pareto-optimal surface for these two objectives. In total, five solutions were identified to form the pareto-optimal set of solutions for the four objectives. Similar to the above analysis, only two were extracted for further investigation. These two solutions were selected based on the same criteria used previously.

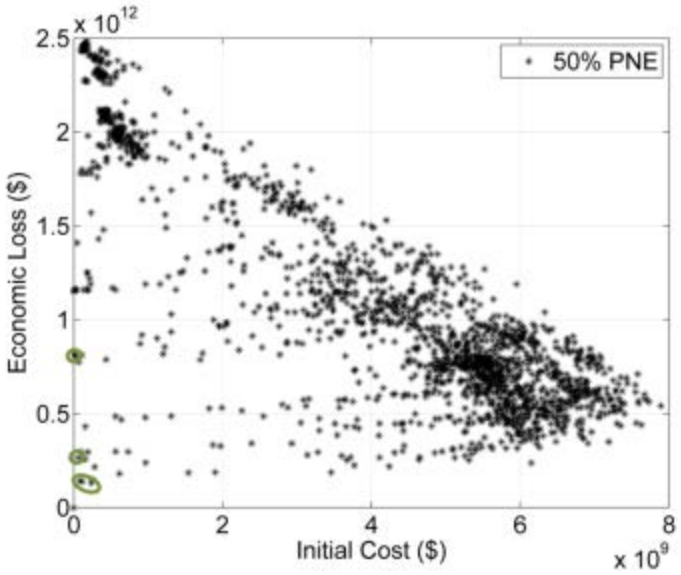

Figure 8-7: Percentile Values for Economic Loss vs. Initial Cost for Los Angeles County at MCE using Social Vulnerability with Pareto Optimal Surface Labeled

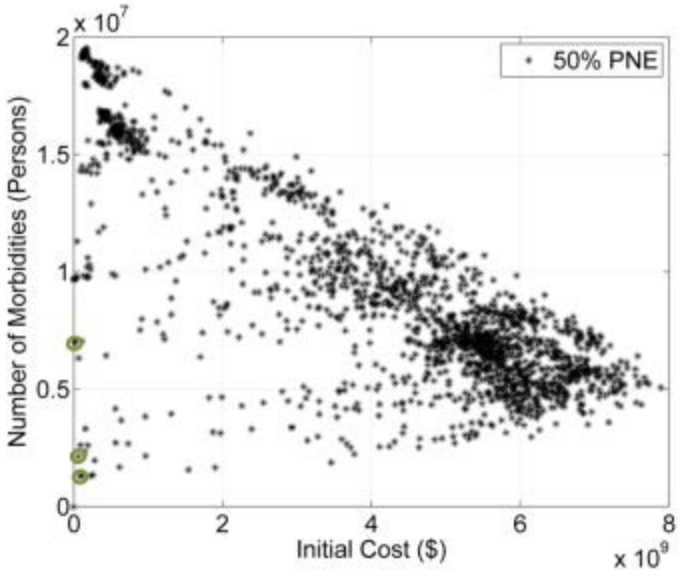

Figure 8-8: Percentile Values for Number of Morbidities vs. Initial Cost for Los Angeles County at MCE using Social Vulnerability with Pareto Optimal Surface Labeled

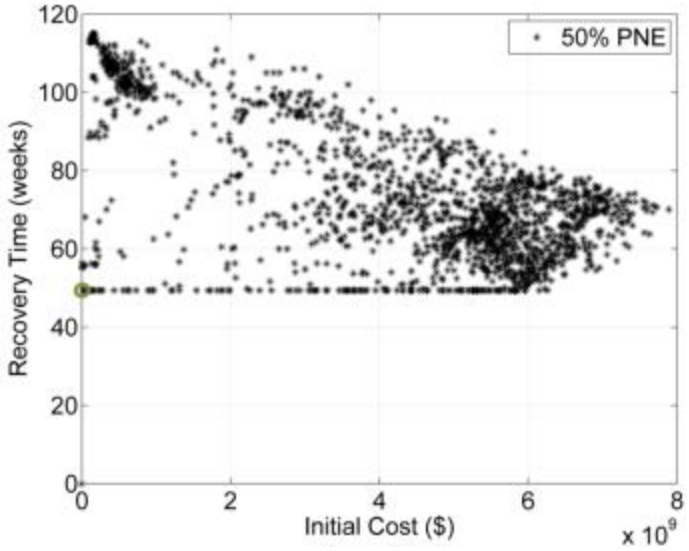

Figure 8-9: Percentile Values for Recovery Time vs. Initial Cost for Los Angeles County at MCE using Social Vulnerability with Pareto Optimal Surface Labeled

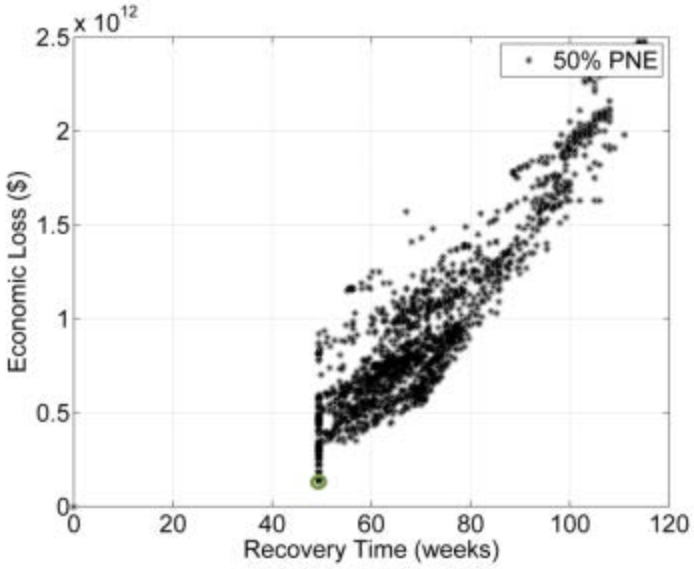

Figure 8-10: Percentile Values for Economic Loss vs. Recovery Time for Los Angeles County at MCE using Social Vulnerability with Pareto Optimal Surface Labeled

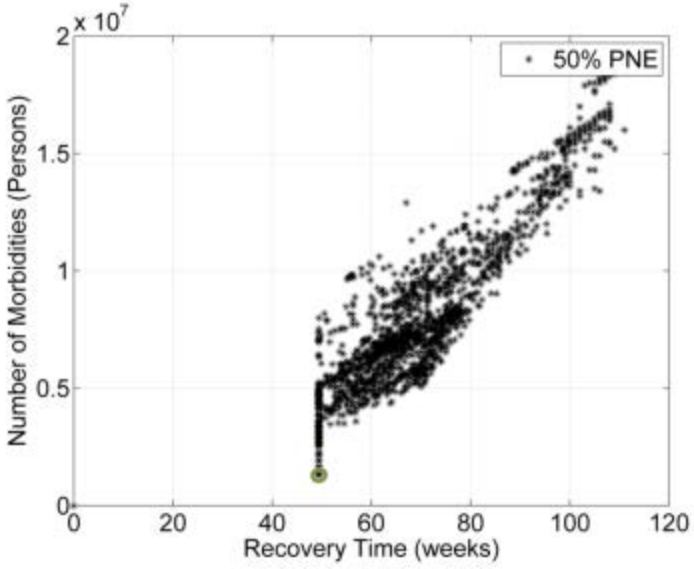

Figure 8-11: Percentile Values for Number of Morbidities vs. Recovery Time for Los Angeles County at MCE using Social Vulnerability with Pareto Optimal Surface Labeled

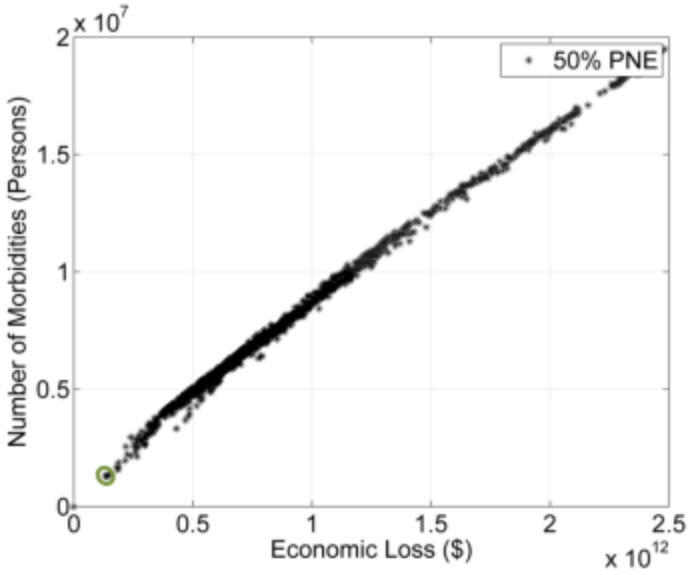

Figure 8-12: Percentile Values for Number of Morbidities vs. Economic Loss for Los Angeles County at MCE using Social Vulnerability with Pareto Optimal Surface Labeled

In reviewing Figure 8-1 through Figure 8-12, one can see similar trends in the figures which compare the same objectives. Figure 8-1 and Figure 8-7 both compared the economic loss versus the initial cost. In these figures, there was a large cluster of solutions demonstrating a trend which indicated that the higher the initial cost the lower the economic loss, the exact relationship that is to be expected. Similarly, in Figure 8-2 and Figure 8-8, when the number of morbidities was plotted against the initial cost, a similar trend was revealed indicating that the higher the initial cost the fewer estimated number of morbidities. Figure 8-3 and Figure 8-9 provided the comparison between the time to recovery and the initial cost. Similar to the above two comparisons, the general trend reveals that in general, the higher the initial cost, the lower the time to recovery. Figure 8-4 and Figure 8-10 compared the economic loss and the time to recovery, whereas Figure 8-5 and Figure 8-11 compared the number of morbidities with the time to recovery. In both cases, similar trends were revealed that the lower the recovery time, the lower the economic loss and the fewer morbidities. In these figures which compare an objective versus the time to recovery, a vertical lower limit is shown at approximately 52 weeks. This

vertical lower limit suggests that at least one person in the exposed population would be diagnosed with PTSD, and therefore the recovery time could not be less than one year. Upon further inspection, one would find that the estimated repair times might be lower than 52 weeks for some solutions. Finally, Figure 8-6 and Figure 8-12 demonstrated the relationship between the number of morbidities and the economic loss. These two objectives clearly go hand-in-hand providing a linear trend showing that fewer morbidities always correspond to a lower economic loss. These trends, in all cases, were what was to be expected, and were successfully achieved.

8.1.1.3 Identifying the Pareto-Optimal Surface based on MCE Seismic Hazard

The initial population, the two optimal solutions identified in Sec. 1.2.1.1, and the two optimal solutions identified in Sec. 1.2.1.2 are provided in Table 8-5, respectively. These five solutions will be used for conducting the remaining community-level case studies. It should be noted that using a population size of 50 and a maximum number of 100 generations will not generate every possible solution. Therefore, there may be more and more-optimal solutions than the four listed in Table 8-5, or found in the analyses presented above. These input parameters were felt to provide an extensive set of solutions for the illustrative examples presented in this dissertation. However, if the framework was to be used by a decision maker for generating the optimal retrofit plan for their community, then the population size should be increased by at least two orders of magnitude, and likely the maximum number of generations would increase similarly. The computing power to support a population of such size was not available to the author at the time of this dissertation. From Table 8-3, one can see that the four optimal solutions wanted to retrofit all of the three-story and four-story buildings designed by the 1959

Blue Book (i.e. A4 and A7) as these must have represented the most vulnerable structures to the population. The algorithm did not allow the counts to reduce to zero to prohibit numerical instabilities in the computations.

Table 8-33: Initial Population and the Pareto-Optimal Set of Solutions Considering a MCE Seismic Hazard for Los Angeles County

Solution	*Alleles for 1959 Blue Book Designs*						
	A1	*A2*	*A3*	*A4*	*A5*	*A6*	*A7*
1	9586	9586	6898	10432	9586	9586	20220
2	6791	1	1	1	1	1	1
3	6624	1	23	1	44	1	1
4	1	8790	1	1	8790	1	1
5	1	8242	1	1	8242	1	1
Solution	*Alleles for the 1978 NEHRP Designs*						
	A1	*A2*	*A3*	*A4*	*A5*	*A6*	*A7*
1	2261	2261	1627	2460	2261	2261	4867
2	1	1	1	1	1	1	1974
3	1	1	1	1	1	1	1806
4	1464	1	830	1664	1464	1	3972
5	1	1	823	1116	917	1	3425
Solution	*Alleles for the 2005 ASCE-7 Designs*						
	A1	*A2*	*A3*	*A4*	*A5*	*A6*	*A7*
1	261	261	188	213	261	261	414
2	1509	1509	1509	2172	2404	1825	2509
3	4287	3061	3061	3061	3264	3061	3061
4	2949	250	2684	1207	250	1608	250
5	3645	486	3032	958	487	516	2137
Solution	*Alleles for the SDDD-IO Retrofit Designs*						
	A1	*A2*	*A3*	*A4*	*A5*	*A6*	*A7*
1	261	261	188	213	261	261	414
2	5559	6687	4899	6120	6041	4999	3292
3	5054	6360	4595	4758	4302	3220	3061
4	4220	4507	2672	4662	4384	5100	5682
5	4220	4507	2739	4914	4446	4654	6797
Solution	*Alleles for the SDDD-LS Retrofit Designs*						
	A1	*A2*	*A3*	*A4*	*A5*	*A6*	*A7*
1	261	261	188	213	261	261	414
2	5559	6687	4899	6120	6041	4999	3292
3	5054	6360	4595	4758	4302	3220	3061
4	4221	4507	2672	4662	4384	5100	5682
5	4221	4070	2739	4914	4446	4548	6684
Solution	*Alleles for the FEMA P-807 Retrofit Designs*						
	A1	*A2*	*A3*	*A4*	*A5*	*A6*	*A7*
1	-	-	-	213	-	-	413
2	-	-	-	2171	-	-	1509
3	-	-	-	3061	-	-	3061
4	-	-	-	1207	-	-	250
5	-	-	-	958	-	-	2137

8.1.2 Illustrative Examples of the Community Resiliency Framework

In this section, and the remainder of the illustrative examples, five specific solutions were selected and analyzed more closely. The five solutions were provided in Table 8-5. In all cases, these are real solutions which the search algorithm found. In this case study and the following two case studies, the analyses were conducted at six seismic intensities. The six seismic intensities are: 17%, 33%, 50%, 66%, 83%, and 100% of MCE (Sa = 0.3g, 0.7g, 1.2g, 1.6g, 2.1g, and 2.5g, respectively). In the following subsections, the results to analyses using the 2010 Los Angeles County population data with and without the inclusion of social vulnerability are provided. The resulting fragilities for the latter three objectives conditioned on initial cost are provided in Figure 8-13 through Figure 8-30 for the six seismic intensities, respectively. The economic loss, number of morbidities, and recovery time were conditioned on initial cost because these three objectives conflict with initial cost. In each case, the estimated losses are compared for the five solutions, with and without the incorporation of the social vulnerability computations. The green curves are the estimated losses using the social vulnerability computations, and the black curves are without. In each case, the estimated losses were less when the social vulnerability computations were not included for each respective solution. When reviewing the figures, one can see how the axis values increase with increasing seismic intensity. The initial population is S1; it had the highest estimated losses for each seismic intensity regardless of whether the social vulnerability computations were included. Reviewing Figure 8-13 through Figure 8-30, the data is presented on multiple plots. For the objectives economic loss and recovery time, the data is separated based on whether the social vulnerability computations were included or not. This was done because for economic loss, the difference in the curves was not visible at a reasonable scale, therefore they were separated. Looking at the

recovery time fragilities in Figure 8-15, Figure 8-18, Figure 8-21, Figure 8-24, Figure 8-27, and Figure 8-30, the curves presented are actually identical for the two cases (e.g., with and without including the social vulnerability computations). This is because the repair times do not consider the socioeconomic variables and they controlled over the recovery times due to morbidities, where PTSD recovery time is the worst case and set at 52 weeks. Therefore, the recovery times were estimated as the same distributions regardless of whether the social vulnerability computations were included or not. For the objective, number of morbidities, the data was separated onto three plots based on the abscissa values. Note, when viewing Figure 8-14, Figure 8-17, Figure 8-20, Figure 8-23, Figure 8-26, and Figure 8-29, the data was split to demonstrate the distribution (i.e. COV) in each case. The percentile values from each of the 18 fragilities curves were extracted and are compared more closely with discussion in Section 8.5.

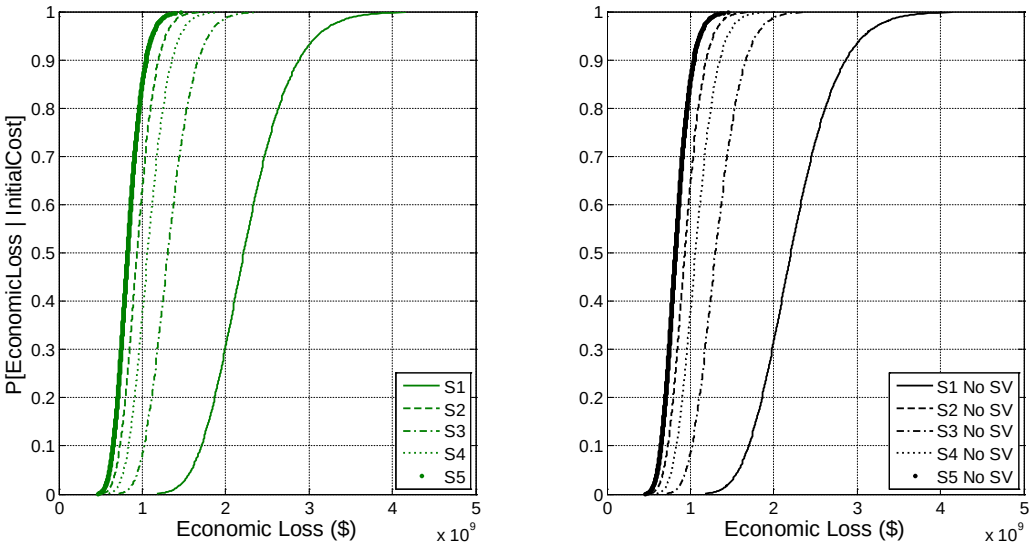

Figure 8-13: Probability of Nonexceedance for Economic Loss Given a Specific Initial Cost at (1/6) MCE using Los Angeles County Population

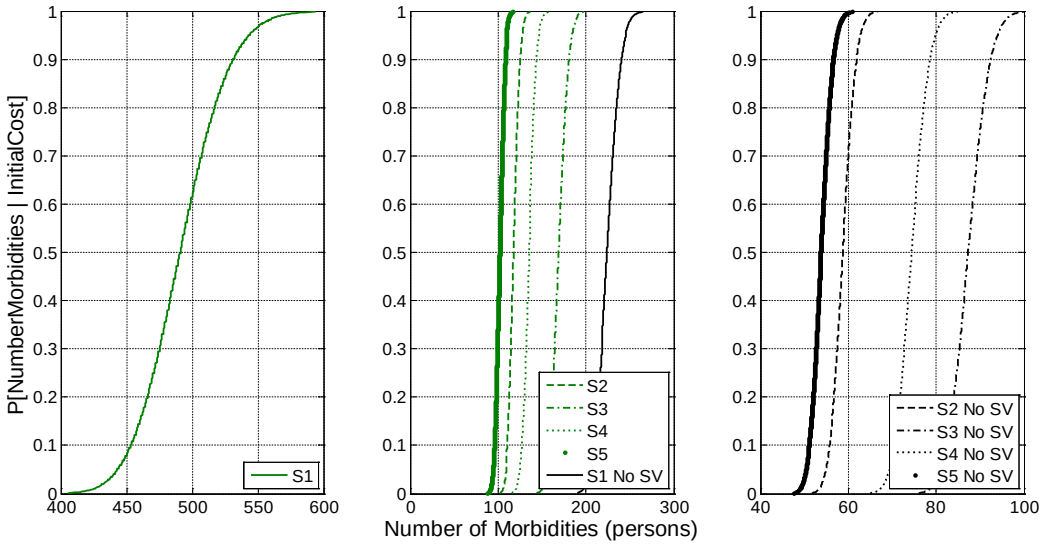

Figure 8-14: Probability of Nonexceedance for the Number of Morbidities Given a Specific Initial Cost at (1/6) MCE using Los Angeles County Population

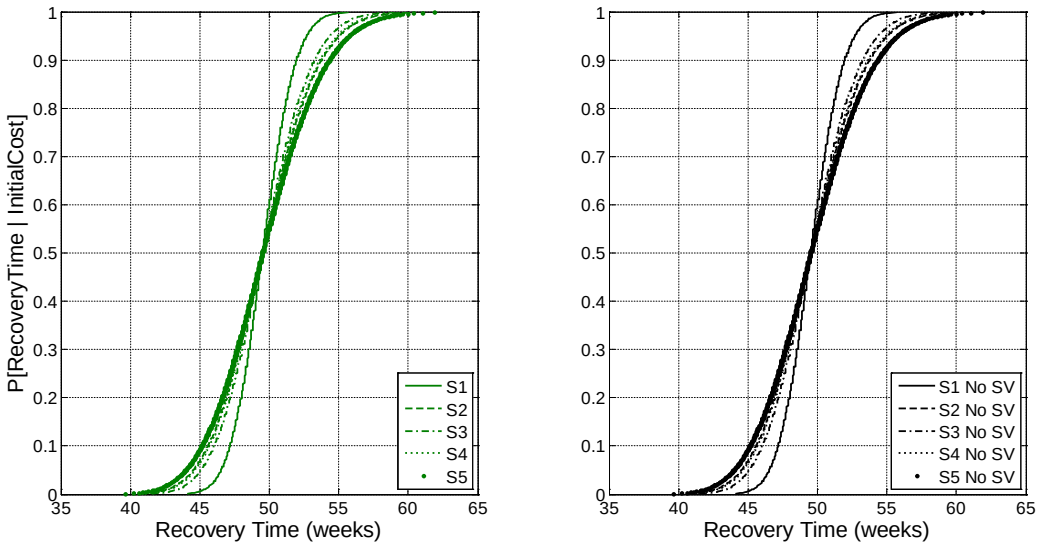

Figure 8-15: Probability of Nonexceedance for the Recovery Time Given a Specific Initial Cost at (1/6) MCE using Los Angeles County Population

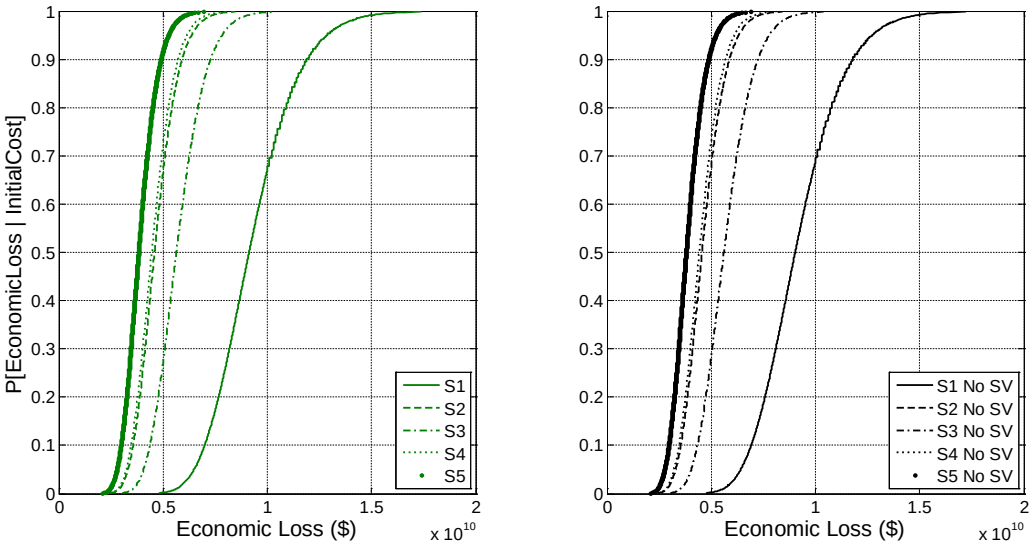

Figure 8-16: Probability of Nonexceedance for Economic Loss Given a Specific Initial Cost at (1/3) MCE using Los Angeles County Population

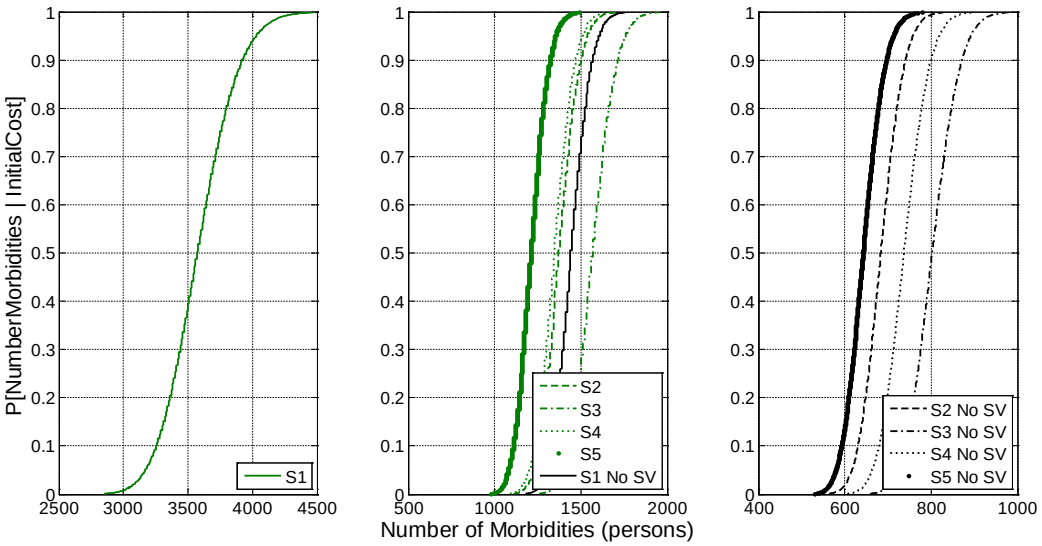

Figure 8-17: Probability of Nonexceedance for the Number of Morbidities Given a Specific Initial Cost at (1/3) MCE using Los Angeles County Population

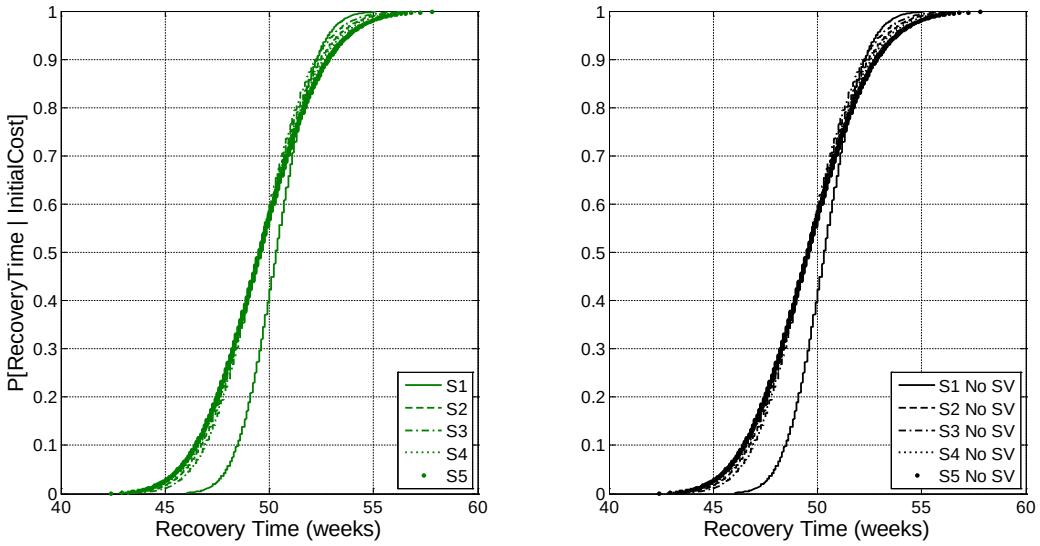

Figure 8-18: Probability of Nonexceedance for the Recovery Time Given a Specific Initial Cost at (1/3) MCE using Los Angeles County Population

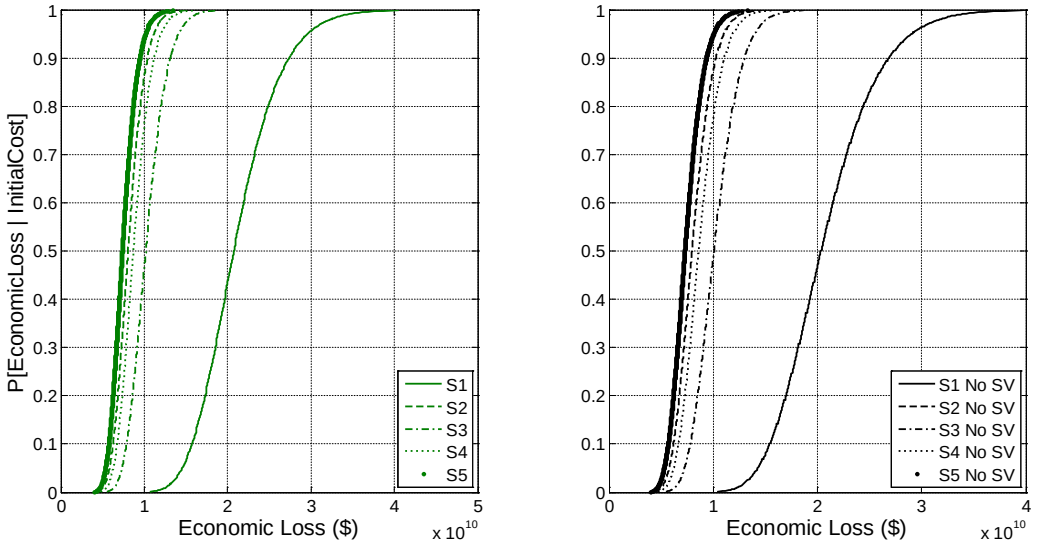

Figure 8-19: Probability of Nonexceedance for Economic Loss Given a Specific Initial Cost at (1/2) MCE using Los Angeles County Population

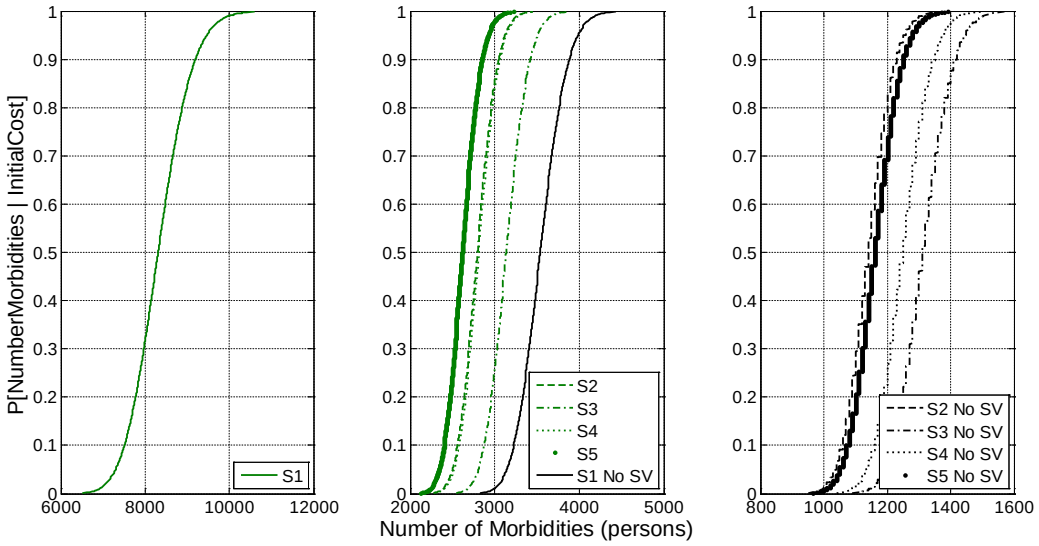

Figure 8-20: Probability of Nonexceedance for the Number of Morbidities Given a Specific Initial Cost at (1/2) MCE using Los Angeles County Population

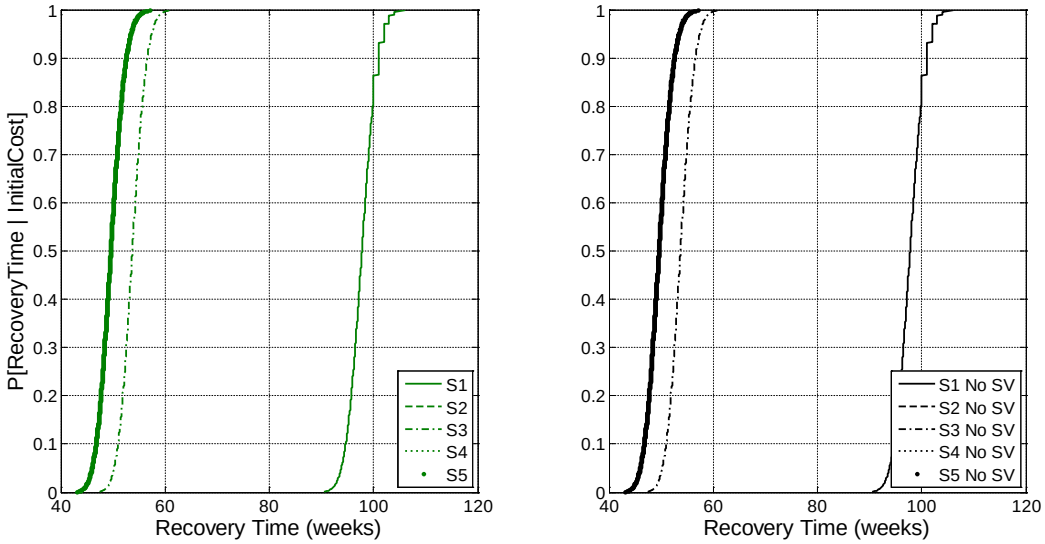

Figure 8-21: Probability of Nonexceedance for the Recovery Time Given a Specific Initial Cost at (1/2) MCE using Los Angeles County Population

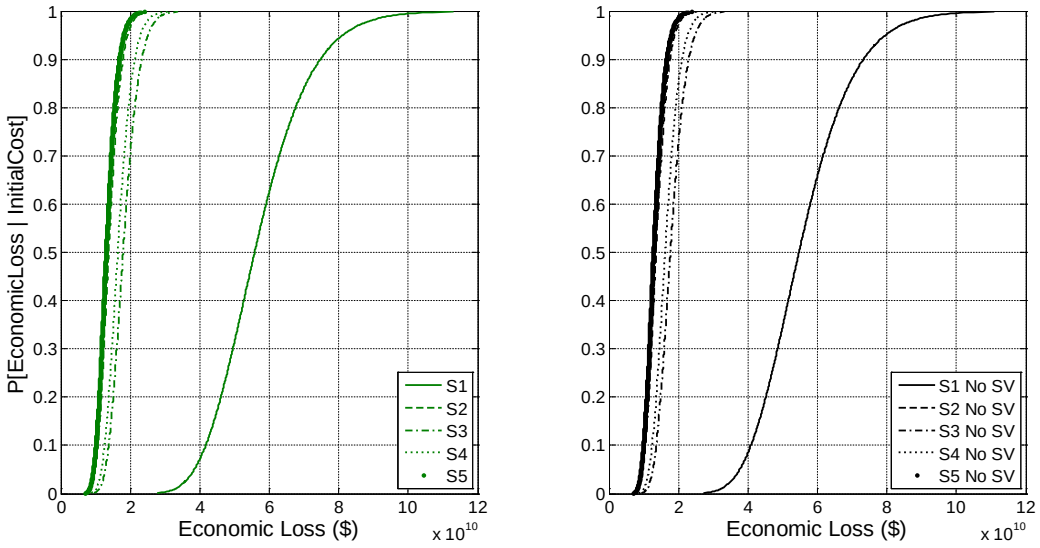

Figure 8-22: Probability of Nonexceedance for Economic Loss Given a Specific Initial Cost at (2/3) MCE using Los Angeles County Population

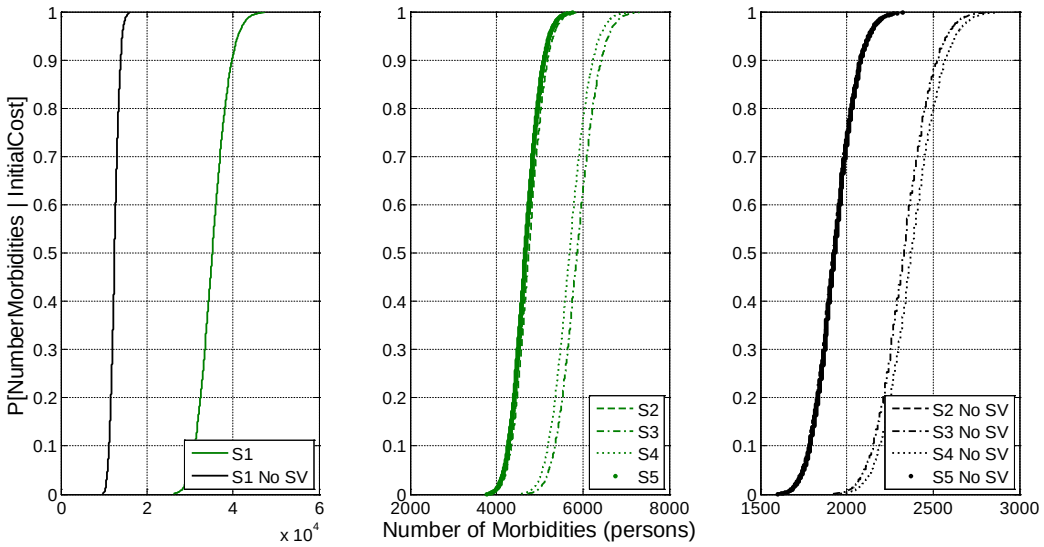

Figure 8-23: Probability of Nonexceedance for the Number of Morbidities Given a Specific Initial Cost at (2/3) MCE using Los Angeles County Population

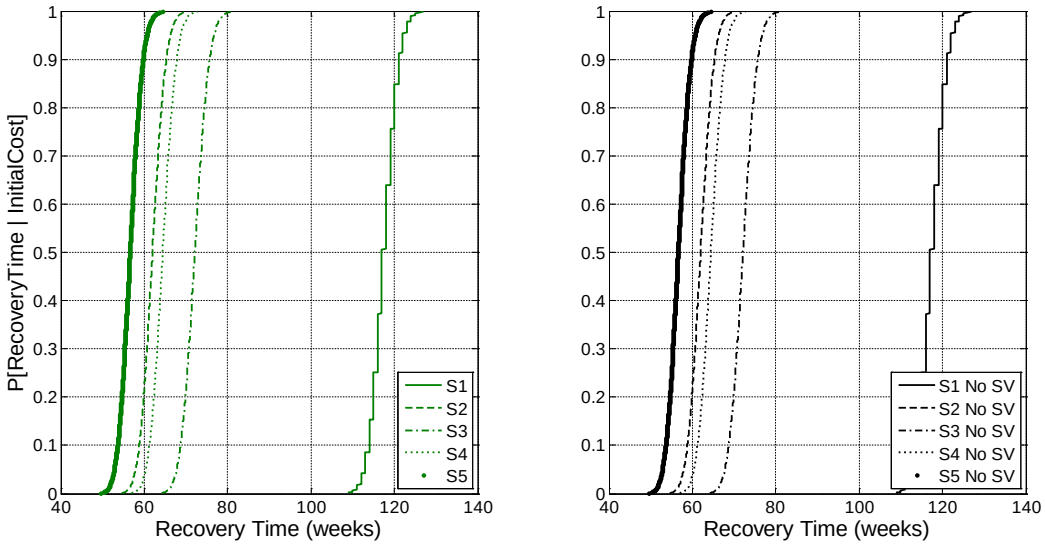

Figure 8-24: Probability of Nonexceedance for the Recovery Time Given a Specific Initial Cost at (2/3) MCE using Los Angeles County Population

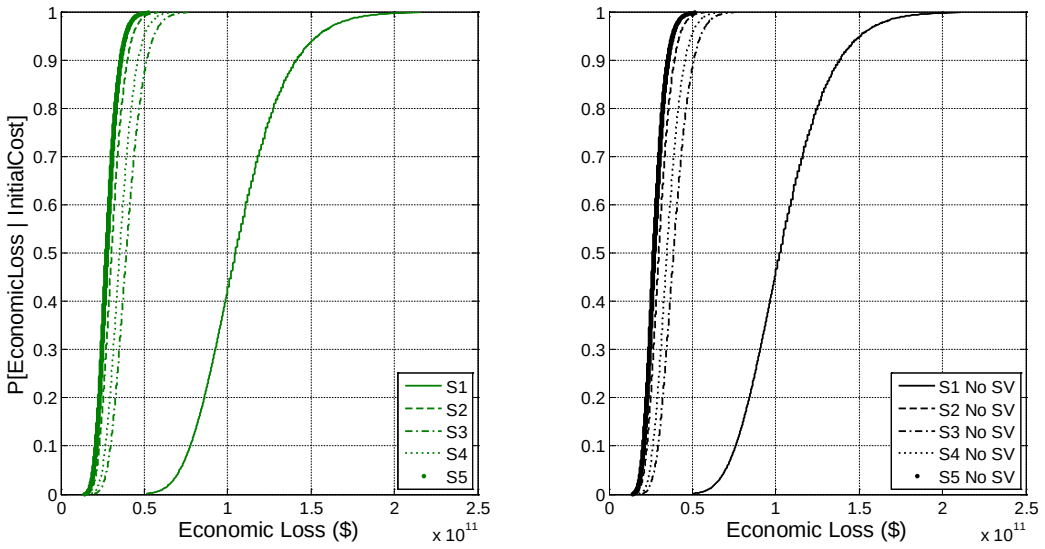

Figure 8-25: Probability of Nonexceedance for Economic Loss Given a Specific Initial Cost at (5/6) MCE using Los Angeles County Population

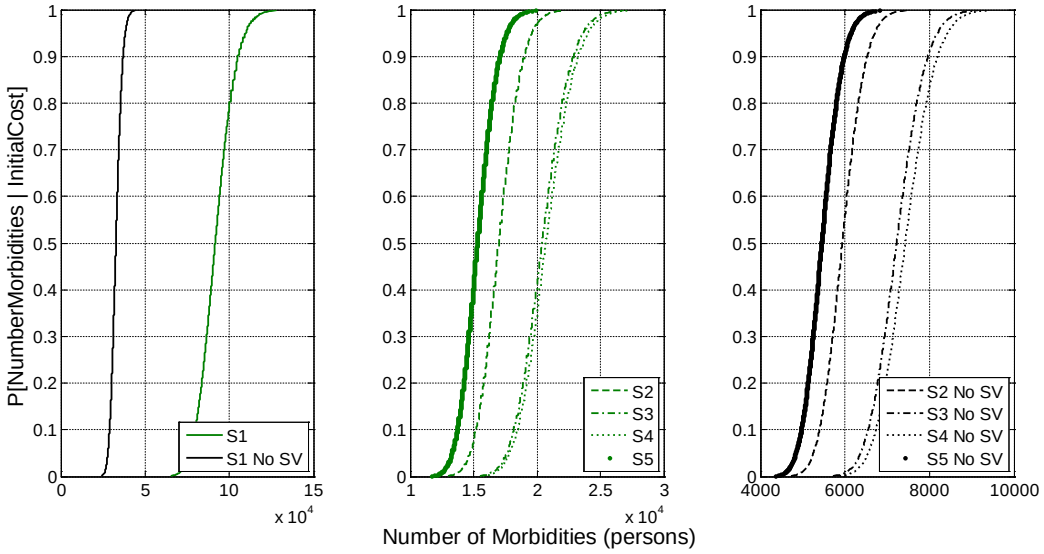

Figure 8-26: Probability of Nonexceedance for the Number of Morbidities Given a Specific Initial Cost at (5/6) MCE using Los Angeles County Population

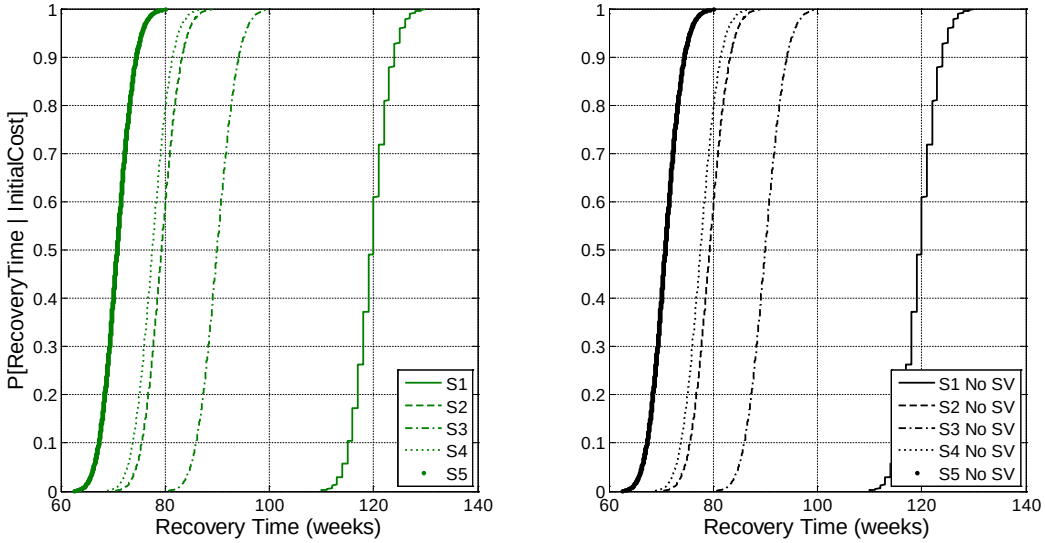

Figure 8-27: Probability of Nonexceedance for the Recovery Time Given a Specific Initial Cost at (5/6) MCE using Los Angeles County Population

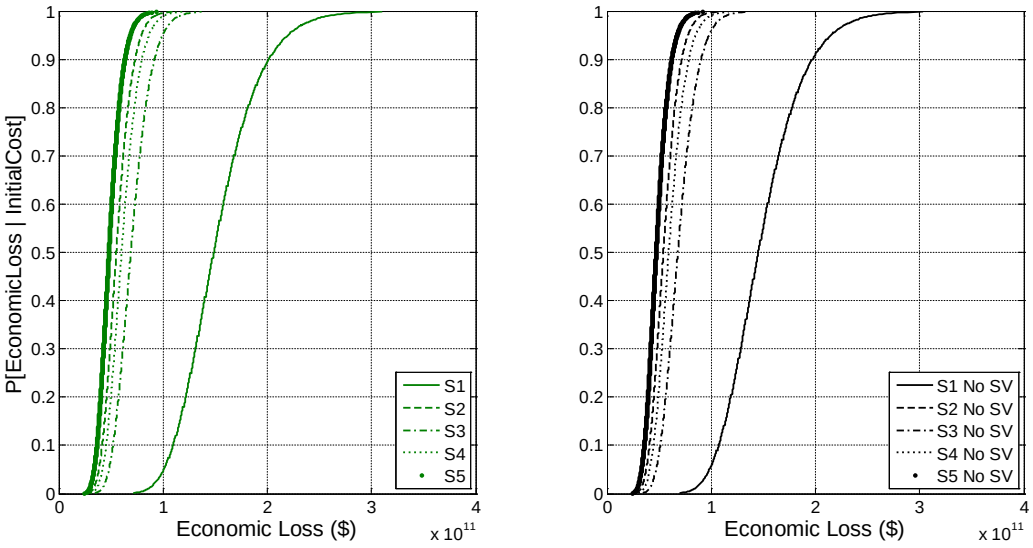

Figure 8-28: Probability of Nonexceedance for Economic Loss Given a Specific Initial Cost at MCE using Los Angeles County Population

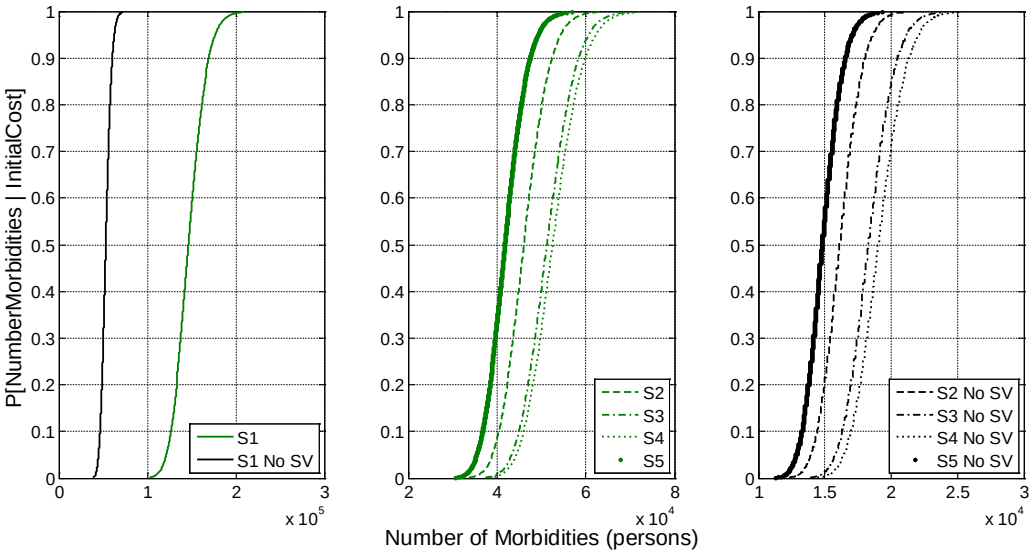

Figure 8-29: Probability of Nonexceedance for the Number of Morbidities Given a Specific Initial Cost at MCE using Los Angeles County Population

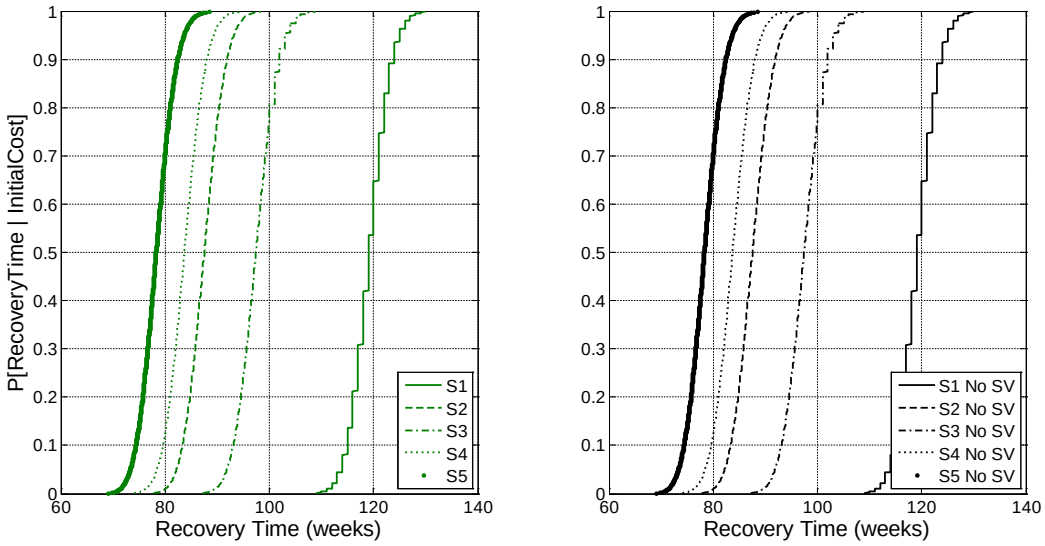

Figure 8-30: Probability of Nonexceedance for the Recovery Time Given a Specific Initial Cost at MCE using Los Angeles County Population

8.2 Case Study 2: Forecasted Population for Los Angeles County, California

The second set of case studies were conducted using the 2010 U.S. census data for East Los Angeles, California. This area has a very high population of ethnic minorities with a much lower mean annual income and with a lower education attainment distribution than Los Angeles County. Potential population growths for Los Angeles County could converge to having similar demographics as East Los Angeles, and therefore using this community's demographics were of interest. The values input for each subcategory are provided in Table 8-4.

Table 8-34: East Los Angeles Community Inputs

Variable	*Subcategory*	*Input Value*
Total Population Size		126,496
Mean Annual Income		$37,982
Mean Household Size		4.09
Percentage of Households with Children		42.6%
Age	Child (0 - 9 y.o.)	17.2%
	Adolescent (10 - 19 y.o.)	18.1%
	Young Adult (20 - 29 y.o.)	16.1%
	Middle-Aged Adult (30 - 45 y.o.)	21.6%
	Older Adult (46 - 64 y.o.)	18.4%
	Elder (65+ y.o.)	8.4%
Ethnicity/Race	Majority	1.5%
	Minority	98.5%
Family Structure	Single	19.5%
	Partnered	80.5%
	Parent	42.6%
Gender	Female	50.3%
	Male	49.7%
Socioeconomic Status	Low	50.3%
	Moderate	34.9%
	Upper	14.5%

The five solutions provided in Table 8-5 were analyzed at the same six seismic intensities investigated before, but with the East Los Angeles population data. The resulting fragilities for the latter three objectives conditioned on initial cost are provided in Figure 8-31 through Figure 8-48 for the six seismic intensities, respectively. Similar to the above case study, the estimated losses are compared for the five solutions, with and without the incorporation of the social vulnerability computations. The green curves are the estimated losses using the social vulnerability computations, and the black curves are without. In each case, the estimated losses were less when the social vulnerability computations were not included for each respective solution. When reviewing Figure 8-31 through Figure 8-48, one can see how the axis values increase with increasing seismic hazard intensity, similar to the case study above. The initial population is S1, had the highest estimated losses for each seismic intensity regardless of

whether the social vulnerability computations were included. The approach used for presenting the data in the above section is repeated here. The percentile values from each of the 18 fragilities curves using the East Los Angeles population data were extracted and are compared more closely with discussion in Section 8.5.

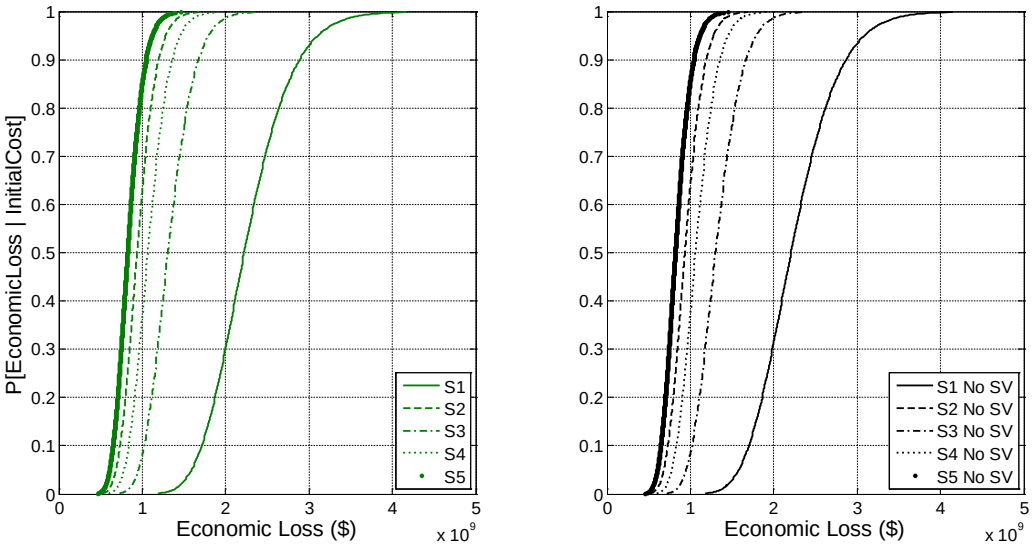

Figure 8-31: Probability of Nonexceedance for Economic Loss Given a Specific Initial Cost at (1/6) MCE using East Los Angeles Population

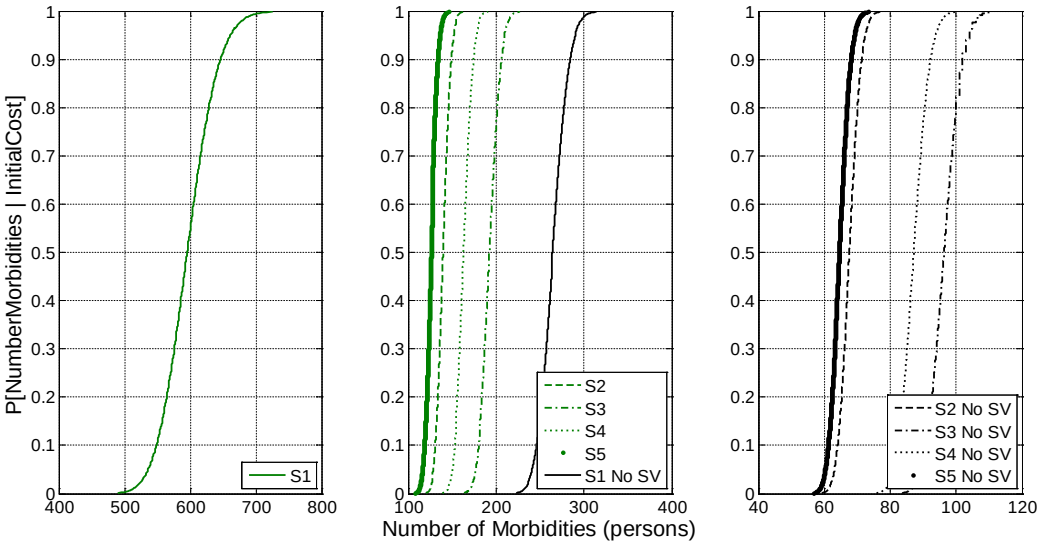

Figure 8-32: Probability of Nonexceedance for the Number of Morbidities Given a Specific Initial Cost at (1/6) MCE using East Los Angeles Population

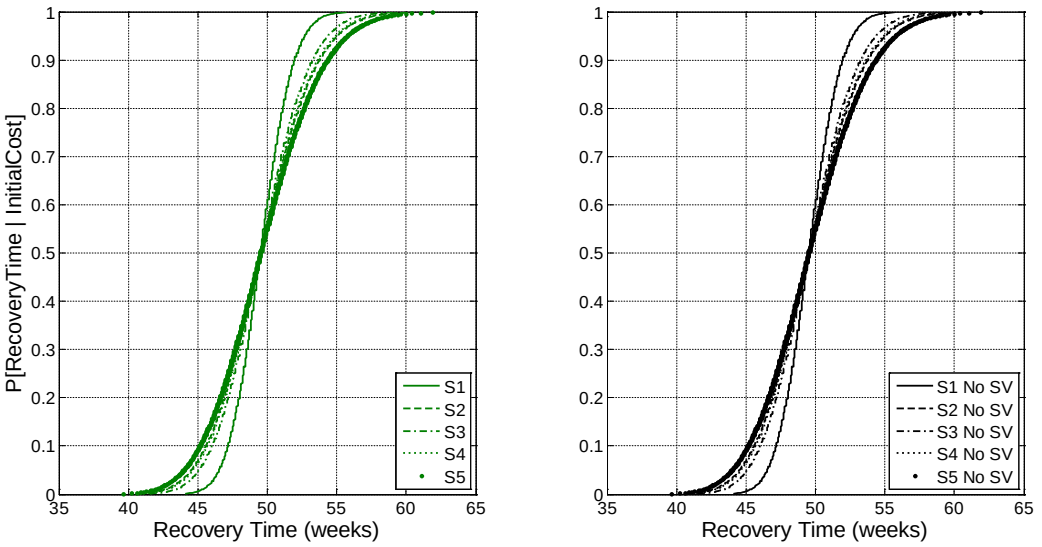

Figure 8-33: Probability of Nonexceedance for the Recovery Time Given a Specific Initial Cost at (1/6) MCE using East Los Angeles Population

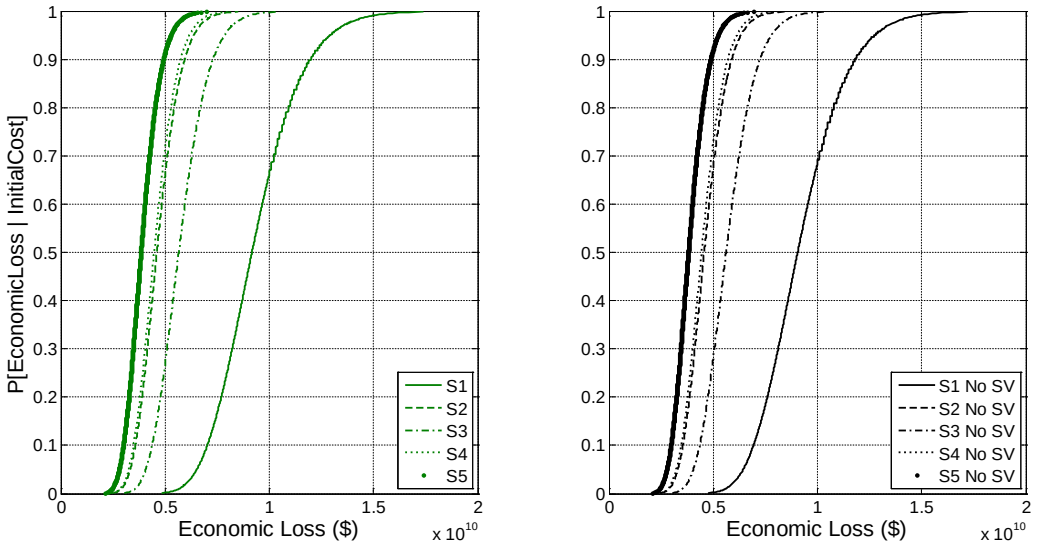

Figure 8-34: Probability of Nonexceedance for Economic Loss Given a Specific Initial Cost at (1/3) MCE using East Los Angeles Population

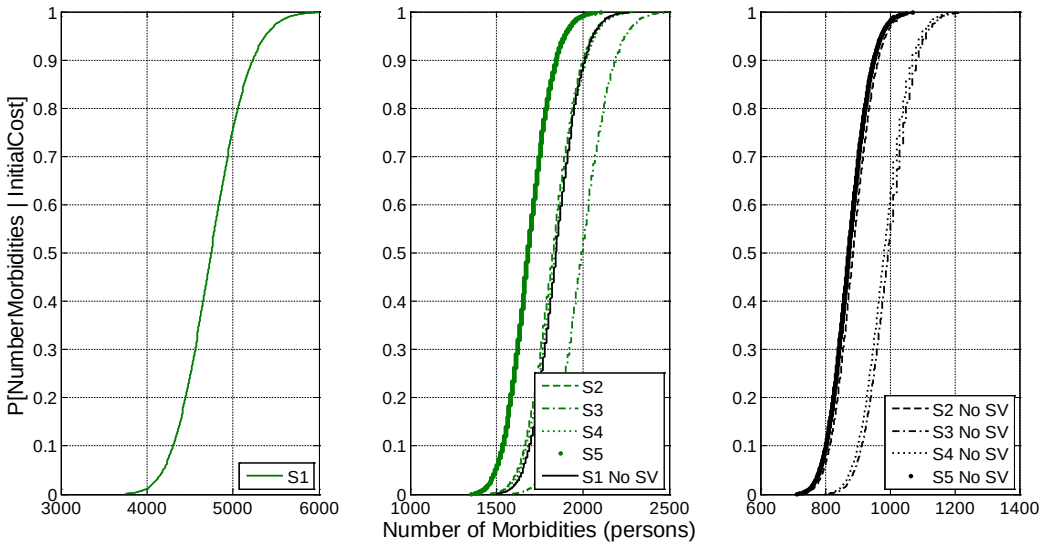

Figure 8-35: Probability of Nonexceedance for the Number of Morbidities Given a Specific Initial Cost at (1/3) MCE using East Los Angeles Population

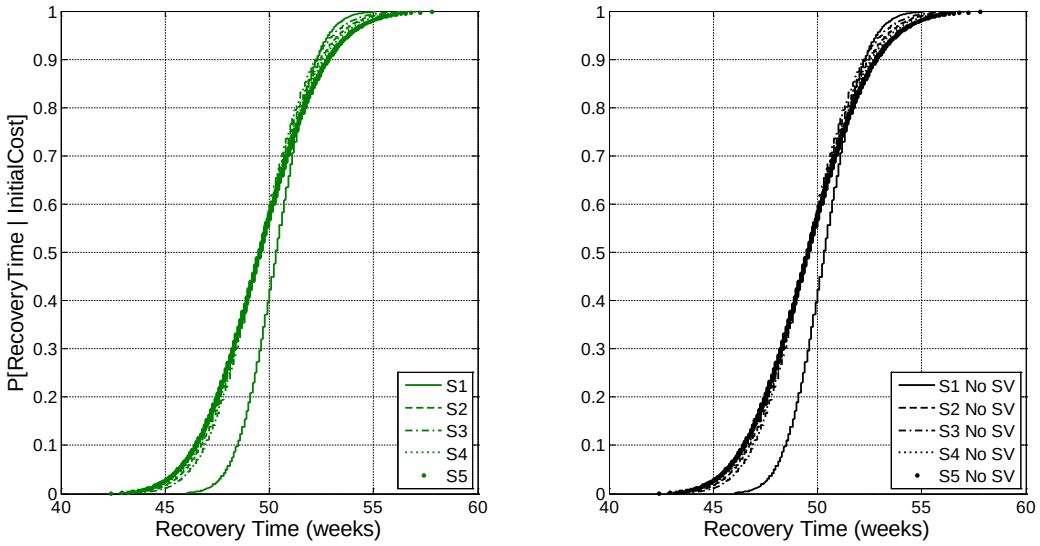

Figure 8-36: Probability of Nonexceedance for the Recovery Time Given a Specific Initial Cost at (1/3) MCE using East Los Angeles Population

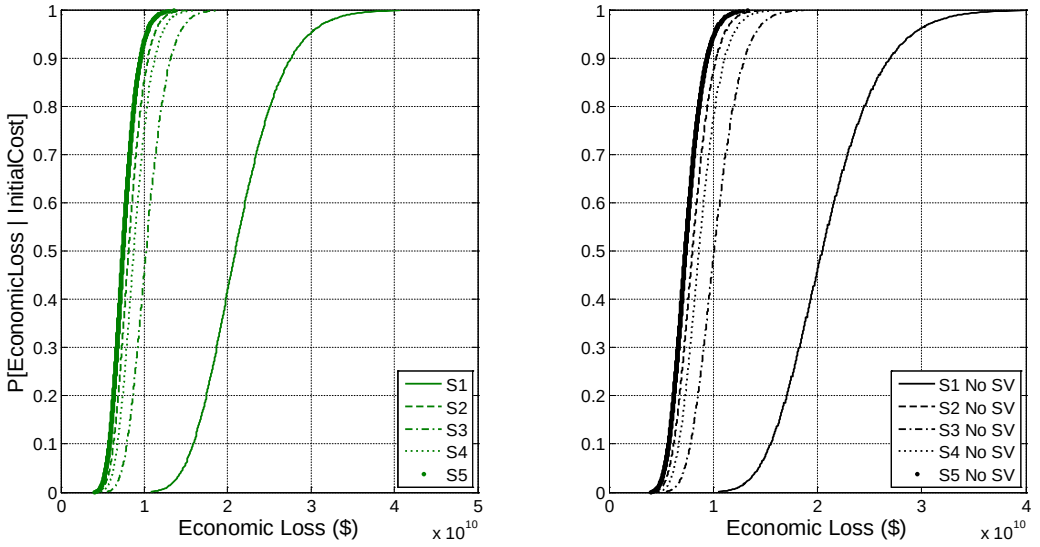

Figure 8-37: Probability of Nonexceedance for Economic Loss Given a Specific Initial Cost at (1/2) MCE using East Los Angeles Population

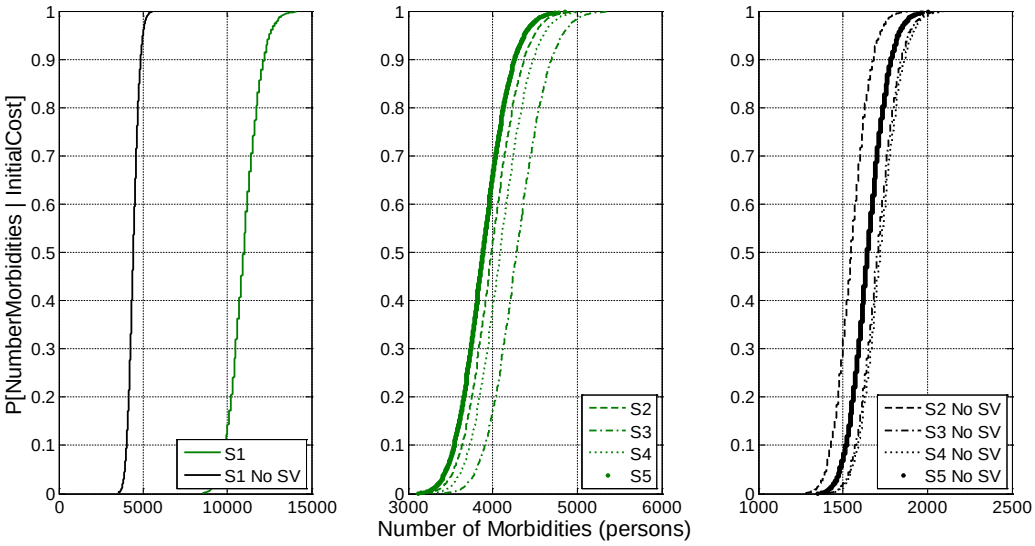

Figure 8-38: Probability of Nonexceedance for the Number of Morbidities Given a Specific Initial Cost at (1/2) MCE using East Los Angeles Population

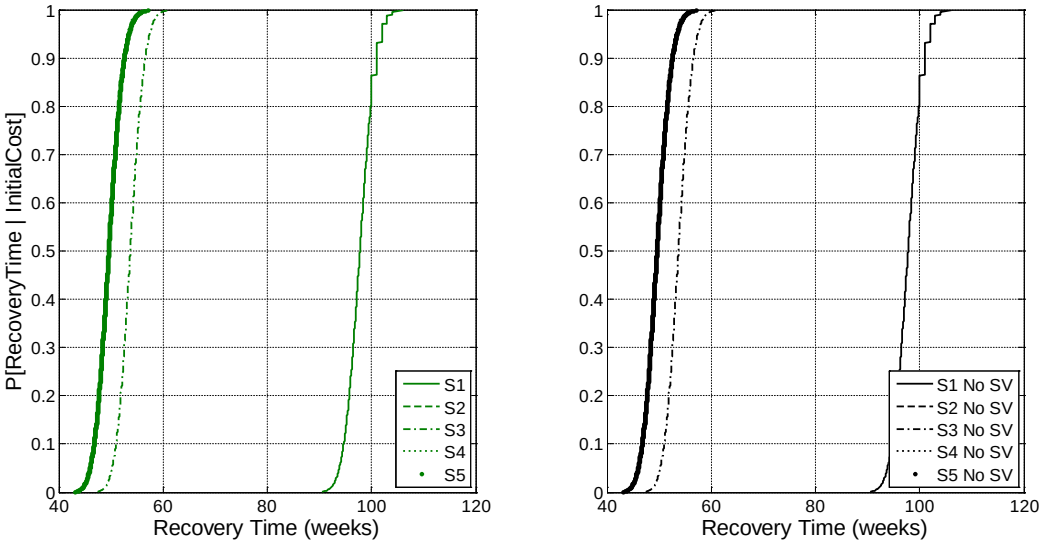

Figure 8-39: Probability of Nonexceedance for the Recovery Time Given a Specific Initial Cost at (1/2) MCE using East Los Angeles Population

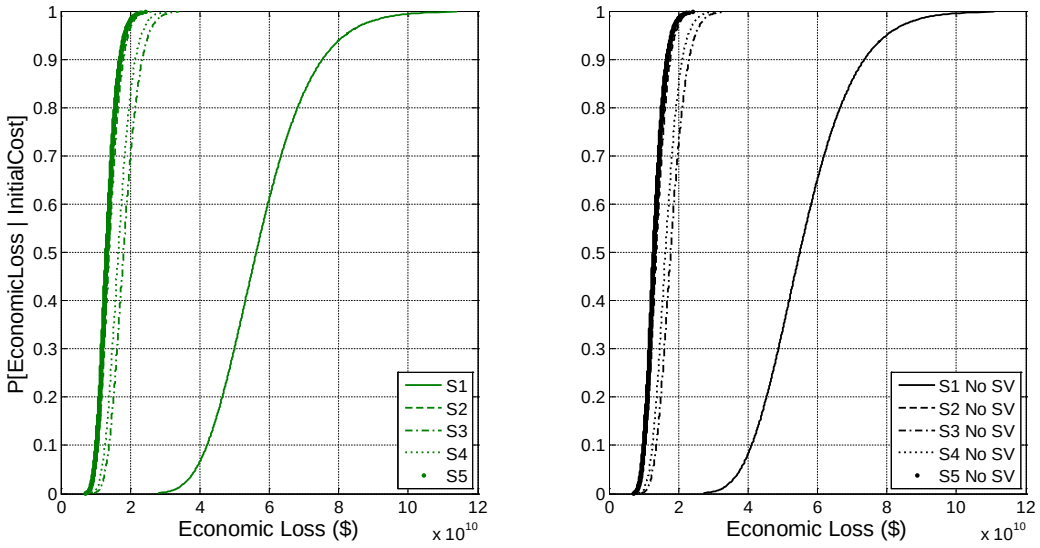

Figure 8-40: Probability of Nonexceedance for Economic Loss Given a Specific Initial Cost at (2/3) MCE using East Los Angeles Population

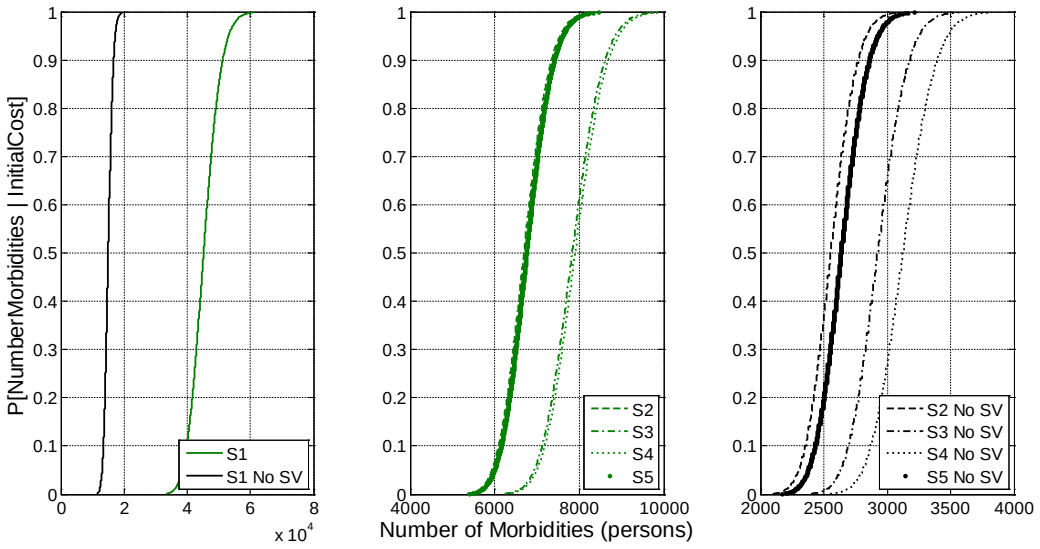

Figure 8-41: Probability of Nonexceedance for the Number of Morbidities Given a Specific Initial Cost at (2/3) MCE using East Los Angeles Population

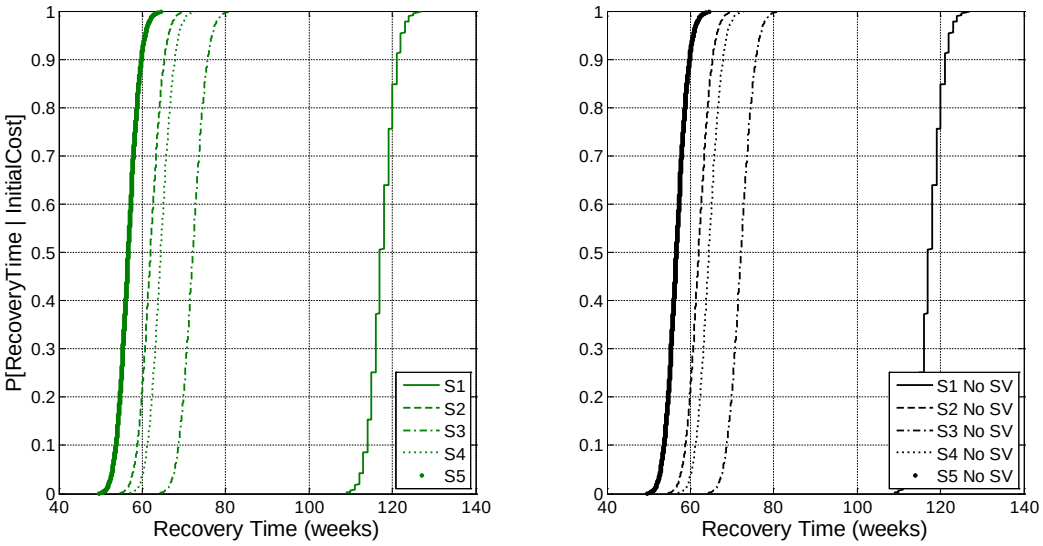

Figure 8-42: Probability of Nonexceedance for the Recovery Time Given a Specific Initial Cost at (2/3) MCE using East Los Angeles Population

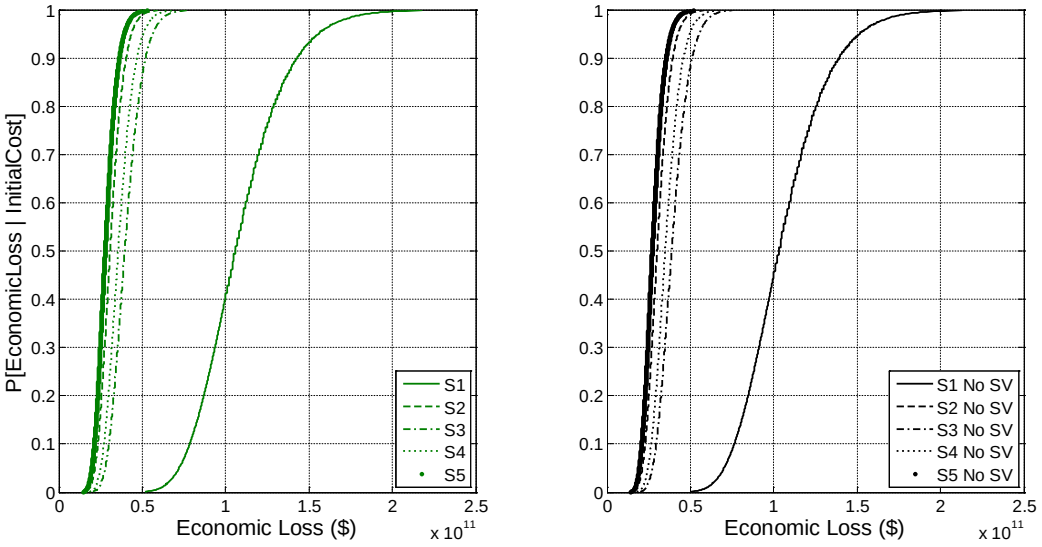

Figure 8-43: Probability of Nonexceedance for Economic Loss Given a Specific Initial Cost at (5/6) MCE using East Los Angeles Population

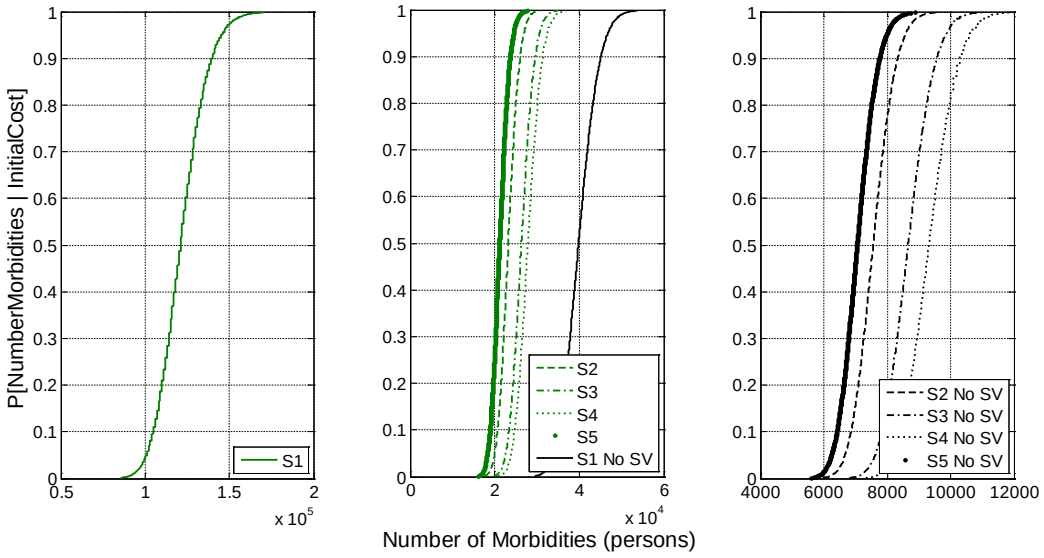

Figure 8-44: Probability of Nonexceedance for the Number of Morbidities Given a Specific Initial Cost at (5/6) MCE using East Los Angeles Population

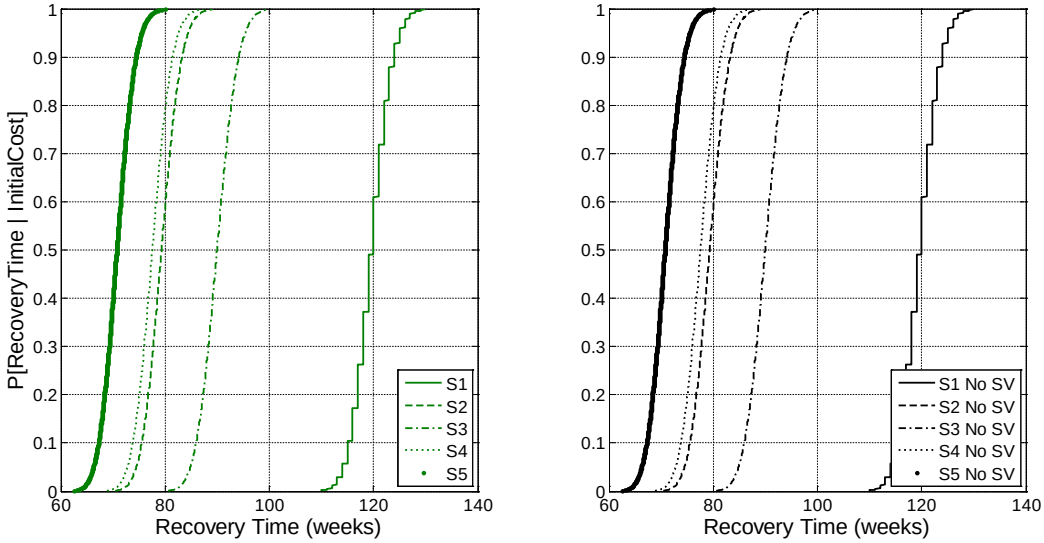

Figure 8-45: Probability of Nonexceedance for the Recovery Time Given a Specific Initial Cost at (5/6) MCE using East Los Angeles Population

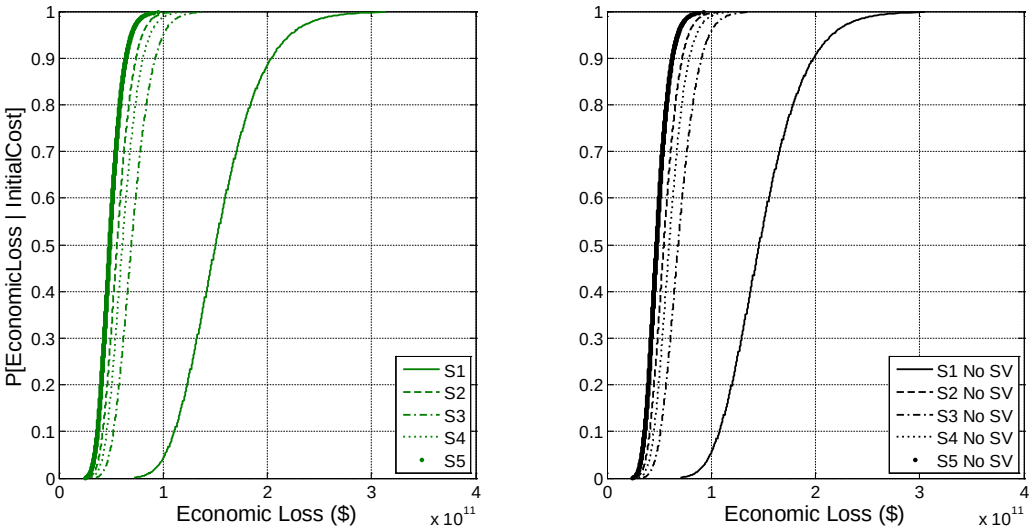

Figure 8-46: Probability of Nonexceedance for Economic Loss Given a Specific Initial Cost at MCE using East Los Angeles Population

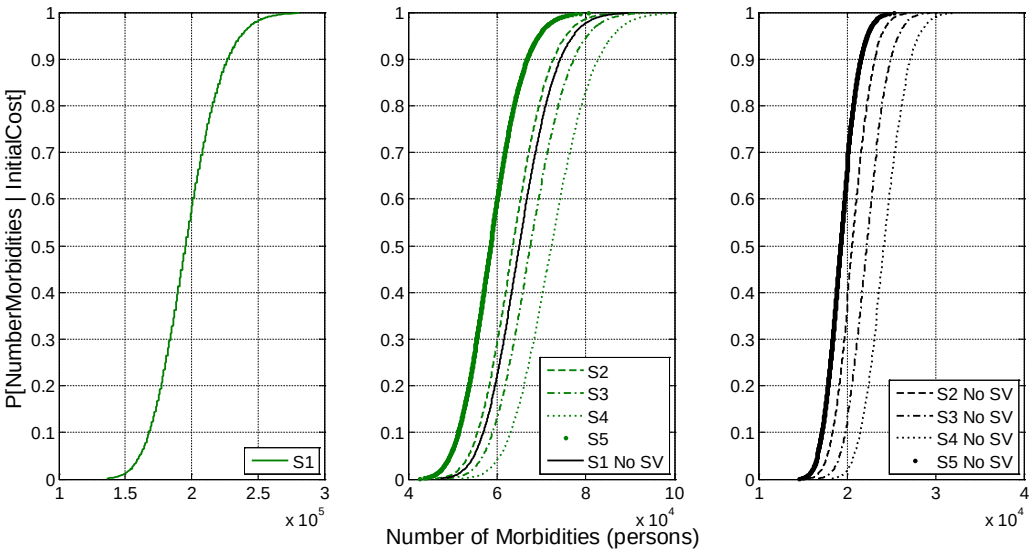

Figure 8-47: Probability of Nonexceedance for the Number of Morbidities Given a Specific Initial Cost at MCE using East Los Angeles Population

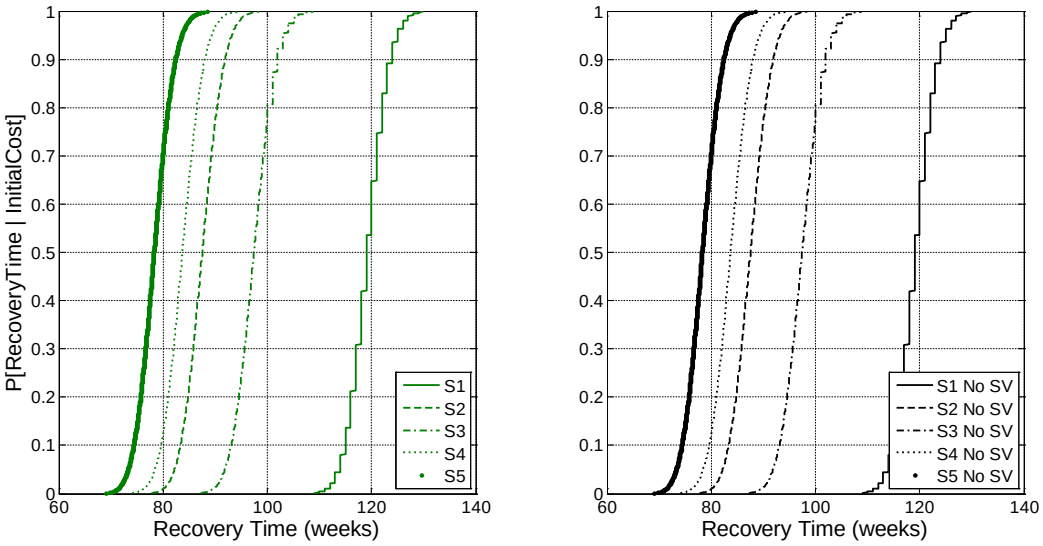

Figure 8-48: Probability of Nonexceedance for the Recovery Time Given a Specific Initial Cost at MCE using East Los Angeles Population

8.3 Case Study 3: Forecasted Population for Los Angeles County, California

The final set of case studies were conducted using the 2010 U.S. census data for Daly City, California. This area has an above average population of ethnic minorities, but with a higher mean annual income than Los Angeles County, and a higher educational attainment distribution. Potential population growths for Los Angeles County could converge to having similar demographics as Daly City, and therefore using this community's demographics were of interest. The values input for each subcategory are provided in Table 8-5.

Table 8-35: Daly City Community Inputs

Variable	*Subcategory*	*Input Value*
Total Population Size		101,123
Mean Annual Income		$89,180
Mean Household Size		3.23
Percentage of Households with Children		35.5%
Age	Child (0 - 9 y.o.)	10.5%
	Adolescent (10 - 10 y.o.)	11.5%
	Young Adult (20 - 29 y.o.)	15.9%
	Middle-Aged Adult (30 - 45 y.o.)	21.2%
	Older Adult (46 - 64 y.o.)	27.3%
	Elder (65+ y.o.)	13.4%
Ethnicity/Race	Majority	13.9%
	Minority	86.1%
Family Structure	Single	26.7%
	Partnered	73.3%
	Parent	35.5%
Gender	Female	50.6%
	Male	49.4%
Socioeconomic Status	Low	23.8%
	Moderate	37.8%
	Upper	35.6%

The five solutions provided in Table 8-5 were analyzed at the same six seismic intensities investigated before, but with the Daly City population data. The resulting fragilities for the latter three objectives conditioned on initial cost are provided in Figure 8-49 through Figure 8-66 for the six seismic intensities, respectively. Similar to the above case studies, the estimated losses were compared for the five solutions, with and without the incorporation of the social vulnerability computations. The green curves are the estimated losses using the social vulnerability computations, and the black curves are without. In each case, the estimated losses were less when the social vulnerability computations were not included for each respective solution. When reviewing Figure 8-49 through Figure 8-66, one can see how the axis values increase with increasing seismic hazard intensity, similar to the case studies above. The initial population is S1, had the highest estimated losses for each seismic intensity regardless of

whether the social vulnerability computations were included. The approach used for presenting the data in the above sections is repeated here. The percentile values from each of the 18 fragilities curves using the Daly City population data were extracted and are compared more closely with discussion in Section 8.5.

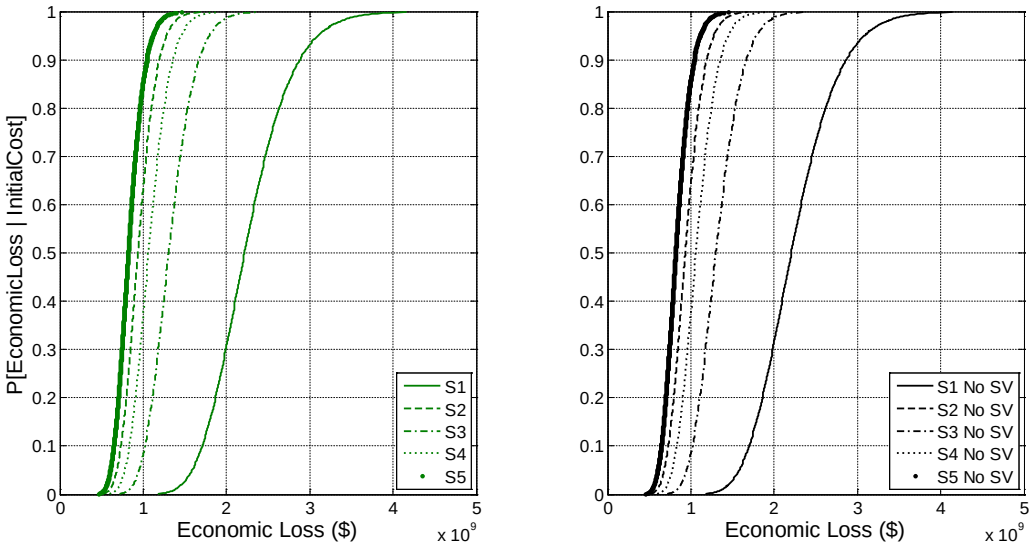

Figure 8-49: Probability of Nonexceedance for Economic Loss Given a Specific Initial Cost at (1/6) MCE using Daly City Population

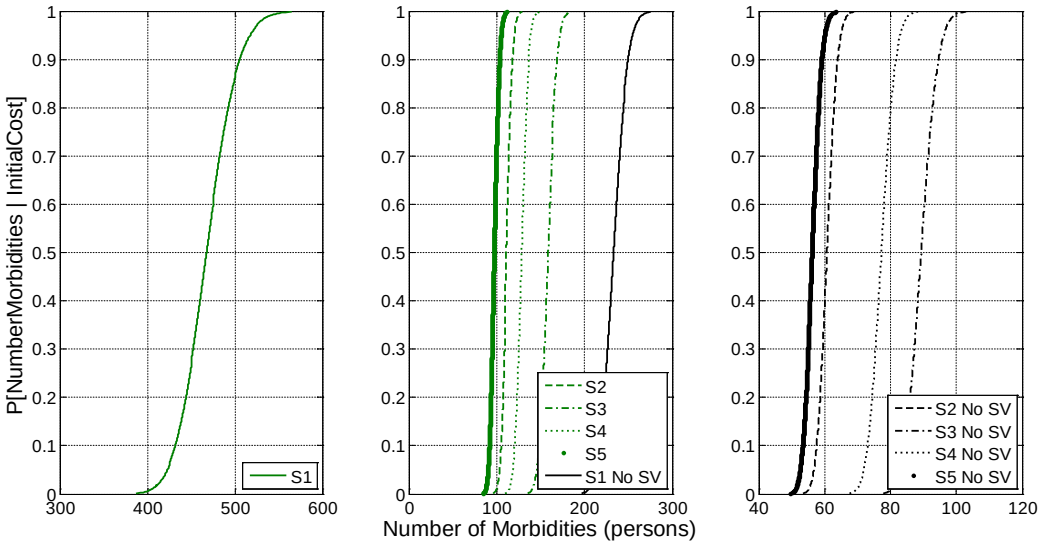

Figure 8-50: Probability of Nonexceedance for the Number of Morbidities Given a Specific Initial Cost at (1/6) MCE using Daly City Population

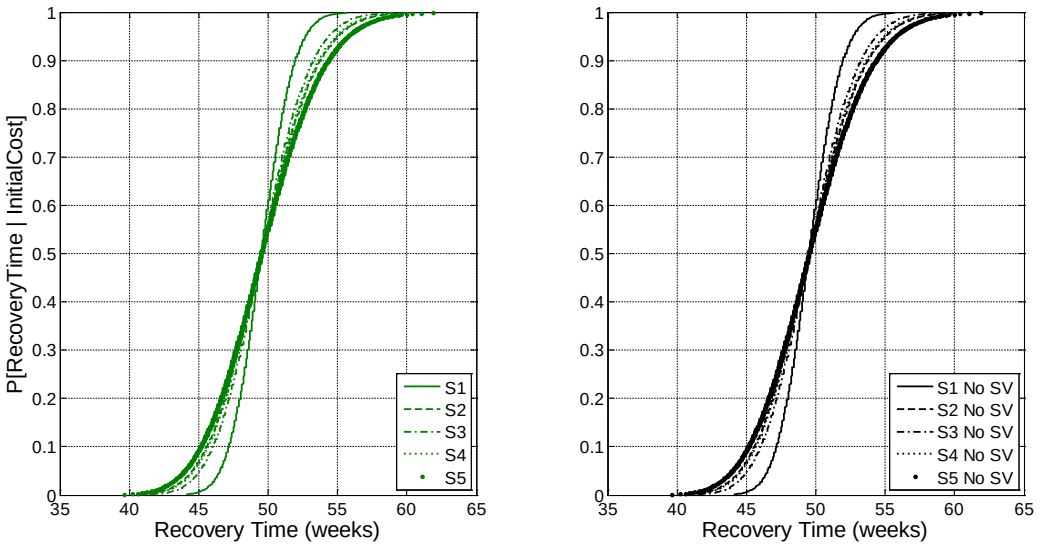

Figure 8-51: Probability of Nonexceedance for the Recovery Time Given a Specific Initial Cost at (1/6) MCE using Daly City Population

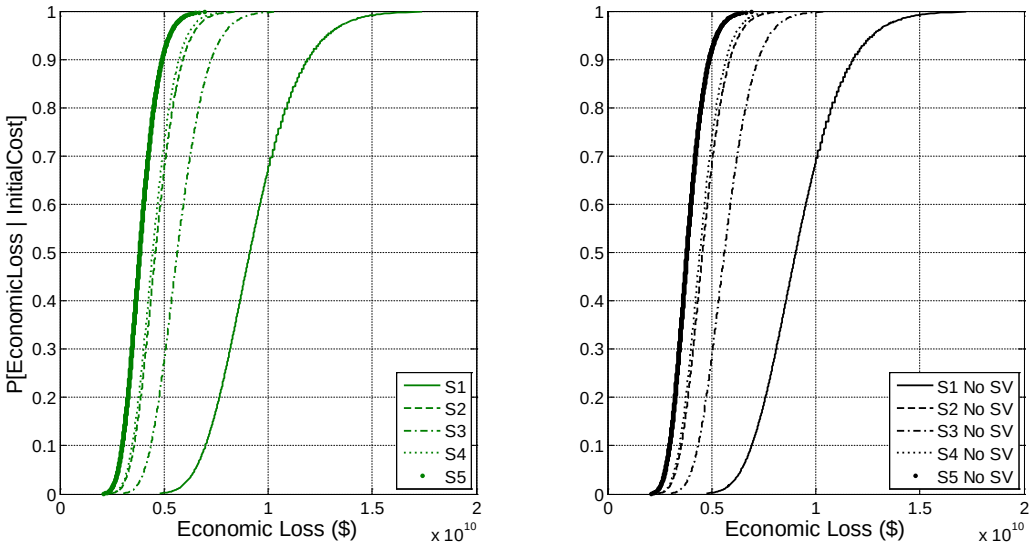

Figure 8-52: Probability of Nonexceedance for Economic Loss Given a Specific Initial Cost at (1/3) MCE using Daly City Population

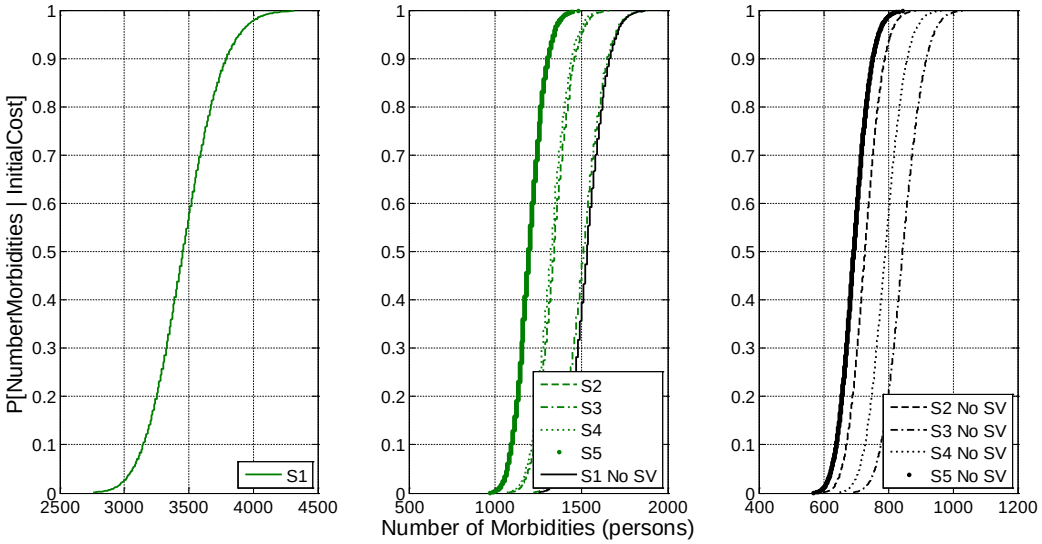

Figure 8-53: Probability of Nonexceedance for the Number of Morbidities Given a Specific Initial Cost at (1/3) MCE using Daly City Population

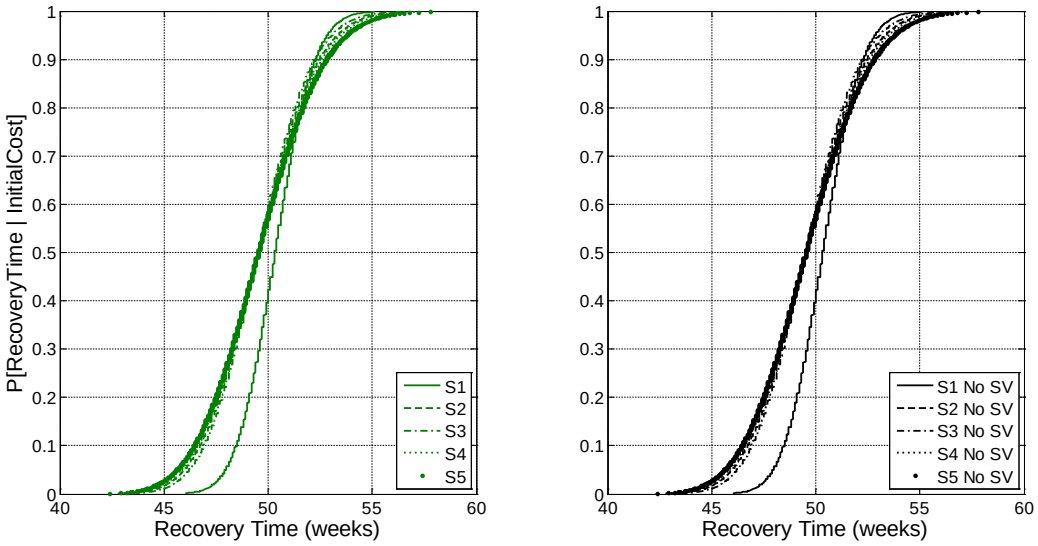

Figure 8-54: Probability of Nonexceedance for the Recovery Time Given a Specific Initial Cost at (1/3) MCE using Daly City Population

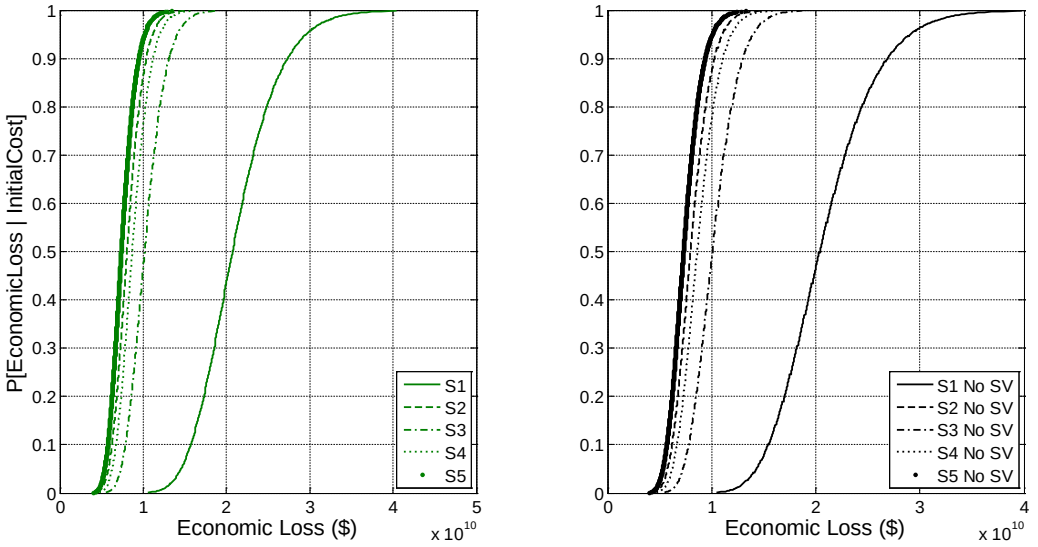

Figure 8-55: Probability of Nonexceedance for Economic Loss Given a Specific Initial Cost at (1/2) MCE using Daly City Population

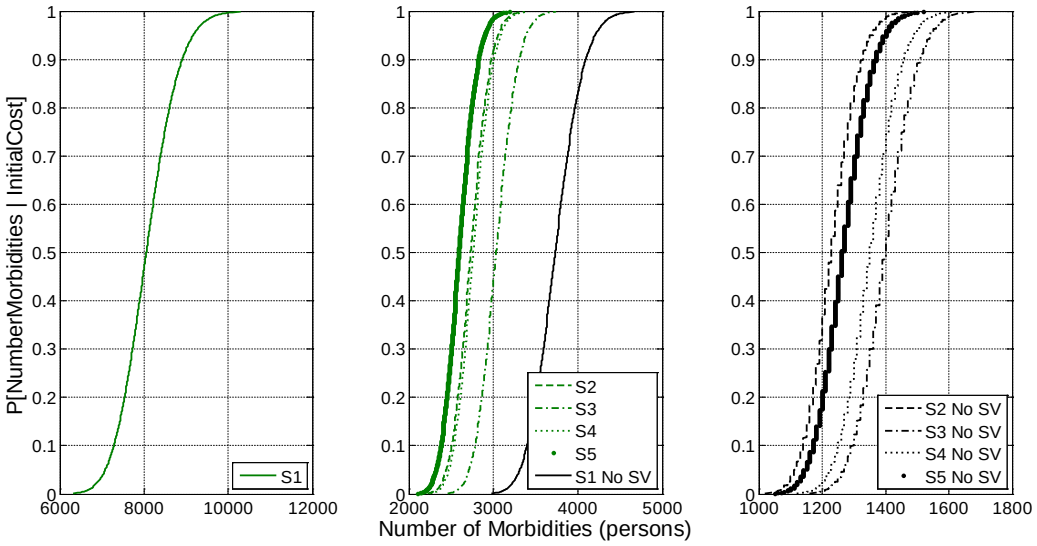

Figure 8-56: Probability of Nonexceedance for the Number of Morbidities Given a Specific Initial Cost at (1/2) MCE using Daly City Population

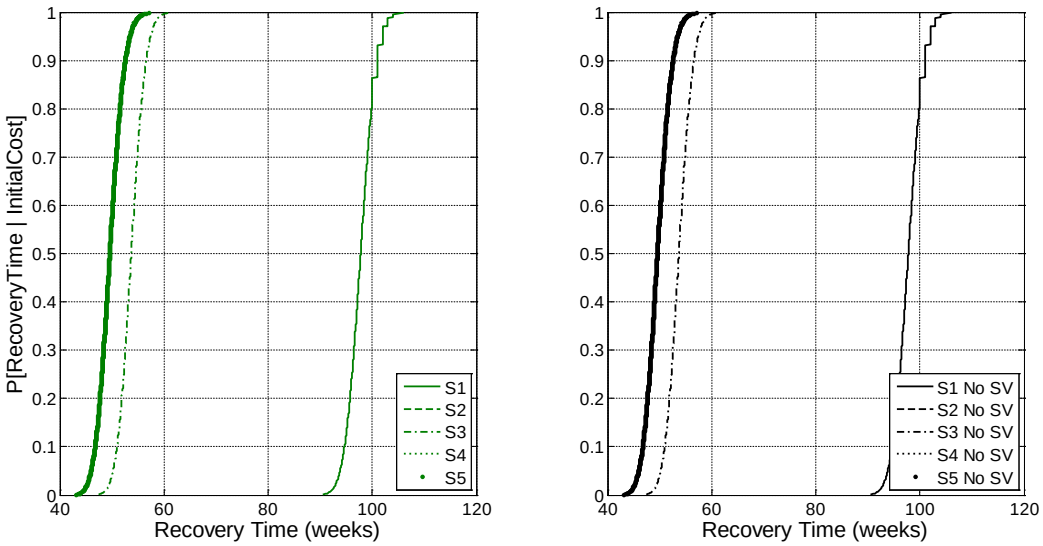

Figure 8-57: Probability of Nonexceedance for the Recovery Time Given a Specific Initial Cost at (1/2) MCE using Daly City Population

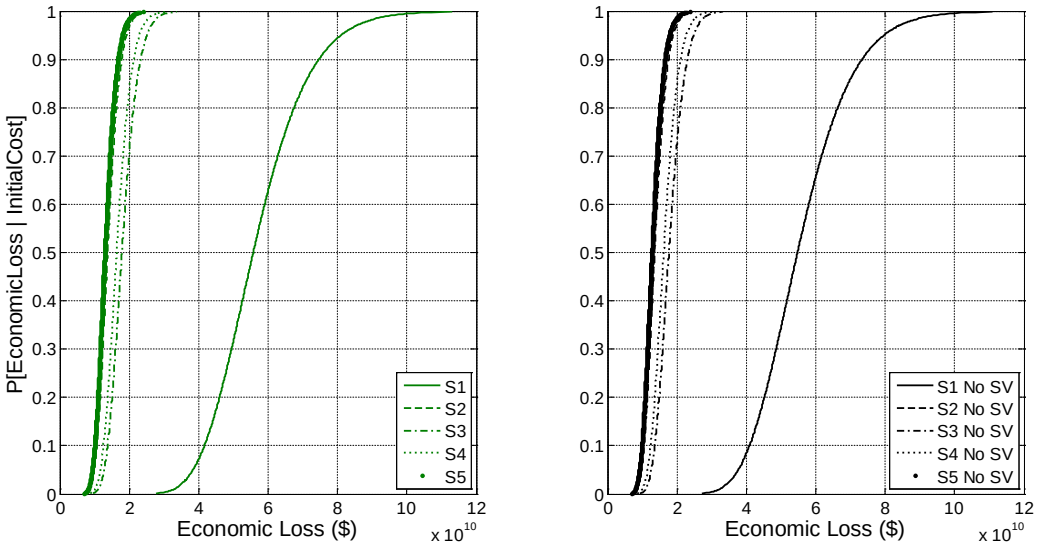

Figure 8-58: Probability of Nonexceedance for Economic Loss Given a Specific Initial Cost at (2/3) MCE using Daly City Population

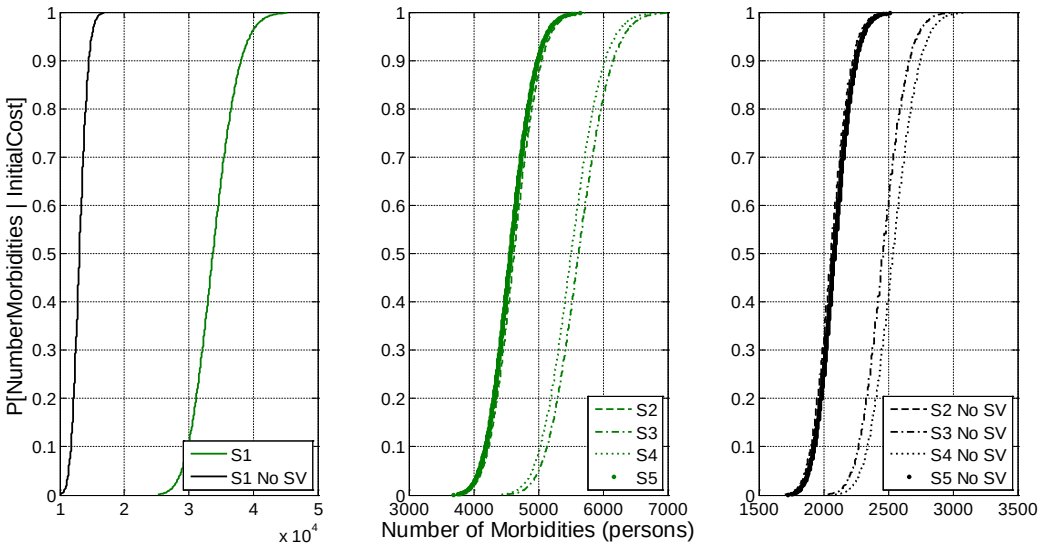

Figure 8-59: Probability of Nonexceedance for the Number of Morbidities Given a Specific Initial Cost at (2/3) MCE using Daly City Population

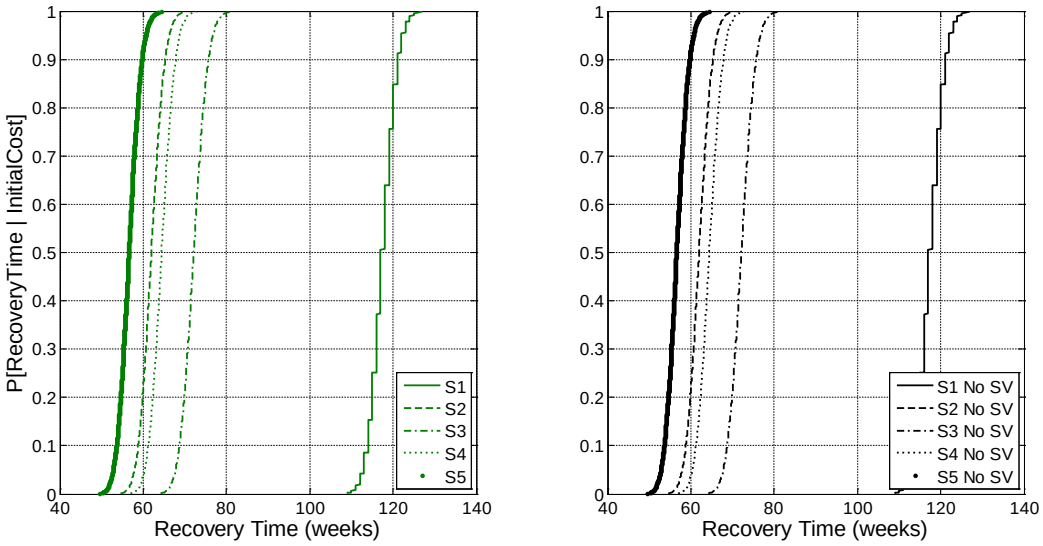

Figure 8-60: Probability of Nonexceedance for the Recovery Time Given a Specific Initial Cost at (2/3) MCE using Daly City Population

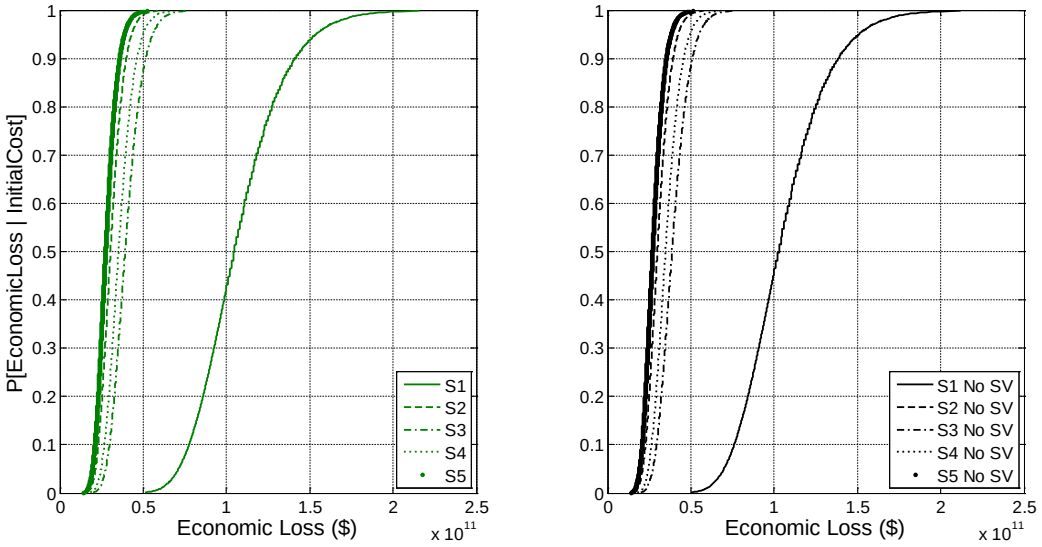

Figure 8-61: Probability of Nonexceedance for Economic Loss Given a Specific Initial Cost at (5/6) MCE using Daly City Population

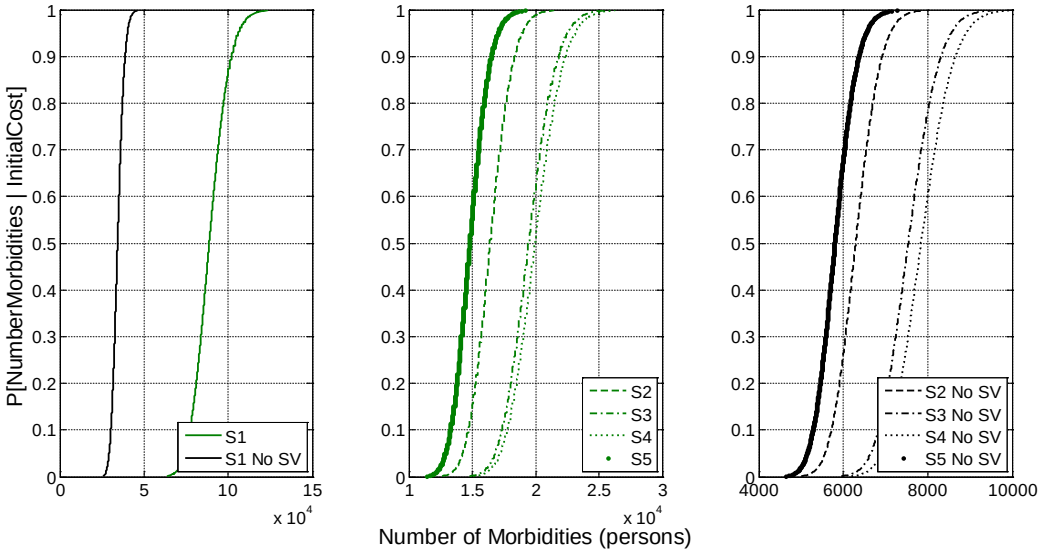

Figure 8-62: Probability of Nonexceedance for the Number of Morbidities Given a Specific Initial Cost at (5/6) MCE using Daly City Population

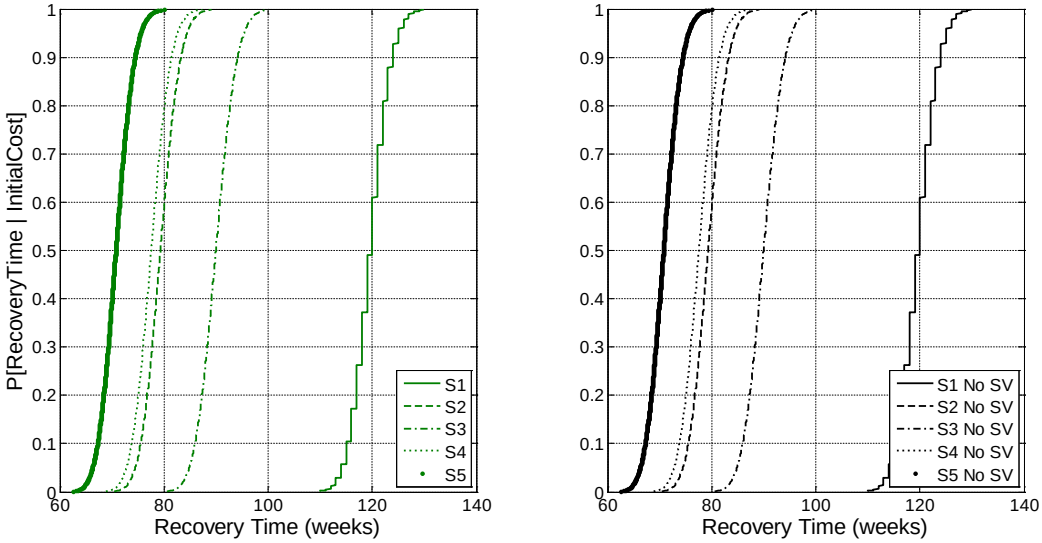

Figure 8-63: Probability of Nonexceedance for the Recovery Time Given a Specific Initial Cost at (5/6) MCE using Daly City Population

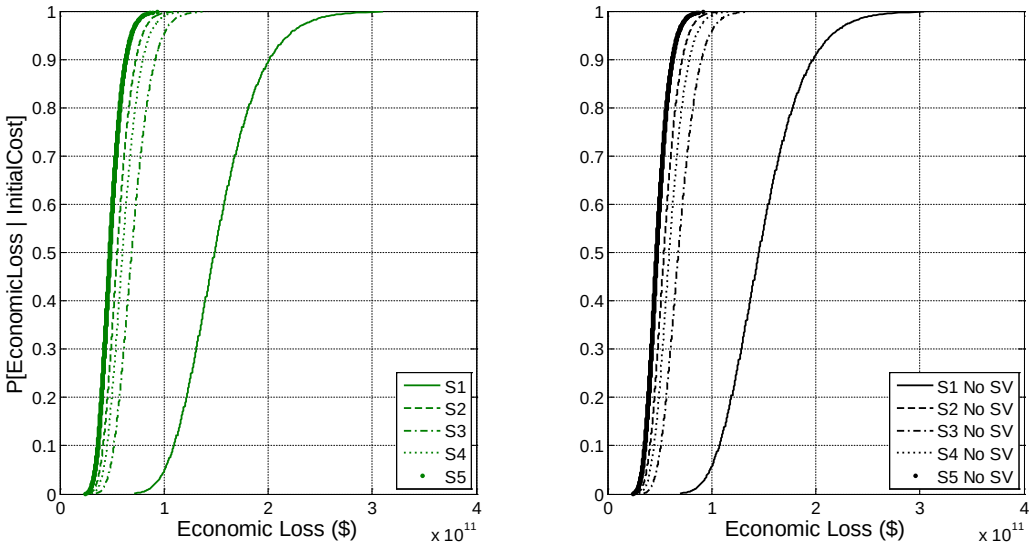

Figure 8-64: Probability of Nonexceedance for Economic Loss Given a Specific Initial Cost at MCE using Daly City Population

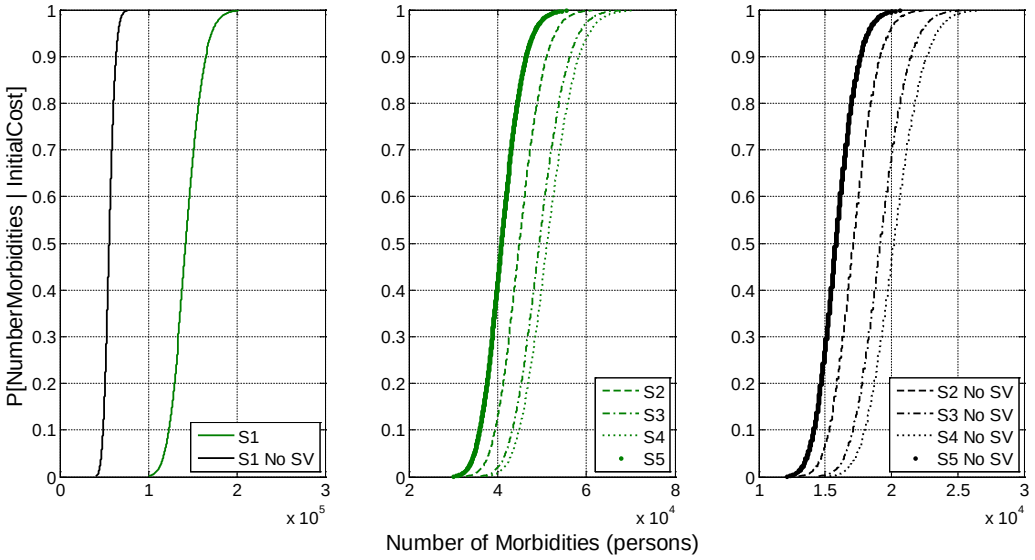

Figure 8-65: Probability of Nonexceedance for the Number of Morbidities Given a Specific Initial Cost at MCE using Daly City Population

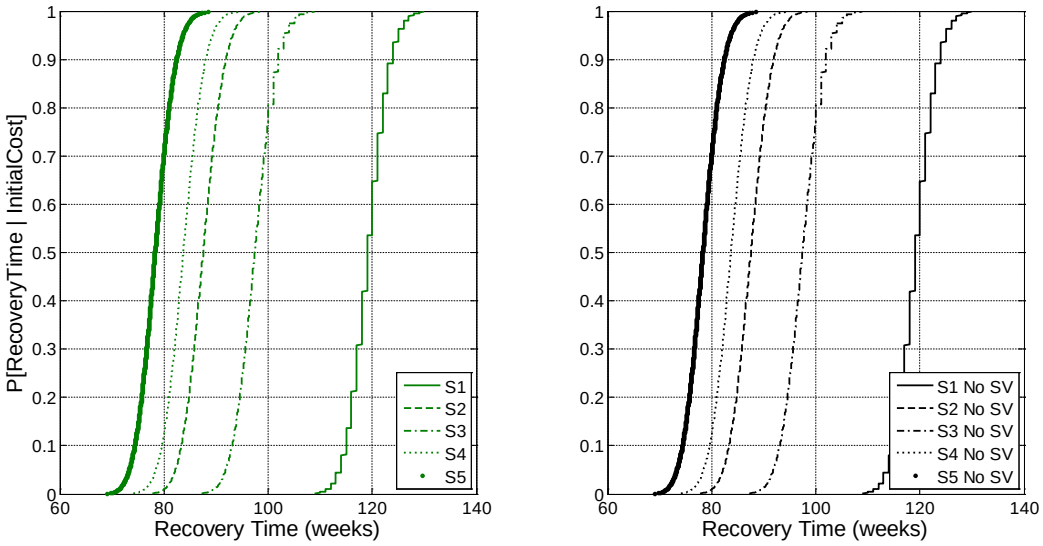

Figure 8-66: Probability of Nonexceedance for the Recovery Time Given a Specific Initial Cost at MCE using Daly City Population

8.4 Case Study 4: Northridge Population – Time of Day Comparison

In the previous examples, the time of day was set to night (2:00am) such that peak occupancy of the residential structures would be achieved. This provides a worst-case scenario for the present archetypes since most of them are residential. There are two other options embedded in the framework for the time of day: an occupancy rate corresponding to mid-work day occupancy occurring at 2:00pm and corresponding to 10% occupancy of residential buildings and 85% occupancy of commercial buildings, and an occupancy rate corresponding to a commuting time at 5:00pm with 15% occupancy of residential buildings and 20% occupancy of commercial buildings. The three occupancies are investigated here using only the initial population provided in Table 8-5 (i.e. solution 1) at a seismic intensity corresponding to a spectral acceleration of 1.1g using the Los Angeles County population data from the 2010 U.S. census data. The results for all three occupancy rates are compared in an effort to demonstrate how the losses could have differed if the 1994 Northridge earthquake would have occurred at a

different time of day. Recall, the 1994 Northridge earthquake occurred around 4:00am. The earthquake also occurred on a holiday weekend, so it is possible that many people were actually out of town. Anytime the fatality count is greater than zero, a tragic loss has occurred, however overall for this earthquake, and given the fact that more than one roadway bridge collapsed, the fatality count of 26 persons was much lower than what could have been expected if the earthquake had occurred on a non-holiday during rush hour.

Based on the associated occupancy rates provided above, one would expect the worst case to be at 2:00am, and the lowest loss estimations to be at 5:00pm during the commute since the framework only considers morbidities occurring in buildings and most of those buildings are residential. This was not the response demonstrated in Figure 8-67 through Figure 8-69 for the respective objectives. The 2:00pm case caused the highest economic loss and highest number of morbidities. This is likely due to the higher occupancy of the four-story commercial building relative to the one-, two-, and three-story residential buildings. Figure 8-69 only shows one curve, because the recovery time was controlled by the recovery time associated with PTSD (one year) which is the same for all three times of day. Although not investigated, it is likely that the 2:00am and 2:00pm loss estimations would differ more significantly at a higher seismic intensity.

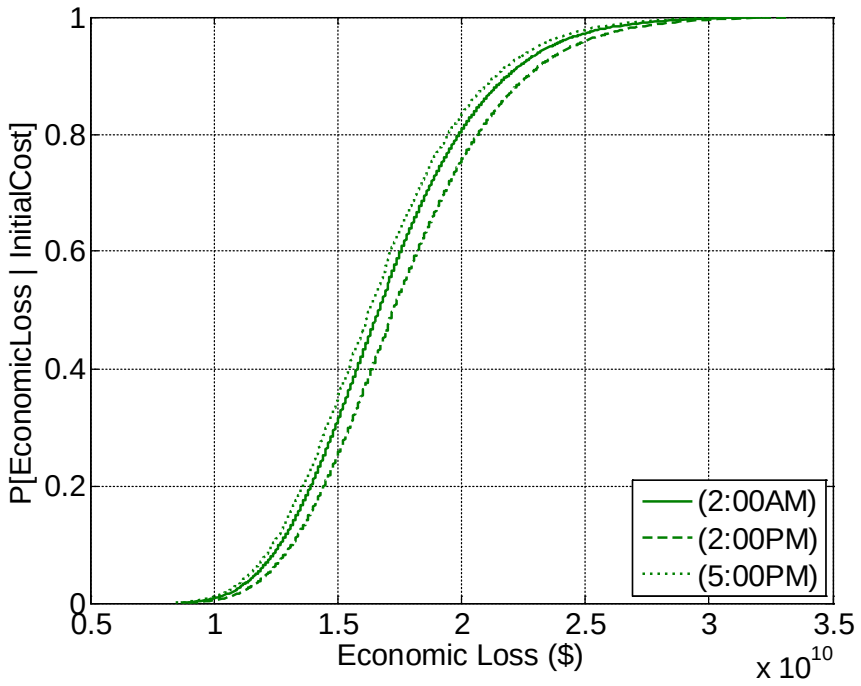

Figure 8-67: Probability of Nonexceedance for Economic Loss Given a Specific Initial Cost using Los Angeles County Population at Three Occupancy Levels and 1994 Northridge Earthquake Equivalent Seismic Hazard

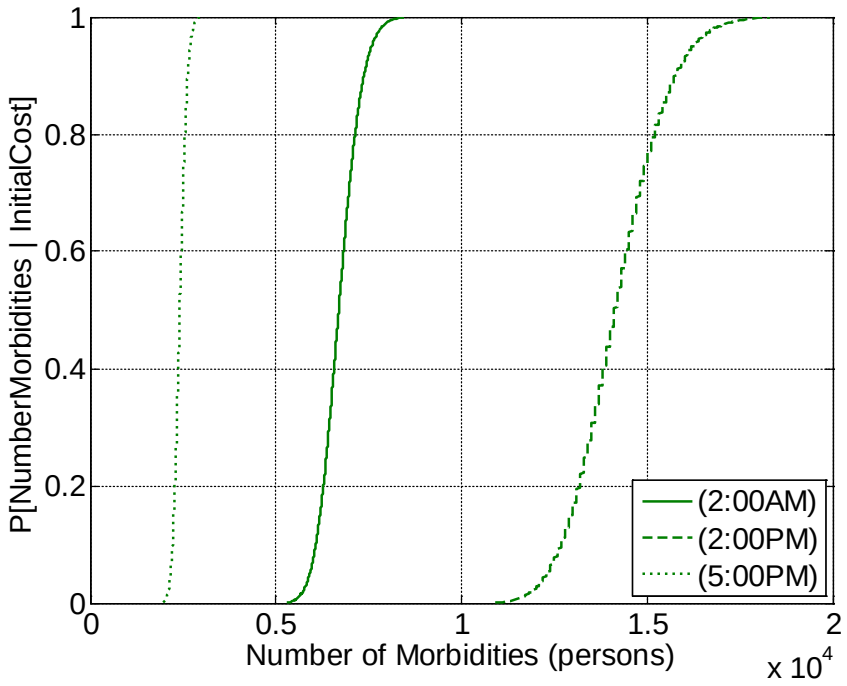

Figure 8-68: Probability of Nonexceedance for Number of Morbidities Given a Specific Initial Cost using Los Angeles County Population at Three Occupancy Levels and 1994 Northridge Earthquake Equivalent Seismic Hazard

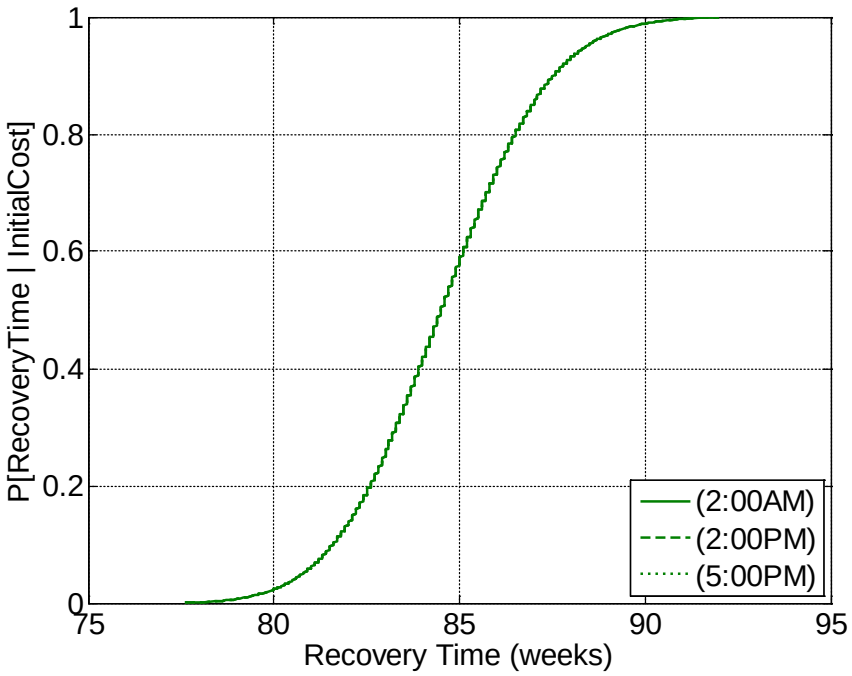

Figure 8-69: Probability of Nonexceedance for Recovery Time Given a Specific Initial Cost using Los Angeles County Population at Three Occupancy Levels and 1994 Northridge Earthquake Equivalent Seismic Hazard

8.5 Discussion

Table 8-6 provides the factors applied to (i.e. the morbidity rates based on the damage states alone) for the three communities analyzed above. The values in Table 8-6 are the product of all the socioeconomic variable factors shown in Eqs. 3-3 and 3-4. When the social vulnerability of the community is not incorporated, these factors go to unity. When the social vulnerability of the community is included, the factors were always over unity, and ranged up to 4.00 for the rate of PTSD diagnosis. The difference in these values when social vulnerability is included versus when it is not included indicates that there will be a difference in the resulting loss estimation values. One can see that although the demographics of these three communities varied, the factors determined for the probability of injury and fatality did not vary significantly with respect to each other. The population with the highest socio-economic status, Daly City,

has the lowest factors applied to all three morbidity rates. The population with the lowest socio-economic status, East Los Angeles, has the highest factors applied to all three morbidity rates. This means one can expect the highest losses to come from East Los Angeles for an identical magnitude earthquake relative to the other two communities. This infers that their higher social vulnerability to earthquakes, and therefore greater precautionary measures should be investigated in that community. The factors in Table 8-6 also demonstrate that socioeconomic status is a higher contributor to social vulnerability than ethnicity in the framework since Daly City and East Los Angeles both have high ethnic minority populations, but Daly City also has a high socioeconomic status. Although only these three populations were investigated here, where all of the factors in Table 8-6 were higher than unity when the social vulnerability computations were included, a population could exist where these factor are less than unity. Such a population was not explored here, and may only be representative of a virtual community with modified inputs from any U.S. census data. Factors lower than unity would be representative of a community with very low social vulnerability.

Table 8-36: Factors for Morbidity Computations

Community	*With Social Vulnerability*		*Without Social Vulnerability*
	Injury and Fatality Rates	*PTSD Rate*	
Los Angeles County	1.67	3.52	1.00
East Los Angeles	1.71	4.00	1.00
Daly City	1.57	3.26	1.00

To further demonstrate the significance of including the socioeconomic variables in loss estimation and mitigation planning, the percentile values were extracted from the economic loss and number of morbidities fragilities above for two solutions, S1 and S2 as an example. S1 was selected since it is the initial population, and S2 was selected to represent one of the optimal

solutions. The percentile values were not further investigated for the recovery time since these values matched for the analyses when using and not using the social vulnerability computations. The percentile values are tabulated with a percent difference comparison for economic loss and for the number of morbidities for all three populations where the percent differences are in bold. Moving from left to right in Table 8-7, the percent differences increase with increasing seismic intensity. The percent differences are higher for the initial population than for the optimal solution S2 for the economic loss computation in Table 8-7. In Table 8-8, the percent differences for the number of morbidities are very severe at all seismic intensities for both solutions. Recall that the economic loss is a compilation of the repair costs, contents damage, and the costs due to morbidities (medical costs and downtime). Therefore, if the highest contributor to economic loss is repair costs (say for the initial population where the building stock is mostly old and structurally deficient), then we would expect to see a larger difference in economic loss values when using versus not using the social vulnerability computations. The number of morbidities, on the other hand, is completely based upon the morbidities which incorporate the factors shown in Table 8-6, therefore regardless of the mitigation level of the building stock, we would expect to see major differences in the morbidity count when including the social vulnerability computations. One point that was noted in discussion of Table 8-6 was that the East LA population would be considered the most vulnerable, followed by Los Angeles County, leaving Daly City to be the least vulnerable of the three populations. Reviewing the percent differences in Table 8-7 and Table 8-8, the largest percent difference values are for East LA, followed by Los Angeles County, leaving Daly City with the smallest percent difference values for both economic loss and the number of morbidities in most cases. These results are exactly what one would expect, and from this, one can conclude that the more socially

vulnerable the population is, the more important it is to include social vulnerability into the loss estimations and mitigation planning to avoid under-prediction of the losses.

Table 8-37: 50th Percentile and Percent Difference for Economic Loss

Population	*Solution*	*Seismic Intensity*					
		1/6MCE	*1/3MCE*	*1/2MCE*	*2/3MCE*	*5/6MCE*	*MCE*
Los Angeles County	S1 No SV ($)	2.20E+09	9.03E+09	2.03E+10	5.47E+10	1.02E+11	1.45E+11
	S1 With SV ($)	2.22E+09	9.12E+09	2.07E+10	5.58E+10	1.05E+11	1.48E+11
	Difference (%)	**0.91**	**1.00**	**1.97**	**2.01**	**2.94**	**2.07**
	S2 No SV ($)	8.15E+08	3.79E+09	7.25E+09	1.28E+10	2.68E+10	4.67E+10
	S2 With SV ($)	8.19E+08	3.81E+09	7.34E+09	1.30E+10	2.72E+10	4.76E+10
	Difference (%)	**0.49**	**0.53**	**1.24**	**1.56**	**1.49**	**1.93**
East LA	S1 No SV ($)	2.21E+09	9.05E+09	2.04E+10	5.49E+10	1.03E+11	1.46E+11
	S1 With SV ($)	2.22E+09	9.16E+09	2.09E+10	5.62E+10	1.06E+11	1.50E+11
	Difference (%)	**0.45**	**1.22**	**2.45**	**2.37**	**2.91**	**2.74**
	S2 No SV ($)	8.16E+08	3.80E+09	7.28E+09	1.28E+10	2.69E+10	4.71E+10
	S2 With SV ($)	8.20E+08	3.83E+09	7.39E+09	1.31E+10	2.75E+10	4.83E+10
	Difference (%)	**0.49**	**0.79**	**1.51**	**2.34**	**2.23**	**2.55**
Daly City	S1 No SV ($)	2.21E+09	9.03E+09	2.04E+10	5.47E+10	1.03E+11	1.45E+11
	S1 With SV ($)	2.22E+09	9.12E+09	2.07E+10	5.57E+10	1.05E+11	1.48E+11
	Difference (%)	**0.45**	**1.00**	**1.47**	**1.83**	**1.94**	**2.07**
	S2 No SV ($)	8.15E+08	3.79E+09	7.26E+09	1.28E+10	2.68E+10	4.68E+10
	S2 With SV ($)	8.18E+08	3.81E+09	7.33E+09	1.30E+10	2.72E+10	4.76E+10
	Difference (%)	**0.37**	**0.53**	**0.96**	**1.56**	**1.49**	**1.71**

Table 8-38: 50th Percentile and Percent Difference for the Number of Morbidities

Population	*Solution*	*Seismic Intensity*					
		1/6MCE	*1/3MCE*	*1/2MCE*	*2/3MCE*	*5/6MCE*	*MCE*
Los Angeles County	S1 No SV (persons)	224	1440	3540	12500	32700	53000
	S1 With SV (persons)	491	3570	8310	35200	91600	146000
	Difference (%)	**119**	**148**	**135**	**182**	**180**	**175**
	S2 No SV (persons)	53.7	642	1160	1920	5440	14800
	S2 With SV (persons)	102	1210	2610	4660	15300	41700
	Difference (%)	**90**	**88**	**125**	**143**	**181**	**182**
East LA	S1 No SV (persons)	265	1840	4410	15000	39800	65000
	S1 With SV (persons)	595	4740	11000	45200	121000	195000
	Difference (%)	**125**	**158**	**149**	**201**	**204**	**200**
	S2 No SV (persons)	64.5	871	1640	2630	7040	19200
	S2 With SV (persons)	126	1680	3880	6750	21100	58500
	Difference (%)	**95**	**93**	**137**	**157**	**200**	**205**
Daly City	S1 No SV (persons)	233	1530	3730	13000	34300	55700
	S1 With SV (persons)	467	3450	8050	33700	88700	142000
	Difference (%)	**100**	**125**	**116**	**159**	**159**	**155**
	S2 No SV (persons)	56.1	692	1260	2080	5790	15800
	S2 With SV (persons)	97	1190	2590	4560	14800	40800
	Difference (%)	**73**	**72**	**106**	**119**	**156**	**158**

The percentile values for the three populations are plotted in Figure 8-70 - Figure 8-75. The percentile values for economic loss and the number of morbidities versus the seismic intensity are provided in Figure 8-70 and Figure 8-71 for the Los Angeles County population. One can see from these figures that when comparing the estimated losses between using the social vulnerability computations versus not using them, the difference between values increases as the seismic intensity increases. The differences between S1 loss estimations were more significant than S2. That is to say, when computing loss estimations for a less resilient building stock, it is even more imperative to include social vulnerability into the loss estimations. Figure 8-72 and Figure 8-73 plot the percentile values for economic loss and the number of morbidities, respectively, for the East Los Angeles population. This population was deemed the most vulnerable of the three populations, and this conclusion is again apparent in Figure 8-71, Figure 8-73, and Figure 8-75 since Figure 8-73 has much higher ordinate values. Figure 8-74 and Figure 8-75 plot the percentile values for economic loss and the number of morbidities, respectively, for the Daly City population. This population was deemed the least vulnerable of the three populations, however the importance in including the social vulnerability computations is still very significant as provided by the percent differences reported in Table 8-7 and Table 8-8, and the curves presented in the figures. Overall, one can see that not including social vulnerability leads to large underestimations in losses, and this is particularly true for a highly vulnerable population with an outdated or structurally deficient building stock.

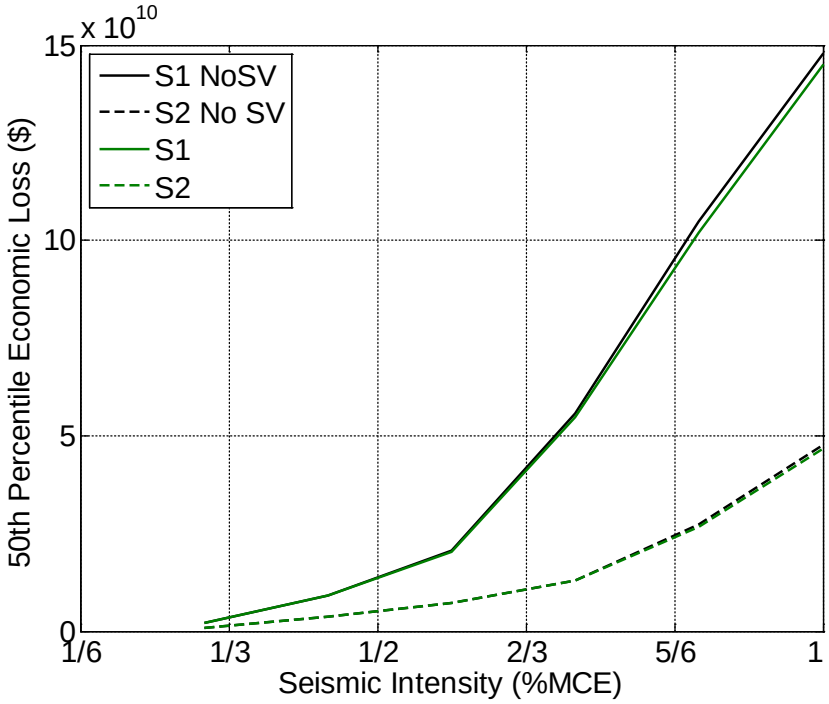

Figure 8-70: 50th Percentile Economic Loss versus Seismic Intensity for the Los Angeles County Population

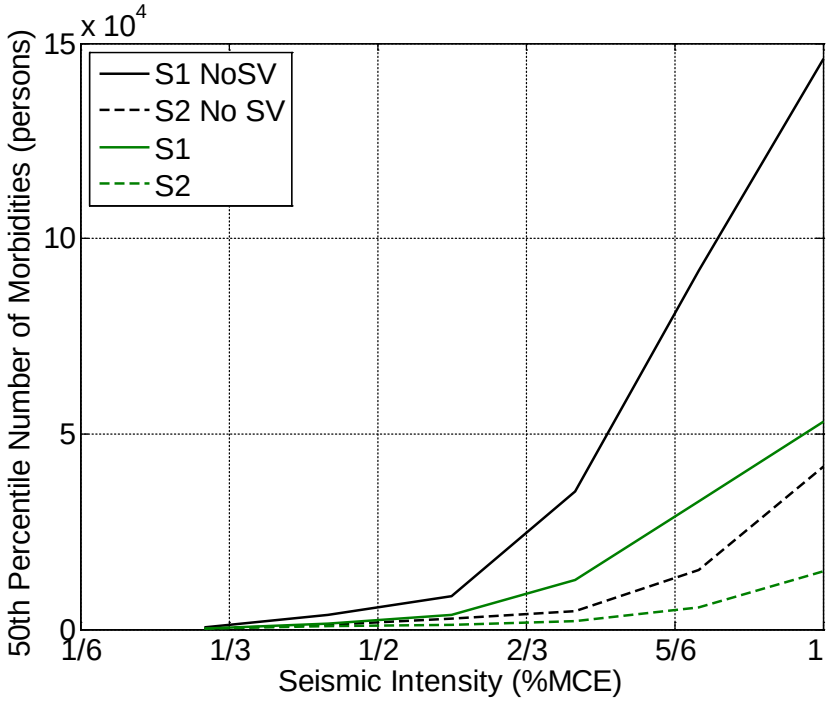

Figure 8-71: 50th Percentile Number of Morbidities versus Seismic Intensity for the Los Angeles County Population

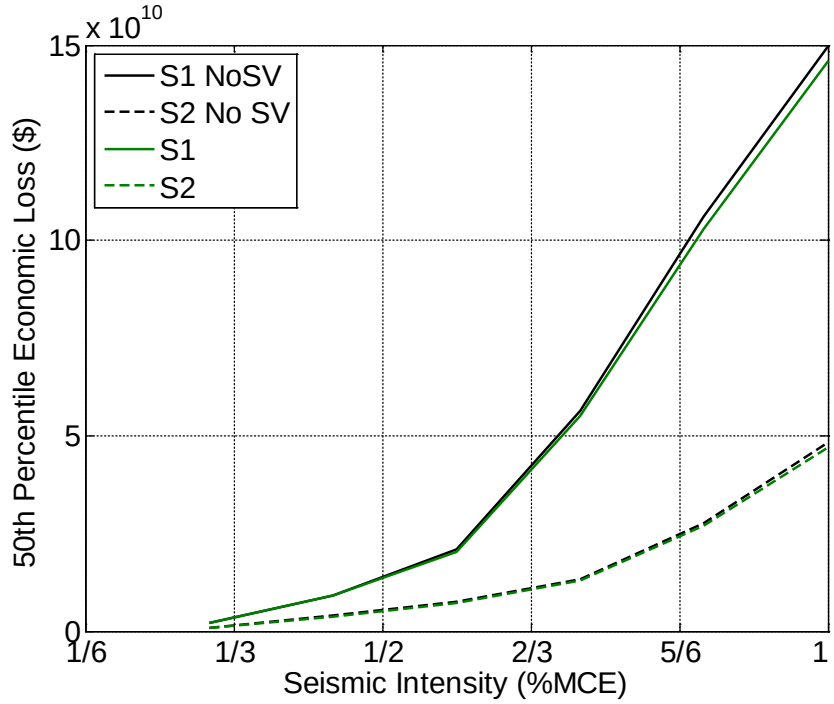

Figure 8-72: 50th Percentile Economic Loss versus Seismic Intensity for the East Los Angeles Population

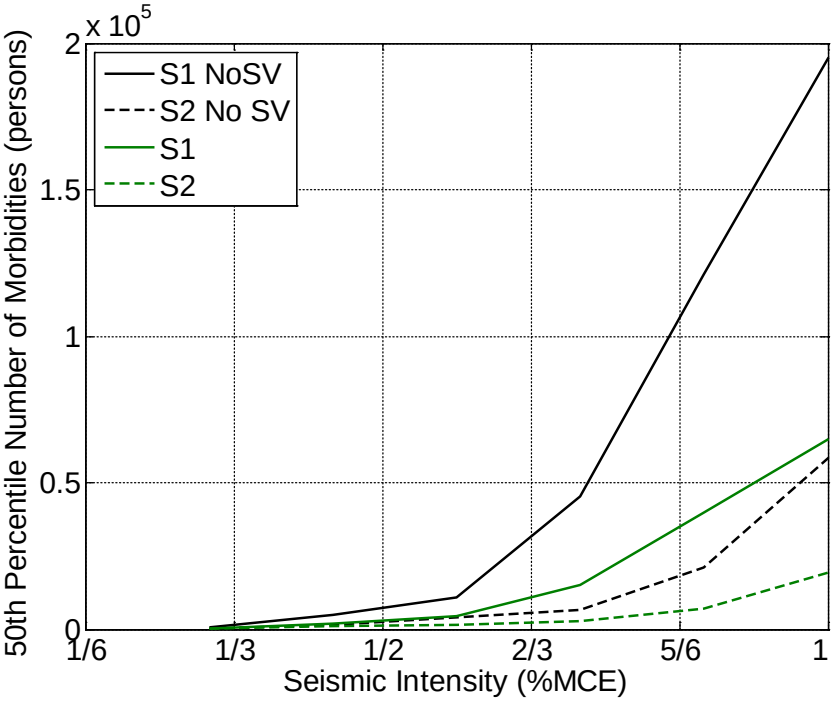

Figure 8-73: 50th Percentile Number of Morbidities versus Seismic Intensity for the East Los Angeles Population

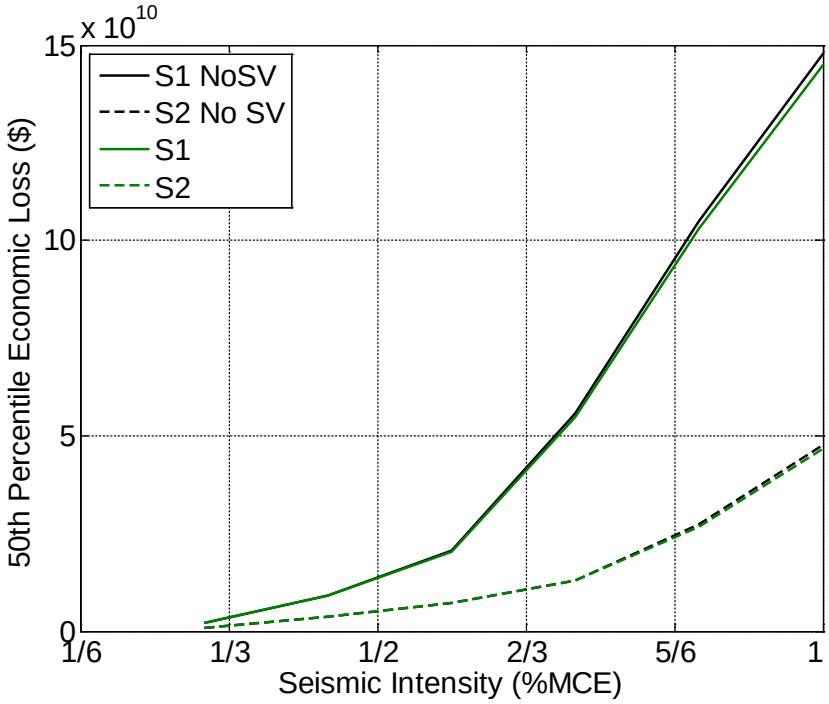

Figure 8-74: 50th Percentile Economic Loss versus Seismic Intensity for the Daly City Population

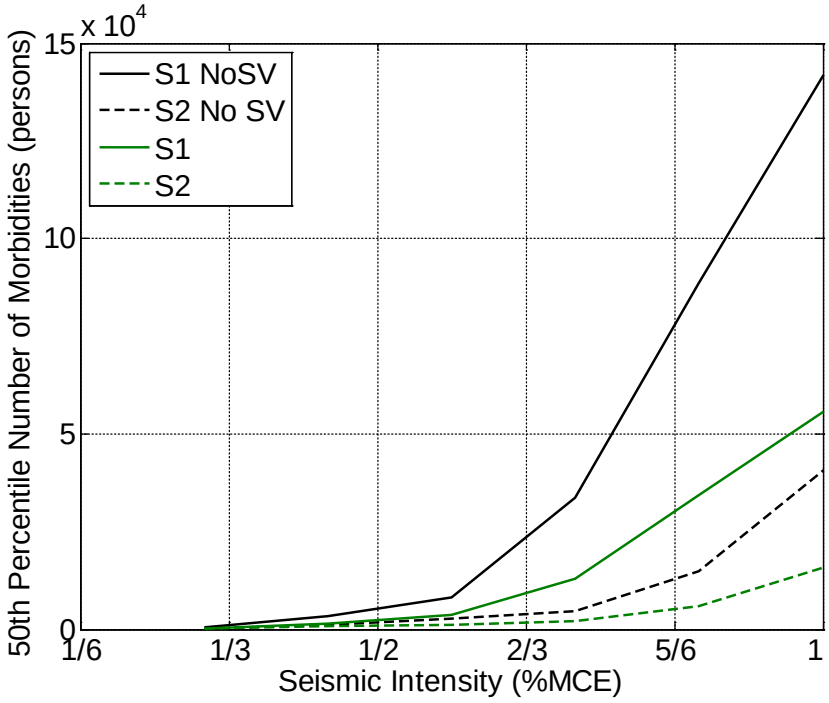

Figure 8-75: 50th Percentile Number of Morbidities versus Seismic Intensity for the Daly City Population

The percent differences between the economic loss determined when including and not including the social vulnerability computations presented in Table 8-7 may seem very small ranging from 0.37% to 2.94%. However, these monetary values are very large, therefore small percent difference still corresponds to millions or billions of dollars difference. Now, if the percentile values for economic loss are extracted from Table 8-7, and added to the initial cost for solutions 1 and 2, then the total financial loss may be investigated. Table 8- 9 provides these computations, along with the percent difference between the total financial losses for the two solutions. In all cases, for all three populations and all seismic intensities, the initial population (i.e. solution 1) has a higher estimated total financial loss. This means that, although there is no associated initial cost, the estimated economic loss, even for very small earthquakes, is greater than the total financial loss for the retrofitted case. Looking at the change in percent difference for each seismic intensity, the most significant difference occurs at 2/3MCE, or at DBE with approximately 76% difference. It is not clear why this is, however it does hold a lot of implications

since this is the seismic intensity that could very well be expected to occur. When considering the reduced number of morbidities associated with the retrofitted solutions, it is clear that retrofitting is better, even if there is a higher associated initial cost.

Table 8- 9: Comparison of Total Financial Loss for Three Case Studies

Solution		*Measure*	*Seismic Intensity*					
			1/6MCE	*1/3MCE*	*1/2MCE*	*2/3MCE*	*5/6MCE*	*MCE*
LA County	S1 With SV	Initial Cost ($)	0	0	0	0	0	0
		Economic Loss ($)	2.22E+09	9.12E+09	2.07E+10	5.58E+10	1.05E+11	1.48E+11
		Sum ($)	2.22E+09	9.12E+09	2.07E+10	5.58E+10	1.05E+11	1.48E+11
	S2 With SV	Initial Cost ($)	5.32E+08	5.32E+08	5.32E+08	5.32E+08	5.32E+08	5.32E+08
		Economic Loss ($)	8.19E+08	3.81E+09	7.34E+09	1.30E+10	2.72E+10	4.76E+10
		Sum ($)	1.35E+09	4.34E+09	7.87E+09	1.35E+10	2.77E+10	4.81E+10
	Percent Difference (%)		**39.14**	**52.39**	**61.97**	**75.75**	**73.59**	**67.48**
East LA	S1 With SV	Initial Cost ($)	0	0	0	0	0	0
		Economic Loss ($)	2.22E+09	9.16E+09	2.09E+10	5.62E+10	1.06E+11	1.50E+11
		Sum ($)	2.22E+09	9.16E+09	2.09E+10	5.62E+10	1.06E+11	1.50E+11
	S2 With SV	Initial Cost ($)	5.32E+08	5.32E+08	5.32E+08	5.32E+08	5.32E+08	5.32E+08
		Economic Loss ($)	8.20E+08	3.83E+09	7.39E+09	1.31E+10	2.75E+10	4.83E+10
		Sum ($)	1.35E+09	4.36E+09	7.92E+09	1.36E+10	2.80E+10	4.88E+10
	Percent Difference (%)		**39.10**	**52.38**	**62.10**	**75.74**	**73.55**	**67.45**
Daly City	S1 With SV	Initial Cost ($)	0	0	0	0	0	0
		Economic Loss ($)	2.22E+09	9.12E+09	2.07E+10	5.57E+10	1.05E+11	1.48E+11
		Sum ($)	2.22E+09	9.12E+09	2.07E+10	5.57E+10	1.05E+11	1.48E+11
	S2 With SV	Initial Cost ($)	5.32E+08	5.32E+08	5.32E+08	5.32E+08	5.32E+08	5.32E+08
		Economic Loss ($)	8.18E+08	3.81E+09	7.33E+09	1.30E+10	2.72E+10	4.76E+10
		Sum ($)	1.35E+09	4.34E+09	7.86E+09	1.35E+10	2.77E+10	4.81E+10
	Percent Difference (%)		**39.19**	**52.39**	**62.02**	**75.71**	**73.59**	**67.48**

Further investigation of Table 8- 9 reveals that the total financial loss, and therefore the percent differences, for the three populations are approximately the same. Only three significant digits are provided, so these values appear to be equal. However, if more significant digits were

provided a slight difference would be seen in all cases. Recall from Chapter 3, that the economic loss was computed by summing the repair costs, relocation costs, contents damage, cost due to injury, due to fatality, cost due to medical treatment of PTSD, and the downtime due to PTSD. All of these values are independent of the community's economics except the last measure, downtime due to PTSD. The downtime due to PTSD is computed using the mean annual income of the community. Thus, the similarity in Table 8- 9 between the Los Angeles County population and the Daly City population occurs due to the similarity in the mean annual income for these two populations, $81,729 and $89,180 for Los Angeles County and Daly City, respectively, and the similar factors in Table 8-6. The mean annual income for East Los Angeles was reported as $37,982, significantly less than the other two, and the factors in Table 8-6 were higher. Referring back to Table 8-8, one can see that the percentile values of the number of morbidities for solution 2 are very similar for the Los Angeles County and Daly City populations at all six seismic intensity levels. At all six seismic intensity levels, the number of morbidities for East Los Angeles was higher. In fact, the number of morbidities estimated for East Los Angeles is approximately 39% higher than the estimates for either of the other two populations. Taking this one step further, the estimated number of work hours lost in one year due to employees suffering from posttraumatic stress disorder may be determined for the current (i.e. initial) population. The percentile value for this measure at DBE (i.e. 2/3MCE), using Eqns. 3-30 and 3-32 was computed as 7,200, 9,500, and 6,800 hours for Los Angeles County, East Los Angeles, and Daly City, respectively. Dividing the mean annual income for these three populations by 260 work days per year at 8 hours per day, providing an equivalent hourly rate for all three populations, the total dollars lost due to downtime, not medical costs, caused by persons having PTSD may be computed as $74 million, $45 million, and $76 million, for Los Angeles

County, East Los Angeles, and Daly City, respectively. These values further demonstrate that the mental health of the population is critical for economic prosperity and recovery following disastrous events such as earthquakes, and further demonstrate the need for seismic mitigation.

Chapter 9: Conclusions, Contributions, and Recommendations

A multi-objective optimization problem was solved via genetic algorithm using socioeconomic and engineering variables to improve community resiliency by identifying optimal retrofit plans for the woodframe building stock of the community. The retrofit plans may be used by decision makers in determining where mitigation funds may best be allocated by providing the associated risk with each retrofit plan. The associated risk was based upon four contributors: initial cost, economic loss, number of morbidities, and recovery time. Additionally, the loss in quality of life for the population was demonstrated using complementary measures such as the number of building collapses, the number of persons sheltering out-of-place, the number of persons injured, killed, and diagnosed with PTSD, along with the estimated recovery time. The primary and complementary measures were determined by modeling the influence that age, ethnicity and race, family structure, gender, socioeconomic status, the age, density and quality of the built environment, and building performance have on community seismic resiliency. Following an extensive literature survey and meta-data analysis, it may be concluded that socio-economic variables can be quantified in a meaningful way in order to be included in engineering frameworks. In this study, the probability of the morbidities, the economic loss, the recovery time, and the loss in quality of life were all modeled to be dependent on the socioeconomic variables.

Due to the large quantity of at-risk soft-story woodframe buildings in California, and with California being the focal area of the applied framework, these building types were desired to serve as archetypes in the present framework. Prior to inclusion into the framework, the seismic behavior of these buildings, post-retrofit, needed to be experimentally investigated to obtain

proper performance data An experimental study was conducted to investigate the adequacy of soft-story woodframe buildings retrofitted by performance-based seismic retrofit procedures and the FEMA P-807 retrofit procedure. The results of the experimental studies confirmed that soft-story buildings retrofitted by performance-based seismic design procedures provide excellent seismic performance when subjected to very large

earthquakes. The results also demonstrated that soft-story woodframe buildings retrofitted following the FEMA P-807 procedure perform better than design expectations and can withstand large earthquakes without collapsing.

Additionally, these experimental tests provided the means to develop a metric for correlating physical building damage to woodframe structures with peak inter-story drifts. The metric became the basis of the damage states used in this study and were the connective tie between physical building damage, morbidity rates, economic loss, and recovery time.

In total, 37 archetypes were modeled and analytically tested for usage in the framework. Design procedures dating back to 1959 and through 2014 state-of-the-art were followed in designing the archetypes. The analytical analyses demonstrated the increase in performance provided by each newer design code for identical floor plans. The performance-based seismic retrofits were superior to buildings design by seismic design codes, while the performance of FEMA P-807 retrofitted buildings was worse than PBSR and the modern seismic design code, but fell within the performance of the structurally obsolete buildings. This investigation on the historical seismic performance of woodframe buildings confirms the improvement of seismic provisions with time; a comforting conclusion.

There are many assumptions and approximations embedded into the framework which can leave to exponentially increasing uncertainty in the estimated losses. With this in mind, the

framework was calibrated to meet several reported loss values for the 1994 Northridge earthquake, the most recent earthquake disaster in the United States. Several illustrative examples were conducted as applications of the combined socioeconomic and engineering framework for optimizing community resiliency. The county of Los Angeles, California was the focal point for the illustrative examples. The population based on the 2010 U.S. census data for Los Angeles county, as well as two forecasted populations using the 2010 U.S. census data for East Los Angeles and Daly City, California were analyzed. The application of the framework demonstrated that of the three populations, the one with the lowest socioeconomic status (i.e. East Los Angeles) was the most vulnerable to an earthquake disaster, and provided the highest estimated losses for economic loss, number of morbidities, and recovery time over the other two populations. The application of the framework also demonstrated that the population with the highest socioeconomic status (i.e. Daly City) was the least vulnerable and produced the lowest estimated losses of the three populations. These results revealed that socioeconomic status was a higher contributor to social vulnerability than ethnicity or race. This conclusion fits in well with what other researchers have reported [Cutter et al. (2003), Cutter and Finch (2008)].

Through applying the framework to select populations in California, it was effectively demonstrated that extreme losses should be expected if a very large earthquake were to occur on the current woodframe building stock. For a maximum considered earthquake (e.g. 2475 year return period), economic loss estimations exceeded $148 billion. This amount was reduced to as much as $47 billion for one of the retrofit plans investigated in the illustrative examples. For this same size earthquake, the number of morbidities was estimated at approximately 146,000 people under the current woodframe building stock. This count was reduced to as much as 41,700 persons for one of the retrofit plans investigated. The recovery time was reduced from 119

weeks to as little as 78 weeks by retrofitting. The discussed values were taken at a 50% probability of nonexceedance with the social vulnerability computations included.

For a design basis earthquake (i.e. 475 year return period), the estimated economic loss and number of morbidities for the current buildings tock in Los Angeles County, California was reported as $56 billion and 35,200 persons, respectively. These values were reduced to as much as $13 billion and 4,660 persons, respectively. The recovery time was reduced from 117 weeks to 56 weeks by retrofitting. In the retrofitted case, the recovery time was controlled by the time for PTSD recovery and the building repair time was less than one year.

The reduced loss values in both cases are still unfortunately high, although they were reduced by approximately an order of magnitude. A greater reduction could potentially be made if the input parameters to genetic algorithm were increased allowing for more solutions to be explored. It is believed that if the algorithm would have been allowed to run for much longer, it would have identified more and more optimal solutions that would reduce the estimated losses to lower values that those discussed above.

Through the illustrative examples, it was effectively demonstrated that by not including social vulnerability into the loss estimations, large underestimations in losses result. This was consistent in all examples for all loss estimates, except recovery time since the repair times were not modeled using the social vulnerability parameters. In all exemplified applications, the total financial loss (e.g., initial cost + economic loss) was higher for the initial population (i.e. un-retrofitted case). When combining this financial savings with the reduced number of morbidities, it is clear that the higher initial cost associated with retrofitting the woodframe building stock greatly outweighs the risks and losses associated with not retrofitting.

The largest difference in total financial loss was demonstrated to occur at a DBE seismic intensity. This finding was interesting, and should further encourage retrofit since a DBE event is very likely to occur in focal communities.

The resulting losses were further investigated to demonstrate how important including the emotional health of the population is for the community's economy and recovery. The percentile values for the total number of work hours lost due to employees having PTSD was estimated as 7,200 hours, 9,500 hours, and 6,800 hours for Los Angeles County, East Los Angeles, and Daly City, respectively for a DBE seismic intensity. These hour estimates equated to $74 million, $45 million, and $76 million, respectively, financial loss for the commercial industry based on the mean annual income for the three communities. Considering these large estimated losses for a design bases earthquake, it is clear that including the mental health of the population is critical for economic prosperity and recovery following disastrous events such as earthquakes. Considering 2,000 work-hours on average for a person per year, 7,200 work-hours lost by a DBE event may not seem like much for a population around the size of 1,000,000 people. The input values for determining the annual work-hours lost may be on the low side of estimating the number of hours lost due to presenteeism and absenteeism, and should be further explored.

A study was conducted to demonstrate the difference in estimated losses based on the time of day. This application was based on the 1994 Northridge earthquake. Considering the woodframe building stock, the time of occurrence for the Northridge earthquake was a worst-case time since the early morning hours (i.e. 4:00am) was modeled to have peak occupancy of the residential structures. The illustrative example demonstrated that if the earthquake had occurred during the lowest residential occupancy hour (i.e. 5:00pm commute) the losses would

have been lower. This is an interesting conclusion and demonstrates a short-coming in the framework. The reason that the estimated losses were not much higher, especially the morbidity rates, following the actual time of day of the 1994 Northridge earthquake is because it did occur when most people were not driving on the roads since there were roadway bridge collapses. The framework only considers losses occurring from the woodframe building stock and therefore does not capture losses occurring from highway bridges, etc. Therefore the framework suggests that what one would assume to be the actual worst time of day for the 1994 Northridge earthquake to occur would be the best time of day considering loss estimations.

In all actuality, there were several limitations to this study. The most significant of which are that the distance variations over the community area from the epicenter were not considered, and that only the woodframe building stock was modeled for the built environment. Additionally, the initial population of the woodframe building stock was based on assumptions from census data, and not necessarily the exact current situation in the community being analyzed. The framework, as it is, is specific to California and could not readily be applied to other locations with seismic hazards such as Memphis, Tennessee, or other parts of the world. This is because the seismic hazard used in the archetype designs, as well as the selected seismic design provisions and soft-story woodframe building archetypes are all specific to California. The framework is generalized and may easily be extended once other region-specific archetypes are incorporated.

There are several major contributions of this dissertation. The soft-story retrofit strategies designed and tested as part of this dissertation can be incorporated into practice to address the current at-risk condition of many communities in California. Thus far an extensive

analysis on the evolution of risk for seismically designed woodframe buildings has not been conducted, but is a complementary output from the archetype designs and analyses.

The socioeconomic parametric models may be used in other studies as a basis for quantifying such qualitative measures, and may be incorporated into other designs and frameworks when the social vulnerability of a place is included as a design objective. The combined socioeconomic and engineering framework may be adopted and applied by local and state decision makers for optimizing the allocation of earthquake mitigation funds amongst its woodframe building stock, and as determining the best retrofit plan for their at-risk communities. The framework may also be incorporated into existing system level studies which desire to include social vulnerability and the quality of life within their models.

Future work by the author will include addressing some of the limitations described above, including extending the framework to include emergency facilities and buildings of all structural types, as well as the aftermath potential of tsunamis and fire hazards. The author will design a set of archetypes for the Memphis, Tennessee region, and apply the framework to local communities in that region. Additionally, the author plans to develop similar socioeconomic variable factors for other hazards so as to extend the framework to other natural and human-induced hazards.

References

Ali, M., Farooq, N., Bhatti, M.A., and Kuroiwa, C., (2011). "Assessment of prevalence and determinants of posttraumatic stress disorder in survivors of earthquakes in Pakistan using Davidson Trauma Scale." *Journal of Affective Disorders*, 136(3), pp. 238-243.

Altindag, A., Ozen, S., and Aytekin, S. (2005). "One-year follow-up study of posttraumatic stress disorder among earthquake survivors in Turkey." *Comprehensive Psychiatry* 46: 328-333.

ASCE (2005). "Minimum Design Loads for Buildings and Other Structures, ASCE/SEI 7-05." American Society of Civil Engineers, Reston, Virginia. ISBN 978-0-7844-1085-1.

ATC (2010). "Here Today – Here Tomorrow: The Road to Earthquake Resilience in San Francisco – A Community Action Plan for Seismic Safety." Applied Technology Council (ATC) Project 52-2, Redwood City, CA.

ATC 3-06 (1978). "Tentative provisions for the development of seismic regulations for buildings." Applied Technology Council, Redwood City, California.

Bahmani, P. and de Lindt, J. (2014). "Experimental and Numerical Assessment of Woodframe Sheathing Layer Combinations for Use in Strength-Based and Performance-Based Design." *J. Struct. Eng.*, .1061/(ASCE)ST.1943-541X.0001134 , E4014001.

Beavers, J.E. (2002). "A review f seismic hazard description in US design codes and procedures." *Prog. Struct. Engng. Mater, 4:46-63.* Copyright 2002 John Wiley and Sons, Ltd.

Black, G., Davidson, R., Pei, S., van de Lindt, J. (2010). "Empirical loss analysis to support definition of seismic performance objectives for woodframe buildings." *Structural Safety*, vol. 32, pp. 209-219.

Bodvarsdottir, I., and Elklit, A., (2004). "Psychological reactions in Icelandic earthquake survivors." *Scandinavian Journal of Psychology*, 45, pp. 3-13.

Borden, K.A., and Cutter, S.L., (2008). "Spatial patterns of natural hazards mortality in the United States." *International Journal of Health Geographics*, 7(1), pp. 64 - 80.

Bruneau, M., Chang, S., Eguchi, R., Lee, G., O;Rourke, T., Reinhorn, A., Shinozuka, M., Tierney, K., Wallace, W., and Winterfedlt, D. (2003). "A Framework to Quantitatively Assess and Enhance the Seismic Resilience of Communities." *Earthquake Spectra*, vol. 19, no. 4, pp. 733-752.

Cairo, J., Dutta, S., Nawaz, H., Hashmi, S., Kasl, S., and Bellido, E. (2010). "The Prevalence of Posttraumatic Stress Disorder Among Adult Survivors in Peru." *Disaster Med Public Health Preparedness,* 4: 39-45.

CBO (2012). The Veterans Health Administration's Treatment of PTSD and Traumatic Brain Injury Among Recent Combat Veterans. Congress of the United States, Congressional Budget Office. Pub. No. 4097.

Cerda, M., Paczkowki, M., Galea, S., Nemethy, K., Pean, C., and Desvarieux, M. (2013). "Psychopathology in the Aftermath of the Haiti Earthquake: A Population-based Study of Posttraumatic Stress Disorder and Major Depression." *Depression and Anxiety,* 30: 413-424.

CGS (2009). "HAZUS Loss Estimations for California Scenario Earthquakes." Prepared by the California Geological Survey Department of Conservation for the California Emergency Management Agency, California.

Chang, C., Connor, K., Lai, T., Lee, L., and Davidson, J. (2005). "Predictors of Posttraumatic Outcomes Following the 1999 Taiwan Earthquake." *The Journal of Nervous and Mental Disease,* 193(1): 40-46.

Chou, Y., Huang, N., Lee, C., Tsai, S., Chen, L. and Chang, H. (2004). "Who Is at Risk of Death in an Earthquake?" *American Journal of Epidemiology*, 160(7): 688-695.

CIA (2011). "Appendix B. International Organizations and Groups. World Factbook." Central Intelligence Agency. .cia.gov/library/publications/the-world-factbook/appendix/appendix-b.html#. Retrieved on December 1, 2014.

Comfort, L.K. "Risk and Resilience: Interorganizational Learning Following the Northridge Earthquake of January 17, 1994." *Journal of Contingencies and Crisis Management*, 1994. Vol. 2(3): pgs. 174-188.

Cutter, S., Barnes, L., Berry, M., Burton, C., Evans, E., Tate, E., and Webb, J. (2008). "A place-based model for understanding community resilience to natural disasters." *Global Environmental Change*, vol. 18, pp. 598-606.

Cutter, S.L. and Finch, C., (2008). "Temporal and spatial changes in social vulnerability to natural hazards." *Proceedings of the National Academy of Sciences of the United States of America*, vol. 105, no. 7, pp. 2301 – 2306.

Cutter, S.L., Boruff, B.J., and Shirley, W.L., (2003). "Social Vulnerability to Environmental Hazards." *Social Science Quarterly*, 84(2), pp. 242 - 260.

Cutter, S.L., (1996). "Vulnerability to environmental hazards." *Progress in Human Geography*, vol. 20, no. 4, pp. 529 – 539.

Davidson, R., Zhao, H., and Kumar, V. (2003). "Quantitative Model to Forecast Changes in Hurricane Vulnerability of Regional Building Inventory." *Journal of Infrastructure Systems*, bol. 9, no. 2, pp. 55-63.

Davidson, R.A., (1997). "An Urban Earthquake Disaster Risk Index." The John A. Blume Earthquake Engineering Center, Stanford University, report no. 121, Blume Center, Stanford, California.

Deb, K., (2008). Multi-Objective Optimization using Evolutionary Algorithms, Chichester, United Kingdom: John Wiley and Sons, LTD, 2008. Print.

Dell'Osso, L., Carmassi, C., Stratta, P., Massimetti, G., Akiskal, K., Akiskal, H., Maremmani, I., Rossi, A., (2013). "Gender differences in the relationship between maladaptive behaviors and post-traumatic stress disorder. A study on 900 L'Aquila 2009 earthquake survivors." *Frontiers in Psychiatry*, 3, pp. 111 - 120.

Dell'Osso, L., Carmassi, C., Massimetti, G., Daneluzzo, E., Di Tommaso, S., and Rossi, A., (2011). "Full and partial PTSD among young adult survivors 10 months after the L'Aquila 2009 earthquake: Gender differences." *Journal of Affective Disorders,* 131, pp. 79-83.

DHS (2003). HAZUS-MH MRI Technical Manual, Department of Homeland Security Emergency Preparedness and Response Directorate, FEMA Mitigation Division, Washington, D.C.

Diebold, J., Moore, K., Hale, T., Mochizuki, G. (2008). "SEAOC Blue Book: Seismic Design Recommendations 1959-2008." *The World Conference on Earthquake Engineering*, Beijing, China.

Dodo, A., Xu, N., Davidson, R., and Nozick, L. (2004). "Optimizing the Selection of Regional Earthquake Mitigation Strategies." *World Conference on Earthquake Engineering*, Vancouver, B.C., Canada. August 1-6, 2004.

Eksi, A., Braun, K., Ertem-Vehid, H., Peykerli, G., Saydam, R., Toparlak, D., and Alyanak, B. (2007). "Risk factors for the development of PTSD and depression among child and adolescent victims following a 7.4 magnitude earthquake." *International Journal of Psychiatry in Clinical Practice*, 11(3): 190-199.

Erdik, M., Sesetyan, K., Demircioglu, M.B., Hancilar, U., and Zulfikar, C. (2011). "Rapid earthquake loss assessment after damaging earthquakes." *Soil Dynamics and Earthquake Engineering*, vol. 31, pp. 247-266.

FEMA (2012a). "Seismic Evaluation and Retrofit of Multi-Unit Wood-Frame Buildings With Weak First Stories, FEMA P-807." prepared by the Applied Technology Council (ATC 71-1 Project) for the Federal Emergency Management Agency, Washington, D.C.

FEMA (2012b). Seismic Performance Assessment of Buildings, FEMA P-58-1. Applied Technology Council (ATC) Project 58-1, Redwood City, CA.

FEMA (2009). "Quantification of Building Seismic Performance Factors". FEMA P695. Washington D.C.

FEMA (2006). "Next-Generation Performance-Based Seismic Design Guidelines, FEMA 445." prepared by the Applied Technology Council (ATC 58 Project) for the Federal Emergency Management Agency, Washington, D.C.

FEMA (2004). Primer for Design Professionals Communicating with Owners and Managers of New Buildings on Earthquake Risk, FEMA 389. Federal Emergency Management Agency, Washington, D.C.

FEMA (2000). "Action Plan for Performance Based Seismic Design, FEMA 349." Prepared by the Earthquake Engineering Research Institute (contract number EMW-92-K-3955, Task 13) for the Federal Emergency Management Agency, Washington, D.C.

FEMA (1996). "Performance Based Seismic Design of Buildings, FEMA 283." Prepared by the Earthquake Engineering Research Center at the University of California at Berkeley (contract number EMW-93-K-4253) for the Federal Emergency Management Agency, Washington, D.C.

Filiatrault, A. and Folz, B., (2002). "Performance-Based Seismic Design of Wood Framed Buildings." *Journal of Structural Engineering*, 128(1), pp. 39–47

FHWA (Federal Highway Administration) (1994). *Technical Advisory: Motor Vehicle Accident Costs*, *Technical Advisory* #750.2, U.S. Department of Transportation, Washington, D.C.

Flores, E., Carnero, A., and Bayer, A. (2014). "Social capital and chronic post-traumatic stress disorder among survivors of the 2007 earthquake in Pisco, Peru." *Social Science and Medicine*, 101: 9-17.

Folz and Filiatrault (2001). "Cyclic Analysis of Wood Shear Walls." *J. Struct. Eng.*, 127(4), 4330441.

Fothergill, A., and Peek, L., (2004). "Poverty and Disasters in the United States: A Review of Recent Sociological Findings." *Natural Hazards*, 32, pp. 89 - 110.

Galea, S., Vlahov, D., Tracy, M., Hoover, D.R., Resnick, H., Kilpatrick, D., (2004). "Hispanic Ethnicity and Post-Traumatic Stress Disorder after a Disaster: Evidence from a General Population Survey after September 11, 2001." *Ann Epidemol*, 14, pp. 520 – 531.

Gall, M., Bordern, K.A., Cutter, S.L., (2009). "When do losses count? Six Fallacies of Natural Hazards Loss Data." *American Meteorological Society*, 90, pp. 799-809.

Gershfeld, M., C. Chadwell, E. Jennings, E. Ziaei, W. Pang, X. Shao, J. van de Lindt, (2014). "Seismic Performance of Distributed Knee-Brace (DKB) System as a Retrofit for Weak-Story Wood-Frame Buildings." *World Conference on Timber Engineering*, Quebec City, Canada, August 10-14, 2014.

GFDRR (2014). "Understanding Risk – Review of Open Source and Open Access Software Packages Available to Quantify Risk from Natural Hazards." Global Facility for Disaster Reduction and Recovery. The World Bank. Published July 1, 2014.

Goetzel, R., Long, S., Ozminkowski, R., Hawkins, K., Wang, S., and Lynch, W. (2004). "Health, Absence, Disability, and Presenteeism Cost Estimates of Certain Physical and Mental Health Conditions Affecting U.S. Employers." *Journal of Occupational and Environmental Medicine*, vol. 46, no. 4, pp. 398-412.

Goldberg, D., (1989). Genetic Algorithms in Search Optimization and Machine Learning, Indiana: Addison Wiley Longman, Inc. 1989. Print.

Han, Y., Davidson, R., Black, G., and Pei, S. (2013). "A regional perspective on defining seismic performance objectives for woodframe buildings." *Structural Safety*, vol. 43, pp. 50-59.

Hsu, C., Chong, M., Yang, P., and Yen, C. (2002). "Posttraumatic Stress Disorder Among Adolescent Earthquake Victims in Taiwan." *J. Am. Aca. Child Adolesc. Psychiatry,* 41(7): 875-881.

IBC (2006). *International Building Code,* International Code Council, Falls Church, VA, 22041.

Jennings, E., J.W. van de Lindt, E. Ziaei, P. Bahmani, S. Park, X. Shao, W. Pang, D. Rammer, G. Mochizuki, and M. Gershfeld, (2014a). "Full-Scale Experimental Verification of Soft-Story-Only Retrofits of Woodframe Buildings with Hybrid Testing." *Journal of Earthquake Engineering*, DOI 10.1080/13632469.2014.975896.

Jennings, E., Ziaei, W. Pang, J.W. van de Lindt, X. Shao, P. Bahmani, (2014b). "Full-Scale Experimental Investigation of Second-Story Collapse Behavior in an Over-Retrofitted First Story of a Woodframe Building." *Journal of Performance of Constructed Facilities*, DOI: 10.1061/(ASCE)CF.1943-5509.0000736.

Jennings, E., van de Lindt, J.W., Ziaei, E., Mochizuki, G., Pang, W., and Shao, X. (2014c). "Retrofit of a Soft-Story Woodframe Buildings using SMA Devices with Full-Scale Hybrid Test Verification," *Engineering Structures*, 80: 469-485.

Jennings, P.C. "Enduring Lessons and Opportunities Lost from the San Fernando Earthquake of February 9, 1971." *Earthquake Spectra*, 1997. Vol. 13(1): pgs. 25 – 44.

Jia, Z., Tian, W., Liu, W., Cao, Y., Yan, J., and Shun, Z. (2010a). "Are the elderly more vulnerable to psychological impact of natural disaster? A population-based survey of adult survivors of the 2008 Sichuan earthquake." *BMC Public Health*, 10:172-183.

Jia, Z., Tian, W., He, X., Liu, W., Jin, C., and Hansheng, D. (2010b). "Mental health and quality of life survey among child survivors of the 2008 Sichuan earthquake." *Qual. Life Res.*, 19: 1381-1391.

Jin, Y., Xu, J., Liu, H., and Liu, D. (2014). "Posttraumatic Stress Disorder and Posttraumatic Growth Among Adult Survivors of Wenchuan Earthquake After 1 Year: Prevalence and Correlates." *Archives of Psychiatric Nursing*, 28, pp. 67-73.

Kessler, R. and Greenberg, P. (2002). "Chapter 67: The Economic Burden of Anxiety and Stress Disorders." *Neuropsychopharmacology: The Fifth Generation of Progress*. Ch. 67, pp. 981-992.

Kessler, R. and Frank, R. (1997). "The impact of psychiatric disorders on work loss days." *Psychological Medicine*, vol. 27, pp. 861-873.

Kilic, C., and Ulusol, M., (2003). "Psychological effects of the November 1999 earthquake in Turkey: an epidemiological study." *Acta Psychiatr Scand*, 108, pp. 232 - 238.

Kun, P., Tong, X., Liu, Y., Pei, X., and Luo, H., (2013). "What are the determinants of post-traumatic stress disorder: age, gender, ethnicity or other? Evidence from 2008 Wenchuan earthquake." *Public Health*, 127, pp. 644 – 652.

Kuo, H.W., Wu, S.J., Ma, T.C., Chiu, M.C., Chou, S.Y., (2007). "Posttraumatic symptoms were worst among quake victims with injuries following the Chi-chi quake in Taiwan." *Journal of Psychosomatic Research*, 62, pp. 495 – 500.

Line, P. (2006). "Benchmarking Seismic Base Shear to Historical Practice." *Wood Design Focus*, 16(1). American Wood Council/American Forest and Paper Association.

Liu, X., Ma, X., Hu, X., Qiu, C., Wang, Y., Wang, Q., Zhang, W., Zhang, J., and Li, T. (2012). "A Risk Score for Predicting Post-traumatic Stress Disorder in Adults in Chinese Earthquake Area." *The Journal of International Medical Research*, 40: 2191-2198.

Liu, Z., Yang, Y., Ye, Y., Zeng, Z., Xiang, Y., and Yuan, P. (2010). "One-year follow-up study of post-traumatic stress disorder among adolescents following the Wen-Chuan earthquake in China." *BioScience Trends*, 4(3): 96-102.

Ma, X., Liu, X., Hu, X., Qiu, C., Wang, Y., Huang, Y., Wang, Q., Zhang, W., and Li, T. (2011). "Risk indicators for post-traumatic stress disorder in adolescents exposed to the 5.12 Wenchuan earthquake in China." *Psychiatry Research*, 189: 385-391.

Mahue-Giangreco, M., Mack, W., Seligson, H., Bourque, L.B., (2001). "Risk Factors Associated with Moderate and Serious Injuries Attributable to the 1994 Northridge Earthquake, Los Angeles, California." *Ann Epidemiol*, 11, pp. 347 - 357.

May (2006). "Societal Implications of Performance-Based Earthquake Engineering." PEER Report 2006/12. Center for American Politics and Public Policy, University of Washington. Pacific Earthquake Engineering Research Center, University of California, Berkeley.

McAllister, T. (2013). "Developing Guidelines and Standards for Disaster Resilience of the Built Environment: A Research Needs Assessment." NIST Technical Note 1795.

McIntosh, R.D., and Pezeshk, S. (1997). "Comparison of Recent U.S. Seismic Codes." *Journal of Structural Engineering*, 123(8), 993-1000.

McMillen, J., North, c., and Smith, E. (2000). "What Parts of PTSD Are Normal: Intrusion, Avoidance, or Arousal? Data from the Northridge, California, earthquake." *Journal of Traumatic Stress*, 13(1): 57-73.

Montazeri, A., Baradaran, H., Omidvari, S., Azin, S., Ebadi, M., Garmaroudi, G., Harirchi, A., and Shariati, M. (2005). "Psychological distress among Bam earthquake survivors in Iran: a population-based study." *BMC Public Health*, 5(4).

Norris, F.H., Stevens, S.P., Pfefferbaum, B., Wyche, K.F., and Pfefferbaum, R.L., (2008). "Community Resilience as a Metaphor, Theory, Set of Capacities, and Strategy for Disaster Readiness." *American Journal of Community Psychology*, vol. 41, pp. 127-150.

Norris, F., Friedman, M., Watson, P., Byrne, C., Diaz, E., and Kaniasty, K. (2002a). "60,000 Disaster Victims Speak: Part I. An Empirical Review of the Empirical Literature, 1981-2001." *Psychiatry*, vol. 65, no. 3, pp. 207-239.

Norris, F., Friedman, M., and Watson, P. (2002b). "60,000 Disaster Victims Speak: Part II. Summary and Implications of the Disaster Mental Health Research." *Psychiatry*, vol. 65, no. 3, pp. 240-260.

Pang, W., Ziaei, E., and Filiatrault, A. (2012). "A 3D Model for Collapse Analysis of Soft-story Light-frame Wood Buildings." *World Conference on Timber Engineering*, Auckland, New Zealand.

Pang, W. and Rosowsky, D. (2010). "Direct Displacement Procedure for Performance-Based Seismic Design of Multistory Woodframe Structures." Technical Report MCEER-10-0001.

Pang, W., Rosowsky, D., Pei, S., and van de Lindt, J.W., (2010). "Simplified Direct Displacement Design of Six-Story Woodframe Building and Pretest Seismic Performance Assessment." *Journal of Structural Engineering*, 136(7), pp. 813–825.

Pang, W., Rosowsky, D., Pei, S., and van de Lindt, J. (2007). "Evolutionary parameter hysteretic model for wood shearwalls." *J. Struct. Eng.*, 133(8), 1118-1129.

Park, S., van de Lindt, J.W., Cox, D., Gupta, R. (2013). "Concept of Community Fragilities for Tsunami Coastal Inundation Studies." *Natural Hazards Review*, 14(4): 220-228.

Park, S. and van de Lindt, J. (2009). "Formulation of Seismic Fragilities for a Wood-Frame Building Based on Visually Determined Damage Indexes." *Journal of Performance of Constructed Facilities*, 23(5): 346-352.

Peek, L. and Stough, L.M., (2010). "Children with Disabilities in the Context of Disaster: A Social Vulnerability Perspective." *Child Development*, 81(4), pp. 1260 – 1270.

Peek, L., (2008). "Children and Disasters: Understanding Vulnerability, Developing Capacities, and Promoting Resilience – An Introduction." *Children, Youth and Environments*, 18(1): 1-29.

Peek-Asa, C., Ramirez, M., Shoaf, K., Seligson, H., and Kraus, J. (2000). "GIS Mapping of Earthquake-Related Deaths and Hospital Admissions from the 1994 Northridge, California, Earthquake." *Ann Epidemiol*, 10: 5-13.

Peek-Asa, C., Kraus, J.F., Bourque, L.B., Vimalachandra, D., Yu, J., Abrams, J., (1998). "Fatal and hospitalized injuries resulting from the 1994 Northridge earthquake." *International Journal of Epidemiology*, 27: 459-465.

Pei, S. and J. van de Lindt, (2010). "User's Manual for SAPWood for Windows Seismic Analysis Package for Woodframe Structures." NEEShub (nees.org).

Pei, S. (2007). "Loss Analysis and Loss Based Seismic Design for Woodframe Structures." Dissertation. Department of Civil and Environmental Engineering. Colorado State University.

Perilla, J., Norris, F.H., and Lavizzo, E.A., (2002). "Ethnicity, culture, and disaster response: Identifying and explaining ethnic differences in PTSD six months after Hurricane Andrews." *Journal of Social and Clinical Psychology*, 21(1), pp. 20-45.

Porter, K., and Cobeen, K., (2009). "Loss Estimates for Large Soft-Story Woodframe Buildings in San Francisco." Proc. ATC-SEI Conference on Improving the Seismic Performance of Existing Buildings and Other Structures, Dec. 9-11, 2009, San Francisco, CA. Applied Technology Council and Structural Engineering Institute of ASCE.

Porter, K., Shoaf, K., and Seligson, H. (2006). "Value of Injuries in the Northridge Earthquake." Earthquake Spectra, Technical Note. vol. 22, no. 2 pp. 555-563.

Porter, K.A. (2003). "An overview of PEER's performance-based earthquake engineering methodology." Proceedings of Ninth International Conference on Applications of Statistics and Probability in Civil Engineering. San Francisco, California.

Porter, K.A., and Kiremidjian, A.S. (2001). Assembly-based vulnerability of buildings and its uses in seismic performance evaluation and risk management decision-making, Technical Report No. 309. Stanford, CA: John A. Blume Earthquake Engineering Center, Stanford University.

Priebe, S., Grappasonni, I., Mari, M., Dewey, M., Petrelli, F., and Costa, A., (2009). "Posttraumatic stress disorder six months after an earthquake." *Soc Psychiatry Psychiatr Epidemol,* 44, pp. 393-397.

Priestley, M.J.N. (1998). "Displacement-Based Approaches to Rational Limit States Design of New Structures." Leynot Address, Proc. *11 European Conf. Earthquake Engineering,* Paris.

Ramirez, C., and Miranda, E. (2009). "Building-Specific Loss Estimation Methods and Tools for Simplified Performance-Based Earthquake Engineering." The John A. Blume Earthquake Engineering Center, Stanford University, report no. 171, Blume Center, Stanford, California.

Ramirez, M., Kano, M., Bourque, L.B., Shoaf, K.I., (2005). "Child and Household Factors Associated with Fatal and Non-Fatal Pediatric Injury During the 1999 Kocaeli Earthquake." *International Journal of Mass Emergencies and Disasters*, 23(2): 129-147.

Rashed, T. and Weeks, J. (2003). "Assessing the vulnerability to earthquake hazards through spatial multicriteria analysis of urban areas." *International Journal of Geographical Information Science,* vol. 17, no. 6, pp. 547-576.

Reitherman, R., and Cobeen, K. (2003). "Design Documentation of Woodframe Project Index Buildings", CUREE Publication No. 29. The CUREE-Caltech Woodframe Project. Funded by the Federal Emergency Management Agency.

Ritchie, A.M. "Managing Infrastructure Problems That Arise From Earthquakes". *Materials Performance*. April 2003, pgs. 2-5.

Rojas, H., Peseshk, S., Foley, C. (2008). "Automated Risk-Based Seismic Design Method for Optimal Structural and Non-Structural System Performance." *Analysis and Computation Specialty Conference, Structures Congress2008.*

RSMeans Online (2014). "Construction Cost Estimator." Reed Construction Data Inc. rsmeans.reedconstructiondata.com.

Samant, L., Porter, K., Cobeen, K., Tobin, L., Kornfield, L., Seligson, H., Alejandrino, S., and Kidd, J., (2009). "Mitigating San Francisco's Soft-Story Building Problem." *Proc. ATC-SEI Conference on Improving the Seismic Performance of Existing Buildings and Other Structures, Dec. 9-11, 2009, San Francisco, CA.* Applied Technology Council and Structural Engineering Institute of ASCE.

Schierle, G. G. (2003). "Northridge Earthquake Field Investigations: Statistical Analysis of Woodframe Damage." CUREE Publication No. W-09. The CUREE-Caltech Woodframe Project Funded by the Federal Emergency Management Agency.

Schmidtlein, M.C., Deutsch, R.C., Piegorsch, W.W., and Cutter, S.L., (2008). "A Sensitivity Analysis of the Social Vulnerability Index." *Risk Analysis,* 28(4), pp. 1099-1113.

Seismology (1959). Recommended Lateral Force Requirements and Commentary, Seismology Committee, Structural Engineers Association of California. Sacramento, California.

Siegel, J. (2000). "Emotional Injury and the Northridge, California Earthquake." *Natural Hazards Review*, 1: 204-211.

Sharan, P., Chaudhard, G., Kavathekar, S., and Saxena, S. (1996). "Preliminary Report of Psychiatric Disorders in Survivors of a Severe Earthquake." *American Journal of Psychiatry*, 153(4): 556-558.

Shao, W., van de Lindt, J.W., Bahmani, P., Pang, W., Ziaei, E., Symans, M.D., Tian, J., and Dao, T. (2014). "Real Time Hybrid Simulation of a Multi-Story Wood Shear Wall with First-Story Experimental Substructure Incorporating a Rate-Dependent Seismic Energy Dissipating Device." *Special Issue on Real Time Hybrid Testing in Smart Structures and Systems, In Press*.

Shoaf, K., Nguyen, L., Sareen, H., and Bourque, L. (1998). "Injured as a Result of California Earthquakes in the Past Decade." *Disasters*, 22(3): 218-235.

Spence, R., So, E., and Scawthorn, C. (2011). "Human Casualties in Earthquakes Progress in Modelling and Mitigation." *Advanced in Natural and Technological Hazards Research*, vol. 29. DOI 10.1007/978-90-481-9455-1.

Sudaryo, M., Besral, Endarti, A., Rivany, R., Phalkey, R., Marx, M., and Guha-Sapir, D. (2012). "Injury, disability and quality of life after the 2009 earthquake in Padong, Indonesia: a prospective cohort study of adult survivors." *Global Health Action*, 5.

Tanaka, H., Kuwagata, Y., Takaoka, M., Morimoto, F., Mizushima, Y., Yamamura, H., and Shimazu, T. (1997). "Morbidity and Mortality of Hospitalized Patients After the 1995 Hanshin-Awaji Earthquake." *International Notes.* Presented at the *Society for Academic Emergency Medicine* annual meeting, May 1996, Denver, CO.

Tian, J. and Symans, M. (2012) High-Performance Seismic Retrofit of Soft-Story Wood-Framed Buildings Using Energy Dissipation Systems. Structures Congress 2012: pp. 1790-1801.

Trayer, G. (1956). "The Rigidity and Strength of Frame Walls." *FPL Report No. 896*, Forest Products Laboratory, Madison, WI.

UBC (1988). "Uniform Building Code." International Conference of Building Officials, Whittier, California, 90601.

UBC (1970). "Uniform Building Code." International Conference of Building Officials, Whittier, California, 90601.

U.S. Census Bureau. (2012, August 28). "State and County Quickfact." Retrieved November 2014, from http://quickfacts.census.gov.

Usami, M. et al. (2012). “Relationships between Traumatic Symptoms and Environmental Damage Conditions among Children 8 Months after the 2011 Japan Earthquake and Tsunami.” *PLOS ONE*, 7(11).

Van de Lindt, J.W., Symans, M.D., Pang, W., Shao, X., and Gershfeld, M. (2012) “The NEES-soft project: Seismic risk reduction for soft-story woodframe buildings,” World Conference on Earthquake Engineering, International Association for Earthquake Engineering (IAEE), Tokyo.

Van de Lindt, J., and Gupta, R. (2006). “Damage and Damage Prediction for Wood Shearwalls Subjected to Simulated Earthquake Loads.” *Journal of Performance of Constructed Facilities*, 20(2): 176-184.

Van de Lindt, J. (2005). “Damage-Based Seismic Reliability Concept for Woodframe Structures.” *Journal of Structural Engineering*, 131(4): 668-675.

Van de Lindt, (2004). “Evolution of Wood Shear Wall Testing, Modeling, and Reliability Analysis: Bibliography.” *Practice Periodical on Structural Design and Construction*, vol. 9, no. 1, pp. 44 – 53.

Van de Lindt, J. and Niedzwecki, J. (2000). “A Time Variant Approach to Performance-Based Engineering.” *Structures Congress*, May 8-10, Philadelphia, PA.

Xu., J. and He, Y., (2012). “Psychological health and coping strategy among survivors in the year following the 2008 Wenchuan earthquake.” *Psychiatry and Clinical Neurosciences*, 66, pp. 210 – 219.

Zahran, S., Peek, L., Snodgrass, J.G., Weiler, S., and Hempel, L., (2011). “Economics of Disaster Risk, Social Vulnerability, and Mental Health Resilience.” *Risk Analysis*, vol. 31, no. 7, pp. 1107 – 1119.

Zahran, S., Peek, L., and Brody, S.D., (2008). “Youth Mortality by Forces of Nature.” *Children, Youth and Environments*, 18(1), pp. 371-388.

Appendix A

1. Example of fitting a lognormal distribution using distribution parameters.

The lognormal probability density function (pdf) may be expressed as

$$f_x(x;\mu,\sigma) = \frac{1}{x\sigma\sqrt{2\pi}} e^{-\frac{(\ln x-\mu)^2}{2\sigma^2}}, x > 0 \qquad \textit{Eq. A - 1}$$

The lognormal cumulative distribution function (CDF) may be expressed as

$$F_x(x;\mu,\sigma) = \frac{1}{2}\left[1 + erf\left(\frac{\ln x-\mu}{\sigma\sqrt{2}}\right)\right] = \Phi\left(\frac{\ln x-\mu}{\sigma}\right) \qquad \textit{Eq. A - 2}$$

where μ and σ are the mean and standard deviation, respectively, of the associated normal distribution. They represent the two distribution parameters where μ may be called the location parameters and σ the scale parameter.

In MATLab, there are three commands associated with fitting the lognormal distribution, *lognfit*, *lognpdf*, and *logncdf*. The lognormal distribution's pdf and CDF may be developed by using the parametric values provided in the tables below as follows.

$$\left[Y_{pdf}\right] = lognpdf(X,\mu,\sigma) \qquad \textit{Eq. A - 3}$$

$$[Y_{CDF}] = logncdf(X,\mu,\sigma) \qquad \textit{Eq. A - 4}$$

where *X* is the rank-ordered vector of the random variable (e.g., peak inter-story drift, number of persons diagnosed with PTSD, etc.), is the fitted probability vector of the pdf (i.e. the probability density function vector), and is the fitted probability vector of the CDF (i.e. the cumulative distribution function vector).

2. Unit Cost of New Construction (cost per square foot)

Floor Plan	*Design Procedure*											
	1959 Blue Book		*1978 NEHRP*		*ASCE7-05*		*SDDD-LS*		*SDDD-IO*		*FEMA P-807*	
	μ	σ	μ	σ	μ	σ	μ	σ	μ	σ	μ	σ
1	150	⅓μ	150	⅓μ	150	⅓μ	150	⅓μ	150	⅓μ	-	-
2	160	⅓μ	160	⅓μ	160	⅓μ	160	⅓μ	160	⅓μ	-	-
3	162	⅓μ	162	⅓μ	162	⅓μ	162	⅓μ	162	⅓μ	-	-
4	167	⅓μ	167	⅓μ	167	⅓μ	167	⅓μ	167	⅓μ	167	⅓μ
5	150	⅓μ	150	⅓μ	150	⅓μ	150	⅓μ	150	⅓μ	-	-
6	160	⅓μ	160	⅓μ	160	⅓μ	160	⅓μ	160	⅓μ	-	-
7	152	⅓μ	152	⅓μ	152	⅓μ	152	⅓μ	152	⅓μ	152	⅓μ

3. Unit Time of New Construction (time (month))

Floor Plan	*Design Procedure*											
	1959 Blue Book		*1978 NEHRP*		*ASCE7-05*		*SDDD-LS*		*SDDD-IO*		*FEMA P-807*	
	μ	σ	μ	σ	μ	σ	μ	σ	μ	σ	μ	σ
1	7	⅓μ	7	⅓μ	7	⅓μ	7	⅓μ	7	⅓μ	-	-
2	7	⅓μ	7	⅓μ	7	⅓μ	7	⅓μ	7	⅓μ	-	-
3	12	⅓μ	12	⅓μ	12	⅓μ	12	⅓μ	12	⅓μ	-	-
4	12	⅓μ	12	⅓μ	12	⅓μ	12	⅓μ	12	⅓μ	12	⅓μ
5	7	⅓μ	7	⅓μ	7	⅓μ	7	⅓μ	7	⅓μ	-	-
6	7	⅓μ	7	⅓μ	7	⅓μ	7	⅓μ	7	⅓μ	-	-
7	12	⅓μ	12	⅓μ	12	⅓μ	12	⅓μ	12	⅓μ	12	⅓μ

4. Cost of Retrofit (cost per square foot)

Floor Plan	*Design Procedure*							
	ASCE7-05		*SDDD-LS*		*SDDD-IO*		*FEMA P-807*	
	μ	σ	μ	σ	μ	σ	μ	σ
1	9	⅓μ	28	⅓μ	34	⅓μ	-	-
2	9	⅓μ	28	⅓μ	34	⅓μ	-	-
3	4.5	⅓μ	14	⅓μ	17	⅓μ	-	-
4	20.7	⅓μ	8.4	⅓μ	10.2	⅓μ	2.7	⅓μ
5	9	⅓μ	28	⅓μ	34	⅓μ	-	-
6	9	⅓μ	28	⅓μ	34	⅓μ	-	-
7	2.25	⅓μ	7	⅓μ	8.5	⅓μ	2.25	⅓μ

5. Repair Costs (cost per unit ($/unit))

Unit	*Parameters*	*Damage State 1*	*Damage State 2*	*Damage State 3*	*Damage State 4*	*Damage State 5*
Interior Wall (64sf)	μ	0.0	453	453	1109	-
	σ	0.0	14	14	32	-
Exterior Wall (64sf)	μ	0.0	445	445	1328	-
	σ	0.0	13	13	37	-
Ceiling (64sf)	μ	0.0	245	245	409	-
	σ	0.0	8	8	13	-
Window (each)	μ	0.0	-	-	239	-
	σ	0.0	-	-	8	-
Water Heater (each)	μ	0.0	-	-	752	-
	σ	0.0	-	-	20	-

6. Repair Times (time per unit (hour/unit))

Unit	*Parameters*	*Damage State 1*	*Damage State 2*	*Damage State 3*	*Damage State 4*	*Damage State 5*
Interior Wall (64sf)	μ	0.0	8	8	18.5	-
	σ	0.0	0.5	0.5	0.5	-
Exterior Wall (64sf)	μ	0.0	9	9	22.5	-
	σ	0.0	0.75	0.75	0.75	-
Ceiling (64sf)	μ	0.0	5	5	7.5	-
	σ	0.0	0.5	0.5	0.5	-
Window (each)	μ	0.0	-	-	3	-
	σ	0.0	-	-	0.25	-
Water Heater (each)	μ	0.0	-	-	5.25	-
	σ	0.0	-	-	0.375	-

7. Number of Units per Floor Plan

Unit	*Floor Plan*						
	1	*2*	*3*	*4*	*5*	*6*	*7*
Interior Wall (64sf)	12	26	62	115	14	16	201
Exterior Wall (64sf)	μ	28	106	115	15	23	98
Ceiling (64sf)	σ	44	56	214	22	23	316
Window (each)	15	28	51	58	6	12	47
Water Heater (each)	1	1	3	10	1	1	4

8. Morbidity Rates (% of population)

Morbidity Rates	*Parameters*	*Damage State 1*	*Damage State 2*	*Damage State 3*	*Damage State 4*	*Damage State 5*
Injury Severity Level 1	μ	0.0	0.005	0.025	0.1	0.3
	σ	0.0	⅓μ	⅓μ	⅓μ	⅓μ
Injury Severity Level 2	μ	0.0	0.0005	0.00225	0.01	0.4
	σ	0.0	⅓μ	⅓μ	⅓μ	⅓μ
Injury Severity Level 3	μ	0.0	0.000005	0.0003	0.001	0.2
	σ	0.0	⅓μ	⅓μ	⅓μ	⅓μ
Injury Severity Level 4	μ	0.0	0.0000005	0.0000003	0.00001	0.03
	σ	0.0	⅓μ	⅓μ	⅓μ	⅓μ
Injury Severity Level 5	μ	0.0	0.0000005	0.0000003	0.00001	0.05
	σ	0.0	⅓μ	⅓μ	⅓μ	⅓μ
PTSD	μ	0.0	0.000005	0.0003	0.001	0.2
	σ	0.0	⅓μ	⅓μ	⅓μ	⅓μ

Appendix B

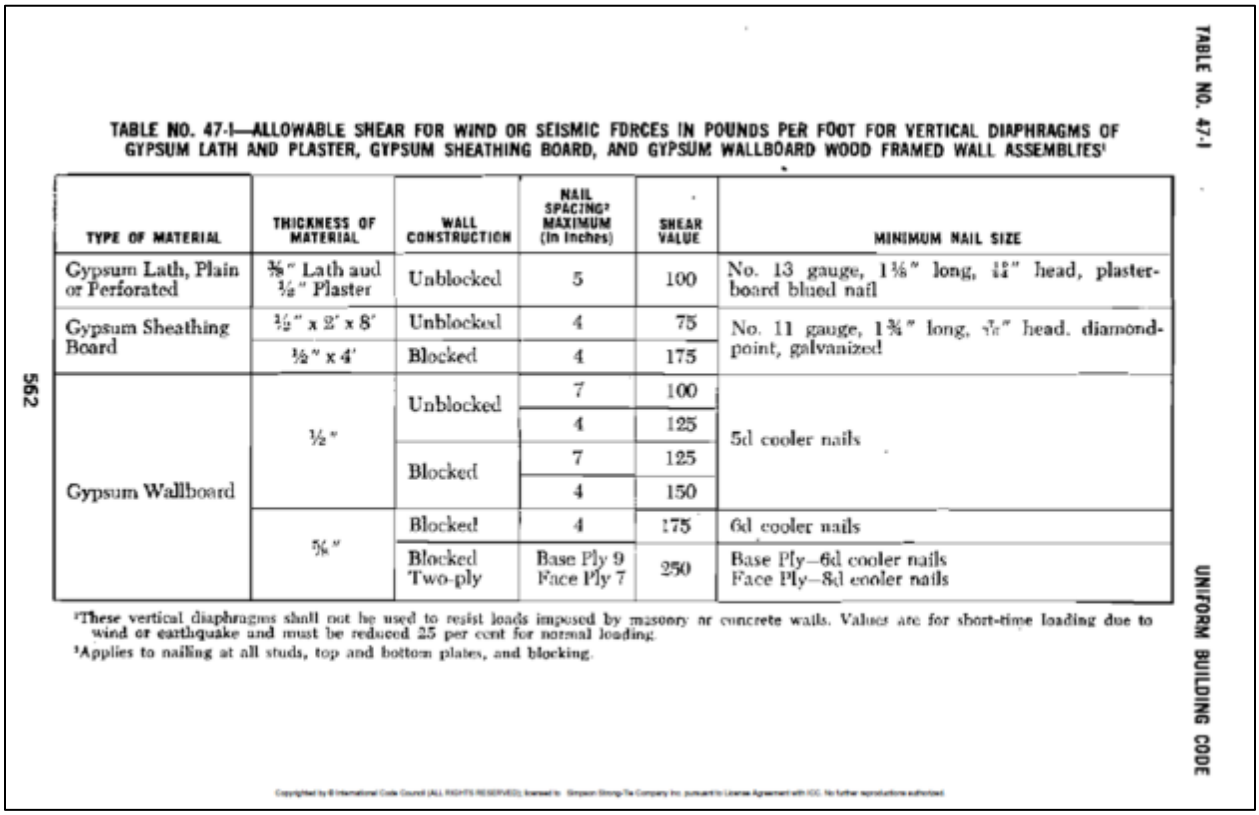

TABLE NO. 47-I

TABLE NO. 47-I—ALLOWABLE SHEAR FOR WIND OR SEISMIC FORCES IN POUNDS PER FOOT FOR VERTICAL DIAPHRAGMS OF GYPSUM LATH AND PLASTER, GYPSUM SHEATHING BOARD, AND GYPSUM WALLBOARD WOOD FRAMED WALL ASSEMBLIES[1]

TYPE OF MATERIAL	THICKNESS OF MATERIAL	WALL CONSTRUCTION	NAIL SPACING[2] MAXIMUM (In Inches)	SHEAR VALUE	MINIMUM NAIL SIZE
Gypsum Lath, Plain or Perforated	⅜" Lath and ½" Plaster	Unblocked	5	100	No. 13 gauge, 1⅛" long, ⅐" head, plasterboard blued nail
Gypsum Sheathing Board	½" x 2' x 8'	Unblocked	4	75	No. 11 gauge, 1¾" long, 7/16" head, diamond-point, galvanized
	½" x 4'	Blocked	4	175	
Gypsum Wallboard	½"	Unblocked	7	100	5d cooler nails
			4	125	
		Blocked	7	125	
			4	150	
	⅝"	Blocked	4	175	6d cooler nails
		Blocked Two-ply	Base Ply 9 Face Ply 7	250	Base Ply—6d cooler nails Face Ply—8d cooler nails

[1]These vertical diaphragms shall not be used to resist loads imposed by masonry or concrete walls. Values are for short-time loading due to wind or earthquake and must be reduced 25 per cent for normal loading.

[2]Applies to nailing at all studs, top and bottom plates, and blocking.

562

UNIFORM BUILDING CODE

Copyrighted by © International Code Council (ALL RIGHTS RESERVED), licensed to Simpson Strong-Tie Company Inc. pursuant to License Agreement with ICC. No further reproductions authorized.

Figure B-1: 1970 UBC Allowable Shear for Gypsum Materials

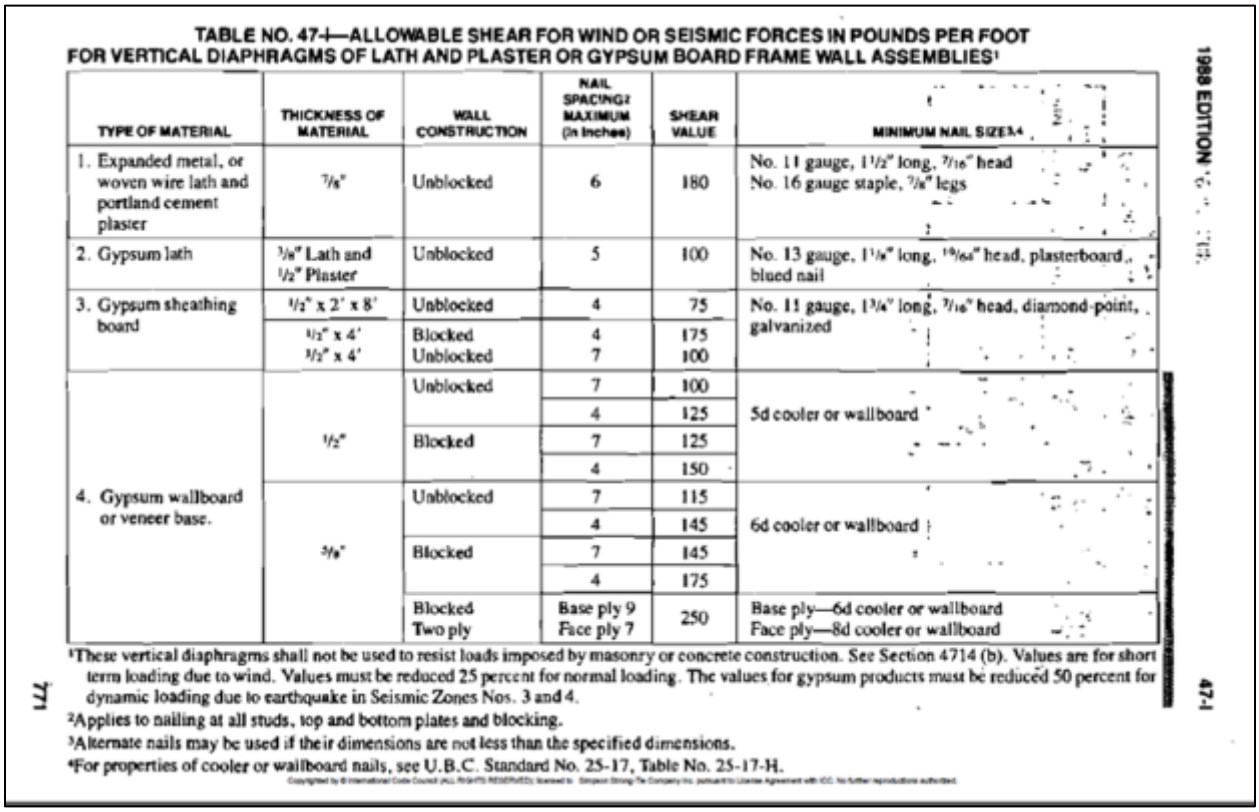

TABLE NO. 47-I—ALLOWABLE SHEAR FOR WIND OR SEISMIC FORCES IN POUNDS PER FOOT FOR VERTICAL DIAPHRAGMS OF LATH AND PLASTER OR GYPSUM BOARD FRAME WALL ASSEMBLIES[1]

TYPE OF MATERIAL	THICKNESS OF MATERIAL	WALL CONSTRUCTION	NAIL SPACING[2] MAXIMUM (In Inches)	SHEAR VALUE	MINIMUM NAIL SIZES[3,4]
1. Expanded metal, or woven wire lath and portland cement plaster	7/8"	Unblocked	6	180	No. 11 gauge, 1 1/2" long, 7/16" head No. 16 gauge staple, 7/8" legs
2. Gypsum lath	3/8" Lath and 1/2" Plaster	Unblocked	5	100	No. 13 gauge, 1 1/8" long, 19/64" head, plasterboard blued nail
3. Gypsum sheathing board	1/2" x 2' x 8'	Unblocked	4	75	No. 11 gauge, 1 3/4" long, 7/16" head, diamond-point, galvanized
	1/2" x 4' 1/2" x 4'	Blocked Unblocked	4 7	175 100	
4. Gypsum wallboard or veneer base.	1/2"	Unblocked	7	100	5d cooler or wallboard
			4	125	
		Blocked	7	125	
			4	150	
	5/8"	Unblocked	7	115	6d cooler or wallboard
			4	145	
		Blocked	7	145	
			4	175	
		Blocked Two ply	Base ply 9 Face ply 7	250	Base ply—6d cooler or wallboard Face ply—8d cooler or wallboard

[1]These vertical diaphragms shall not be used to resist loads imposed by masonry or concrete construction. See Section 4714 (b). Values are for short term loading due to wind. Values must be reduced 25 percent for normal loading. The values for gypsum products must be reduced 50 percent for dynamic loading due to earthquake in Seismic Zones Nos. 3 and 4.

[2]Applies to nailing at all studs, top and bottom plates and blocking.

[3]Alternate nails may be used if their dimensions are not less than the specified dimensions.

[4]For properties of cooler or wallboard nails, see U.B.C. Standard No. 25-17, Table No. 25-17-H.

Copyrighted by © International Code Council (ALL RIGHTS RESERVED) licensed to Simpson Strong-Tie Company Inc. pursuant to License Agreement with ICC. No further reproductions authorized.

Figure B-2: 1988 UBC Allowable Shear for Gypsum Materials

Appendix C

The resulting curves from the multi-record IDA analysis are provided in Figure C-1 through Figure C-37 for the first story of each of the 37 archetypes. For the IDA, the FEMA P-695 suite of 22 bi-axial ground motions were scaled to forty spectral accelerations starting with 0.1g and ending with 4.0g at increments of 0.1g. The peak inter-story drift response, from either principle building direction, were extracted from each scaled ground motion and plotted.

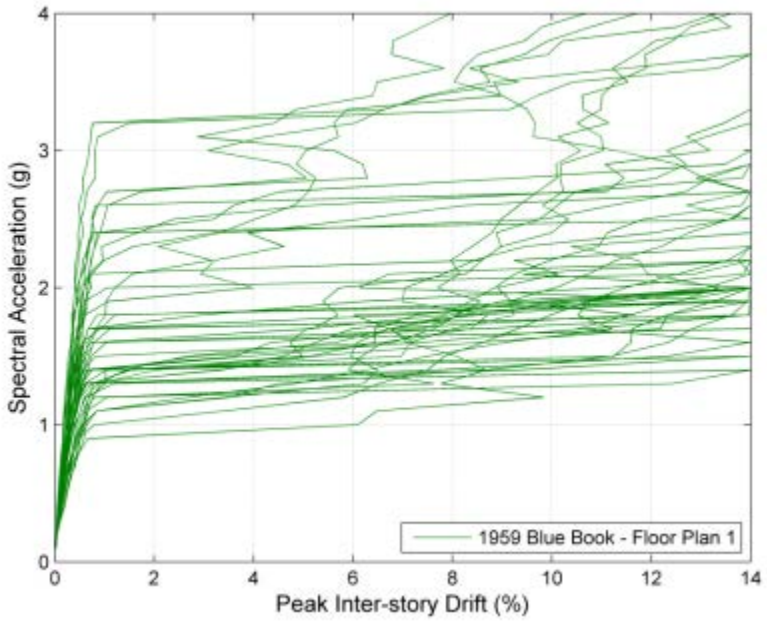

Figure C-1: Multi-Record IDA for Floor Plan 1, 1959 Blue Book Design

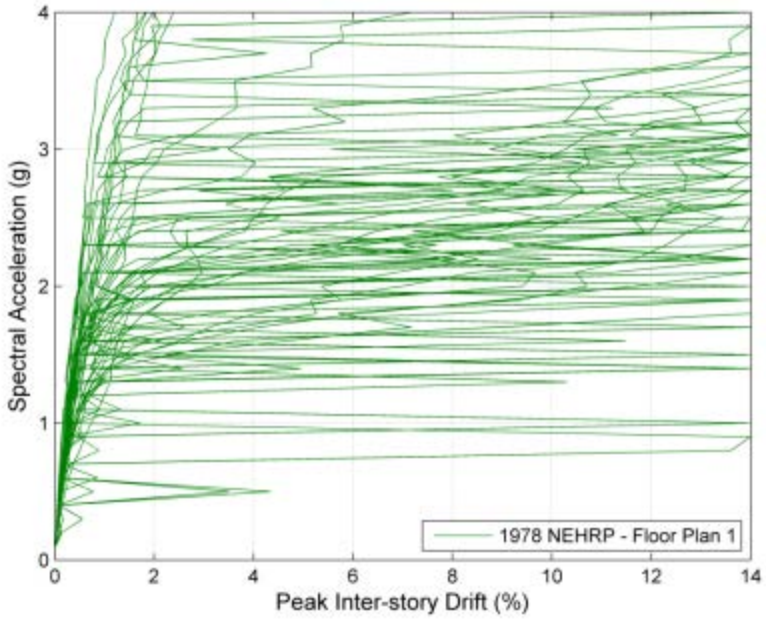

Figure C-2: Multi-Record IDA Floor Plan 1, 1978 NEHRP Design

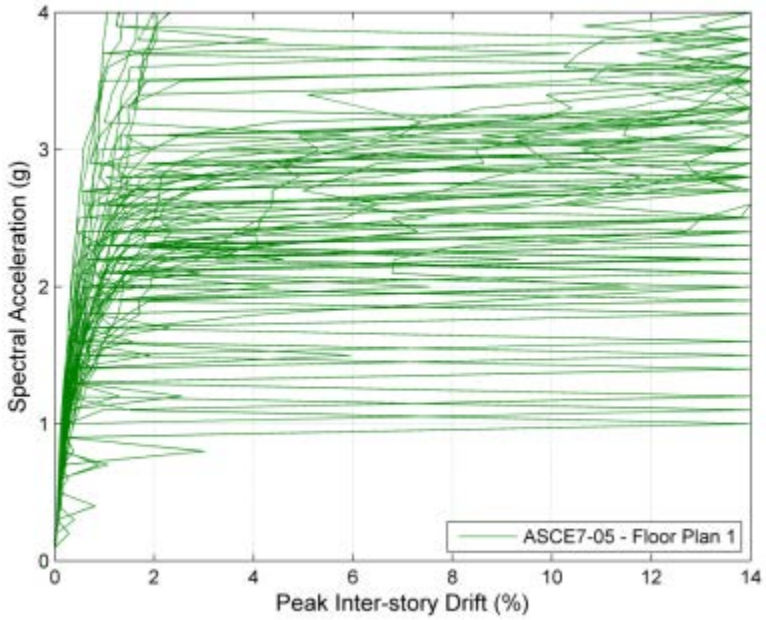

Figure C-3: Multi-Record IDA for Floor Plan 1, ASCE7-05 Design

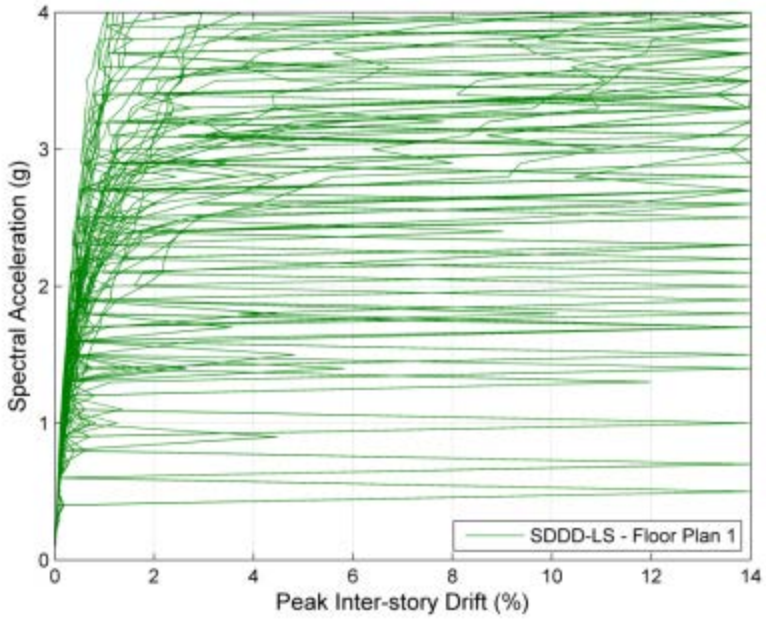

Figure C-4: Multi-Record IDA for Floor Plan 1, SDDD-LS Retrofit Design

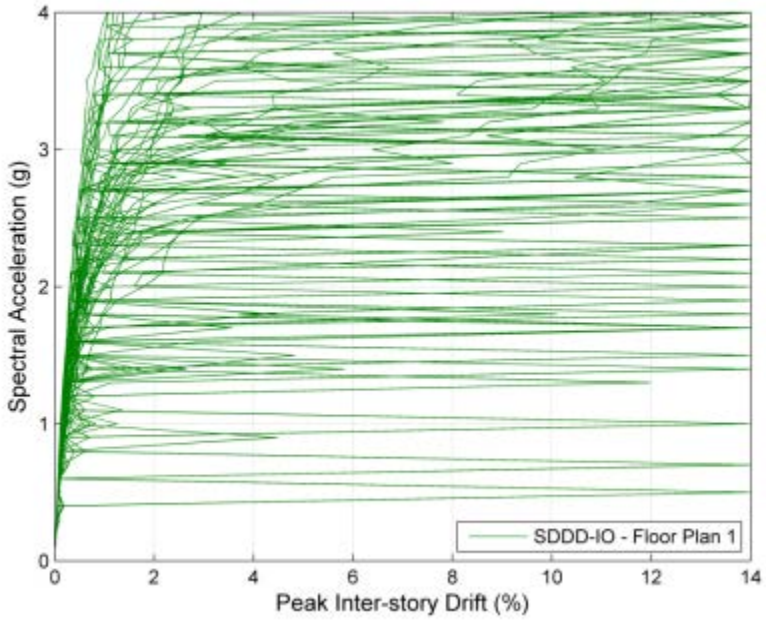

Figure C-5: Multi-Record IDA for Floor Plan 1, SDDD-IO Retrofit Design

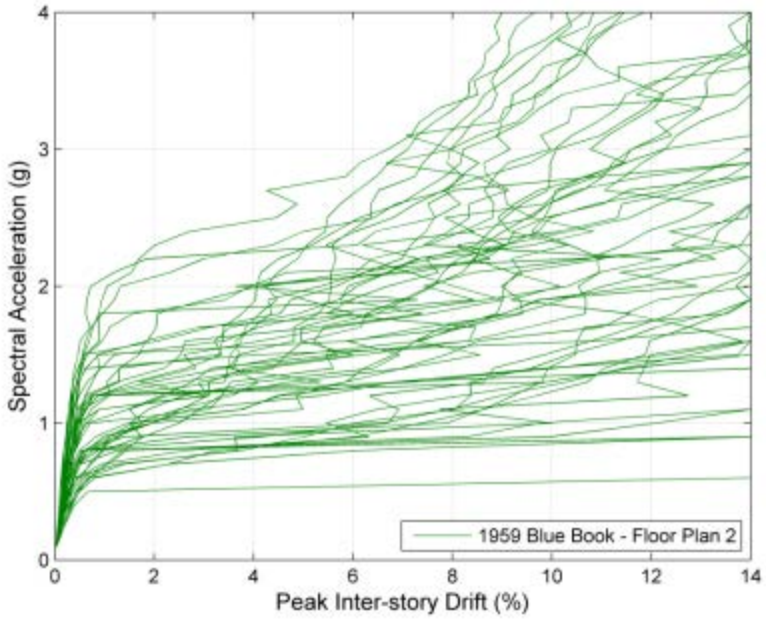

Figure C-6: Multi-Record IDA for Floor Plan 2, 1959 Blue Book Design

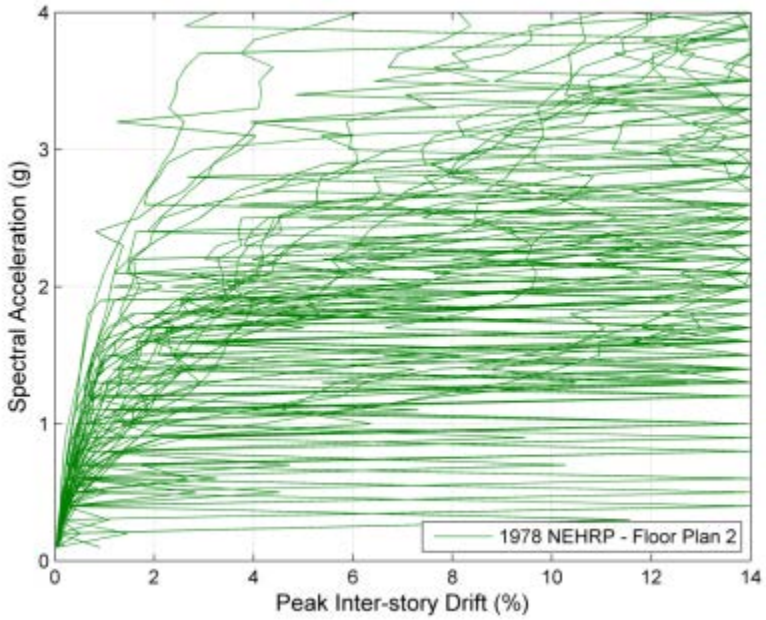

Figure C-7: Multi-Record IDA Floor Plan 2, 1978 NEHRP Design

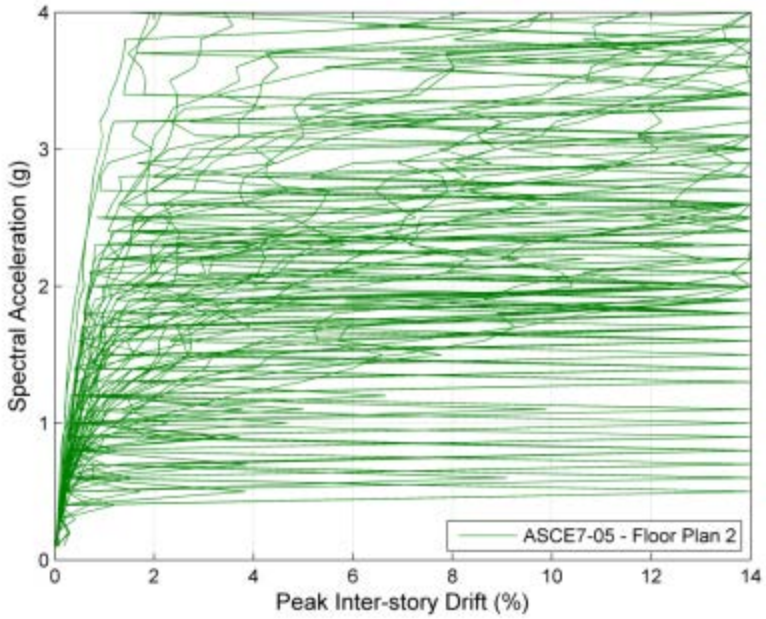

Figure C-8: Multi-Record IDA for Floor Plan 2, ASCE7-05 Design

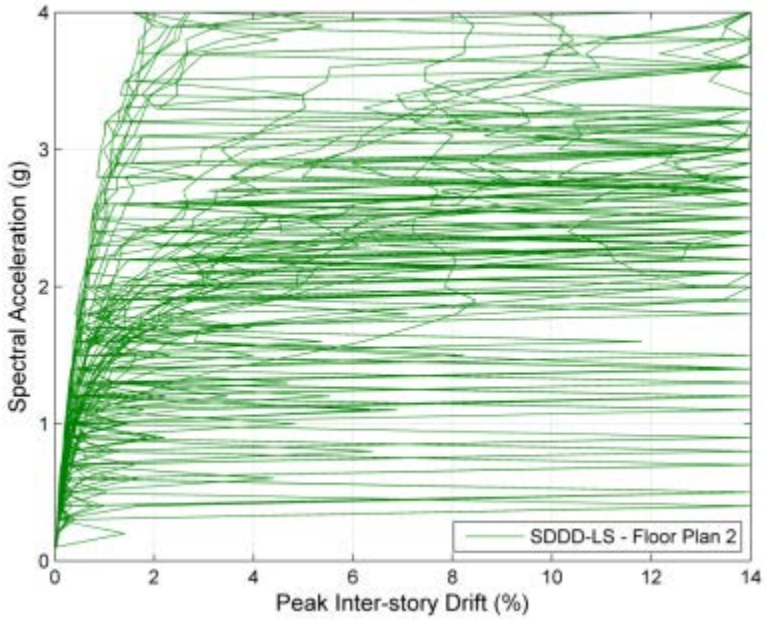

Figure C-9: Multi-Record IDA for Floor Plan 2, SDDD-LS Retrofit Design

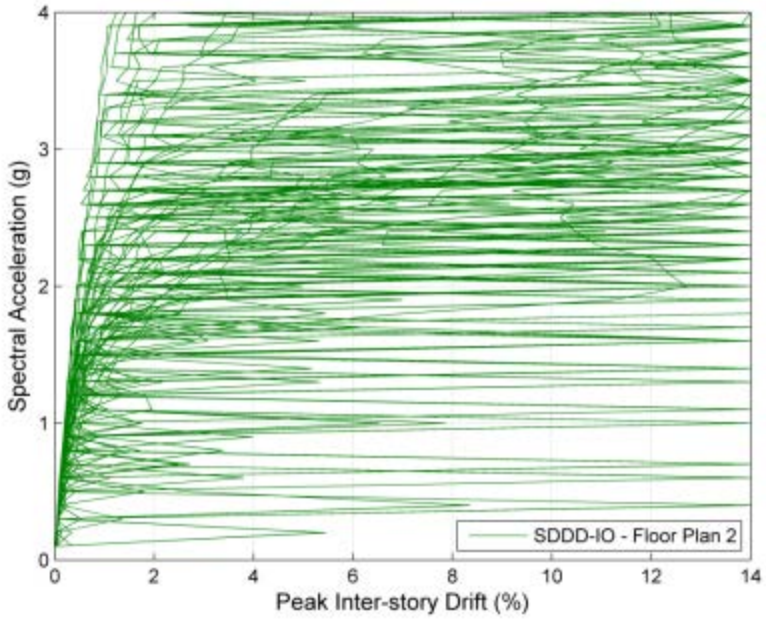

Figure C-10: Multi-Record IDA for Floor Plan 2, SDDD-IO Retrofit Design

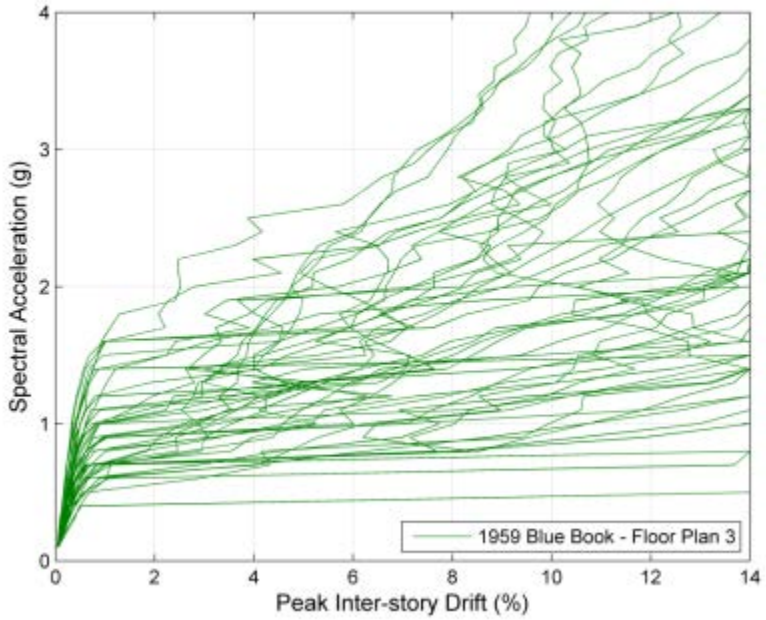

Figure C-11: Multi-Record IDA for Floor Plan 3, 1959 Blue Book Design

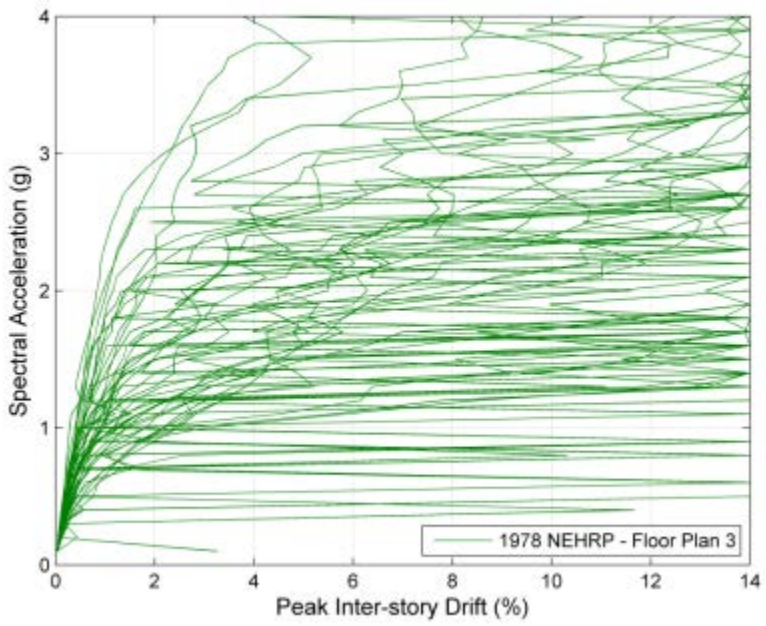

Figure C-12: Multi-Record IDA Floor Plan 3, 1978 NEHRP Design

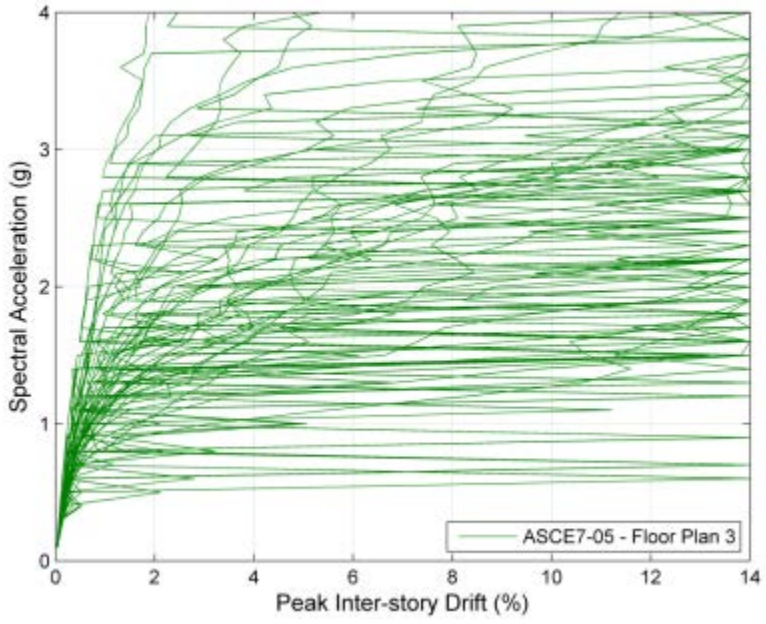

Figure C-13: Multi-Record IDA for Floor Plan 3, ASCE7-05 Design

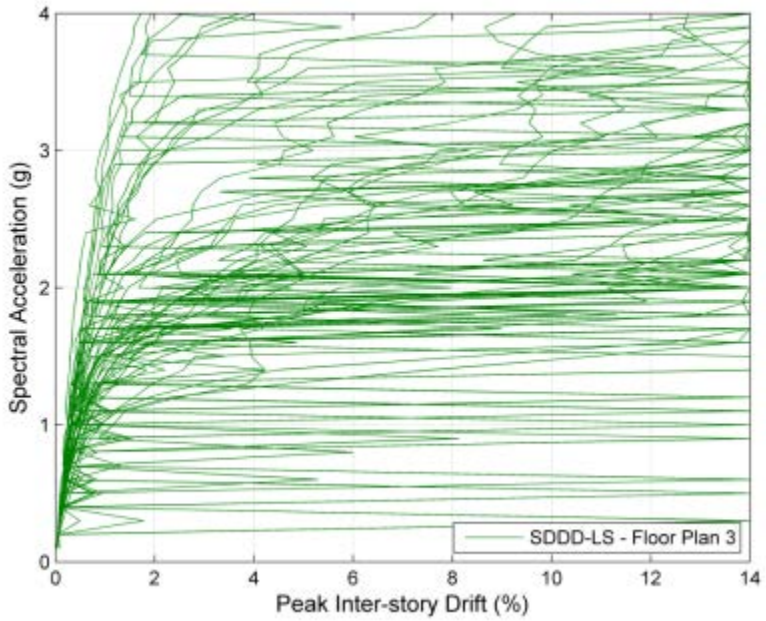

Figure C-14: Multi-Record IDA for Floor Plan 3, SDDD-LS Retrofit Design

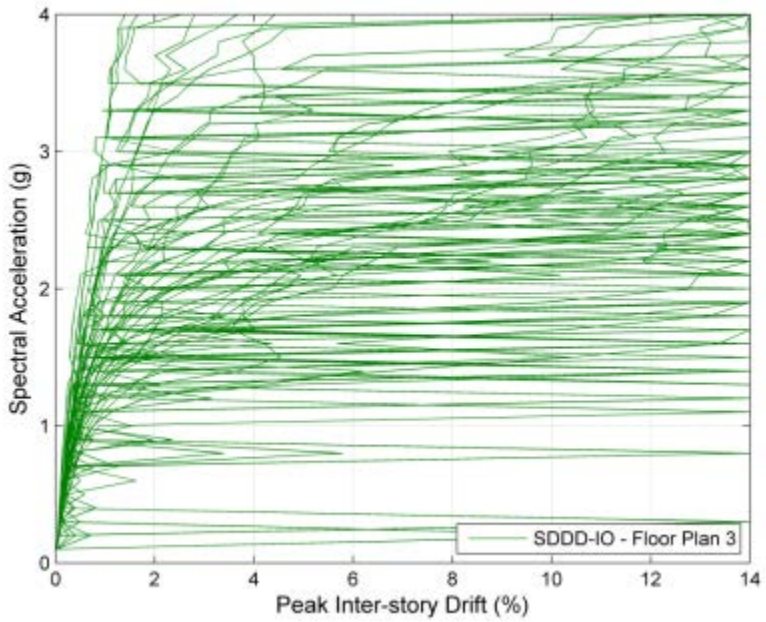

Figure C-15: Multi-Record IDA for Floor Plan 3, SDDD-IO Retrofit Design

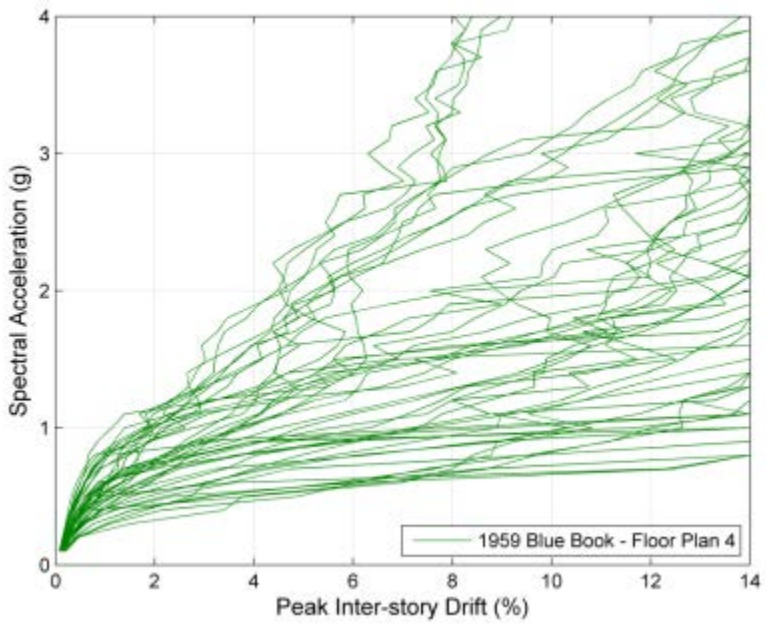

Figure C-16: Multi-Record IDA for Floor Plan 4, 1959 Blue Book Design

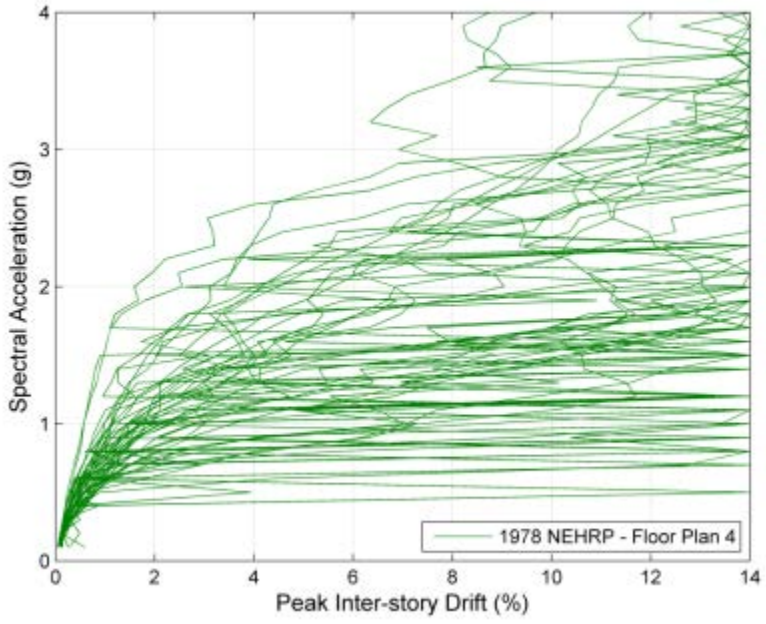

Figure C-17: Multi-Record IDA Floor Plan 4, 1978 NEHRP Design

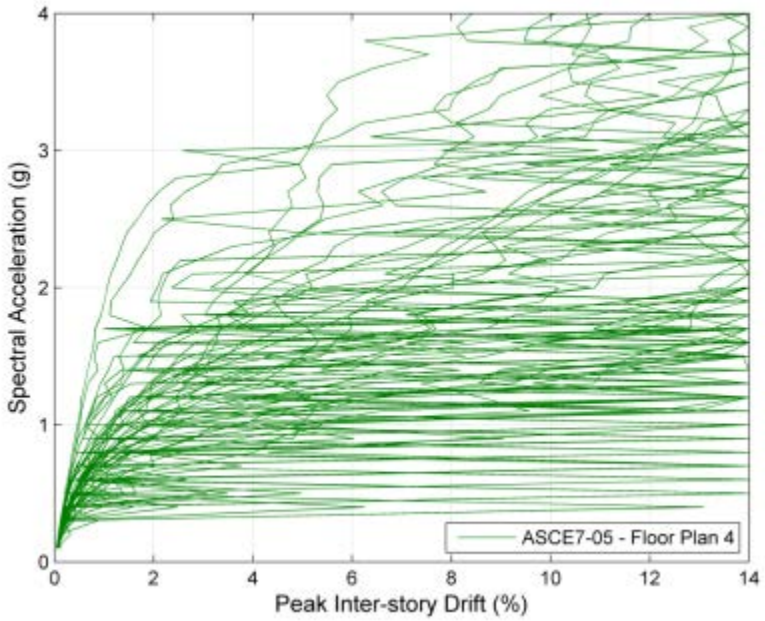

Figure C-18: Multi-Record IDA for Floor Plan 4, ASCE7-05 Design

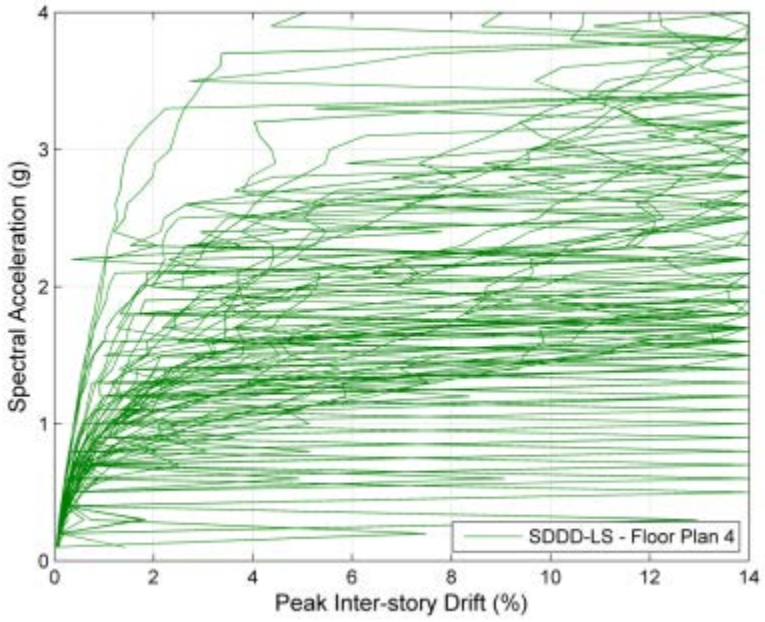

Figure C-19: Multi-Record IDA for Floor Plan 4, SDDD-LS Retrofit Design

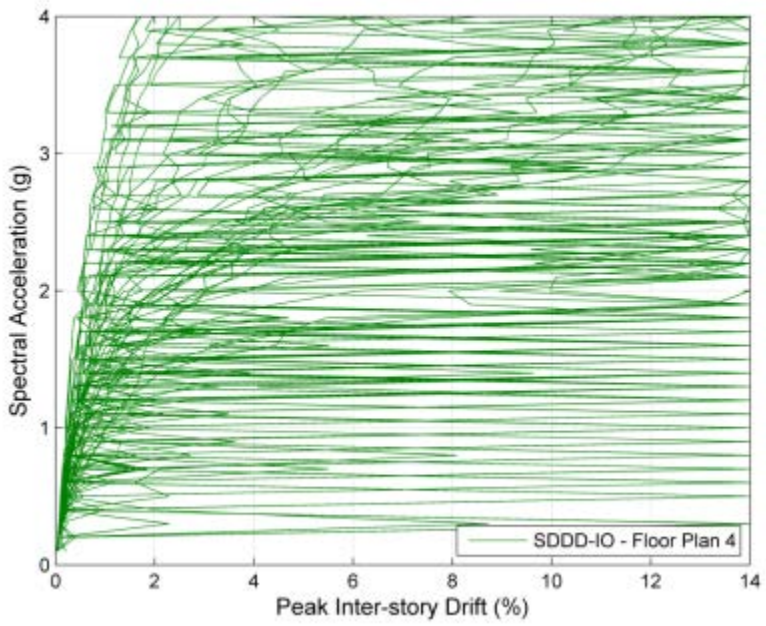

Figure C-20: Multi-Record IDA for Floor Plan 4, SDDD-IO Retrofit Design

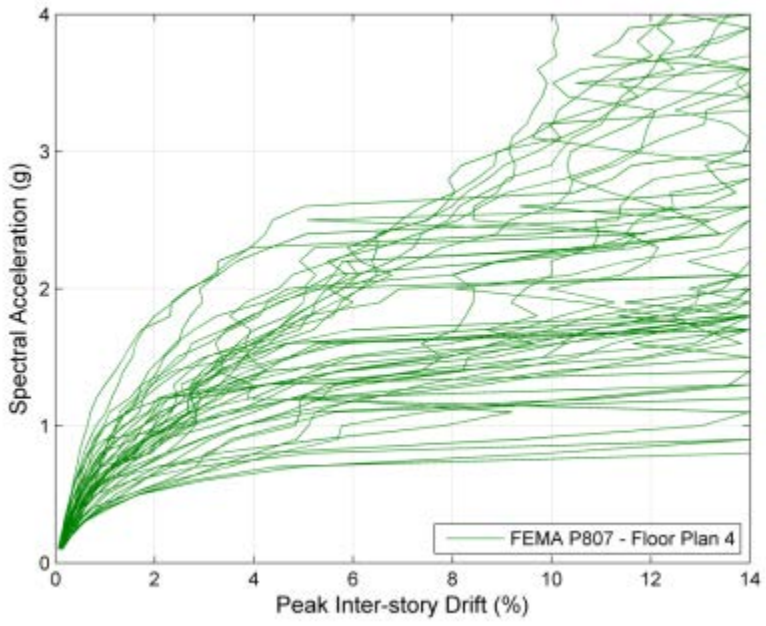

Figure C-21: Multi-Record IDA for Floor Plan 4, FEMA P-807 Retrofit Design

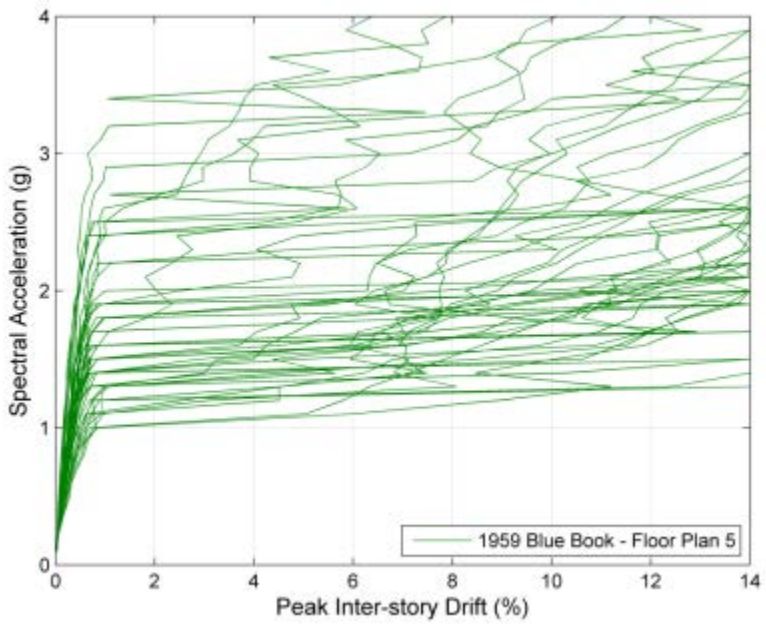

Figure C-22: Multi-Record IDA for Floor Plan 5, 1959 Blue Book Design

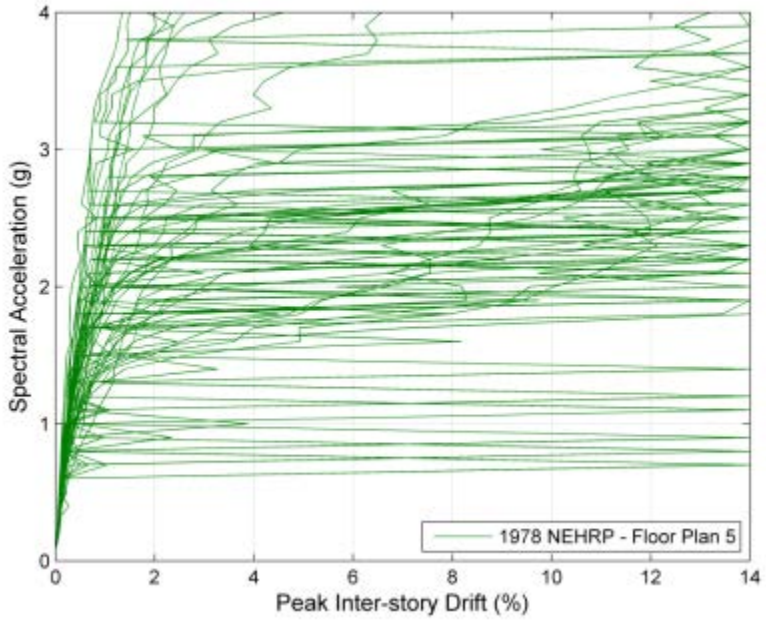

Figure C-23: Multi-Record IDA Floor Plan 5, 1978 NEHRP Design

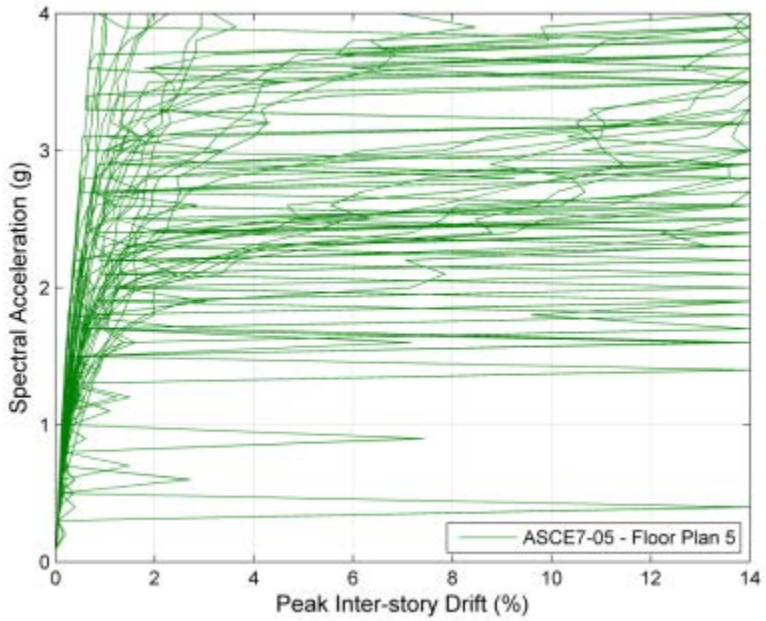

Figure C-24: Multi-Record IDA for Floor Plan 5, ASCE7-05 Design

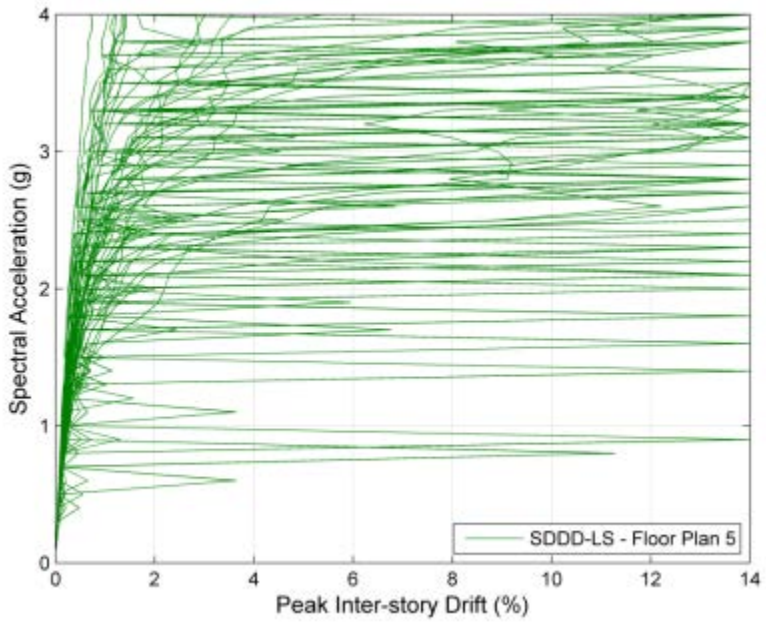

Figure C-25: Multi-Record IDA for Floor Plan 5, SDDD-LS Retrofit Design

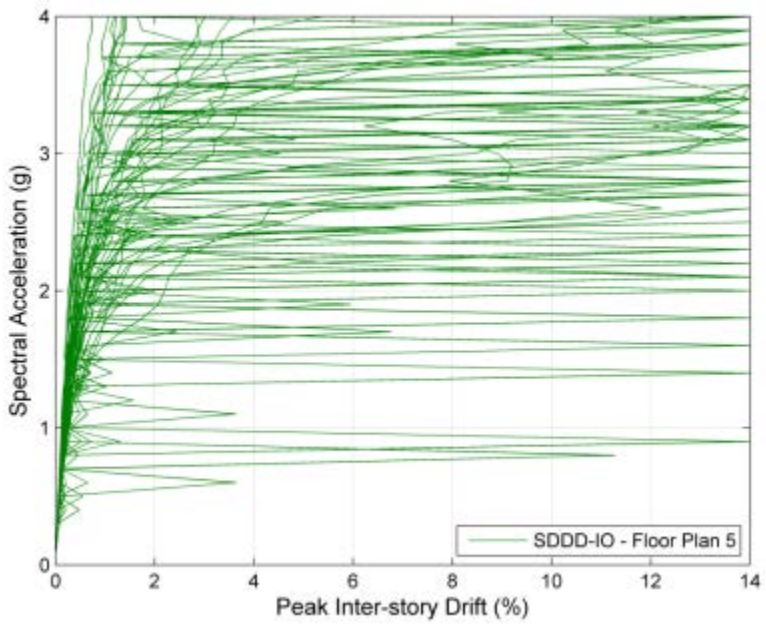

Figure C-26: Multi-Record IDA for Floor Plan 5, SDDD-IO Retrofit Design

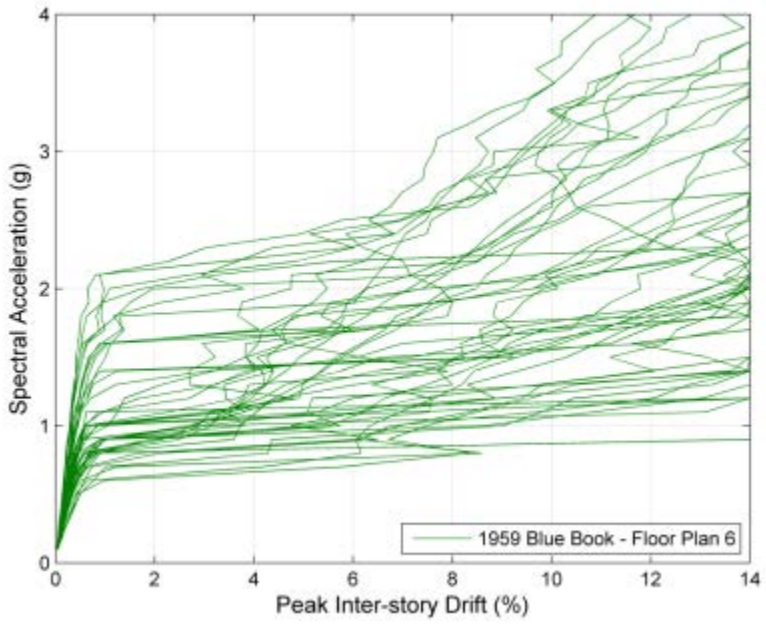

Figure C-27: Multi-Record IDA for Floor Plan 6, 1959 Blue Book Design

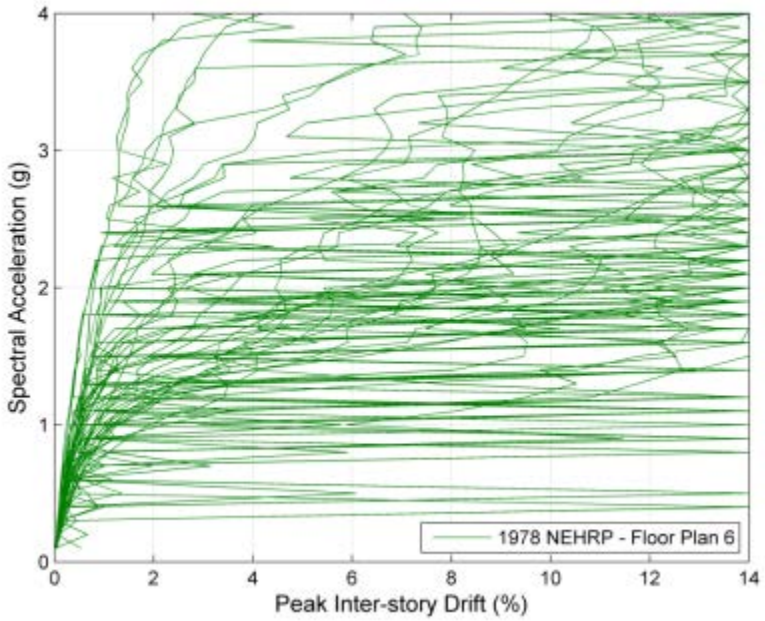

Figure C-28: Multi-Record IDA Floor Plan 6, 1978 NEHRP Design

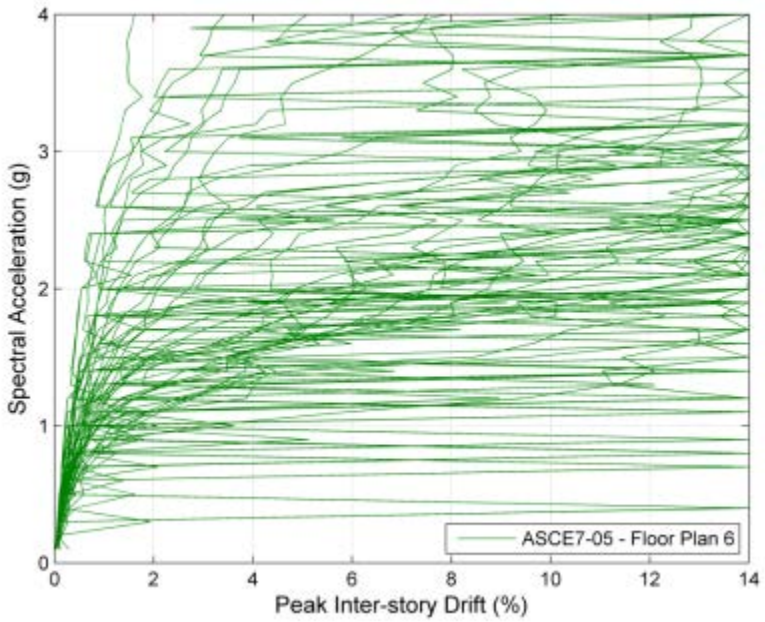

Figure C-29: Multi-Record IDA for Floor Plan 6, ASCE7-05 Design

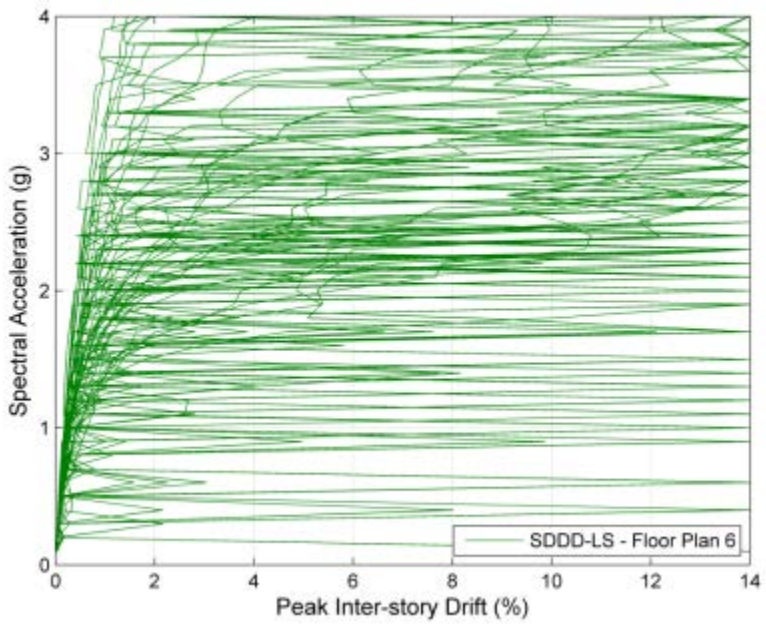

Figure C-30: Multi-Record IDA for Floor Plan 6, SDDD-LS Retrofit Design

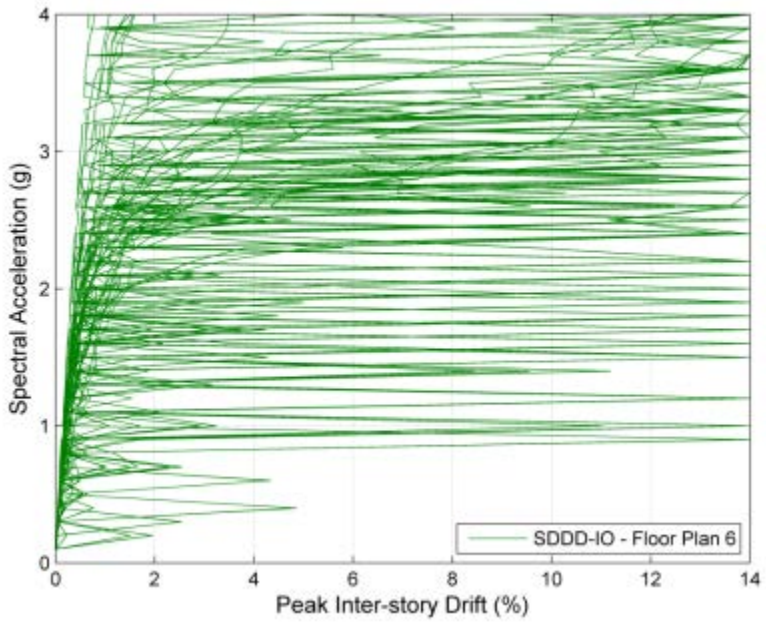

Figure C-31: Multi-Record IDA for Floor Plan 6, SDDD-IO Retrofit Design

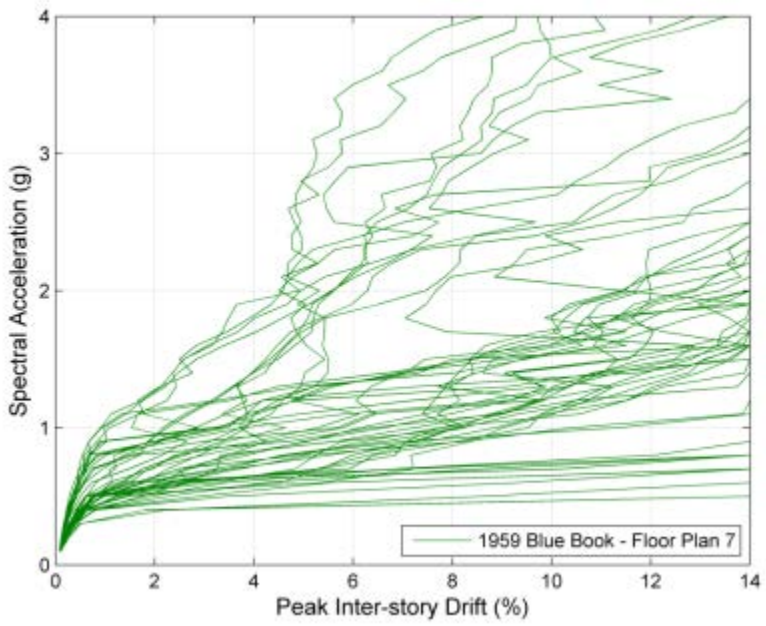

Figure C-32: Multi-Record IDA for Floor Plan 7, 1959 Blue Book Design

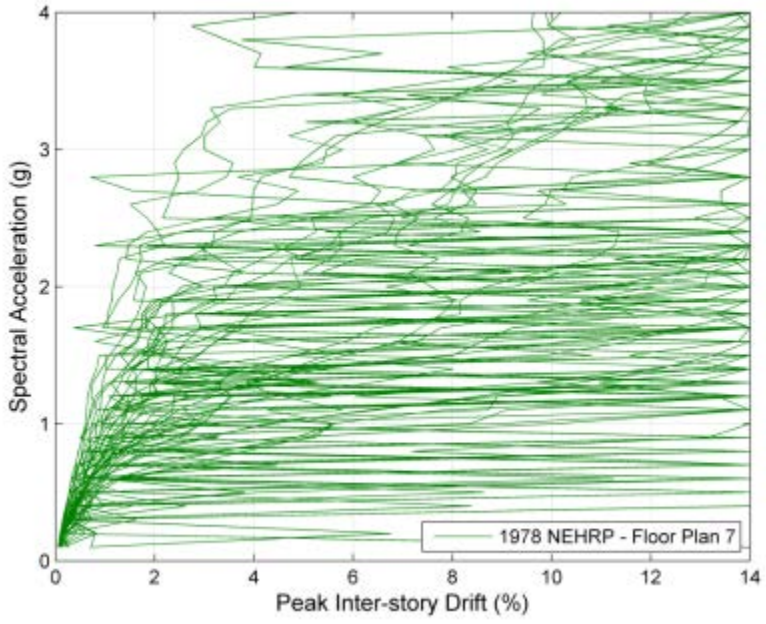

Figure C-33: Multi-Record IDA Floor Plan 7, 1978 NEHRP Design

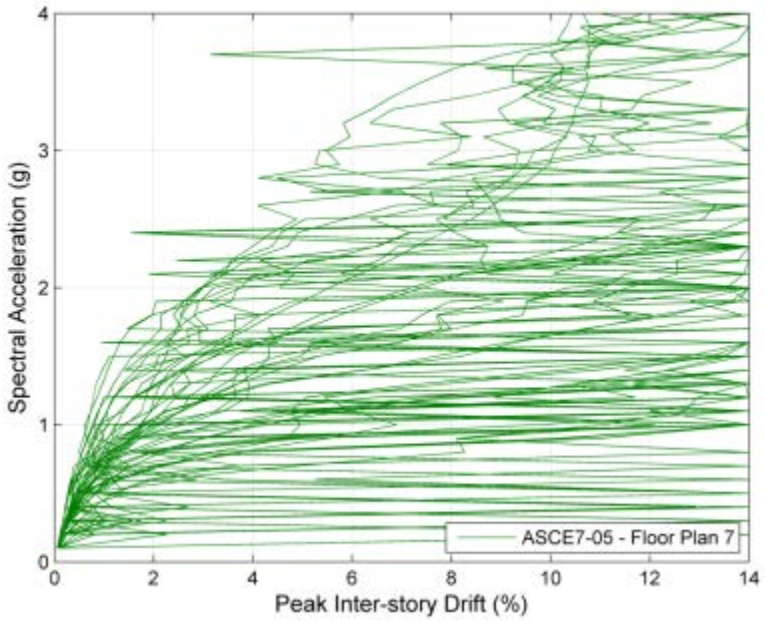

Figure C-34: Multi-Record IDA for Floor Plan 7, ASCE7-05 Design

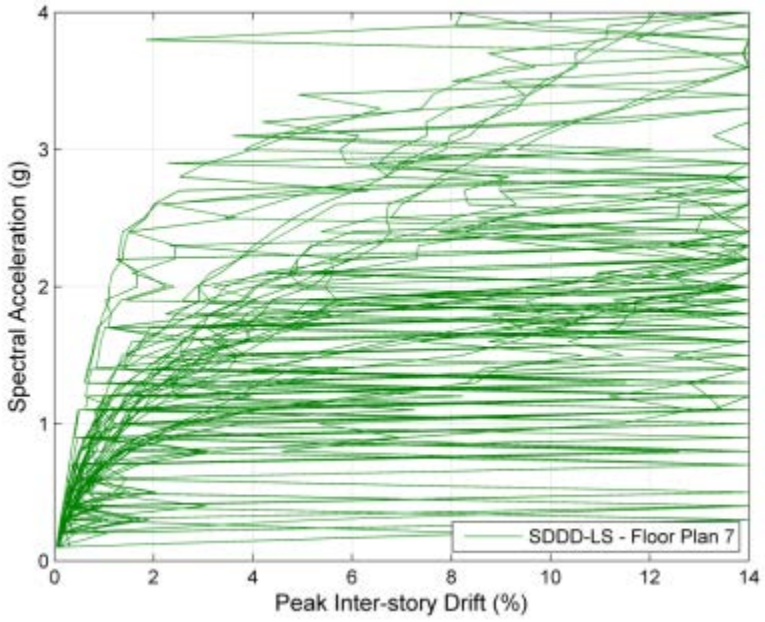

Figure C-35: Multi-Record IDA for Floor Plan 7, SDDD-LS Retrofit Design

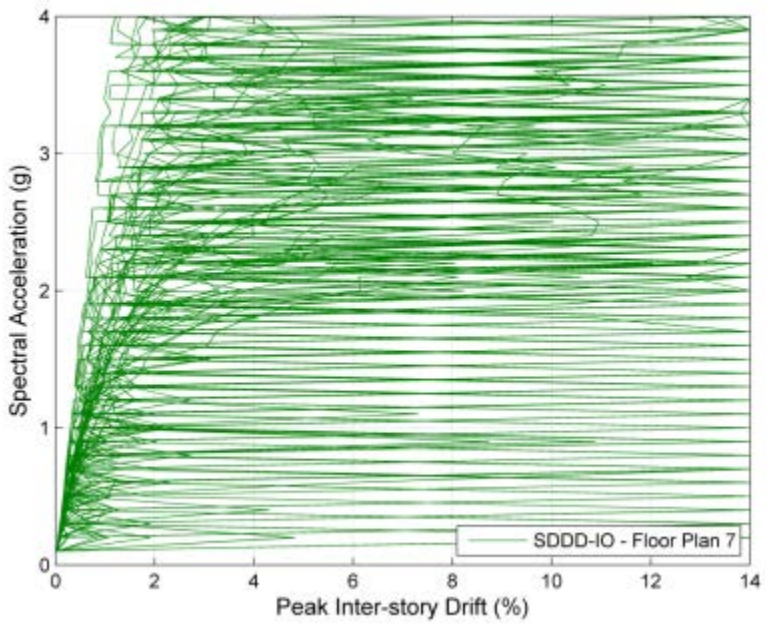

Figure C-36: Multi-Record IDA for Floor Plan 7, SDDD-IO Retrofit Design

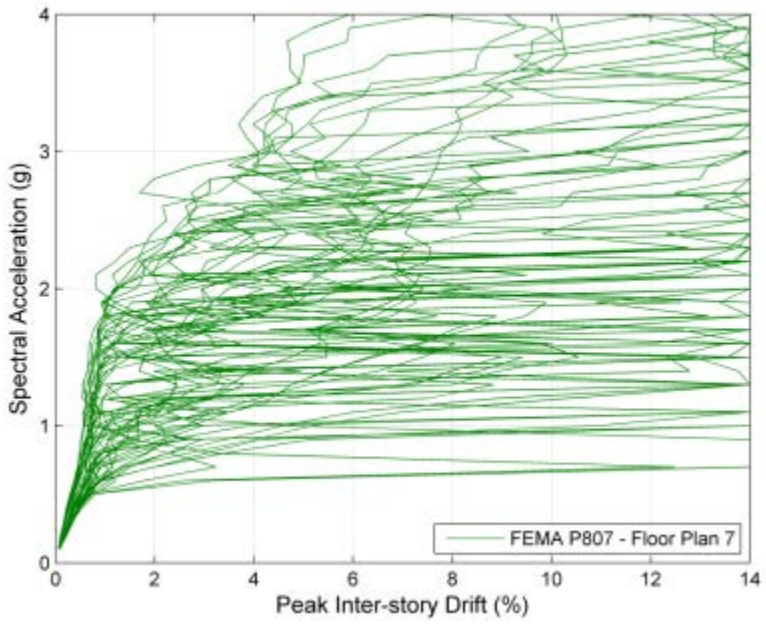

Figure C-37: Multi-Record IDA for Floor Plan 7, FEMA P-807 Retrofit Design

Appendix D

Case Study 1 Results:

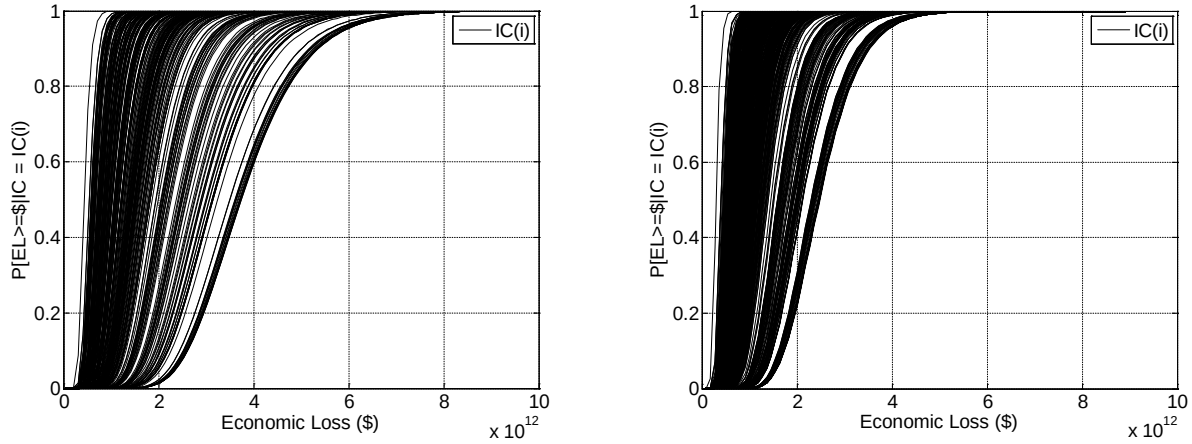

(a) (b)

Figure D-1: Probability of Economic Loss Conditioned on Initial Cost:
a) with Social Vulnerability Factors; b) without Social Vulnerability Factors

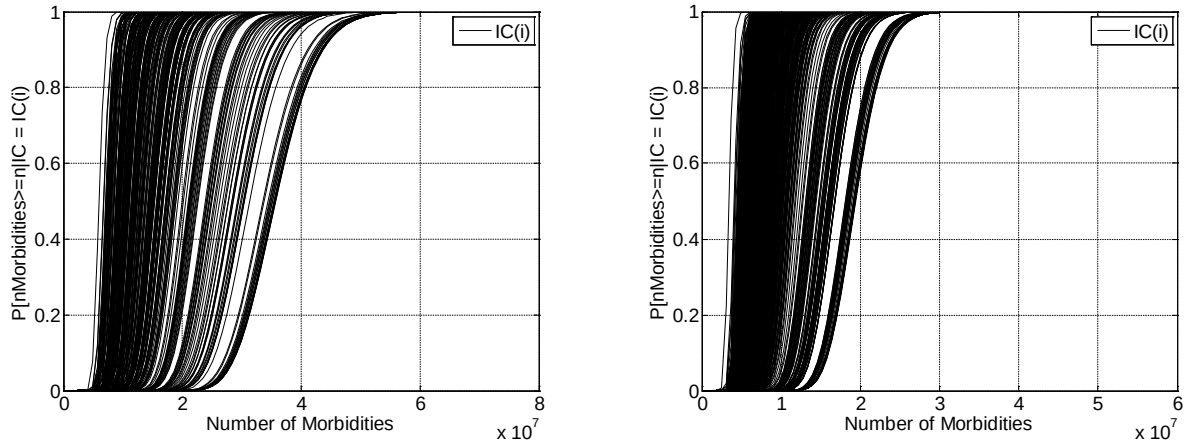

(a) (b)

Figure D-2: Probability of Morbidity Conditioned on Initial Cost:
a) with Social Vulnerability Factors; b) without Social Vulnerability Factors

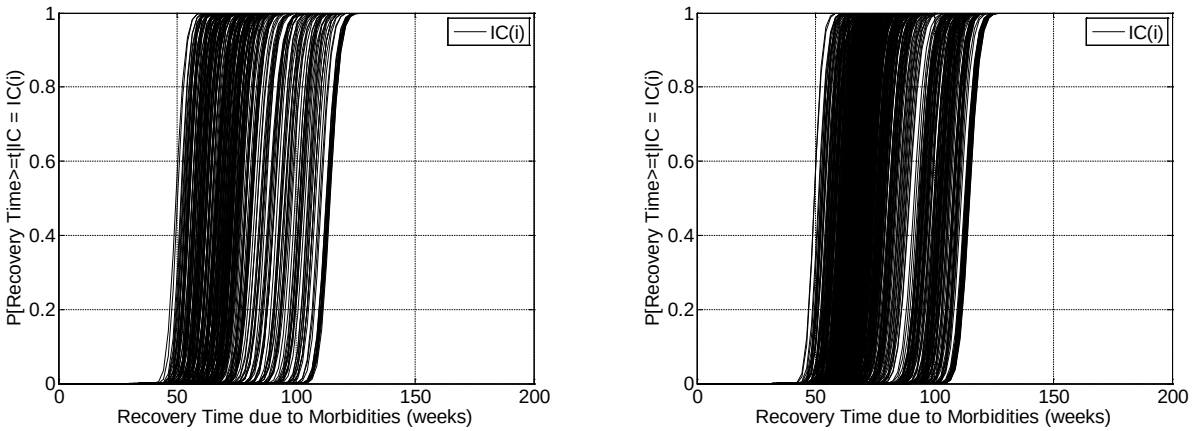

(a) (b)

Figure D-3: Probability of Recovery Time Conditioned on Initial Cost:
a) with Social Vulnerability Factors; b) without Social Vulnerability Factors

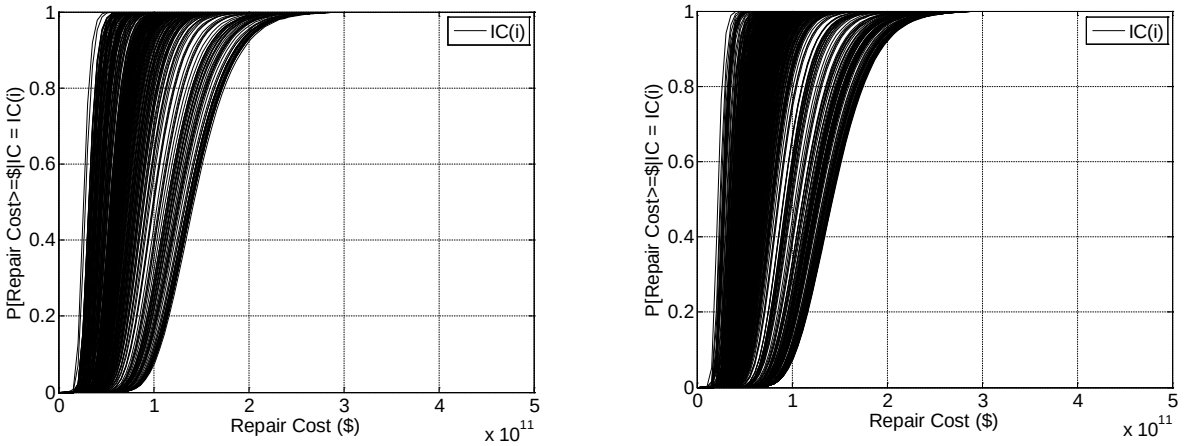

(a) (b)

Figure D-4: Probability of Repair Cost Conditioned on Initial Cost:
a) with Social Vulnerability Factors; b) without Social Vulnerability Factors

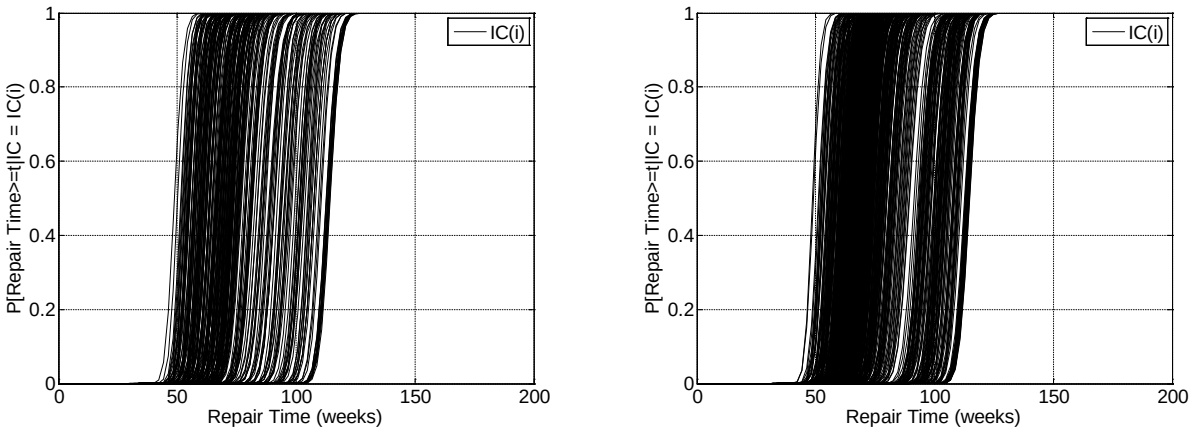

(a) (b)

Figure D-5: Probability of Repair Time Conditioned on Initial Cost:
a) with Social Vulnerability Factors; b) without Social Vulnerability Factors

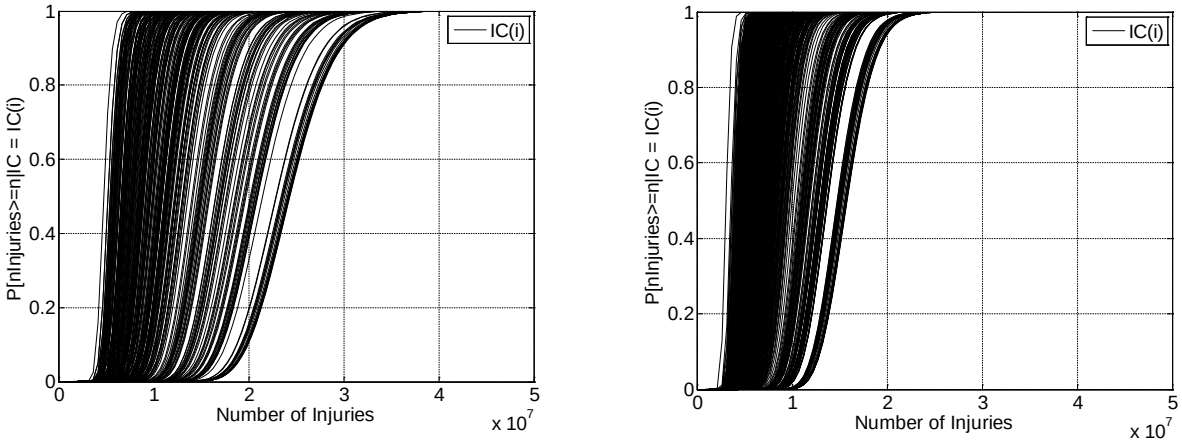

(a) (b)

Figure D-6: Probability of Injury Conditioned on Initial Cost:
a) with Social Vulnerability Factors; b) without Social Vulnerability Factors

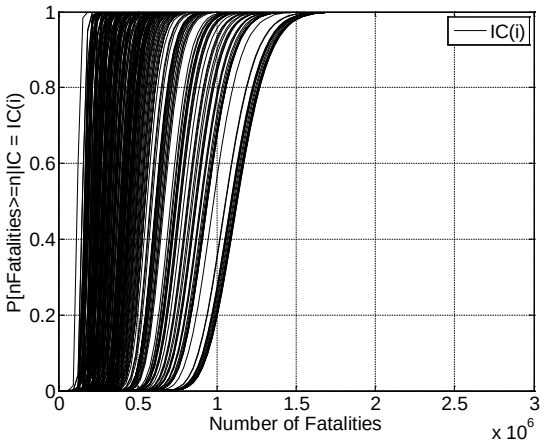

(a)

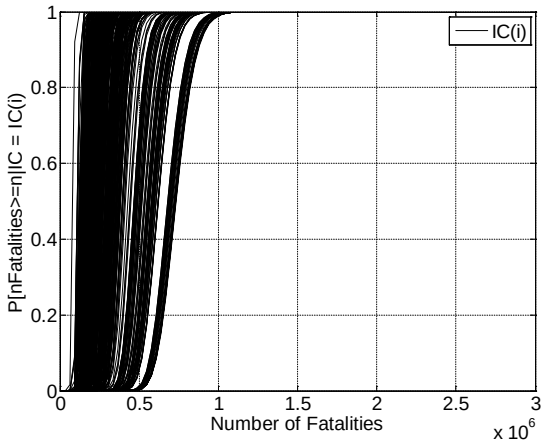

(b)

Figure D-7: Probability of Fatality Conditioned on Initial Cost:
a) with Social Vulnerability Factors; b) without Social Vulnerability Factors

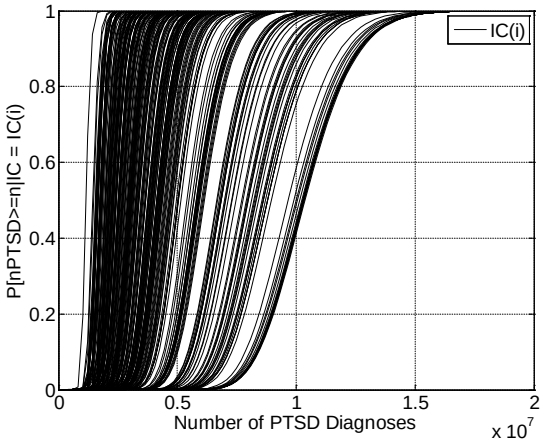

(a)

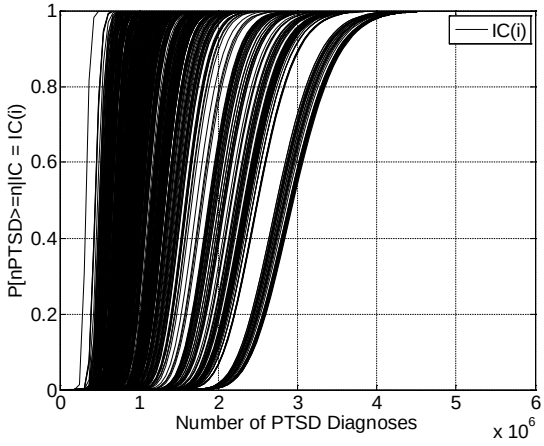

(b)

Figure D-8: Probability of PTSD Diagnosis Conditioned on Initial Cost:
a) with Social Vulnerability Factors; b) without Social Vulnerability Factors

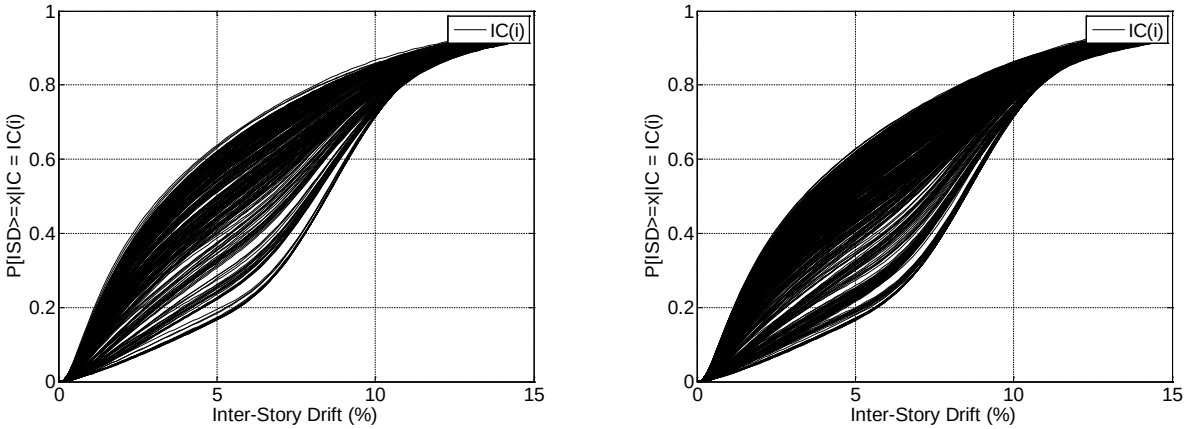

(a) (b)

Figure D-9: Probability of Community Inter-Story Drift Conditioned on Initial Cost: a) with Social Vulnerability Factors; b) without Social Vulnerability Factors

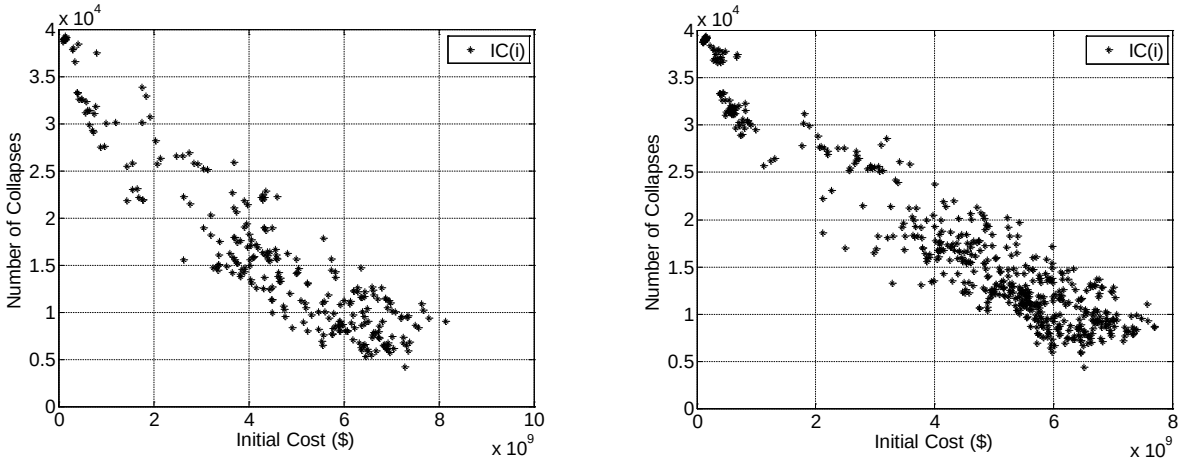

(a) (b)

Figure D-10: Number of Building Collapses versus Initial Cost: a) with Social Vulnerability Factors; b) without Social Vulnerability Factors

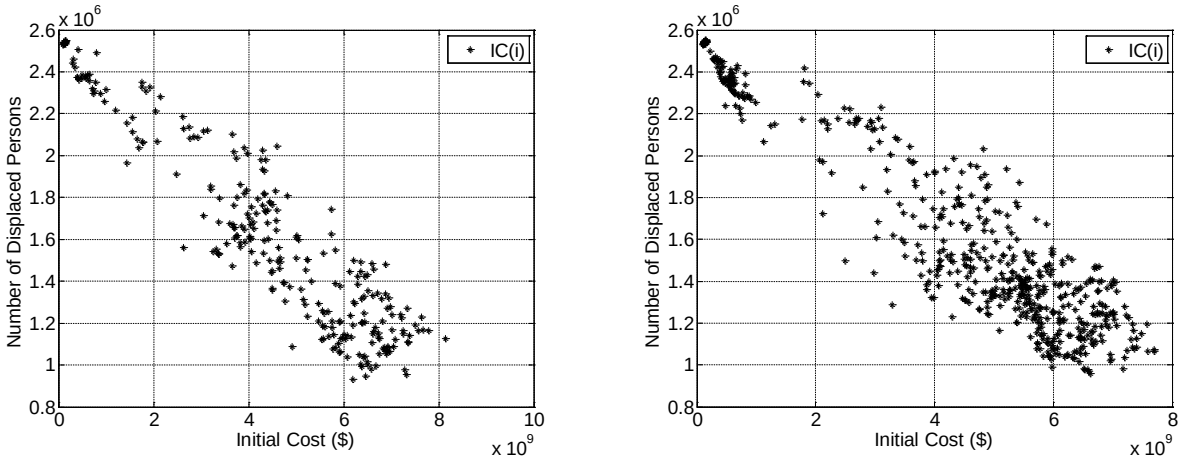

(a) (b)

Figure D-11: Number of Displaced Persons versus Initial Cost:
a) with Social Vulnerability Factors; b) without Social Vulnerability Factors